Investigations into the stability of growth factor induced-vasculature and the effects of synthetic biomaterials on heart remodelling after myocardial infarction

Dr. Stephan Dobner

Supervisor: Neil H. Davies, PhD

Thesis presented for the Degree of DOCTOR OF PHILOSOPHY in the Department of Surgery, Faculty of Health Sciences, UNIVERSITY OF CAPE TOWN

February 2011

I, Dr. Stephan Dobner, hereby:

(a) grant the University of Cape Town free licence to reproduce the above thesis in whole or in part, for the purpose of research;

(b) declare that:

(i) the above thesis is my own unaided work, both in concept and execution, and that apart from the normal guidance from my supervisor, I have received no assistance.

(ii) neither the substance nor any part of the above thesis has been submitted in the past, or is being, or is to be submitted for a degree at this University or at any other university.

Signature: ……

Date: ……

Acknowledgements

First and foremost, I would like to thank Dr. Neil Davies, for being a tremendous supervisor and mentor. His daily advice was instrumental for the completion of this thesis and I surely tested his patience on a number of occasions. I will always fondly remember our morning discussions of experiments (and cricket) over a cup of coffee.

I would like to thank Prof. Peter Zilla, the director of the Cardiovascular Research Unit, for giving me the opportunity to take my first steps towards becoming a physician-scientist. His relentless pursuit of combining clinical medicine and science in a financially challenging environment is truly inspiring.

I am immensely grateful towards Dr. Deon Bezuidenhout, Johann Eygelaar and Christian Schmidt for their contributions to this project. Without Deon and Johann, many of the experiments would not have been possible and I've enjoyed working alongside them every single moment.

Many thanks to Subash Govender, Melanie Black and Helen Ilsley, for helping me with all the histology. While I knew myself to be lucky being able to rely on them during my time in Cape Town, I have since then gained even more appreciation of their excellent work.

I would like to thank Noel Markgraaf and Raymond Michaels, for sharing their expertise and assisting me during countless hours of surgical procedures.

I thank my dear colleagues, Louise Bezuidenhout and Thomas Franz, for their friendship and continuous support and making me see the light at the end of the tunnel during the many not so bright moments one inevitable encounters while conducting research.

Finally, I would like to thank Mona Bracher for taking me under her wings in the laboratory, teaching me many of the things that I know today and making me feel at home far away from home.

This project was supported financially by Medtronic Inc., Minneapolis, USA.

Publications arising from this thesis

Davies N*, **Dobner S***, Bezuidenhout D, Schmidt C, Beck M, Zisch AH, Zilla P.; *The dosage dependence of VEGF stimulation on scaffold neovascularisation.* **Biomaterials. 2008 Sep;29(26):3531-8. Epub 2008 Jun 9**

Dobner S, Bezuidenhout D, Govender P, Zilla P, Davies N.; *A synthetic non-degradable polyethylene glycol hydrogel retards adverse post-infarct left ventricular remodeling.* **J Card Fail. 2009 Sep;15(7):629-36. Epub 2009 May 7**

Other publications

Franz T, Human P, Dobner S, Reddy BD, Black M, Ilsley H, Wolf MF, Bezuidenhout D, Moodley L, Zilla P.; *Tailored sizes of constrictive external vein meshes for coronary artery bypass surgery.* **Biomaterials. 2010 Dec;31(35):9301-9. Epub 2010 Sep 22.**

Abbreviations

ACE	angiotensin-converting enzyme
aFGF	acidic fibroblast growth factor
Akt	protein kinase B
Ang-1/Angpt1	angiopoietin-1
Ang-2/Angpt2	angiopoietin-2
Anpep	alanyl (membrane) aminopeptidase
ARB	angiotensin receptor blocker
Bai1_predicted	brain-specific angiogenesis inhibitor 1
BDNF	brain-derived neurotrophic factor
bFGF	basic fibroblast growth factor
CAM	chorioallantoic membrane
Ccl2	chemokine (C-C motif) ligand 2, MCP-1
CD	cluster of differentiation
Cdh5_predicted	cadherin 5
Col18a1	collagen, type XVIII, alpha 1
Col4a3	collagen, type IV, alpha 3
Ctgf	connective tissue growth factor
CVD	cardiovascular disease
CXCL	chemokine (C-X-C motif) ligand
CXCR	C-X-C chemokine receptor
DAPI	4',6-diamidino-2-phenylindole
DNA	deoxyribonucleic acid
DTT	dithiothreitol
EC	endothelial cell
ECG	electrocardiogram
Ecgf	thymidine phosphorylase
ECM	extracellular matrix
EDD	end-diastolic diameter
Edg1	sphingosine-1-phosphate receptor 1
EDV	end-diastolic volume
EGF	epidermal growth factor
ELISA	enzyme-linked immunosorbent assay
Epas1	endothelial PAS domain protein 1, Hif2a
EPC	endothelial progenitor cell
ePTFE	expanded tetrafluoroethylene
ERK	extracellular-signal-regulated kinase
ESD	end-systolic diameter
ESV	end-systolic volume
F2	thrombin, coagulation factor II
FGF	fibroblast growth factor
FGFR	fibroblast growth factor receptor
Figf	C-fos induced growth factor, VEGF-D
Flt-1	Fms-related tyrosine kinase 1, VEGFR1
FS	fractional shortening
Fzd5	frizzled homolog 5 (Drosophila)
HF	heart failure
HGF	hepatocyte growth factor
HIF-1α	hypoxia inducible factor 1
HSC	haematopoietic stem cell

HSPG	heparan sulfate proteoglycan
HUVEC	human umbilical vein endothelial cell
Id	inhibitor of DNA binding
Ifna1	interferon α-1
Ifnb1	interferon β-1
Ifng	interferon γ
IGF-1	insulin-like growth factor-1
IHD	ischemic heart disease
IL	interleukin
Itga5	Integrin α5 (fibronectin receptor alpha)
Itgav_predicted	integrin α-V Cd51
Itgb3	integrin β-3
Jag1	jagged 1
Kdr	kinase insert domain protein receptor, VEGFR2
KGF	keratinocyte growth factor
L. esculentum lectin	Lycopersicon esculentum lectin
LAD	left anterior descending coronary artery
Lama5	laminin-α5
LDL	low-density lipoprotein
Lect1	leukocyte cell derived chemotaxin 1
Lep	leptin OB
LV	left ventricular
Mapk14	mitogen activated protein kinase 14
Mdk	midkine
MI	myocardial infarction
MM	multiple myeloma
MMP	matrix metalloproteinase
MMPs	matrix metalloproteinase-sensitive
MRI	magnetic resonance imaging
NO	nitric oxide
Npr	natriuretic peptide receptor A/guanylate cyclase A
Nrp1	Neuropilin 1
Nrp2	Neuropilin 2
p75NTR	p75 neurotrophin receptor
PAI-1	plasminogen activator inhibitor-1
PBS	phosphate buffered saline
PCR	polymerase chain reaction
PDGF	platelet-derived growth factor
PDGFR	platelet-derived growth factor receptor
PECAM	platelet/endothelial cell adhesion molecule 1 CD31
PEDF	pigment epithelium-derived factor
PEG	polyethylene glycol
Pgf	placental growth factor
PI3K	phosphatidylinositol 3-kinase
Plau	plasminogen activator
PLCγ	phospholipase Cγ
Plg	plasminogen
PlGF	placental growth factor
PPC	perivascular progenitor cell
Ptgs1	prostaglandin-endoperoxide synthase 1
PU	polyurethane
q-RT-PCR	quantitative real-time polymerase chain reaction

RGD	Arginine-Glycine-Aspartic acid
RNA	ribonucleic acid
ROS	reactive oxygen species
Sca-1	murine homolog of CD34
SDF-1	stromal-cell derived factor-1
siRNA	small interfering RNA
SMC	smooth muscle cell
SPECT	single photon emission computed tomography
Sphk1	Sphingosine kinase 1
ST	ST segment in electrocardiogram
Tbx4_predicted	T-box 4
Tek	TEK tyrosine kinase, endothelial Tie-2, Tie2
TGF	transforming growth factor
TGF-α	transforming growth factor-α
TGF-β	transforming growth factor-β
Tgfbr1	transforming growth factor-β receptor 1
Thbs4	thrombospondin 4
TIMP	tissue inhibitor of matrix metalloproteinase
TNF	tumour necrosis factor
Trk	neurotrophic tyrosine kinase receptor
VEGF	vascular endothelial growth factor
VEGFR	vascular endothelial growth factor receptor
VIS	Visiopharm Integrated Systems
VPF	vascular permeability factor
VS	vinyl sulfone
vWF	von Willebrand factor

Table of Contents

Investigations into the stability of growth factor induced-vasculature and the effects of synthetic biomaterials on heart remodelling after myocardial infarction

ABSTRACT

In recent years, therapeutic neovascularization has emerged as a promising strategy to treat a number of cardiovascular pathologies, yet the creation of stable vasculature is still a major challenge for which no adequate solution currently exists. Numerous strategies, including delivery of growth factors and employment of biomaterial scaffolds, have been proposed to address this problem. However, these approaches have yet to be widely adopted or validated, perhaps because there is inadequate knowledge of the appropriate growth factor dosage rates and material compositions for such a purpose. This work was based on the hypothesis that optimization of growth factor delivery rate and duration, combined with a biomaterial scaffold, could lead to an improved strategy for therapeutic neovascularization. To test this hypothesis, a novel in vivo model system that allows for characterization of stability and mural cell investment of newly created vessels was designed. Using this model, the effects of numerous growth factors on vessel development were tested, with vascular endothelial growth factor-A^{165} (VEGF) emerging as the most potent initiator of neovascularization in initial experiments. Subsequent studies revealed that VEGF concentration plays a critical role in the nature and persistence of neovessels in a biomaterial scaffold. When VEGF was delivered at 150ng/day for 42 days, scaffold neovessels were found to be stable for up to 2.5 months after withdrawal of VEGF. At this timepoint, vessels induced by a 10-fold higher concentration of VEGF had regressed to levels comparable with PBS controls. Upon identifying advantageous delivery conditions for VEGF to induce therapeutic neovascularization, a rat myocardial infarction model was employed to investigate whether these findings might be applied in the setting of myocardial ischemia, as this remains one of the major pathologies hypothesized to benefit greatly from therapeutic neovascularization. In this model, VEGF delivery was combined with an injectable polyethylene glycol (PEG) hydrogel, which had previously been shown to effectively deliver VEGF in vivo.

Surprisingly, injection of non-degradable PEG hydrogels alone revealed that synthetic biomaterial injections into infarcted myocardium could result in retardation of post-infarct left-ventricular remodelling. Importantly though, despite using a non-degradable material, the beneficial effects observed - complete prevention of wall thinning and significant (33.3% and 43.3%) reductions in end-diastolic diameter increase at 2 and 4 weeks - did not persist until the 3-month time-point. An additional hypothesis, that enzymatically degradable hydrogels could be a required compromise to overcome the inflammatory response observed with non-degradable PEG whilst still providing mechanical support, was not supported by further experiments. Finally, the potential of enzymatically degradable PEG hydrogels for the sustained delivery of growth factors to the myocardial infarct (injury) site and promotion of angiogenesis was tested. Prolonged VEGF delivery did not lead to improved left ventricular function after myocardial infarction. These findings suggest that not only are the time and mode of growth factor delivery critical variables that determine the efficacy of therapeutic angiogenesis, but also that the PEG hydrogel described may need further refinement to allow for its use as a growth factor delivery vehicle in context of myocardial ischemia.

1. INTRODUCTION

Cardiovascular disease (CVD) is the most common cause of death in the industrialized world today. In 2005, CVD accounted for 35.2% of all deaths in the United States[1]. Risk factor identification, an emphasis on disease prevention, the development of novel drugs and advances in invasive medical therapies have contributed to declining death rates from cardiovascular disease. Yet the socioeconomic burden of these diseases remains high. A drop off in mortality resulting from myocardial infarction (MI) observed in recent decades was paralleled by an increase in the incidence of heart failure (HF) [2], with up to one third of patients developing heart failure after a coronary attack. Furthermore, the rising epidemic of Diabetes Mellitus will contribute to a substantial increase in peripheral arterial disease over the next decades[3-5]. In all more than 80 million American adults presently suffer from one or more types of cardiovascular disease. The cost of CVD in 2008, estimated at $448.5 billion[1], underlines that new therapies and effective strategies to prevent cardiovascular disease are urgently needed. Over the last 10 years, promoting angiogenesis - the formation of new blood vessels - has emerged as one of the more promising concepts to treat cardiovascular disease[6]. While progress has been made in understanding basic mechanisms regulating therapeutic angiogenesis, the translation into clinical practice has been disappointing. A major obstacle remains the establishment of a stable mature neovasculature. The future success of therapeutic angiogenesis will depend on developing strategies to minimize the leakiness of newly generated vessels and to create a vascular bed that resists regression at least for months, if not years.

1.1. History of Angiogenesis

The 1971 New England Journal of Medicine publication by the late Judah Folkman stating that tumour growth is angiogenesis-dependent can be viewed as the beginning of the modern era of angiogenesis research [7]. Folkman not only predicted that without developing a microvasculature most tumours would be restricted to a size of 1-2 millimetres and that tumours would be capable of secreting molecules promoting the growth of the microvasculature, he also anticipated the

discovery of angiogenesis inhibitors that would make it possible to prevent the arising of new capillary sprouts [7]. Still, it required developing methods to culture endothelial cells[8,9], assays to assess angiogenesis in vivo, and discovering the first angiogenic growth factor, basic fibroblast growth factor (bFGF/FGF2) in the 1970´s[10], to silence many sceptics. The first successful use of anti-angiogenic therapy to treat a teenage patient suffering from progressive pulmonary haemangiomatosis was reported in 1988[11,12]. Based on experimental evidence and its anti-angiogenic properties elucidated in animal studies, Judah Folkman had suggested low-dose interferon-α after conventional therapies had failed.

In 1989, another pro-angiogenic protein, vascular endothelial growth factor A (VEGF-A) [13] was discovered, and the first angiogenesis inhibitor, thrombospondin-1[14,15], was identified. While most research was initially directed towards limiting angiogenesis to prevent tumours from growing, the idea of promoting microvascular growth to improve perfusion and recover function in ischemic tissues appealed to cardiovascular researchers.

The concept of using angiogenic factors was based on Folkman's research on tumours and proposed as early as 1977. 15 years later, Yanagisawa-Miwa et al. [16] and Jeffrey M Isner's group in 1994 were amongst the first to report the potential benefits of therapeutic angiogenesis[17].

1.2. Angiogenesis and Vasculogenesis

Angiogenesis is instrumental during the growth and repair of organs. A transitory physiological angiogenic response can be observed during wound healing or during the female reproductive cycle[18,19]. An imbalance or chronic activation may on the other hand lead to cancer or the promotion of arthritis or proliferative retinopathy[6].

Historically discussed separately, it is becoming increasingly clear that during embryonic as well as during adult life, the two main mechanisms that contribute to neovascularization, vasculogenesis and angiogenesis[20], are not mutually exclusive[21]. Vasculogenesis describes the de novo development of blood vessels from progenitor cells, the prime example being the

formation of the primary capillary plexus by differentiating angioblasts during embryonic development[20]. The growth of new blood vessels by sprouting and extension from the pre-existing vasculature is referred to as angiogenesis (or sprouting angiogenesis) and can further be distinguished from non-sprouting angiogenesis, during which a vessel splits into two by forming a transcapillary pillar or posts of extracellular matrix (ECM)[20]. Vasculogenesis and angiogenesis simultaneously contribute to the expanding neovasculature during wound healing, tumour growth or inflammation[21].

A first hint that vasculogenesis might indeed occur and contribute to neovascularization in adult life stems from a 1997 study by Asahara et al.[22], suggesting that a subset of CD34+ human endothelial progenitor cells could differentiate into cells that show characteristics comparable with endothelial cells. Young and his colleagues confirmed the hypothesis in 2002, when they showed that endothelial progenitor cells (EPCs) derived from the bone marrow integrate into the vasculature of newly born mice[23]. Both pro-[24-27] and anti-angiogenic[28,29] stimuli have since been shown to operate by affecting endothelial progenitor cells. EPCs not only play a significant role during pathological angiogenesis, they also contribute to vascular quiescence and homeostasis[30] and as a source of angiogenic factors modulate angiogenesis and vasculogenesis.

1.3. Molecular mechanisms of angiogenesis

The endothelial cell (EC) is the primary cell involved in angiogenesis[31]. Activation of the EC marks the beginning of the angiogenic response. ECs then acquire invasive, migratory and proliferative characteristics[32,33].

By blocking a stabilizing signal usually transmitted through the Angiopoietin-1 (Ang-1) – Tie-2 axis, Angiopoietin-2 (Ang-2) plays a prominent role in destabilizing the vessel by promoting the detachment of pericytes and smooth muscle cells (SMCs)[34]. The VEGF and Notch signalling pathways orchestrate the EC sprouting and migration by breaking up cell adhesion proteins, such as vascular endothelial cadherin, claudins and occludin and loosening inter-endothelial cell

contacts[35-37]. ECs then invade and break down the extracellular matrix, migrate towards an angiogenic stimulus/gradient, proliferate and reorganize into a new vascular sprout[38]. While tip cells, a group of selected endothelial cells, instigate the new sprout and migrate towards a VEGF gradient [39-42], the activation of Notch receptor in the remaining stalk cells compromises the ability of those cells to respond to VEGF [43] by increasing the ratio of VEGFR1 to VEGFR2. As a consequence, stalk cells proliferate to form the body of the extending capillary. During vessel sprouting, the extracellular matrix undergoes extensive remodelling mediated by proteinases, including matrix metalloproteinases (MMPs) and plasminogen activators[44-48]. This delicate process is controlled by their respective inhibitors, the tissue inhibitors of matrix metalloproteinases (TIMPs) and plasminogen activator inhibitor (PAI-1) ensuring a balance between degradation of the extracellular matrix, thereby providing space for the sprouting vessel, while preventing excessive ECM breakdown that would lead to the removal of critical support and guidance signals and possibly vessel collapse[44,49-52]. Once the sprout has reached its final length, the endothelial cells differentiate, form a lumen and a new basement membrane is synthesized[44].

1.4. Stabilization of the neovasculature

After the formation of a new vessel, the recruitment of mural cells helps to stabilize the immature vasculature[53]. Multiple molecular pathways regulate this process, referred to as arteriogenesis. One of the mechanisms characterized best is the recruitment of pericytes expressing the platelet-derived growth factor receptor-β [(PDGFR)-β] by endothelial cells secreting platelet-derived growth factor-B (PDGF-B)[54]. Ang-1, secreted by perivascular cells, also plays a prominent role in vessel maturation[55] by assisting the interaction of ECs with both mural cells and the extracellular matrix, as does TGF-β through promoting extracellular matrix deposition and differentiation of mesenchymal to mural cells [56-58]. Recent evidence suggests that platelet-derived growth factor receptor β-positive (PDGFRβ+) perivascular progenitor cells (PPCs) can be recruited to sites of active vascular remodelling from the bone marrow that also contribute to vessel maturation [59,60].

1.5. Neovascular regression

Creating stable vascular networks after growth factor delivery remains challenging and the strategies will likely differ from tissue to tissue. While prolonged exposure to a single growth factor (VEGF) has been shown to result in the creation of persisting neovessels in heart and liver[61], overexpression of VEGF in the trachea was described to consistently lead to a regression of the induced neovasculature, independent of the duration of growth factor exposure[62]. Therefore, tissue-specific differences in the recruitment of supporting mural vascular cells likely exist. In some tissues prolonged exposure to a single growth factor may allow the establishment of signalling gradients necessary to recruit supporting vascular mural cells while in others a diverse set of angiogenic growth signals may be required for the recruitment of support cells to achieve vascular stability. Apart from supporting mural cells, neovessel stability may benefit from the early establishment of blood flow, as exposure to mechanical shear stress during laminar blood flow has been identified as a critical regulator of EC apoptosis[63]. Transduction of these mechanical stresses has been described to culminate in the activation of pro-survival signalling pathways, such as PI3K/Akt[64-66], while a reduction in shear stress has been linked to elevated levels of MMPs (e.g. MMP-2, MMP-9, MT1-MMP) [67-69], which may critically modify EC interactions with the extracellular matrix. Increasing evidence suggests that while membrane-type MMPs control EC tube formation[46,70-73], an important function of secreted MMPs, such as MMP-1, MMP-9 and MMP-10, is regulating vascular regression[74,75]. The extracellular matrix is thus not only inherently involved in the regulation of the initiation of angiogenesis and lumen formation, but also in promoting vascular stability[44].

Recent evidence suggests that clinical trials to promote neovascularization and the recovery of ischemic tissues after injury may have been hampered by the inability to create a stable vascular network[76]. Developing more efficient approaches will likely depend on acquiring a deeper understanding of the mechanisms involved in both promoting a mature vascular phenotype and governing neovascular regression.

1.6. Growth factors and angiogenesis

As growth factors are a central focus of this study, their involvement in angiogenesis is reviewed in some detail in the following section.

1.6.1. VEGF A

Vascular endothelial growth factor A was first identified by Senger and colleagues[77] in 1983. Found in the supernatant of a guinea pig tumour cell line, it was originally named vascular permeability factor (VPF) due to its striking ability to enhance vascular permeability. A few years later, in 1989, Ferrara and colleagues successfully isolated this protein from the supernatant of bovine pituitary cells[13] giving it its current name, vascular endothelial growth factor. Subsequent sequencing would later disclose the two proteins to be identical.

To date, the human VEGF family encompasses 5 members: Placental growth factor (PlGF), VEGF-A, VEGF-B, VEGF-C and VEGF-D[78]. As part of the VEGF/PDGF super-gene family[79], these growth factors share a number of characteristic features: their homodimeric structure, conservation of 8 cysteines at distinct positions and three disulfide bonds (S-S) that form three loops within the peptide.

The name-giving attribute of VEGF-A is its potent stimulatory effect on vascular endothelial cells. By promoting vascular endothelial cell growth, survival, migration and the formation of tubules [80-82], VEGF-A has emerged as a major conductor of the angiogenic response, for example during cyclical angiogenesis in female reproductive organs[19]. VEGF-A increases vascular permeability, promotes monocyte chemotaxis[83] and is involved in the recruitment of vascular endothelial growth factor receptor 1^+ ($VEGFR1^+$) inflammatory cells [$VEGFR1^+$-haematopoietic stem cells (HSCs)]. The important interaction between VEGF and the chemokine stromal-cell derived factor-1, whose receptor CXCR4 is expressed on endothelial progenitor cells (EPCs), raises the possibility that co-mobilisation of EPCs and HSCs and recruitment to areas of active

neovascularisation is essential for angiogenesis [24,84] and the remodelling of the extracellular matrix [25,85,86].

VEGF-A isoforms mainly differ in their heparin-binding ability, which is an important determinant of their bioavailability. Whereas VEGF-A 121 is freely diffusible, the isoforms 189 and 206 are almost entirely bound to the extracellular matrix or cell surfaces[78]. VEGF-A 165 shows more balanced properties and is significantly available in both the free as well as the heparin-bound form.

VEGF exerts its effects by binding to a family of tyrosine kinase receptors, VEGFR1, -2 and -3[78]. The receptors consist of an extracellular ligand-binding domain, arranged in 7 immunoglobulin-like domains, apart from VEGFR3, in which 1 domain is replaced by a disulfide bridge, a transmembrane spanning region and the intracellular portion containing the tyrosine kinase domain. While VEGF-A binds to VEGFR1 and -2, PlGF and VEGF-B exclusively bind to VEGFR1, VEGF-C and VEGF-D mediate their actions via VEGFR2 and VEGFR3[78].

Knockout studies have revealed essential roles during development for both VEGF-A and its receptors. Inactivation of a single VEGF-A allele results in embryonic lethality between days 11 and 12[87]. VEGFR1, also known as Flt-1, is indispensable for the normal development of blood vessels during embryogenesis[88,89]. Mice lacking VEGFR2 die between day 8.5 and 9.5 in utero owing to an inadequate vasculogenic response and failure to form blood-islands[90].

VEGF-A transmits its main mitogenic, angiogenic (chemotactic and pro-survival signal) and permeability-enhancing effects via VEGFR2 (human form also known as KDR, mouse: Flk-1)[78]. VEGFR1 has been shown to compete with VEGFR2 for VEGF-A, and by acting as a trap for VEGF-A, a role for VEGFR1 as a regulator for the pro-angiogenic effects - induced by VEGF-A through VEGFR2 - has been suggested[91,92]. Soluble VEGFR1 has previously been shown to be

responsible for the avascularity of the cornea[93]. VEGFR3 (Flt-4) is primarily located on lymphatic endothelial cells and is essential for lymphatic endothelial cell development and function[94].

After VEGF binds to the extracellular binding domain, the receptor molecules dimerize thereby activating the intracellular tyrosine kinase[78]. The two main signal transduction pathways activated via VEGFRs are the Phospholipase Cγ (PLCγ) pathway[95] and the PI3K pathway[96]. The PI3K pathway is switched on downstream of VEGFR2 and-3[96]. Through the activation of Akt, also known as protein kinase B, this pathway mediates EC survival[97]. It is also involved in controlling the actin cytoskeleton and thus important for EC migration and vascular tube formation. Interestingly, binding of different ligands to the VEGFRs initiates selective phosphorylation site patterns and differential downstream signalling (VEGF-A[98] and PlGF[99] after binding to VEGFR1). The transmission of signals via the VEGFRs can be switched off either by dephosphorylation[100] (by phosphotyrosine phosphatases) or by internalization and/or degradation of the receptor[96]. Apart from the VEGFRs 1-3, a few co-receptors exist, namely neuropilins and heparan sulfate (HS) proteoglycans (HSPGs), which adjust downstream VEGF signalling. Neuropilin-1 more efficiently presents VEGF165 to VEGFR2 thereby promoting the transduction of its signal[101].

Via the transcription factor hypoxia inducible factor 1 (HIF-1α), oxygen tension is a major regulator of VEGF gene expression[102]. A binding site for HIF-1α has been discovered in the promoter region of the VEGF gene[103]. Several growth factors have also been shown to up-regulate VEGF expression, amongst them EGF (endothelial growth factor), TGF-α, TGF-β, keratinocyte growth factor (KGF), IGF-1 (insulin-like growth factor), FGF and PDGF[104-106]. Inflammatory cytokines like IL-1-α and IL-6[107,108] or oncogenic mutations[109-111](ras, wnt-signalling pathway) may also alter VEGF gene expression.

To date, VEGF-A represents one of the most investigated growth factors for therapeutic angiogenesis and besides FGF remains the only one previously tested in phase III clinical trials.

1.6.2. VEGF-C

Vascular endothelial growth factor C signals via VEGFR2 and -3[94,112] and is critically involved in the development of the lymphatic vasculature. At active sites of lymphatic vessel development, VEGF-C is expressed along with VEGFR3[113,114]. Gene targeting studies have substantiated the importance of VEGF-C for the development of the lymphatic vasculature, showing that mice lacking VEGF-C die between day 15.5 and 17.5 in utero due to severe tissue oedema resulting from their failure to develop lymphatic vessels[113]. In tumour models, cells overexpressing VEGF-C have been associated with increased lymphangiogenesis and a higher potential to invade the lymphatic system[115-117].

It has also been demonstrated that VEGF-C is capable of inducing a strong angiogenic response. Cao and colleagues reported that VEGF-C stimulates the proliferation and chemotaxis of porcine ECs[118]. A pro-survival effect on ECs and a potential to enhance migration have also been described[115]. In a mouse cornea angiogenesis assay, VEGF-C delivery generated capillary sprouts at a high density comparable to VEGF-A[118]. When the lymphatic vasculature was also examined, VEGF-C was shown to create a comparable number of both blood and lymphatic vessels[119]. Due to the decreased leakiness of the neovasculature compared to VEGF-A induced neovessels, the study authors even suggested VEGF-C as a potential alternative angiogenic growth factor to its family member[119]. In a variety of other animal models such as the chicken embryo chorioallantoic membrane[118,120,121] and a mouse ischemic hindlimb model[122], the pro-angiogenic properties of VEGF-C have been confirmed. Other reports have challenged these findings[120,121,123] and the extent to which VEGF-C may increase neovascularization remains controversial.

In a recent report, Benest and co-workers adapted a rat mesenteric angiogenesis model for lymphangiogenesis[124]. One of their most interesting findings was that the presence of lymphatic tissue is critical when considering the pro-angiogenic properties of VEGF-C, showing an inverse

correlation between blood and lymphatic vessel density. In the vicinity of a lymphatic vascular network, the pro-angiogenic effects of VEGF-C were significantly reduced[124].

1.6.3. PLGF

Placental growth factor, a highly expressed growth factor in the placenta, was discovered in 1991 by Maria Graziella Persico[125]. PlGF binds and activates VEGFR1 to induce downstream signalling[125,126]. PlGF knockout mice, though born without any obvious abnormalities in the vascular system, demonstrate an impaired angiogenic response after ischemia[127]. Furthermore, studies have shown that as a result of reduced angiogenesis PlGF$^{-/-}$ mice have a hindered ability to develop adipose tissue in a murine model of diet-induced obesity[128].

Reports indicate that PlGF-induced vessels possess a more stable phenotype than vessels created by VEGF-A delivery. A possible explanation offered has been the ability of PlGF to target not only ECs[127], but also smooth muscle cells, and macrophages, the three main cell types involved in the growth of collaterals[31,129]. Luttun and colleagues have shown that these cell types all express higher levels of the PlGF-binding receptor Flt-1 during collateral growth[130].

PlGF has been postulated to shape angiogenesis in diverse ways[131]. Apart from its direct effect on ECs via VEGFR1, PlGF has also been shown to compete VEGF-A off of VEGFR-1, allowing VEGF-A to bind and signal through VEGFR2 instead[132]. By binding to VEGFR1, PlGF is also believed to regulate the sensitivity of cells towards the VEGF/VEGFR2 axis. In inflammatory cells, monocytes or smooth muscle cells residing in wound or tumour stroma, PlGF may potentially influence angiogenesis by upregulating VEGF[133].

Some of the mechanisms involving PlGF in the regulation of pathological angiogenesis have recently been described. Tumour angiogenesis and vascular leakage are impaired in PlGF $^{-/-}$ mice. A critical way for PlGF to enhance tumour angiogenesis[127] is the mobilization of haematopoietic progenitor cells from the bone marrow[134]. Interestingly, synergistic effects

existing between PlGF and VEGF have also been demonstrated to exhibit a profound effect on pathological angiogenesis, as PlGF was shown to promote pathological angiogenesis by triggering crosstalk between VEGFR-1 and VEGFR-2[99,127,130].

Even though PlGF has not been as thoroughly investigated as VEGF, it has demonstrated its usefulness for therapeutic angiogenesis in a number of experimental settings[130]. In ischemic myocardium, PlGF has been reported to induce angiogenesis and arteriogenesis more efficiently than VEGF without triggering typical side effects seen with VEGF, such as the generation of haemangiomas[130]. PlGF-treated animals recovered better in an ischemic hindlimb model than animals in the VEGF-treated group, mainly by exerting a more powerful effect on collateral side branch growth[130]. With PlGF, Carmeliet's group was further able to create a stable vasculature that persisted for more than a year[130]. In yet another report, Kolakowski and colleagues confirmed PlGF's potential to promote angiogenesis in the heart[135]. Delivery of 1µg PlGF into the heart 2 weeks after myocardial infarction led to improved cardiac function measured via maximal LV pressure, maximal dP/dt, and ejection fraction, and PlGF was further shown to increase the thickness of the border zone wall and reduce dilation of the left ventricular cavity after MI[135].

1.6.4. Ang-2

Angiopoietins and their main receptor, the tyrosine kinase Tie-2, are closely involved in the creation of new vessels and in determining their long-term fate[136]. Apart from promoting EC survival, sprouting and migration, the angiopoietin-Tie-2 axis has been shown to be involved in the recruitment of pericytes[137,138] whilst also mediating anti-permeability and anti-inflammatory effects[139]. Tie receptors are mainly expressed by ECs. Angiopoietin-1 (Ang-1) and angiopoietin-2 (Ang-2) transmit distinct actions via the Tie2 receptor, which is reflected in their expression patterns. Ang-1 is expressed by perivascular cells and in a paracrine way preserves the quiescent state of the mature vasculature[55,140]. By activating Tie-2 and thereby initiating the activation of the downstream signalling pathway PI3K, Ang-1 promotes endothelial cell survival,

motility, tube formation and sprouting[140-143]. Ang-2, the antagonistic ligand for Tie-2, is synthesized by ECs themselves, stored in Weibel-Palade bodies, and released upon stimulation[144]. It has a fundamental role in the initiation of angiogenesis by destabilizing the endothelium[34,145] and loosening the contacts between endothelial and perivascular cells[34,146-148]. Hypoxia has been identified as an important stimulus for the up-regulation of Ang-2 mRNA[149]. Other stimuli controlling the expression levels of Ang-2 include growth factors like VEGF[150] and bFGF[150], angiotensin II[151], leptin[152] and TNF-α[153].

Further evidence underlying the importance of angiopoietins and the Tie receptors during angiogenesis stems from gene targeting studies. Tie-$2^{-/-}$ mice die between day 9.5 and 12.5 in utero due to deficiencies in the development of the vascular system leading to vessel rupture, haemorrhage and impaired heart function[57,154]. These mice further have a reduced number of endothelial and perivascular cells, implicating Tie-2 with both the survival of ECs and the generation of a more stable vasculature. The phenotype of Ang-$1^{-/-}$ mice resembles that of Tie-2-deficient mice[155], while Tie-1 knockout mice die after day 13.5 due to shortcomings in the vascular system, apparent by haemorrhages and oedema[57,156].

Contrary to vessels induced by VEGF alone, Ang-1, when co-delivered with VEGF, has been shown to generate leakage-resistant blood vessels, emphasizing the role of Ang-1 in the maturation of the vasculature[157]. Of note, in the presence of VEGF, Ang-2 supports the growth of blood vessels and sprouting angiogenesis, while effectively blocking the maturation signals mediated by Ang-1[145]. In the absence of VEGF, Ang-2 leads to endothelial cell death and regression of the neovasculature[145].

1.6.5. PDGF-BB

Platelet-derived growth factor was first purified in 1979[158,159]. Initially two PDGF genes were discovered, PDGF-A and PDGF-B, which were shown to homo- or heterodimerize into the active

forms PDGF-AA, PDGF-AB or PDGF-BB[160]. In 2000 and 2001, two more members of the PDGF-family, PDGF-CC[161], and PDGF-DD[162,163] were described. A key difference between the early members and PDGF-CC and PDGF-DD is that the latter ones are released in a latent form and proteolytic cleavage of an amino-terminal CUB domain is required to activate these growth factors[164].

Two PDGF receptor subunits exist, PDGFRα and PDGFRβ[165]. When PDGF binds to its receptor, each PDGF monomer unites with a receptor subunit to stabilize the PDGFR-complex[166]. PDGF-BB shows a high affinity for both PDGFRα and PDGFRβ and is thus considered the universal ligand for all three receptors: PDGFR$\alpha\alpha$, PDGFR$\beta\beta$ and PDGFR$\alpha\beta$[165].

PDGF-BB plays a crucial role in the recruitment of pericytes to the neovasculature, thereby promoting its stability and the switch to a more mature phenotype[167,168]. PDGFRβ^+-perivascular progenitor cells in tumours have been shown to control the differentiation of pericytes and influence vascular survival[59].

Both PDGF-BB and PDGFRβ null mutants demonstrate substantial microvascular bleeding and die at later stages of gestation[169-171]. A diminished recruitment of vascular smooth muscle cells and pericytes has been identified as the underlying defect[167].

PDGF has emerged as a prominent target for therapeutic angiogenesis. Not only has PDGF a role in the recruitment of vascular progenitor cells[59], but Li and colleagues have also demonstrated that by means of recruiting endothelial and pericyte precursors PDGF-CC is required for the revascularization for ischemic limb and heart tissues[172]. PDGF-BB delivery has furthermore been demonstrated to preserve myocardial contractility after myocardial infarction by both decreasing cardiomyocyte apoptosis and increasing vascular density and regional perfusion[173,174].

1.6.6. bFGF (FGF2)

The first angiogenic growth factor successfully isolated in 1984 by Judah Folkman and co-workers, basic fibroblast growth factor (bFGF) shows strong heparin-binding properties[175,176]. bFGF primarily is bound within the basement membrane in vivo[177]. While bFGF may be mobilized[178] from the ECM, it can also activate endothelial cells in its bound form[179-181]. bFGF is a strong angiogenic factor that stimulates DNA synthesis, migration and plasminogen activator production in endothelial cells[182,183]. To date, bFGF is the only growth factor other than VEGF that has been used in advanced human clinical trials to promote therapeutic angiogenesis[184,185].

Apart from endothelial cells, bFGF also stimulates smooth muscle cells and fibroblasts, making it less selective than VEGF[186]. It binds to a tyrosine kinase receptor family, fibroblast growth factor receptors 1-4 (FGFR1-4)[187]. Interestingly, FGFR expression may be increased on tumour endothelial cells[188]. After bFGF binding, its receptor dimerizes and autophosphorylates tyrosine residues located in its intracellular domain[187]. Importantly, for successful activation of the FGFR by bFGF, the growth factor also needs to bind to heparan-sulfate proteoglycans (HSPGs)[178] to stabilize the complex between the receptor and the ligand. PI3K[189] and the ERK1/2[190,191] pathways have been associated with transmitting the angiogenic signals of bFGF. A soluble form of the extracellular part of FGF1 (aFGF) exists that may bind bFGF and thereby prevent its binding to the target receptors[192]. Thrombospondin-1, an endogenous angiogenesis inhibitor, may similarly regulate bFGF function[192].

bFGF has been shown to play an important role in tumour and inflammatory-mediated angiogenesis[182]. It promotes tumour cell proliferation and survival[193], and has been linked to promoting tumour cell migration and differentiation towards a more invasive phenotype[194-196]. Inhibition of bFGF signalling has been demonstrated to shrink tumours and reduce their vascularization[197]. The requirement of the monocyte chemoattractant protein-1/CC chemokine receptor 2 axis for bFGF-induced neovascularization is exemplary of the contribution of inflammatory cells to angiogenesis[198]. It has been suggested that short-term exposure to bFGF

may act as a pro-inflammatory and pro-angiogenic signal, whereas long-term exposure may communicate anti-inflammatory effects[182].

There is extensive cross talk between bFGF and a number of growth factors. Hepatocyte growth factor has been shown to increase bFGF levels in external auditory canal choleastoma cell cultures[199]. The combination of PlGF and bFGF synergistically enhanced bovine retinal endothelial cell proliferation, survival and migration[200]. Insulin-like growth factor works in concert with bFGF to increase endothelial cell proliferation and survival[200]. When co-delivered with granulocyte colony-stimulating factor, bFGF had a more pronounced angiogenic effect in a mouse ischemic hindlimb model[201]. A synergistic effect on neovascularization has also been reported for PDGF-BB and bFGF, as well as for the combination of VEGF and bFGF. It has been suggested that bFGF may induce neovascularization indirectly by activating the VEGF/VEGFR system[202,203-206]. By simultaneously delivering PDGF-BB and bFGF, Cao and colleagues were able to generate long-lasting vessels in the mouse corneal micropocket assay, concluding that the recruitment of mural cells contributed to vessel stability. When subsequently testing the combination in the hind-limb ischemia model, they found an enhanced stimulation of collateral growth and increased perfusion[207].

1.6.7. BDNF

Brain-derived neurotrophic factor (BDNF) belongs to a family of structurally related neurotrophins that, during their development, support the growth, survival and differentiation of neurons, in both the central and peripheral nervous system[208-213]. Other members include nerve growth factor, neurotrophin-3, neurotrophin-4/5, neurotrophin-6 and neurotrophin-7[214-217]. Synthesized as precursors, neurotrophins require proteolytic cleavage for activation[218]. Neurotrophins bind to two types of receptors, p75NTR and TrkA, TrkB and TrkC, which bind BDNF and neurotrophin-3 selectively[219]. An important role for BDNF in controlling the fate of the cardiac microvasculature during development has been revealed through genetic studies [220].

The pro-angiogenic effects of BDNF have been well documented. In an ischemic hindlimb model, Kermani and colleagues found higher levels of BDNF in the ischemic tissue[221], pointing towards a critical contribution of BDNF post injury. They further demonstrated that overexpression of BDNF has VEGF-like effects on increasing capillary density and enhancing blood flow[221]. Interestingly, the authors not only observed that the activation of TrkB on endothelial cells contributes to the pro-angiogenic effects but also that exogenous BDNF acted as a chemotactic factor recruiting CD11+myeloid cells and Sca1+ hematopoietic cells[221], leading them to conclude that those cells potentially home to the injury site and may contribute to the maturation of the neovasculature. Kim et al. reported that brain-derived endothelial cells express BDNF and that BDNF is able to activate TrkB and p75NTR, which are also expressed on the endothelial cells[219]. When exposed to exogenous BDNF, transformed rat brain endothelial cells showed increased survival, which was mediated through the TrkB receptor and downstream phosphatidylinositol (PI) 3-kinase-Akt signalling. BDNF-treatment also elicited an angiogenic response, confirmed by tube formation and cellular sprouting[219].

In multiple myeloma (MM), a disease that is associated with increased angiogenesis of the bone marrow, remission has been linked to reduced BDNF levels[222,223]. Hu and colleagues have shown that BDNF-signalling through the TrkB receptor is indeed one of the mechanisms responsible for the observed increase in angiogenesis[224]. When co-culturing multiple myeloma cells and human umbilical vein endothelial cells (HUVECs), the authors demonstrated migration and network formation of the endothelial cells and these effects were blocked by an anti-BDNF antibody. Anti-BDNF antibody delivery further stopped tumour growth, induced tumour necrosis and reduced tumour vessel density, underlining the importance of BDNF in this particular tumour[224].

In combination with bFGF, BDNF has shown potential for use in therapeutic angiogenesis[225]. Prolonged release from gelatin hydrogels resulted in enhanced left ventricular function and angiogenesis, measured by means of left ventricular ejection fraction, regional myocardial blood

flow and vessel density, respectively[225]. Interestingly, in an ischemia-reperfusion model, border zone myocytes have been known to express BDNF[226]. Pro-angiogenic effects of BDNF have also been recorded in a rat spinal cord injury model[227].

1.6.8. SDF-1

Over the last few years the chemokine stromal-cell derived factor-1 (SDF-1), also known as CXCL12, has emerged as an essential factor regulating neovascularization[228]. Its receptor, CXCR4 is expressed on a variety of cells participating in angiogenesis, such as hematopoietic cells, endothelial progenitor cells or smooth muscle cell progenitors[228]. An important axis early in development, both SDF-1 and CXCR4 null mice lack the interconnecting vessels that form between the primary capillary plexus and the superior mesenteric artery in the small intestine[229]. SDF-1 has been shown to promote endothelial cell proliferation, differentiation, tube formation and to improve survival of endothelial progenitor cells[230,231].

While SDF-1 alone induces angiogenesis in the matrigel plug assay, a more dramatic angiogenic response has been described after co-delivery with VEGF-A[232,233]. Recent reports have further established an important partnership between SDF-1 and VEGF-A in the regulation of the angiogenic response after ischemic injury. Both SDF-1 and VEGF-A are capable of mobilizing cell populations residing in the bone marrow, CXCR4+ and VEGFR2+ cells, respectively. Furthermore, the retention and incorporation of cells recruited by VEGF-A upregulation into sites of active neovascularization has been shown to be dependent on SDF-1[84].

SDF-1 is upregulated in ischemic tissues[234-240]. It has been hypothesized to be an important factor responding to hypoxia by initiating the angiogenic response and thereby limiting tissue damage[241-243]. In prostate cancer cells, the levels of a variety of angiogenic factors have been shown to be SDF-1 dependent, including VEGF, IL-6, IL-8 and TIMP-2[244]. In these cells, SDF-1 was further shown to limit the synthesis of angiostatin, a prominent angiogenesis inhibitor[244]. Also, by promoting MMP production, SDF-1 facilitates remodelling of active angiogenic sites and

neovessel formation[25,84,245]. SDF-1 dependent recruitment of CXCR4+PDGFR+ckit+ smooth muscle progenitor cells has furthermore been shown to ensure the stability of the newly formed vasculature[246].

After myocardial ischemia, SDF-1 has been demonstrated to reduce cardiomyocyte death[247], decrease infarct size[248], promote neovessel formation[247,249], CXCR4+ckit+ stem cell recruitment and, most importantly, improve cardiac function[247,249].

1.6.9. HGF

Hepatocyte growth factor (HGF), a heparin-binding growth factor[250], combines a unique set of features, making it a promising candidate for biological revascularization and myocardial infarct therapies[251]. HGF has been shown to promote both angiogenesis[252-255] and myocardial hypertrophy, whilst inhibiting apoptosis and fibrosis[256-258].

HGF levels are considerably elevated after acute myocardial infarction[259]. Yasuda and co-workers reported that in humans high HGF levels in the infarct area correlate with reduced ventricular dilation and enhanced cardiac function, thus suggesting a cardioprotective role of HGF[260]. In various animal models of ischemia-reperfusion, HGF has been shown to beneficially affect infarct size and cardiac function, confirming this hypothesis. Miyagawa and colleagues reported that HGF gene therapy ameliorates adverse ventricular remodelling and improves cardiac function in a mouse MI model[261]. Intramyocardial injection of an adenovirus encoding HGF preserved myocardial function and geometry, promoted angiogenesis and led to significant reductions in apoptosis[262]. In another report, HGF gene therapy significantly reduced the ischemic area and increased capillary density and regional myocardial perfusion in a pig myocardial infarct model[263]. The authors further observed a significant decrease in the fibrotic area in the HGF group and improved cardiac function and increased wall thickness when a high dose of HGF (4mg) was administered[263].

Diabetes remains one of the most common underlying causes necessitating revascularization therapies. It is therefore important to note that intramuscular injection of a HGF plasmid into the ischemic hindlimb of diabetic rats significantly increased blood flow and capillary density in a dose-dependent manner[264].

In combination these promising studies have led to the initiation of clinical studies to explore the angiogenic effects and safety of HGF treatment in the setting of peripheral arterial disease[265,266].

1.7. Angiogenesis assays

The major breakthrough that permitted the development of angiogenesis assays was the establishment of cell culture techniques for vascular endothelial cells. While in vitro assays are more easily accessible, more cost effective and easier to quantify, a number of important shortcomings exist in comparison with in vivo assays. Most importantly, endothelial cells in culture remain in an activated state, whereas endothelial cells in vivo are activated only under special circumstances, e.g. during the estrus cycle, or during pathological conditions such as inflammation, tumour growth or wound healing[267-269]. Continued cell passaging may induce the activation of cellular receptors or the loss of cell surface antigens, negatively affecting the reproducibility of experiments. Furthermore, in vitro angiogenesis studies are typically performed on pure endothelial cell cultures, and thus interactions with supporting perivascular cells or the effects of systemic factors cannot be studied. In vitro assessment of endothelial cell proliferation is typically performed either by cell counting (manually or, if available, via flow cytometer) or – to obtain a more accurate measure – by quantifying DNA synthesis (via flow cytometric analysis of the cell cycle or incorporation of radioisotopes). Evaluation of endothelial cell migration comprises the measurement of chemokinesis and chemotaxis, the random and directed migration of cells, respectively. Chemokinesis may be quantified using time-lapse microscopy while chemotaxis towards a concentration gradient is typically determined with transwell or Boyden chamber culture systems. The tube formation assay represents a more advanced in vitro angiogenesis assay that determines the potential of endothelial cells to form tubes, which can

often be enhanced in a three-dimensional model system, such as matrigel, fibrin or collagen. Organ culture assays such as the aortic ring assay, in which the outgrowth of endothelial cells is quantified, reflect the in vivo situation more closely, as endothelial cells interact with surrounding smooth muscle cells, pericytes and the supporting matrix.

The complex regulatory mechanisms that regulate angiogenesis are best studied in vivo. Used for more than 60 years, the chorioallantoic membrane (CAM) assay was the first assay developed for the in vivo assessment of neovascularization[270,271]. A major advantage of this assay is its ready availability. Delivering tissues and reagents to be tested for their angiogenic potential is technically relatively easy and the angiogenic response can be assessed using standard histological techniques. An important downside to consider is that while the assay may be performed on chick embryos aged 5 to 14 days, the responsiveness to angiogenic stimuli varies considerably during this timespan. Due to the extensive capillary bed of the chorioallantoic membrane, it can be challenging to distinguish the pro-angiogenic effects of a given tested substance[272]. Furthermore, quantification of the neovasculature may be complicated by a commonly observed inflammatory response seen around day 8 after delivery of a variety of biologics[273]. Technically more challenging but similar to the CAM assay is the mesenteric window assay[274,275]. Importantly, in this assay, angiogenesis is tested on mammalian tissue, the small gut mesenteric window of rodents. In addition, this assay can be performed on adult laboratory animals and it allows one to distinguish between and quantify capillaries, arterioles and venules.

The corneal angiogenesis assay is currently considered as the gold standard of in vivo angiogenesis assays. As the cornea is essentially avascular, the ingrowth of the peripheral limbal vasculature after implantation of pro-angiogenic tissues of biologics into a corneal pocket can be easily assessed. While surgically challenging and time consuming, the corneal angiogenesis assay allows monitoring of the effects of pro- and anti-angiogenic stimuli over extended periods of time, if delivered via osmotic pumps or slow-release polymers. However, due its avascularity, the immune-privileged cornea represents a somewhat atypical site to assess physiological angiogenesis and therefore findings from this assay need to be carefully interpreted and may not always be adaptable to other tissues.

The matrigel plug assay presents an alternative to the in vivo assays mentioned above. Liquid matrigel is mixed with the test substance and, upon subcutaneous injection into the animal, solidifies at body temperature to form a plug that can easily be explanted and processed for histological analysis. A number of important limitations of this assay exist. The dynamics of neovascularization cannot be non-destructively tracked during the course of the experiment. Moreover, striking regional differences in neoangiogenesis were uncovered after implantation of matrigel plugs into various subcutaneous sites[276-280]. In recent years, the use of chamber assays has become more popular. The rabbit ear, mouse or rat dorsal skinfold or the cranium have been used as implantation sites. In these in vivo assays, intravital microscopy is used to track neovascularisation in real time after removal of a piece of the skin or part of the skull[281]. While a great advantage of the chamber assay is the continuous monitoring of neoangiogenesis, these experiments are technically challenging and imaging may be complicated by suboptimal optical properties as a result of the thickness of the tissue examined. In total, the described assays have contributed significantly to a general increase in mechanistic insight into the process of neovascularization. However, these assays have been established to study the formation of neovessels and assess the angiogenic potential of growth factors; yet prevention of vascular regression is also a critical component of therapeutic neovascularization. In their current format, the ability of these assays to monitor neovascular regression is limited, thus modifications may be required to parse the effects of factors on vascular stability and regression.

1.8. Summary

Therapeutic angiogenesis has emerged as a novel concept to enhance blood flow in ischemic tissues. In recent years, numerous growth factors have been demonstrated to contribute to angiogenesis. A major obstacle that has yet to be overcome is the instability of growth factor-induced neovasculature. Thus far little is known about the factors that determine the long-term fate of growth factor-induced neovasculature. Due to tissue-specific differences, previous studies have shown conflicting results. Whereas delivery of single growth factors has resulted in the development of a stable neovasculature in some tissues, treatment with the same growth factor

regimen can result in rapid neovessel regression in others. Timing and dosage likely are important variables that regulate vascular stability, as are interactions between co-delivered growth factors. While these factors appear crucial in explaining the failed translation of therapeutic angiogenesis from bench to bedside, our understanding of which mechanisms contribute to making neovessels unstable is incomplete, partly due to the lack of appropriate in vivo animal models. A deeper insight into this process is required to exploit the potential of therapeutic angiogenesis.

2. HYPOTHESES

Part of the work described in this thesis is the development of a novel in vivo angiogenesis model that addresses some of the deficiencies in existing models. Using this model and a rat model of myocardial infarction, this thesis tests the following hypotheses:

1. Stability of growth-factor induced neovasculature is highly dosage-dependent
2. Stability of growth-factor induced neovasculature is enhanced by controlled co-delivery of specific factors
3. Targeted delivery of an angiogenic growth factor (VEGF-A) via an injectable biomaterial implant induces a neovasculature that exhibits long-term stability and improves cardiac remodelling and functional recovery after myocardial infarction.

3. RESULTS: Angiogenesis chapter

3.1. Establishment of a subcutaneous in vivo angiogenesis model

In order to track the angiogenic potential of growth factors and to test the long-term stability of newly formed vessels induced by recombinant growth factor delivery, an in vivo angiogenesis model was designed (see chapter 10.1.1, 10.1.3.). The in vivo angiogenesis assay described

here allows for the precise delivery of growth factors to a scaffold and the quantification of vessel growth into the scaffold during and after growth factor delivery. Neovascularization constructs were produced in our laboratory with the generous help of Dr. Deon Bezuidenhout and Mr. Johann Eygelaar. Using spherical microbeads, a revised phase inversion technique was employed to generate polyurethane with well-defined porosity[282]. On the luminal surface, polyurethane tubes used in the experiments were lined with expanded tetrafluoroethylene (ePTFE). This modification allowed for ready tissue-ingrowth into the porous polyurethane but prevented complete closure of the lumen enabling growth factor-delivery to the polyurethane graft via an attached osmotic pump. Osmotic pumps allowed for the establishment of a stable growth factor gradient within the polyurethane graft for extended periods. Depending on the length of the experiment, a variety of osmotic mini-pumps were used for growth factor delivery. A schematic of the vascularization device is depicted in Fig.1, a photograph in Fig.2.

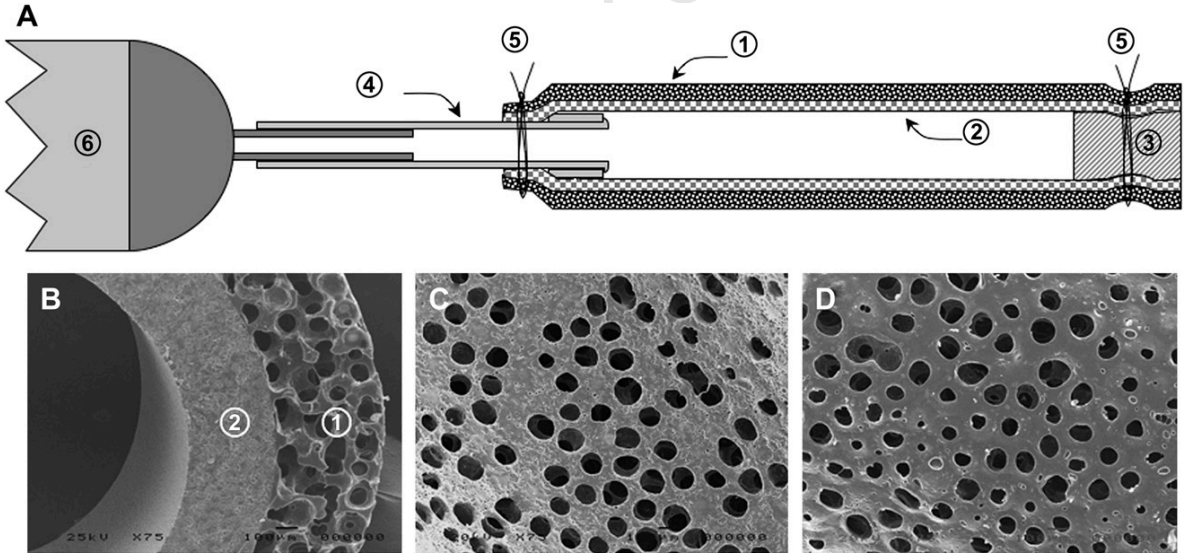

Fig.1. (A) Schematic representation of the vascularisation devices, showing porous polyurethane (1), ePTFE cell barrier (2), plug (3), polyethylene tube assembly (4), silk ligatures (5), and osmotic pump (6). The scanning electron micrographs show the cross-section (B), as well as the lumenal (C) and

The main purpose of these studies was to identify growth factors that significantly contribute to angiogenesis in this model, to characterize the stability of the neovasculature and to identify mechanisms/parameters that contribute to vascular stability.

Fig.2. Photograph of the vascularization device

3.2. Basal levels of vascular ingrowth into the vascularization device

In an initial pilot experiment the basal level of vascular ingrowth into the vascularization device after subcutaneous implantation was determined. Vascularization devices were either implanted alone or attached to phosphate buffered saline-delivering osmotic mini-pumps. Vascularization devices were explanted after 10 days and the angiogenic response was visualized by staining with an antibody targeting CD31.

3.2.1. Results

As expected, the ePTFE barrier prevented ingrowth of organized tissue into the luminal space of the porous polyurethane tube. A small number of individual cells were found within the ePTFE barrier (data not shown).

Subcutaneous implantation of neovascularization devices resulted in 2.11±0.14% of the total graft area being vascularised after 10 days (see Fig. 3, n=4). Delivering phosphate buffered saline via an attached osmotic mini-pump had no significant effect on neovessel formation (2.4±0.27%, n=6, $p>0.05$, representative image shown in Fig.4).

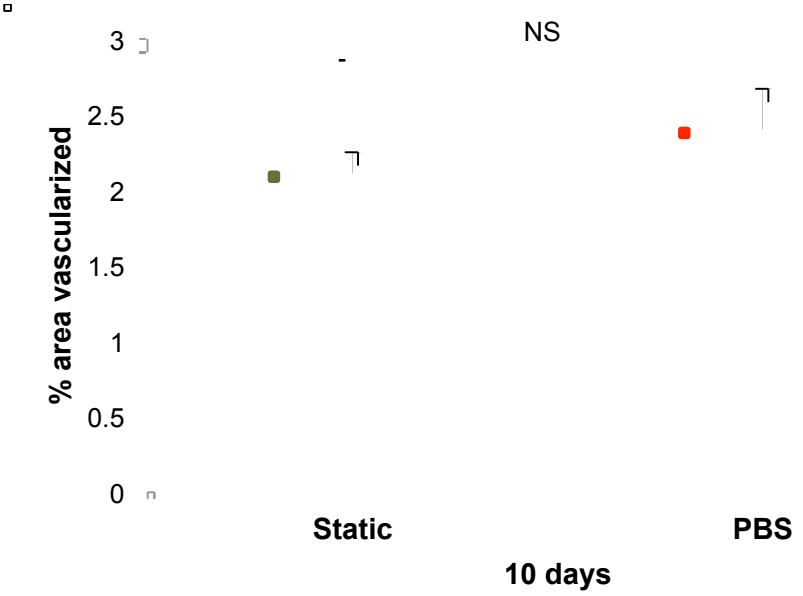

Fig.3. Graph shows baseline vascularization of a polyurethane graft after subcutaneous implantation for 10 days. Delivery of PBS via an attached osmotic mini-pump does not affect neovascularization.

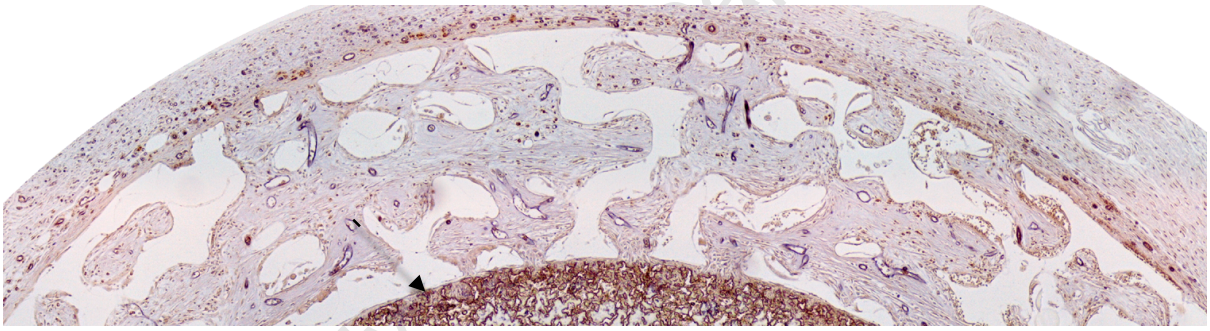

Fig.4. Immunohistochemical staining of CD31 positive vessels in devices explanted after delivery of PBS for 10 days. The ePTFE barrier (black arrow) successfully prevented tissue ingrowth into the lumen of porous polyurethane tubes.

3.2.2. Discussion

Delivery of phosphate-buffered saline did not have an effect on neovascularisation in this assay and is well suited as a negative control for comparison with angiogenic growth factors. For ensuing experiments, growth factors were diluted in phosphate-buffered saline. Importantly, image analysis of neovascularization revealed that vascularisation density within polyurethane

grafts was highly reproducible after PBS delivery, allowing comparison of the angiogenic potential of growth factors tested in different sets of experiments.

3.3. Dynamics of VEGF-induced neovascularization

The vascular endothelial growth factor family plays a particularly prominent role in angiogenesis. Though angiogenesis is most probably controlled by a complex interaction of growth factors at both temporal and spatial levels[31,283], signalling by vascular endothelial growth factor-A[165] (VEGF-A[165]; for the remainder of the thesis referred to as VEGF) is an essential and rate-limiting step in physiological angiogenesis[78].

Therefore, to test whether VEGF promotes neovascularization into polyurethane grafts, VEGF was delivered at 1500ng/day for 5 days. Vascular grafts were explanted after 5 days (n=5) and neovascularisation was subsequently visualized by staining with a CD31-antibody.

3.3.1. Results, day 5

VEGF delivery resulted in significantly higher neovessel formation in comparison with PBS at 5 days. At day 5, 4.83±0.85% of the total graft area was vascularised in the VEGF group as compared to 1.84±0.12% in the PBS control group ($p<0.01$, 1.62 fold increase, n=5).

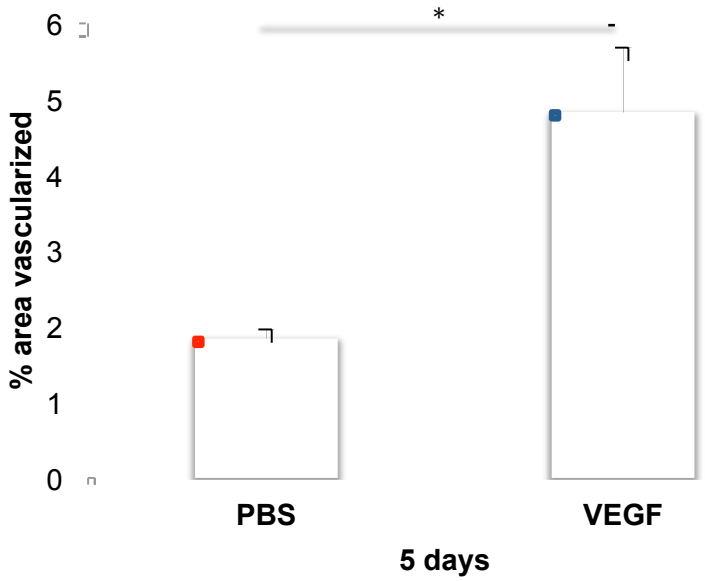

*Fig.5. As early as 5 days after the initiation of VEGF delivery, a significant 1.62 fold increase in angiogenesis is observed (*p<0.01, n=5).*

To investigate whether prolonging the delivery of VEGF could further increase neovascularisation, 1500ng/day of VEGF were delivered for a total of 10 days before harvest of the vascular grafts on day 10 (PBS: n=6, VEGF: n=4). Neovascularisation was again visualized by staining with a CD31-antibody.

3.3.2. Results, day 10

At day 10, 8.76±1.37% of the total graft area was vascularised after VEGF-delivery in comparison with 2.4±0.13% in controls ($p<0.001$, 2.65 fold increase, n=4(VEGF), n=6 (PBS), see Fig.6). Delivery of VEGF for an additional 5 days increased neovascularisation by 81%, nearly doubling the number of neovessels present in the vascularization device. Representative images for polyurethane grafts after PBS and VEGF delivery explanted at day 10 are shown in Fig.7.

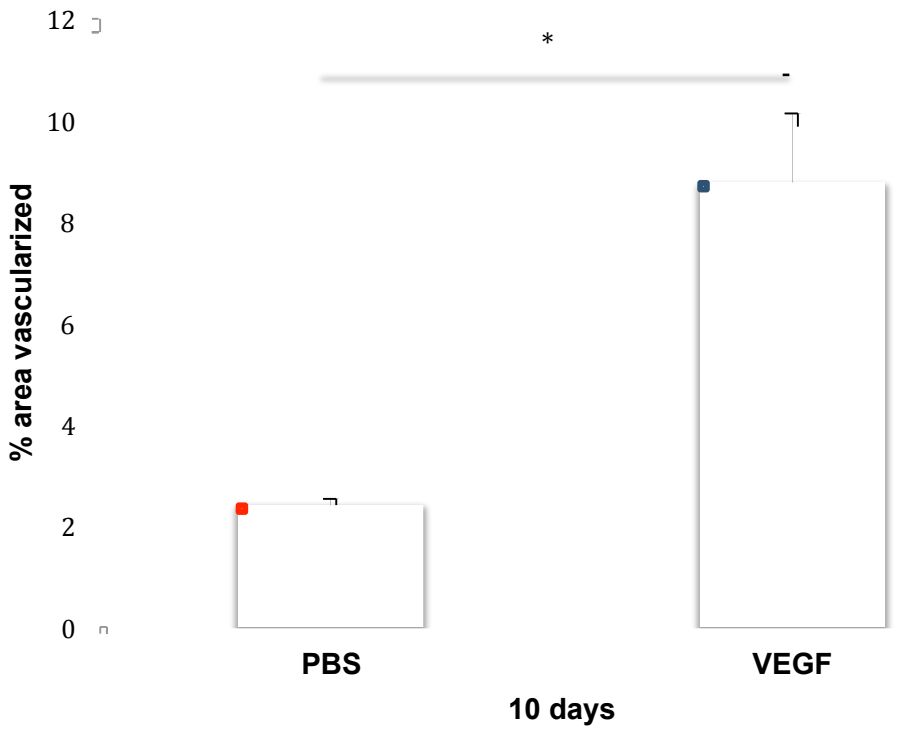

*Fig.6. Prolonged VEGF delivery for 10 days instead of 5 enhances neovessel formation even further (2.65 fold over PBS controls at day 10 (*p<0.001, n=4) in comparison with 1.62 fold at day 5 (p<0.01, n=5).*

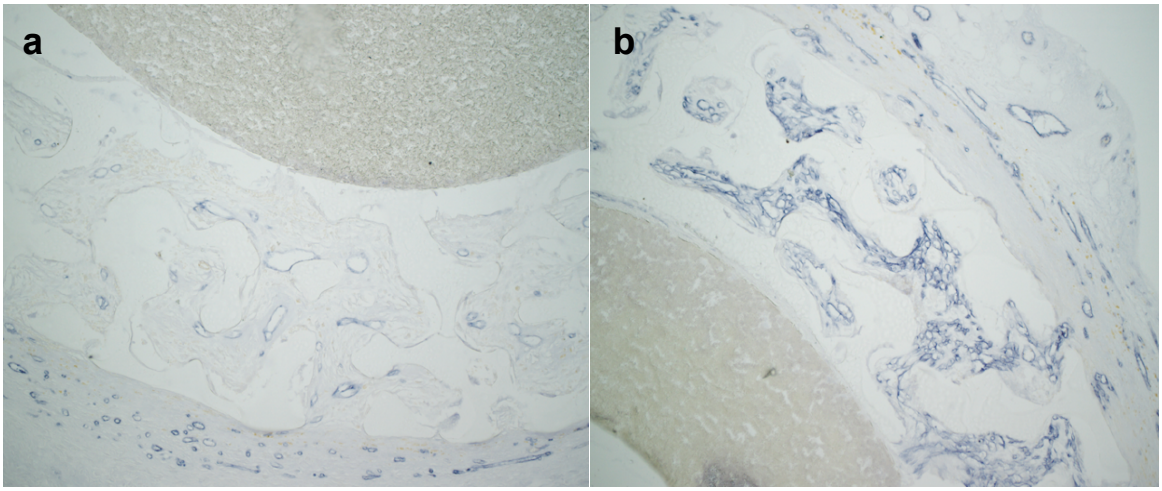

Fig.7. Immunohistochemical staining of CD31 positive vessels in devices explanted after delivery of PBS(a) or 1500ng/day VEGF(b) for 10 days. A dramatic increase in neovascularization is observed after VEGF delivery.

3.3.3. Conclusion

Taken together, these experiments show that the delivery of VEGF significantly increases angiogenesis in the neovascularisation device. Neovessel formation was significantly increased after continuously delivering VEGF for 5 days. Yet, prolonged delivery of VEGF for an additional 5 days had an even more pronounced effect on neovascularisation, almost doubling the number of $CD31^{+}$-vessels in the polyurethane graft. In combination, these experiments show that continuous delivery of VEGF steadily increases neovascularization until day 10.

3.4. Promotion of angiogenesis by the vascular endothelial growth factor family

3.4.1. Rationale

The vascular endothelial growth factor family currently comprises 5 family members. While VEGF, VEGF-C and PlGF have all been shown to enhance angiogenesis, these growth factors establish a neovasculature with distinct features. In comparison with VEGF, Placental growth

factor (PlGF) has been shown to induce a neovasculature that is more stable in nature and better resembling the physiological phenotype. This is most likely based on the ability of PlGF to not only stimulate endothelial cells[127] but also vascular smooth muscle cells and macrophages[31,128]. To determine whether placental growth factor is a more potent angiogenesis stimulus than VEGF in this assay, neovascularization devices were implanted subcutaneously and 1500ng/day PlGF, were delivered via attached osmotic pumps for 10 days (n=6). Furthermore, to determine, whether the promotion of neovascular formation after VEGF delivery is dosage-dependent, 150ng VEGF/day were delivered for 10 days (n=6). After explantation, neovessel formation was assessed via CD31-staining.

3.4.2. Results

Both VEGF and PlGF significantly increased neovascularization after 10 days in comparison with

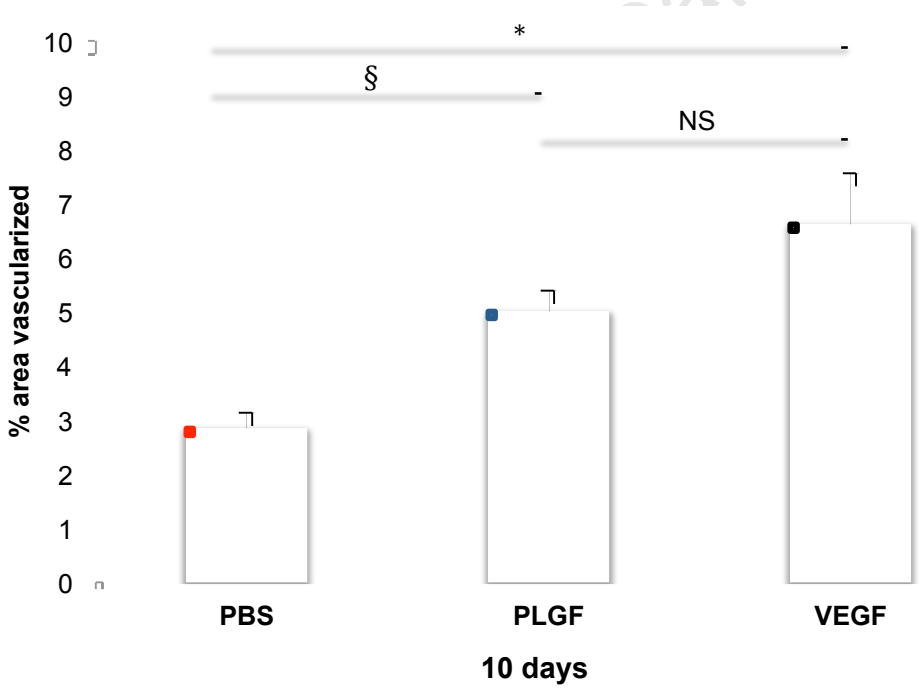

*Fig.8. Daily delivery of either 150ng VEGF (*p<0.01) or 1500ng PlGF (§p=0.001) significantly enhances neovascularization after 10 days by 132% and 76.1%, respectively (n=6). No significant difference in angiogenic potential was observed between delivering 150ng VEGF/day and a 10-fold higher PlGF dosage.*

PBS controls. In PBS grafts, 2.84±0.29% of the total graft area was vascularised. 10-day delivery of 150ng/day VEGF increased neovascularization by 132% (to 6.61% of the total graft area, $p<0.01$), while the delivery of 1500ng/day PlGF increased angiogenesis by 76.1% (to 5%, $p=0.001$), as shown in Fig.8.

3.4.3. Conclusion

These data indicate that VEGF acts as a more potent stimulus for vessel formation in the subcutaneous rat model than PlGF, as lower VEGF concentrations induced angiogenesis as effectively as the highest PlGF dosages examined ($p=0.148$). Furthermore, this experiment provided initial evidence that VEGF-induced angiogenesis into the neovascularization device is dosage-dependent based.

3.5. Vascular endothelial growth factor-C and short-term neovascularization

While vascular endothelial growth factor C has traditionally been considered a lymphangiogenic factor, additional evidence suggests that it acts as an angiogenic stimulus[119,124]. The ability of VEGF-C to induce neovascularization was therefore tested in the subcutaneous rat model. VEGF-C was delivered for 10 days via osmotic pumps at 150ng/day or 600ng/day, respectively, and subsequently neovascularization was assessed by immunohistochemical analysis of CD31.

3.5.1. Results

After osmotic delivery of 150ng VEGF-C per day 2.59±0.2% (n=6) of the polyurethane graft area was vascularized, while delivery of 600ng VEGF-C per day resulted in a vascularization area of 2.74±0.21% (n=6). Neither 10-day delivery of 150ng/day nor 600ng/day VEGF-C had a significant effect on neovascularization in comparison with PBS controls (2.4±0.13%, n=6), [$p=0.2$ (PBS, VEGF-C (600ng/day)); $p=0.45$ (PBS, VEGF-C (150ng/day))].

A possible effect of VEGF-C delivery on lymphatic vessels could not be excluded, as repeated attempts to establish an immunohistochemistry protocol were unsuccessful.

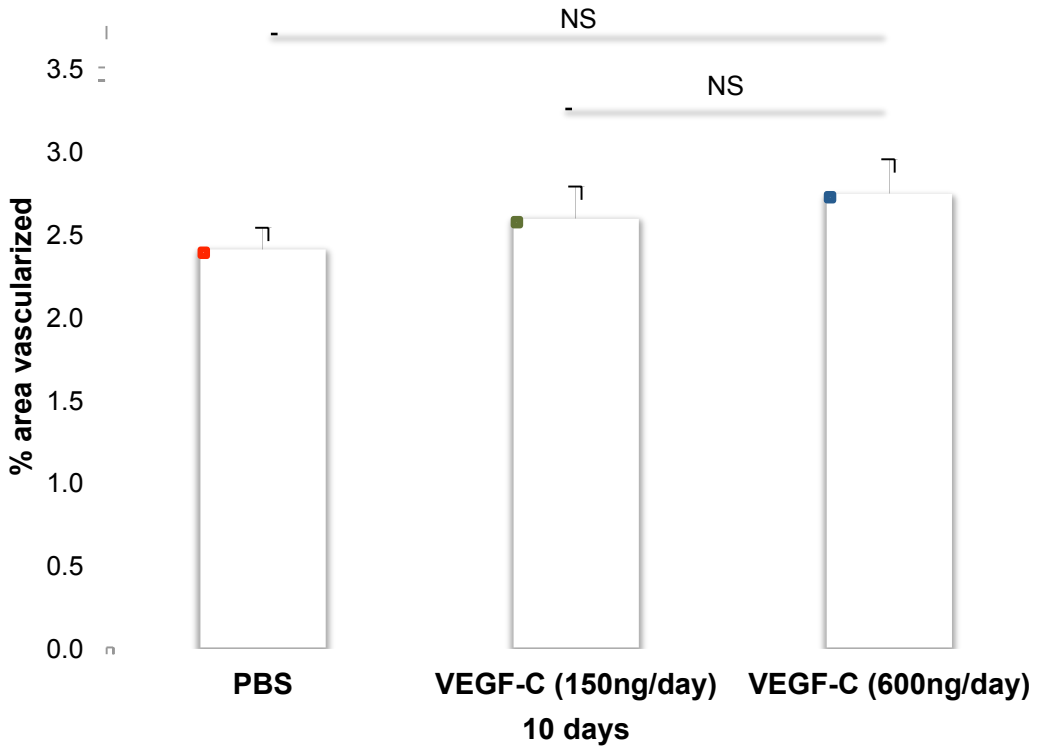

Fig.9. No significant pro-angiogenic effects are observed after the delivery of 150ng/day VEGF-C, 600ng/day VEGF-C or PBS for 10 days.

3.6. Angiogenic potential of brain-derived neurotrophic factor (BDNF) and hepatocyte growth factor HGF

Apart from the VEGF family, numerous growth factors such as hepatocyte growth factor[253,254,262-264] (HGF) and brain-derived neurotrophic factor[219,221,225] (BDNF) have been shown to be potent inducers of angiogenesis.

To determine, whether BDNF or HGF induce angiogenesis at levels similar to VEGF or even exceed VEGF-induced neovascularization in the subcutaneous wound healing model, 1µg/day of HGF or BDNF, respectively, were delivered via osmotic pump for 10 days. Neovessel formation was assessed by immunohistochemical staining for CD31.

3.6.1. Results

BDNF delivery significantly increased neovascularization by 29.6% compared to PBS controls (from 2.4±0.13 to 3.11±0.65%, $p<0.05$, $n=6$ (BDNF, PBS)). Nevertheless, compared to VEGF-induced neovessel formation after 10 days, the observed increase was minimal. Due to the high variability seen in explanted grafts after delivery of 1µg/day HGF, no significant effects on altering the intrinsic angiogenic response after 10 days (2.94±1.12%, $p>0.05$, $n=6$) were seen.

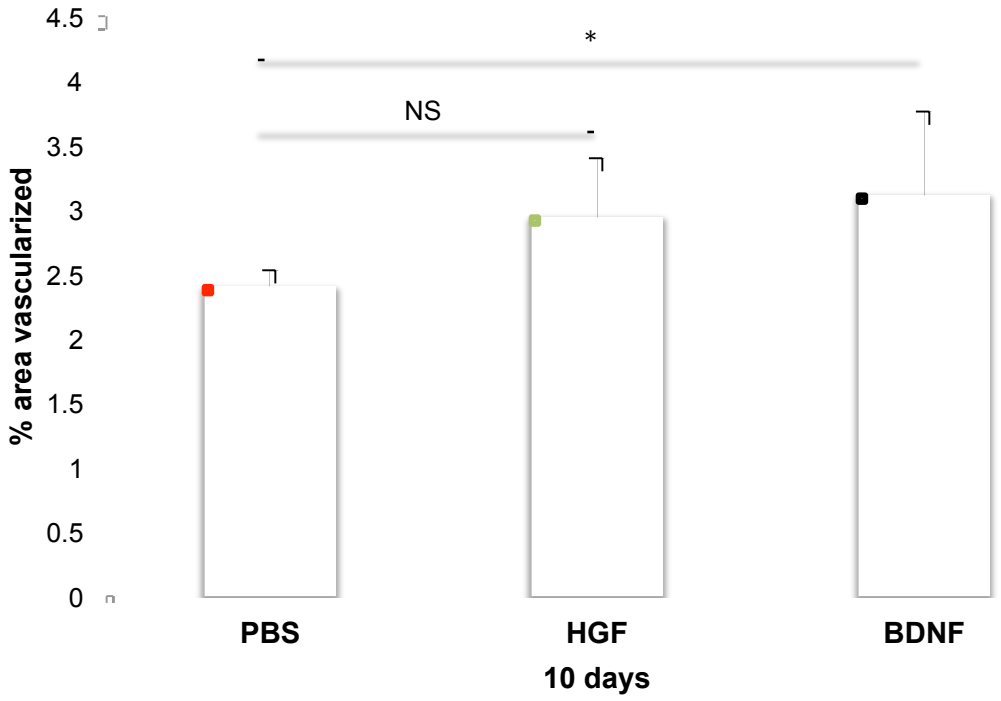

*Fig.10. In comparison with VEGF, BDNF treatment only led to a modest increase in neovascularization after 10 days (29.6% increase over PBS controls, *p<0.05, n=6). No significant increase in angiogenesis was observed after delivering 1µg/day HGF for 10 days.*

3.6.2. Conclusion

Quantification of neovascularization revealed that while HGF and PlGF significantly enhanced angiogenesis in comparison with PBS controls, VEGF was the most potent pro-angiogenic factor (of those tested) when delivered alone. Angiogenesis is controlled by numerous growth factors, and growth factor-interaction is important during neovessel formation. Therefore, to determine

whether short-term neovascularisation could be further increased, the effects of delivering multiple pro-angiogenic growth factors either simultaneously or subsequently were tested next.

3.7. Synergistic angiogenic effects of growth factors

Simultaneous delivery of multiple growth factors may be required to increase neovascularization to achieve therapeutic levels. In concert, bFGF and PDGF have previously been shown to have synergistic effects on promoting angiogenesis[207]. Furthermore, cross talk between vascular endothelial growth factor and angiopoietins is essential for the regulation of neovascular formation and vascular stability[145,157]. Angiopoietin-2 plays a particularly important role in the initiation of angiogenesis; during this phase it is required to destabilize vessels by promoting pericyte and vascular smooth muscle cell detachment, before vascular endothelial growth factor stimulates endothelial cell invasion, proliferation and migration[34].

Therefore to test whether a) the combination of bFGF and PDGF has synergistic effects on promoting angiogenesis and b) whether, in the presence of Ang-2, VEGF-A induces neovascularization more effectively, 1) bFGF and PDGF and 2) Ang-2 and VEGF-A, respectively, were delivered simultaneously. Neovascularization devices were explanted after 10 days and neovessel formation was assessed by immunohistochemical analysis of CD31.

3.7.1. Results – bFGF/PDGF

Quantification of CD31-positive vessels revealed that the simultaneous delivery of 1200ng/day bFGF and PDGF for 10 days had no stimulatory effect on angiogenesis in our rat model. In comparison with controls, the vascularized area remained unchanged at 2.69±0.4% as compared to 2.4±0.14 in PBS controls ($p>0.05$, $n=5$ for both groups).

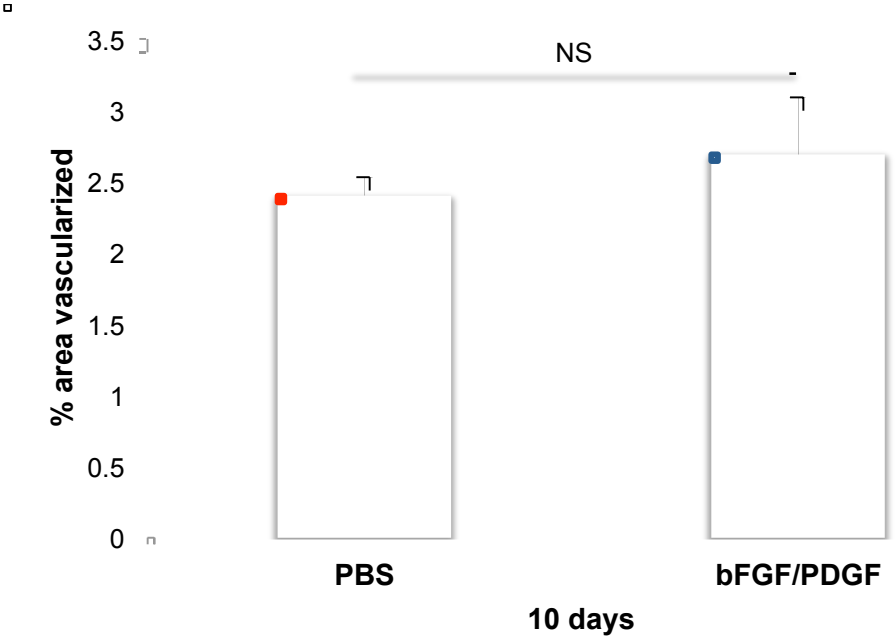

Fig.11. Simultaneous delivery of bFGF and PDGF at 1200 ng/day for 10 days did not induce angiogenesis in the subcutaneous graft model (p>0.05, n=5).

Ang-2/VEGF

2 distinct VEGF dosages (50ng/day and 150ng/day) were tested for their ability to enhance angiogenesis in concert with Ang-2 (15ng/day) after continuous delivery for 10 days. Two hypotheses were tested in this experiment: namely, whether a) the combination of VEGF at a low dosage (50ng/day) with Ang-2 (15ng/day) enhances neovessel formation; and b) whether the simultaneous delivery of VEGF (150ng/day) and Ang-2 (15ng/day) synergistically leads to a more pronounced increase in neovascularization.

3.7.2. Results - Ang-2/VEGF

Sole delivery of 50ng/day VEGF or 15ng/day Ang-2, respectively, did not significantly increase neovascularization compared to PBS controls (n=6 for all groups). To the contrary, 150ng VEGF/day, simultaneous delivery of 50ng VEGF and 15ng Ang-2/day and simultaneous delivery of 150ng VEGF in combination with 15ng Ang-2/day all led to significant increases in angiogenesis in the vascularization device at day 10, by 57, 48 and 80%, respectively. Yet,

despite observing a trend towards an increase in angiogenesis when vascular endothelial growth factor at either dose (particularly for the lower dose of VEGF) was co-delivered with angiopoietin-2, these differences were not significant when compared with VEGF delivery alone (see Fig.12).

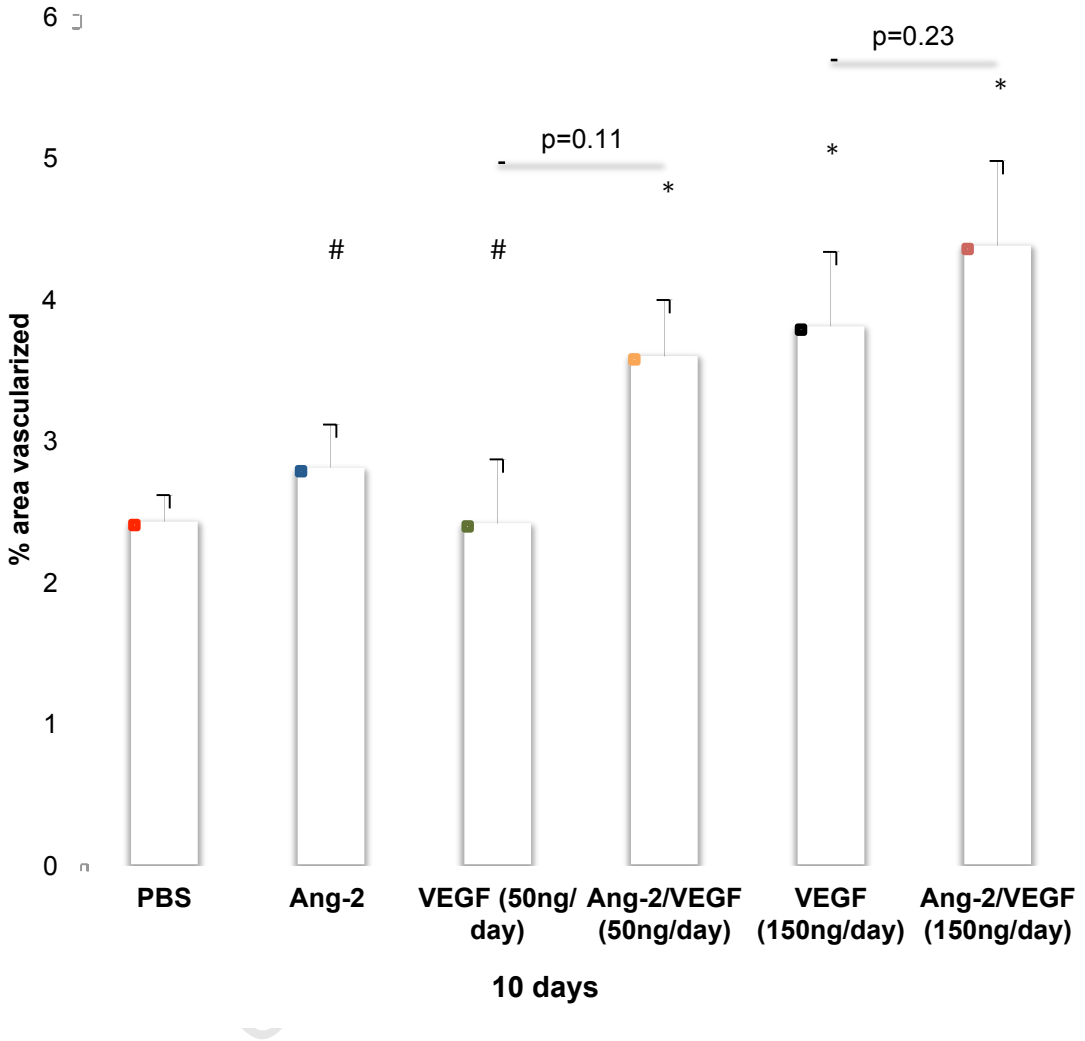

*Fig.12. 150ng VEGF/day, simultaneous delivery of 50ng VEGF and 15ng Ang-2/day and simultaneous delivery of 150ng VEGF in combination with 15ng Ang-2/day promoted neovessel formation at 10 days (*p<0.05 vs PBS). No pro-angiogenic effect was seen after delivery of 15 ng/day Ang-2 or 50ng/day VEGF ($^{\#}$p>0.05). A strong trend towards a synergistic effect was observed when Ang-2 was co-delivered with low VEGF dosages (p=0.11 when compared with sole delivery of VEGF (50ng/day), n=6)*

3.7.2.1. Conclusion - Ang-2/VEGF

While the study was underpowered to show a significant synergistic effect on neovessel formation by the simultaneous delivery of VEGF-A and Ang-2, the observed trend is in conjunction with the current literature[284]. In combination with previous experiments, though, the results suggested that increasing the dose of VEGF-A is a more effective way to increase angiogenesis into vascularization devices in comparison with co-delivery of Ang-2.

3.8. Simultaneous delivery of diverse VEGF family members for the stimulation of neovascularization

VEGF-A, VEGF-C and PLGF activate a diverse set of vascular endothelial growth factor receptors[78]. While VEGF-A binds to both VEGFR1 and -2, its downstream angiogenic effects are transmitted through VEGFR-2. PlGF exclusively binds to VEGFR1, while VEGF-C mediates its actions via VEGFR2 and-3. By competing with VEGF-A for binding to VEGFR-1 and thereby allowing it to bind more to VEGFR-2, PlGF has been proposed to increase pro-angiogenic signalling[132]. Furthermore, while it has been suggested that angiogenic therapy may be improved by simultaneously stimulating blood and lymphatic vessel growth[285], this hypothesis has not yet been tested. To determine whether the concurrent delivery of VEGF-A, VEGF-C and PlGF has synergistic effects on neovascular development, 150ng/day of each growth factor were delivered concurrently over a period of 10 days. Neovessel formation was assessed by immunohistochemical analysis of CD31.

3.8.1. Results

Simultaneous delivery of VEGF-A, VEGF-C and PlGF vascularized 6.39±0.87% of the total graft area after 10 days (n=6), corresponding to a statistically significant 128% increase in vascularization with respect to PBS controls (2.8±0.31%, see Fig.13). Nevertheless, since comparable results were achieved by the sole delivery of 150ng/day VEGF-A for 10 days

(6.61±0.95%, n=6), simultaneous delivery of the three VEGF family members did not further promote neovessel formation at this timepoint.

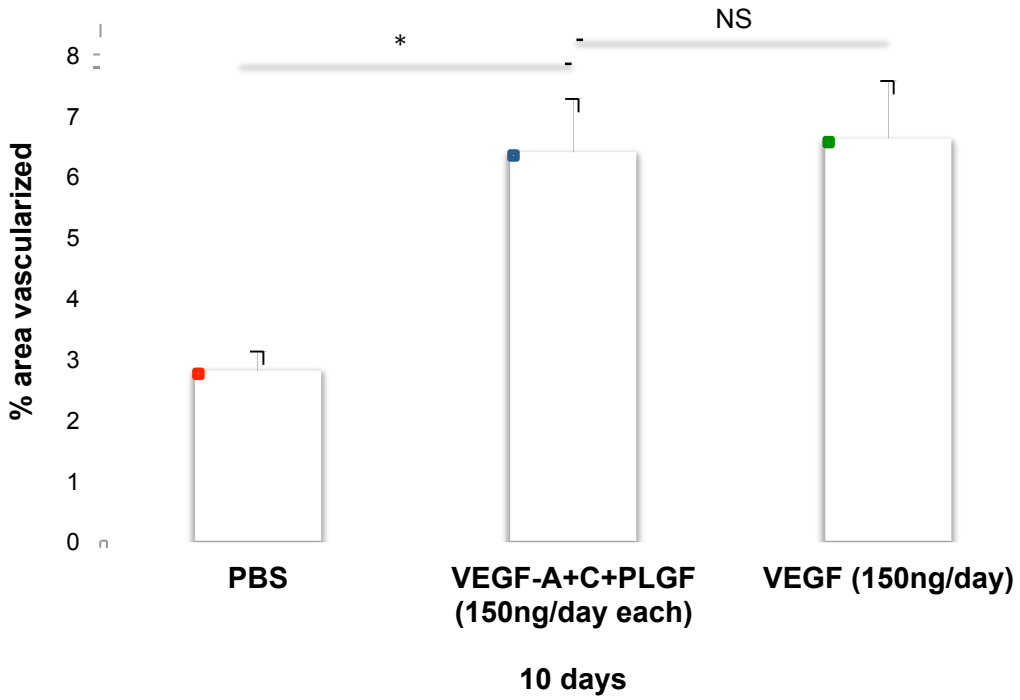

*Fig.13. The concurrent delivery of 150ng/day of VEGF-A, VEGF-C and PlGF significantly enhanced vascularization at 10 days (*p>0.01, n=6). In comparison with sole delivery of 150ng VEGF/day, no additional pro-angiogenic effects were seen by co-delivering VEGF-C and PlGF.*

3.9. Discussion – Growth factor delivery for stimulation of angiogenesis

VEGF-A, PlGF and BDNF significantly increased neovascularization after being continuously delivered for 10 days, with VEGF inducing the most prominent increase in neovessel formation. Furthermore, a trend towards synergistically promoting angiogenesis was observed for VEGF and Ang-2, in accordance with previous reports in the literature. An increase in sample number likely would have confirmed this effect. Since increasing VEGF dosage more effectively induced an increase in neovessel formation, this avenue was no longer pursued. For some other growth factors (HGF, VEGF-C) their previously described angiogenic potential could not be confirmed in this subcutaneous wound-healing model. Multiple potential explanations for this discrepancy

exist. Growth factor stability has been a major concern in therapeutic angiogenesis approaches. The initial experiments with a diverse set of angiogenic growth factors clearly indicate that at least some of the growth factors were stable for extended periods of time when delivered with an osmotic minipump. In addition, an extensive analysis of growth factor stability was performed for VEGF, which is believed to be one of the most unstable growth factors[17] in the body. Both saphenous vein endothelial cell proliferation assays and enzyme-linked immunosorbent assays were performed to confirm VEGF stability up to day 42. These data are presented in chapter 3.10.2., along with experiments describing the effects of continuous VEGF delivery for up to 42 days on neovascularization. A high variability in levels of neovascularization was observed after HGF delivery. An increase in sample number may therefore have allowed for discernment of a more subtle effect of HGF on increasing neovessel formation. The lack of a pro-angiogenic effect observed after HGF treatment may also reflect specific differences that exist between angiogenesis assays, such as delivery method and site. Increases in angiogenesis were reported after adenoviral injection into the myocardium[262,263] as well as after HGF plasmid delivery into the ischemic hindlimb of diabetic rats[264]. VEGF-C also did not promote angiogenesis into neovascularisation devices. Despite analysing its angiogenic potential after delivery at 2 different dosages, it is possible that the correct dosage was not delivered and that a further increase in VEGF-C may have been necessary to induce subcutaneous angiogenesis. Timing and duration of VEGF-C delivery are likely important variables determining its effects on neovascularization and both may have contributed to the negative finding. Other possible explanations include tissue-specific differences in growth factor metabolism in comparison with models described previously, in which an increase in angiogenesis was observed, and differences in the mode/route of growth factor delivery. The combination of bFGF/PDGF was previously shown to synergistically enhance angiogenesis in an ischemic hind-limb model. Cao et al used micropellets, growth factor loaded heparin-sepharose beads and slow-release polymers in a mouse corneal micropocket assay, a matrigel assay and a rat hindlimb ischemia model, respectively[207]. The release kinetics for each of the described methods are not described in further detail in this manuscript and may differ substantially. While osmotic mini pumps were

used to deliver bFGF and PDGF-BB in a rabbit model of hindlimb ischemia in the same report[207], it should be noted that collateral formation and blood flow were measured to show synergistic effects of bFGF and PDGF-BB, and not an increase in capillary density. Analysis of downstream signalling pathway activation may be of interest in determining why the simultaneous delivery of VEGF, VEGF-C and PlGF did not significantly alter neovascularization in comparison with VEGF treatment alone. Overall, the data obtained after delivery of VEGF were the most robust, reproducibly leading to dramatic increases in neovascularization after 5 and 10 days. Initial experiments with varying dosages indicated a dosage-dependent effect on neovessel formation. As VEGF dynamics appeared to be the most interesting finding in the context of this assay that deserved more extensive study, a detailed characterisation of VEGF was carried out. PlGF emerged as another protein that induced significant neo-angiogenesis and since this growth factor has been associated with increased vascular stability, the response to PlGF was investigated for its ability to generate stable vessels.

3.10. Scaffold neovascularisation after VEGF stimulation is dosage dependent

Vascular endothelial growth factor (VEGF) has been extensively studied for short-term vessel ingrowth in tissue regeneration applications to stimulate vascularisation of polymeric scaffolds[286-289]. Initial experiments indicated that, at the 10-day timepoint, VEGF enhances angiogenesis in the vascularization device in a dosage dependent fashion. Yet, little is known about the long-term fate of the neovasculature induced by VEGF stimulation. To test the hypothesis that the concentration of VEGF plays a critical role in the nature and persistence of vasculature formed in a tissue regenerative scaffold, the effects of different concentrations of VEGF on the vascularisation of a porous scaffold in the short-, intermediate- and long-term were evaluated. For up to 6 weeks, 15, 150 and 1500ng VEGF/day were delivered to polyurethane scaffolds by osmotic pumps. The stability of the vessels created as well as their mural cell investiture and perfusion was quantified.

3.10.1. Continuous delivery of VEGF for 10 days

The level of neovascularisation within a porous polyurethane scaffold as visualized by staining with an antibody against CD31 is shown in Fig.14 A–D. Delivery of 15ng/day in this model had no impact but the two higher dosages of 150 and 1500ng/day dramatically increased vessel ingrowth area relative to the control by 159±39 and 286±90%, respectively, corroborating the previous findings for these dosages (Fig. 14E). Regions containing a very high density of small vessels and putative endothelial sacs were observed in explants from the highest VEGF dosage regime but not in the other dosages (Fig 14D).

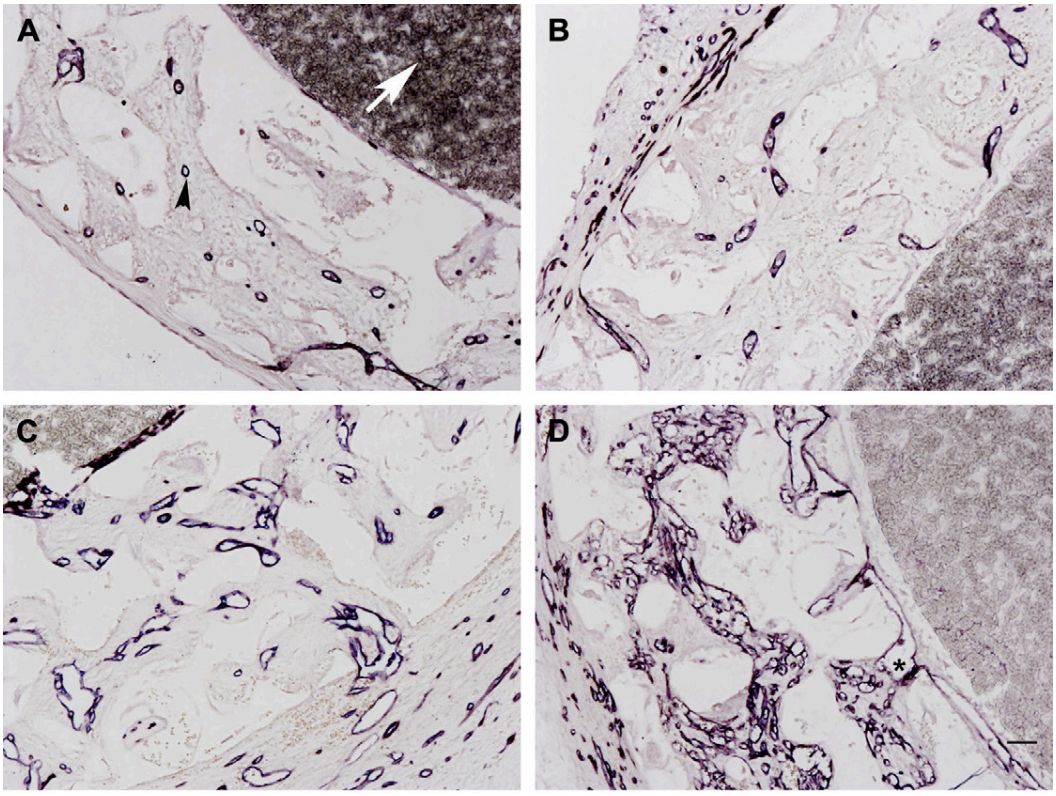

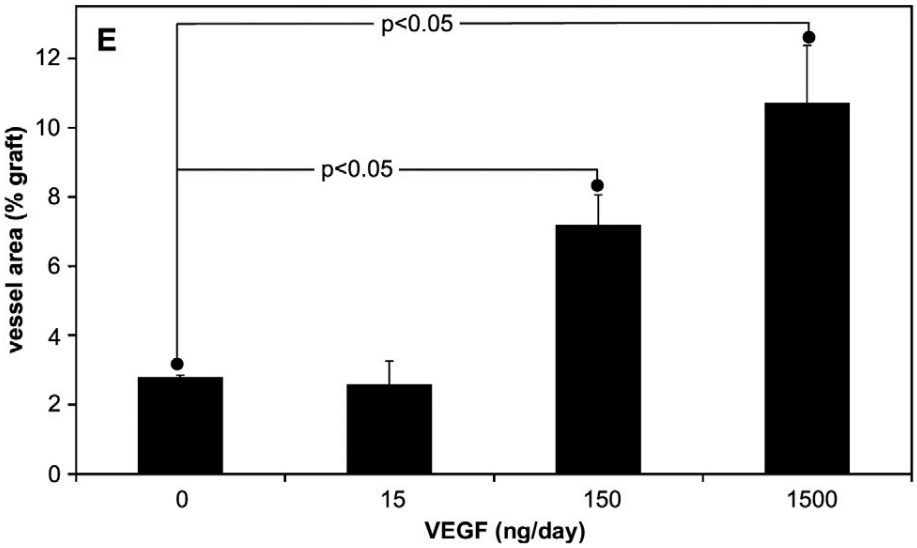

*Fig.14. Immunohistochemical staining of CD31 positive vessels in devices explanted after delivery of (A) 0, (B) 15, (C) 150 and (D) 1500ng VEGF/day for 10 days. Arrowhead indicates a CD31 positive vessel and white arrow indicates ePTFE cell barrier in Fig.14A. *in Fig.14D indicates a putative endothelial sac. Bar represents 50 µm (E). The area of vascularisation was determined as a percentage of the total area available for tissue ingrowth in the polyurethane wall. There was a significant increase in vascularisation relative to the control after delivery of 150 and 1500ng VEGF/day for 10 days (n=4).*

3.10.2. Continuous delivery of VEGF for 20, 30 and 42 days

To determine the stability of VEGF at 37 °C over the maximum delivery period, the VEGF solution used to load the pumps was incubated for 42 days at 37 °C and then used to stimulate endothelial cell growth (see chapter 10.1.5.). The incubated VEGF resulted in a 15% increase in cell number after 2 days compared to media alone ($p<0.05$) with fresh recombinant VEGF producing a similar increase. Furthermore, the VEGF content within an implanted polyurethane device that had VEGF pumped at 1500ng/day (as determined by ELISA, described in chapter 10.1.5.) was found to be similar after 10 and 42 days implantation (226±21 and 257±11ng, respectively). The delivery of VEGF for periods greater than 10 days was then investigated for the two higher dosages. After 20 days the ingrowth was similar to that at 10 days with increases of vessel area within the polyurethane of 120±47 and 273±185% for the 150 and 1500ng/day dosages, respectively (Fig.15A). No endothelial sacs were observed at this time point. At 30 days the situation again was unchanged with regards to the delivery of 150ng/day VEGF (161±65% increase) but the maximum dosage regime now had a lower increase (125±113%) than the medium dosage. Additionally, this increase was not significant with respect to the control ($p>0.2$). The lack of significance derived from maximum dosage explants either having highly elevated vessel ingrowth similar to that observed in the two previous time points for this dosage or a gross appearance and amount of vessels identical to that in the control explants (Fig. 15B, C). At 42 days explants of the 1500ng/day group also had two distinct appearances with the majority indistinguishable from the control and the remainder having considerably increased vessel

ingrowth. Again, the medium dosage had a significant though substantially decreased increase (48±15%) in vessel density whilst the increase in response to the maximal dosage was again insignificant. The average vessel diameter was then determined for the medium and maximal VEGF and control groups at the two earliest time points. Vessel diameter at 10 days was found

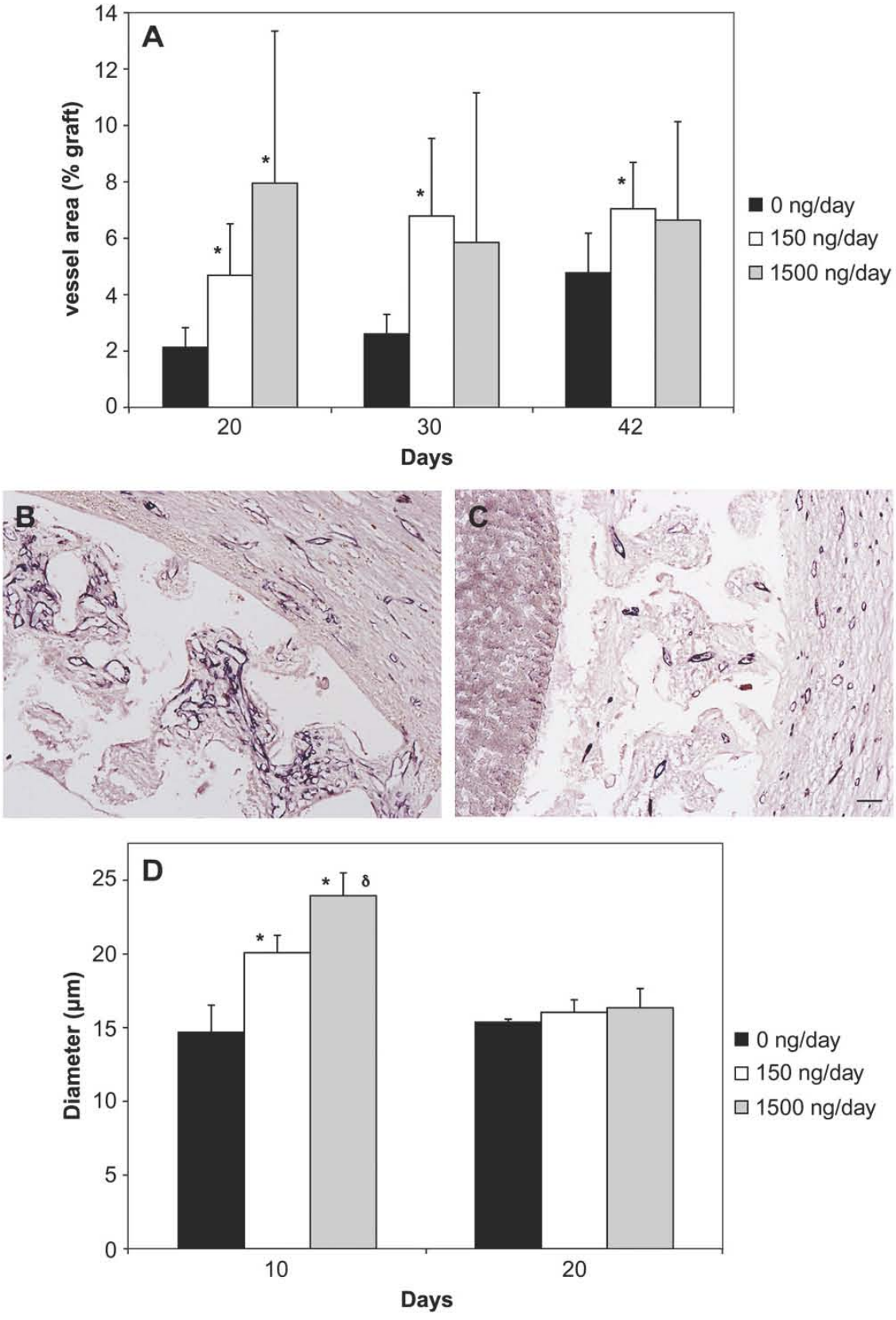

*Fig.15. Constant delivery of VEGF resulted in concentration dependent differences in vascularisation levels. (A) The area of vascularisation was significantly increased by delivery of 150ng VEGF/day for 20, 30 and 42 days. A significant increase was only observed for 20 days of delivery at 1500ng VEGF/day (*p< 0.05 vs. control, n=5–6). (B, C) Immunohistochemical staining for CD31 of two explants that had received VEGF at 1500ng/day for 30 days shows the dramatic differences in outcome. Bar represents 50µm. (D) Analysis of the average vessel diameter after 10 and 20 days of VEGF delivery showed that supply of VEGF for 10 days at 150ng/day increased the average diameter relative to the control and at 1500ng/day increased vessel size relative to both the control and the 150ng VEGF/day dosage. After 20 days delivery, the average diameter for both VEGF groups had reduced to that of the control (*p< 0.05 vs. control, p< 0.05 vs. 150ng VEGF/day, n=4).*

to increase from 14.7±1.84µm for the control group to 20.1±1.17µm for the medium dosage ($p<0.05$) and again to 23.9±1.55µm for the maximal dosage ($p<0.05$ maximum vs. medium dose) (Fig. 15D). By 20 days, the vessel diameters were very similar and the differences observed were not significant (15.4±0.2, 16.0±0.84, and 16.3±1.30µm for control, medium VEGF, and maximal VEGF groups, respectively).

3.10.3. Vessel persistence after discontinuing VEGF delivery

After VEGF had been delivered through the polyurethane device for 42 days at 150 and 1500ng/day, the osmotic pump was removed and the device left in position for a further 80 days. The vessel density showed an overall decline but the medium dosage group still had an elevation over the control (46±11% increase, $p<0.05$) (Fig.16). The maximal dosage group's vessel density was not significantly increased above the control.

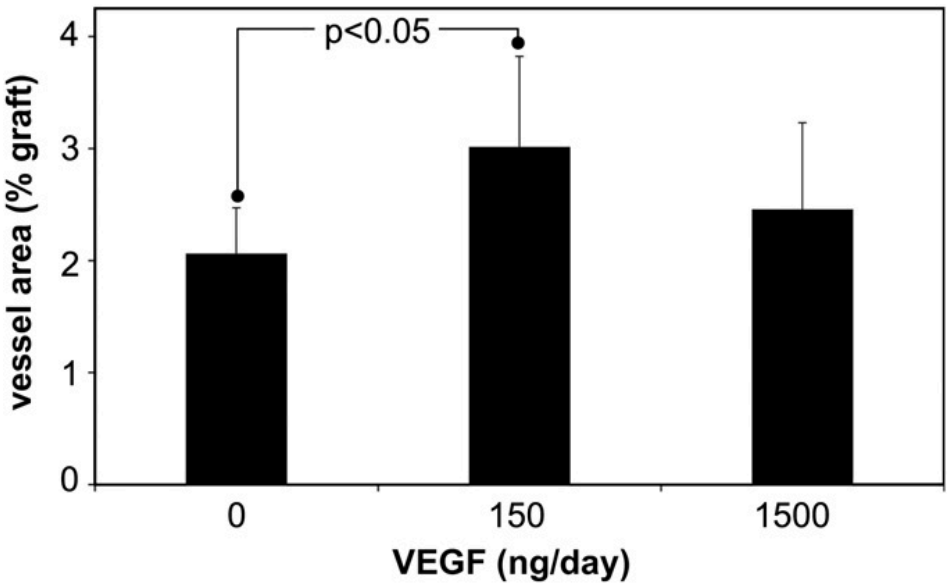

Fig. 16. A persistent increase in vascularisation levels after termination of VEGF supply is dependent on the concentration of VEGF delivered. VEGF was delivered for 42 days and devices were explanted 80 days after pump removal. The delivery of VEGF at a dose of 150ng/day showed a significantly increased vasculature in the graft compared to the control (n=7).

3.10.4. Mural cell coverage of vessels

As mural cell coverage has been extensively implicated in the stability of vessels, the investiture of the newly formed vessels with desmin-positive cells was assessed (Fig.17A). The vessels induced by the medium VEGF dosage had a similar coverage of desmin-positive mural cells to that found on those in the control group (Fig.17B). However, the vessels resulting from the maximal concentration of VEGF showed a significant reduction (29.2±6.6%) in coverage after 20 days of delivery. All groups showed an increase in coverage (51.3±2.9%) at 4 months relative to the 42 days time point.

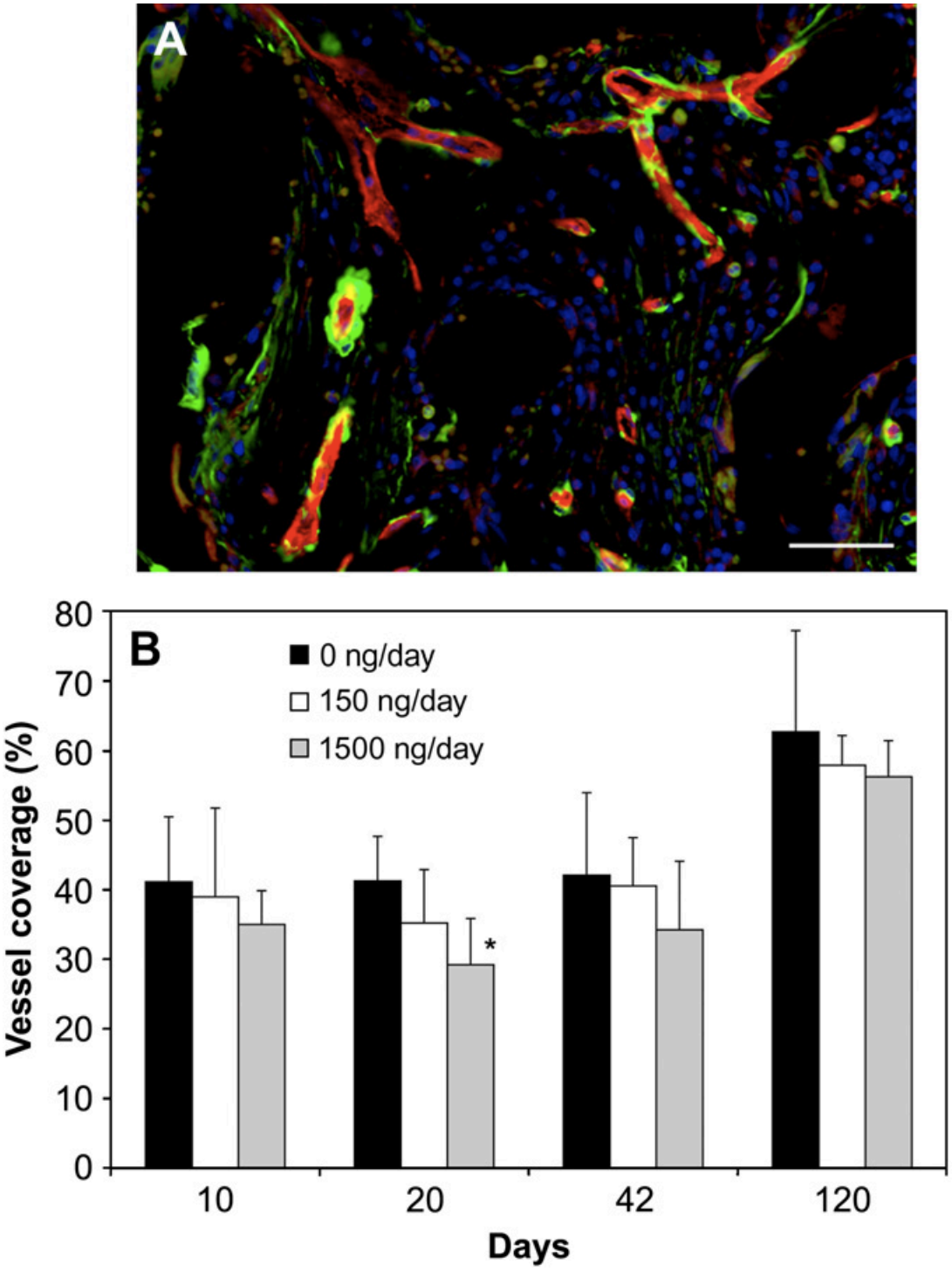

*Fig. 17. Analysis of mural cell coverage of endothelial cells. (A) Micrograph showing fluorescently labelled CD31 (red), desmin (green) and nuclei (blue). The yellow stain results from the overlay of a desmin positive cell and a CD31 positive endothelial cell. Bar represents 50 μm. (B) The percentage of endothelial cells directly in contact with a desmin positive cell was quantified as described in Section 2. Delivery of VEGF at 1500ng/day for 20 days resulted in a significant decrease in endothelial cell coverage (*p<0.05 vs. control, n=4–7).*

3.10.5. Vessel perfusion

When the vessels that had grown into the polyurethane scaffold were identified by physiological perfusion with a biotinylated L. esculentum lectin, it was observed that vessels that had been exposed to VEGF for 20 days had substantially more intense staining than the control group with the high dosage group appearing the brightest (Fig.18A–C). Vessels within the scaffold still stained positive for lectin at the terminal time point but the intensity was much diminished for the VEGF groups and there was no discernible difference between them and the control group (data not shown).

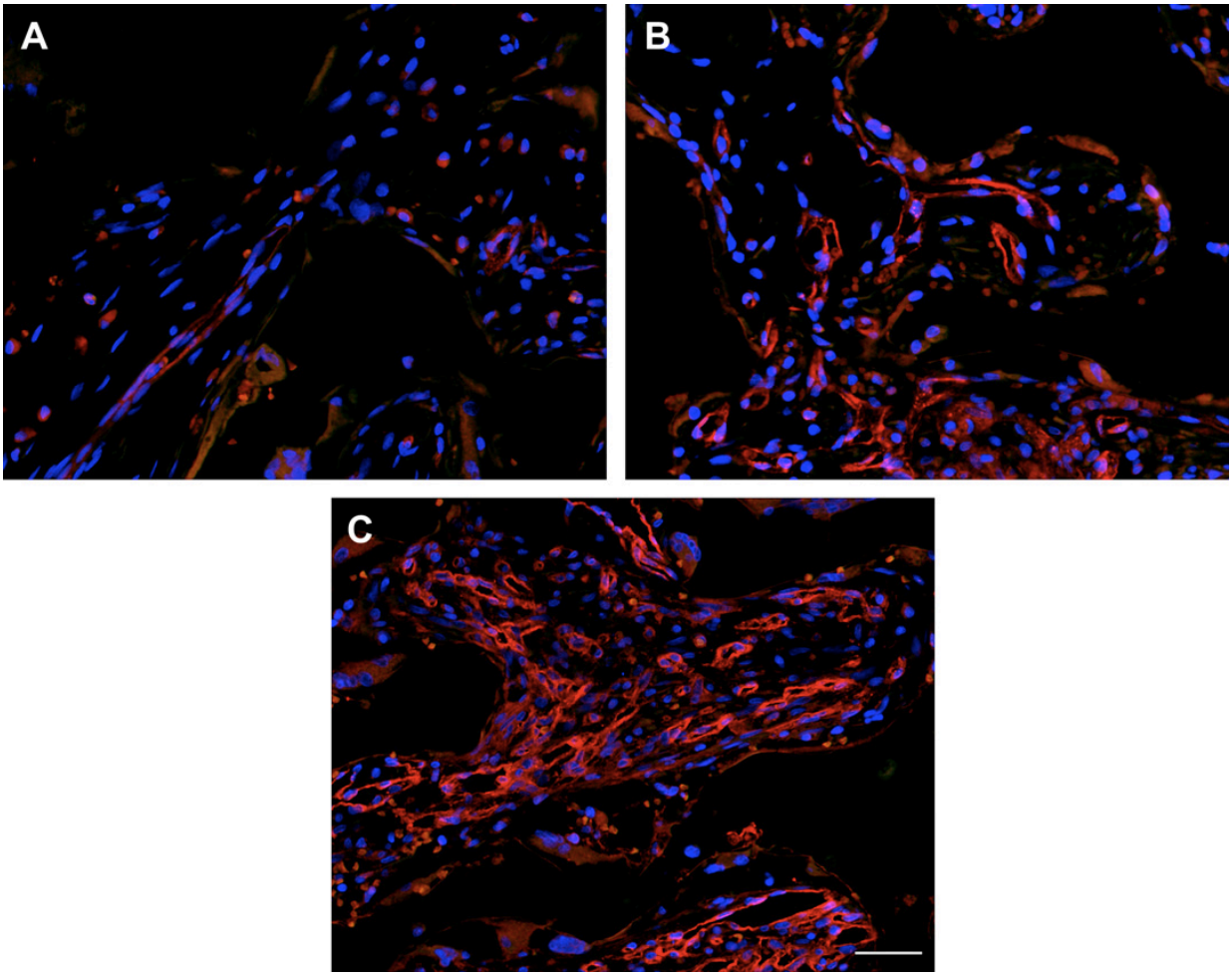

Fig. 18. Analysis of vessel perfusion as determined by Lycopersicon esculentum lectin binding. The bound biotinylated lectin was detected by Cy3-streptavidin (red) after 20 days of delivery of VEGF at (A) 0, (B) 150 and (C) 1500ng/day. The intensity of staining increased with increasing VEGF concentration.

3.10.6. Discussion

VEGF was stable and its concentration in the device maintained at a consistent level for the entire period of VEGF supply. High concentrations of VEGF induced maximal, but transient, vessel growth into porous PU scaffolds, as spontaneous regression occurred even with continued growth factor delivery over a period of 6 weeks. In contrast, medium concentrations of VEGF (150ng/day) induced not only a constant increase in vascularisation during delivery, but also resulted in elevated and functional vascularity for 2.5 months after termination of VEGF delivery. A delivery of VEGF at 15ng/day was found to be insufficient to generate an increase in this angiogenesis model at 10 days whilst 1500ng/day VEGF generated an even more extreme increase than the medium dosage at this time point. As most tissue engineering projects would desire as rapid a connection with the host vasculature as possible, the low dosage was not further investigated. The response to the high dosage would suggest that the burst release observed for many biopolymers[286] might not be deleterious but rather advantageous as long as it is not sustained for an extended period. This caveat stems from the finding that the high dosage eventually resulted in dramatic regression of the neovascularisation that started somewhere between 20 and 30 days of VEGF delivery. The precise timing of the delivery of VEGF may also be important as is evidenced by the study of Gosain and colleagues[290] where in a similar manner to that reported here, VEGF was delivered by osmotic pumps to polyvinyl alcohol sponge discs. However, the delivery of VEGF only began 17 days after disc implantation, when the concentration of endogenous VEGF generated during wound healing started to decrease and it was found that the delivered VEGF did not prevent the regression of vessels. The exact reason for the persistence of an elevated vascularisation for the medium dosage of VEGF is not clear and is almost certainly multi-factorial in nature. This view derives in part from observations on the nature of the vessels generated. The medium dose led at all time points to vessels that morphologically closely resembled those in the control group, though they were larger at 10 days, whilst the maximum dose at 10 days had regions densely filled with smaller vessels, putative endothelial sacs and an average vessel size that was even greater than those in the medium dosage. It is interesting that while both VEGF dosages still had induced substantially

larger areas of vessel ingrowth at 20 days the average vessel size had decreased to that of the control group and there were very few endothelial sacs present. The reason and mechanism(s) for this decrease in size are unclear but must reflect either a very dynamic period of regression of large vessels and sprouting of new smaller vessels or intussusception of the larger vessels. VEGF clearly can induce sprouting and has also been implicated in the regulation of intussusception[291]. The high dose also exhibited a significant decrease in endothelial cell contact with mural cells at 20 days. Again, the medium dose showed no such decline in vessel coverage. The mural cells are assumed to most likely be pericytes and possibly a subset of smooth muscle cells as these cell types have been shown to express the intermediate filament desmin[292]. The association of pericytes with endothelial cells has been variously reported to either be correlated with stabilization of blood vessels[293] or not[294]. Though this study was not designed to comment on this discrepancy, an image analysis assay was established that determines the level of endothelial cell ensheathment by pericytes. This is analogous to the assay designed for whole retinal mounts established by Chan-Ling and co-workers[292], which was found to predict stability of newly developed vessels in the retina. Interestingly the pericyte coverage increased for all groups at the final time point when it might be expected that the vessels that are present would be stable. Finally the VEGF treated implants had a substantial increase in perfusion as determined by lectin binding in the earlier stages with the high dose having the most pronounced increase. L. esculentum lectin binding could rather be altered by differing expression of its ligand (N-acetyl-D-glucosamine) on the endothelial surface and not by a change in perfusion. However, it has been demonstrated that binding of L. esculentum was uniform on normal and inflamed vessels[295]. Additionally decreased lectin binding in peritubular capillaries in diseased kidneys was found to correlate with decreased perfusion as determined by intravitral microscopy analysis of red blood cell velocity[296]. Though a cause for the increased perfusion was not determined, it may result from increased nitric oxide (NO) levels as VEGF causes the increased production of NO via upregulation of endothelial nitric oxide synthase[297] and NO has been determined to increase perfusion in several areas of the body, most probably through its vasodilation of resistance vessels[298]. It is therefore tempting to suggest that the precipitous regression observed for the

high dose regime results from a confluence of the above factors. The vascularised area generated within the scaffold by this dosage was massively elevated over the normal tissue response (even 50–75% higher than the medium dosage) and this elevation was coupled with an increased perfusion. This would probably have resulted in supply far outstripping metabolic demand and caused a dramatic pruning of the newly formed vessels[299]. The extent of pruning may have been exacerbated by the irregular nature and inadequate pericyte coverage of the vessels. The medium dose, however, may avoid this fate by generating vessels that do not cross critical thresholds of difference from physiological vessels. This finding suggests that a single growth factor can induce stable vessels into a scaffold but further work needs to be done to elucidate the minimal delivery period. In conclusion, the concentration of VEGF delivered plays a central role in determining the nature of neovessels, which in turn critically influences the stability of generated vascular constructs.

3.11. Regression of VEGF-induced neovasculature is preceded by the termination of vessel perfusion

While high VEGF dosages (1500ng/day) were highly efficient at inducing neovessels in the short term, the time course experiments suggested that there could be a precipitous regression of vessels after exposure to VEGF at such a high dosage. It was therefore thought worthwhile to examine the kinetics of regression of vessels that had been induced by this dosage in more detail. Early experiments revealed that that VEGF-induced neovascularization reached its maximum around day 10 after implantation. To study the dynamics of vascular regression after termination of VEGF delivery, 1500ng/day VEGF were delivered via osmotic pumps for 10 days; osmotic pumps were removed at day 10 and subsequently the vascularization devices were explanted at the time of and 1, 2, 4, 10 or 20 days after pump removal, respectively. The level of neovascularisation within the scaffolds was visualized by staining with an antibody against CD31 and physiological perfusion was assessed with biotinylated L. esculentum lectin.

3.11.1 Vessel persistence after discontinuing VEGF delivery

During the initial 48 hours after termination of VEGF delivery vascular density remained unchanged (Fig.19). Between day 10+2 and 10+4 a sharp increase in vascular regression was observed and by day 10+4 the number of vessels had decreased by 75.9% in comparison to day 10 (Fig.19). Regression of the neovessels continued at a rapid rate and by day 10+10 the

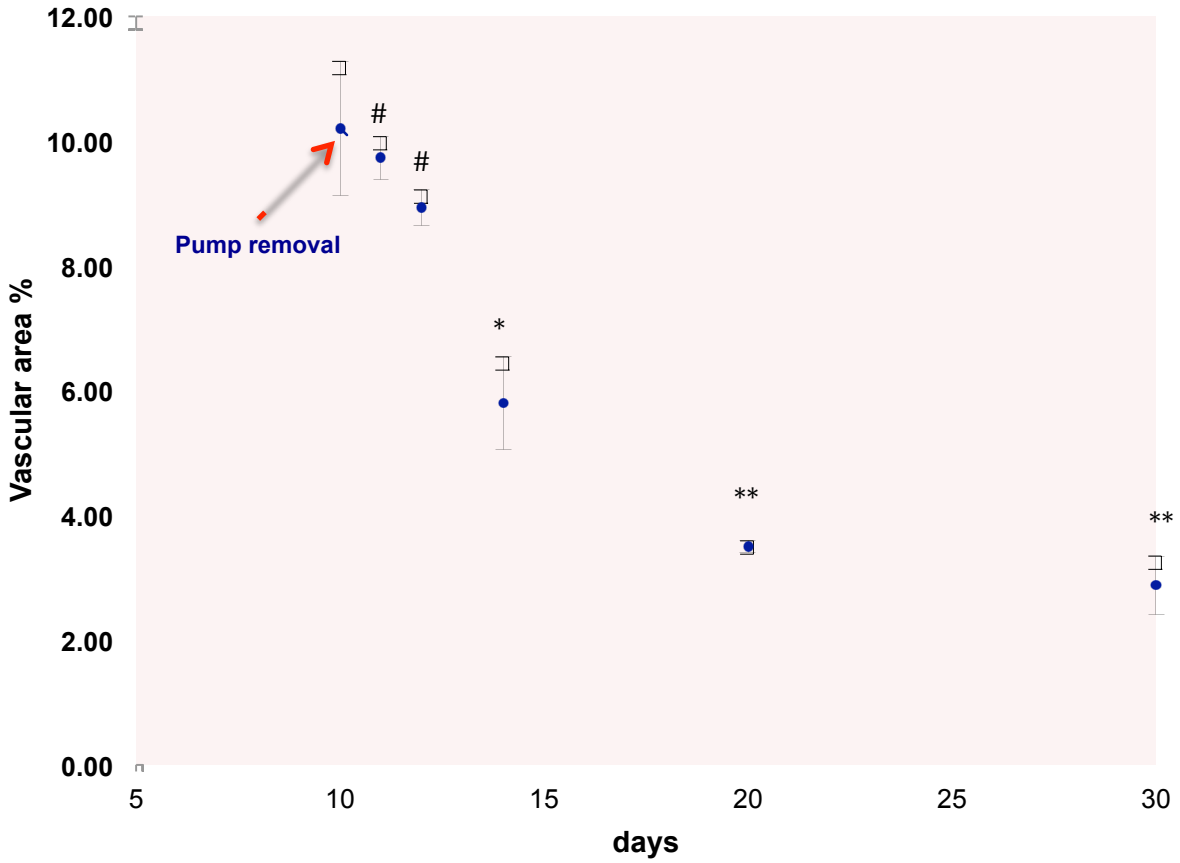

*Fig.19. After termination of VEGF delivery at 10 days (1500ng/day), the induced neovasculature appeared stable for 2 days (#p>0.05 compared with 10 day vascular area after VEGF delivery, n=4-6) before regressing rapidly (*p<0.01, **p<0.001 both compared with 10 day VEGF-induced vascularization, n=4-6). At day 20, 10 days after pump explantation, no significant difference in vascularization between VEGF grafts and PBS controls was observed (p=0.11, n=4).*

neovasculature had regressed completely (-191.4%) to levels comparable with PBS controls harvested at this timepoint. A further decrease was observed on day 10+20 (-254.2% in comparison with 10-day levels).

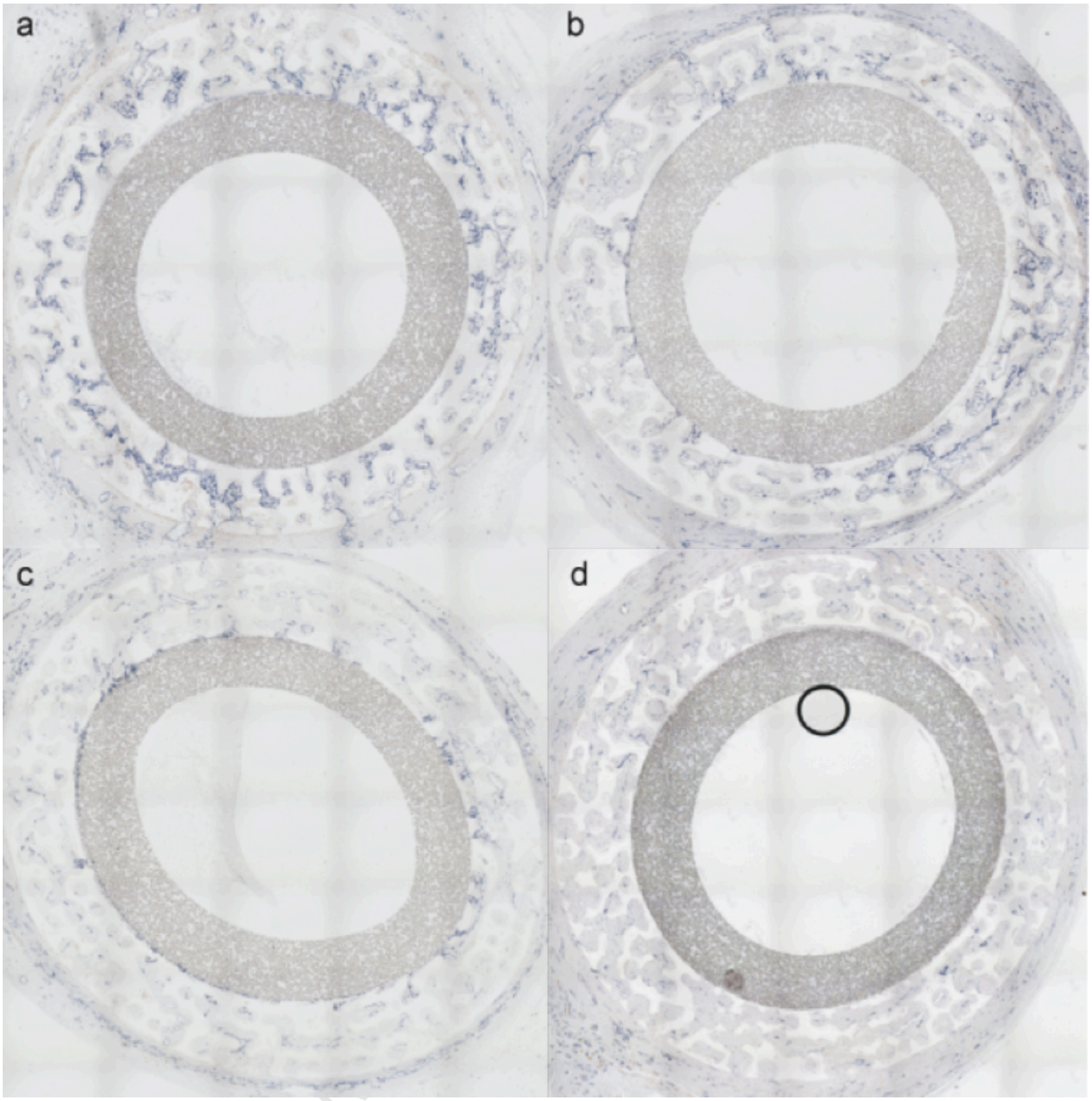

Fig.20. Immunohistochemical staining of neovascular devices for CD31 performed on day 1 (a), 2 (b), 4 (c) and 19 (d) after removal of VEGF-delivering osmotic pumps. As early as day 2 (b) a substantial decrease of $CD31^{+}$-vessels (in blue) is seen. 4 days after termination of VEGF-delivery (c) the neovasculature has entirely regressed to control levels.

3.11.2. Vessel perfusion

Assessment of physiological kidney perfusion confirmed successful delivery of biotinylated L. esculentum lectin in all animals (n=3 for each timepoint). Perfusion at day 1 post pump-removal

(10+1) remained unchanged in vascularization devices in comparison with grafts explanted immediately after pump removal at day 10 (see Fig.21a). Vascular perfusion was still observed 2 days after pump removal albeit at a diminished rate (shown in Fig.21b), but by day 4 after termination of VEGF delivery the perfusion had almost entirely stopped (see Fig.21c). At days 10+4, 10+10 and 10+20, there were no discernible difference in perfusion between VEGF-treated groups and PBS controls.

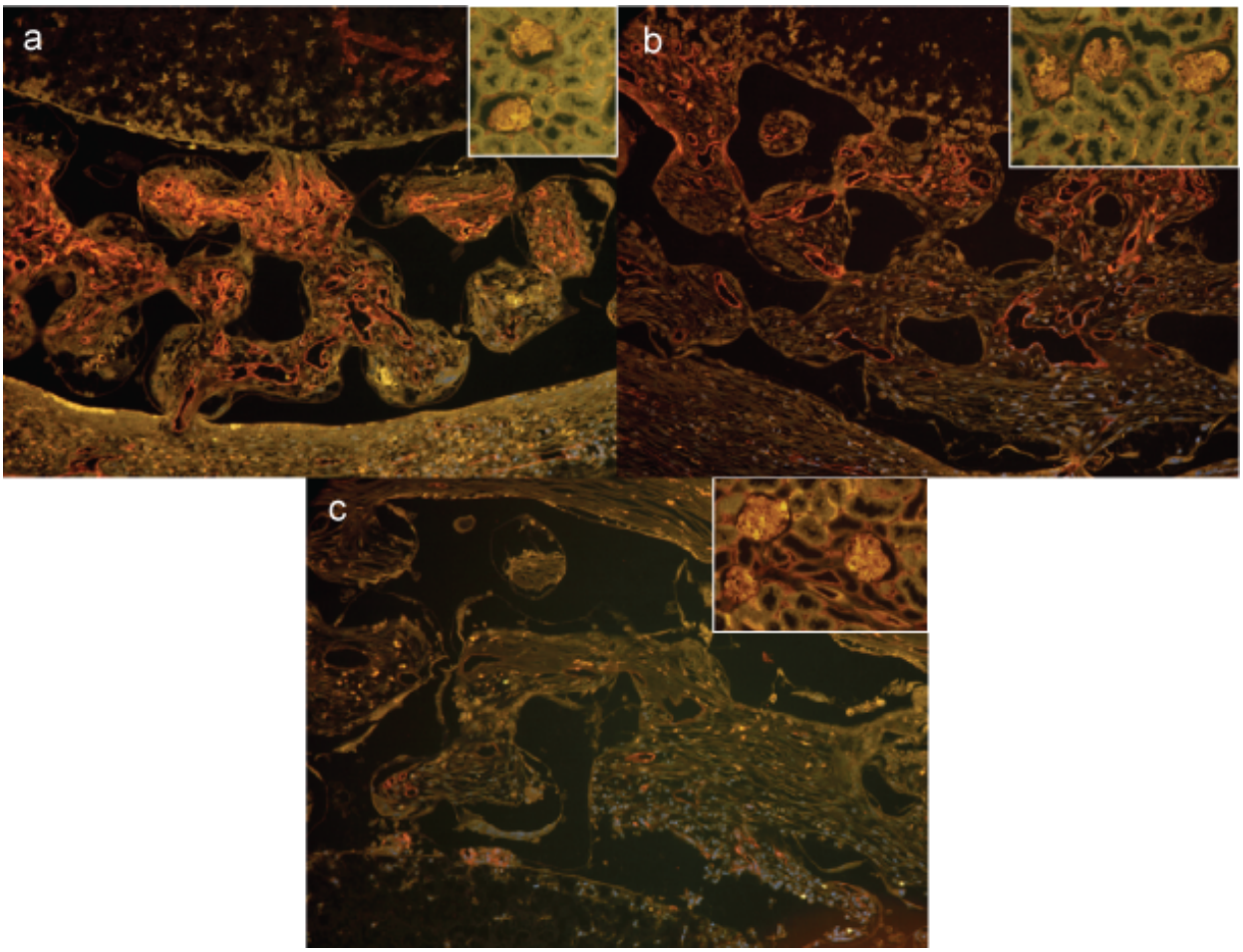

Fig.21. *Vessel perfusion as determined by L. esculentum lectin binding. Successful perfusion with lectin in each animal was confirmed by detecting bound biotinylated lectin with Cy3-streptavidin in kidneys harvested at the time of sacrifice. Kidney perfusion was similar at each timepoint and representative images are shown in respective inserts (framed in white). 1 day after termination of VEGF delivery vascularization devices remain highly perfused (Fig.21a). 48 hours after stoppage of VEGF delivery a profound decrease in perfusion in vascularization devices was observed (Fig.21b). Perfusion of neovessels has almost entirely stopped by day 10+4 (Fig.21c).*

3.11.3. Discussion

The dynamics of vascular perfusion and regression were assessed. Experiments confirmed that short-term delivery of high VEGF dosages does not result in a stable neovasculature. Within 48 hours after termination of VEGF delivery, a dramatic decrease in vascular perfusion was observed (Fig. 21b). 96 hours after VEGF removal perfusion had come to a complete halt (Fig.21c). Regression of the neovasculature occurred at a slower rate [following approximately 48 hours after perfusion] (see Fig. 20). First significant signs of vascular regression became apparent 4 days after termination of VEGF delivery and 10 days after stoppage of VEGF delivery, neovessels had completely regressed and there was no significant difference in comparison with PBS controls.

While the mechanisms underlying vascular regression are currently poorly understood, a number of hypotheses exist that attempt to explain this phenomenon. While it is possible that the deferred regression of vessels resulted from a slow clearance of VEGF from the neovascularisation site, turnover of VEGF in the body has been shown to be rapid[17] and thus this explanation seems unlikely. It is plausible that a lack of metabolic demand precedes the stop in vascular perfusion and initiates the pursuing vascular regression[58]. Growth factor interactions have been shown to be instrumental in regulating neovessel stability. As the previous study had shown that the concentration of VEGF has substantial effects on the maturation of neovessels, it is intriguing to hypothesize that super-physiological growth factor concentrations may prevent the establishment of stabilizing signals mediated by supplementary endogenous growth factors. As a result, this could block the recruitment of stabilizing perivascular cells to the newly forming vessels.

4. INTRODUCTION: Attempts to prevent vascular regression

As stable vasculature is a prerequisite for many therapeutic angiogenesis approaches, it was felt that further attention should be paid to stabilizing the rapid and dramatic increases in neovascularization observed for the high VEGF dosage. Even though it was shown that a

moderate dosage could sustain a stable vasculature, many therapies will benefit from a more rapid connection to the host vasculature.

A number of strategies have been suggested to promote vessel stability. In the body, the survival of many capillary beds throughout the body is dependent on the continuous presence of VEGF[294,300]. Numerous reports have suggested that vascular stability depends on the temporal and spatial interplay of a diverse set of growth factors that help recruit stabilizing perivascular cells. While SDF-1 has been identified as an important regulator initiating angiogenesis in ischemic tissues[234-240], SDF-1-dependent recruitment of CXCR4+PDGFR+ckit+ smooth muscle progenitor cells has also been shown to promote neovascular stability[246]. PlGF has been associated with superior vascular stability[130] in comparison with VEGF likely due to targeting endothelial cells[127], smooth muscle cells and macrophages, all of which are instrumental in the growth of collaterals[31,129]. Synergistic effects existing between PlGF and VEGF exhibit a profound effect on pathological angiogenesis, as PlGF was shown to promote pathological angiogenesis by triggering crosstalk between VEGFR-1 and VEGFR-2[99,127,130]. Furthermore, tumour vessels resistant to VEGFR2 have been described to regress upon treatment with an antibody targeting PlGF (α-PlGF)[301]. As crosstalk between VEGF and PlGF appears to be important in controlling vessel stability, these results suggest that a strategy based on simultaneous delivery of these angiogenic factors may be worth exploring for therapeutic angiogenesis.

Finally, signals derived from ECM turnover play an important role during angiogenesis. MMPs help regulate extracellular matrix remodelling to provide space during vascular sprouting[44-48]. As critical support and guidance signals are mediated through the ECM, a shift in the balance of MMPs and their inhibitors (TIMPs) has been suggested to contribute to determining vascular fate, namely vessel collapse versus vessel stability, after establishment of an immature vascular bed[44,49-52].

Therefore to test the aforementioned hypotheses, the long-term fate of VEGF-induced neovessels was assessed after simultaneous and sequential delivery of VEGF, SDF-1 and PlGF. Furthermore the effects of an MMP-modulating agent on neovessel stability were tested.

4.1. Are low VEGF dosages essential to protect neovessels from regression?

Previous experiments have shown that neovascular stability is dependent on the VEGF dosage. High VEGF-dosages give rise to neovessels that are prone to regression after termination of growth factor delivery. It has been demonstrated that the survival of many capillary beds throughout the body is dependent on the continuous presence of very low levels of VEGF[294,300]. In order test the hypothesis that minimal levels of VEGF are needed to maintain vascular stability and prevent neovessel regression, osmotic pumps were exchanged at day 10, and 15ng VEGF/day were delivered for an additional 10 days subsequent to 10-day delivery of 1500ng VEGF/day. After harvesting neovascularization devices, neovessel formation was assessed by immunohistochemical staining for CD31.

4.1.1. Results

Sequential delivery of 15ng/day VEGF did not successfully prevent or retard the regression of VEGF-induced neovessels. 10 days after the termination of high VEGF delivery (1500ng/day), vascularization in the treatment group was 3.15±0.33% and did not differ significantly from PBS controls (2.54±0.29%, n=6, p=0.2, Fig.22). Historical comparison with highly reproducible data obtained after delivering 1500ng VEGF/day for 10 days and harvesting neovascularization devices at 10 and 20 days, respectively, was performed (for this and ensuing experiments). In comparison with grafts that only had VEGF delivered for 10 days before being explanted at day 20 (10+10) no differences were observed (3.5±0.09%, n=4, p=0.43). A 223.8% reduction was observed on day 20 in comparison with vascularization levels at day 10. Delivery of VEGF dosages in the range of 15ng/day is therefore not sufficient to promote stabilization of the vessels created and this strategy fails to halt the regression seen after terminating the delivery of VEGF at high dosages.

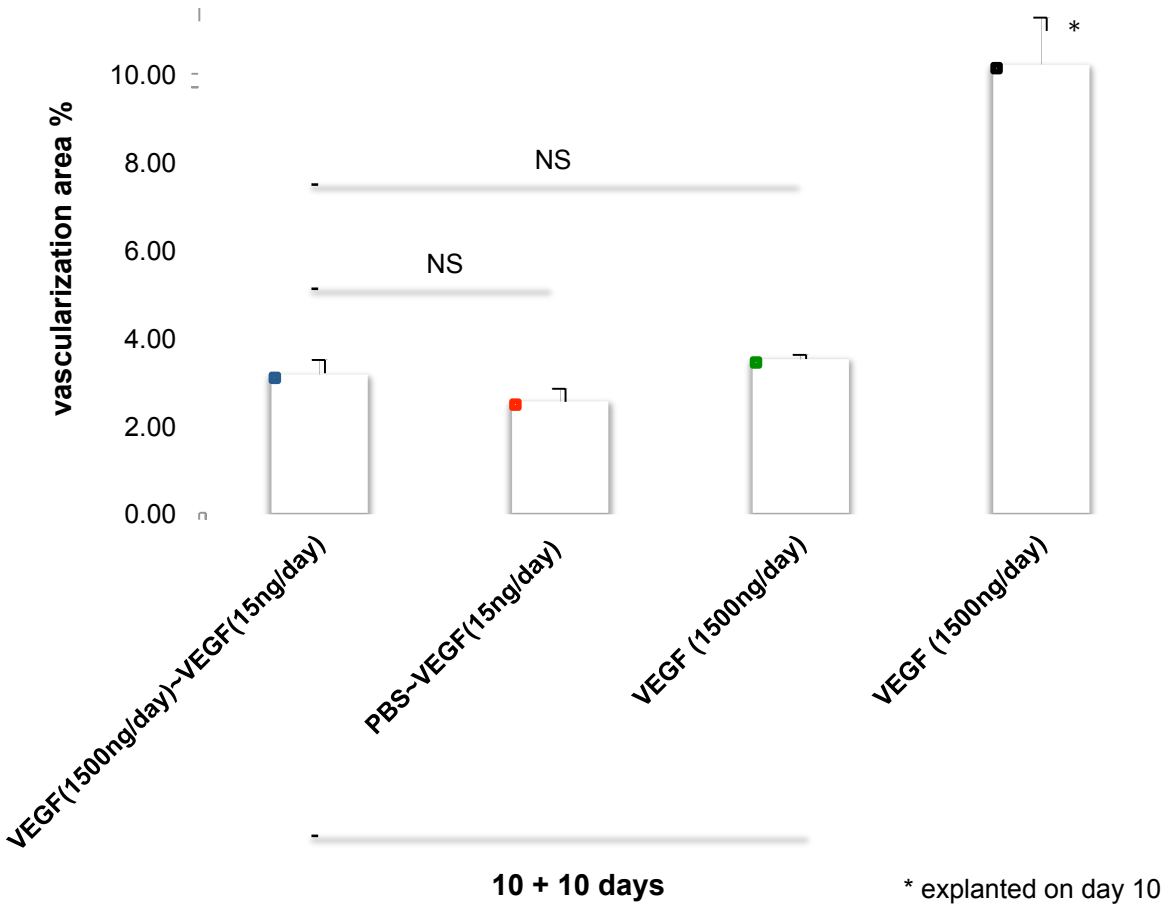

Fig.22. Immunohistochemical analysis of CD31-positive vessels in devices explanted after 20 days. To allow for comparison, historical data depicting vascularization levels seen after 10 days of delivering 1500ng/day VEGF is shown (, black bar). Delivery of 15ng/day VEGF does not prevent or slow down the regression of VEGF-induced neovessels.*

4.2. Does the VEGF-SDF-1 axis contribute to creating vascular stability in therapeutic angiogenesis?

The interaction between SDF-1 and VEGF is critical in regulating the angiogenic response after ischemic injury. SDF-1 has emerged as a major factor regulating the retention and incorporation of progenitor cells recruited by VEGF-A up-regulation into sites of active neovascularization[84] and in particular the SDF-1 dependent recruitment of CXCR4+PDGFR+ckit+ smooth muscle progenitor cells has been shown to enhance the stability of the newly formed vasculature[246].

In order to test the hypothesis that via recruitment of stabilizing progenitor cells SDF-1 enhances the stability of VEGF-induced neovessels in the subcutaneous angiogenesis assay 150ng SDF-1/day were administered for a period of 10 days subsequent to administering 1500ng VEGF/day for 10 days. At day 20 the vascularization devices were explanted and processed for histological analysis.

4.2.1. Results – Sequential delivery of VEGF and SDF-1

Immunohistochemical analysis for $CD31^{+}$-vessels was performed. Vascularization in the treatment group was 2.92±0.11% and did not differ significantly from controls (2.82±0.3%, n=6, p=0.3). Historical comparison with vascularization seen after 10-day delivery of 1500ng VEGF/day shows that the neovasculature has entirely regressed (-249.3%).

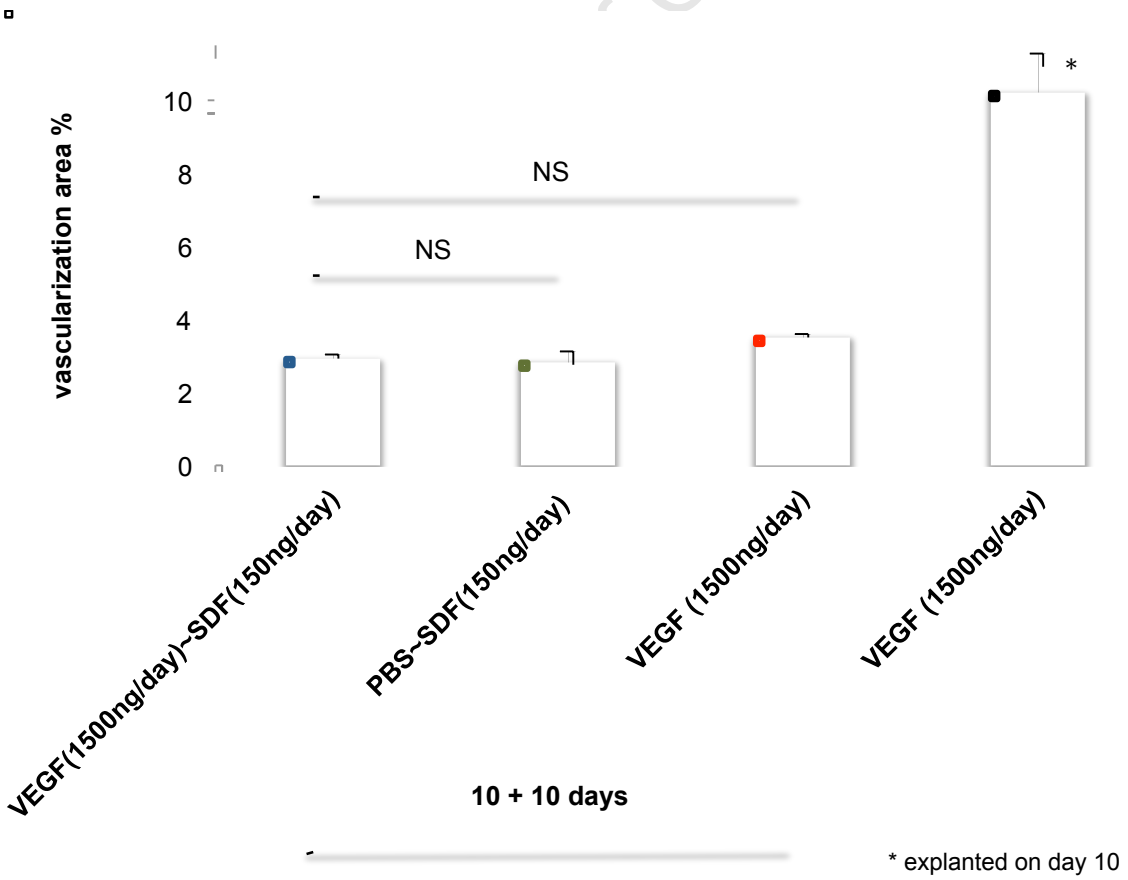

Fig.23. Analysis of CD31+vessels after harvesting vascularization devices at day 20. The sequential delivery of VEGF-A and SDF-1 does not create a more stable vascular bed in comparison with sole delivery of 1500ng VEGF/day. ($p>0.05$). 10 days after termination of VEGF-A delivery the neovasculature has completely regressed to levels seen in the PBS control ($p=0.3$, $n=6$).

Vascularization area measured after sequential delivery of 1500ng VEGF/day and 150ng SDF-1/day was not significantly different compared to levels seen after sole delivery of 1500ng VEGF/day for 10 days (when devices were explanted on day 20). Thus, the subsequent administration of SDF-1 did not promote the stability of VEGF-induced neovascularization.

While the sequential delivery of VEGF and SDF-1 did not have an effect on vascular stability and was unsuccessful in preventing the regression of neovessels, simultaneous delivery of both growth factors may be needed for vessel maturation. Evidence supports that SDF-1 and VEGF enhance neoangiogenesis synergistically when delivered simultaneously. In the matrigel plug assay, co-delivery with VEGF-A[232,233] resulted in a more significant increase in angiogenesis than sole delivery of SDF-1. Furthermore the ability of SDF-1 to promote matrix metalloproteinase production and assist during vessel formation by facilitating the remodelling of active angiogenic sites has been described[25,84,245].

To test the hypothesis that simultaneous delivery of VEGF-A and SDF-1 enhances angiogenesis and promotes vascular stability, VEGF-A and SDF-1 were co-delivered for 10 days. Osmotic pumps were explanted after 10 days and at day 20 after device implantation, vascularization devices were harvested and neovessel formation was assessed by immunohistochemical staining for CD31.

4.2.2. Results – Simultaneous delivery of VEGF and SDF-1

Image analysis performed on vascularization devices harvested on day 20 revealed that

simultaneous delivery of 1500ng VEGF-A/day and 150ng SDF-1/day resulted in a vascularization area of 3.03±0.28% (see Fig.24). This did not differ significantly from controls solely delivering 150ng SDF-1/day (2.48±0.19%, n=6, p=0.076). Importantly, no effect on vascular stability was

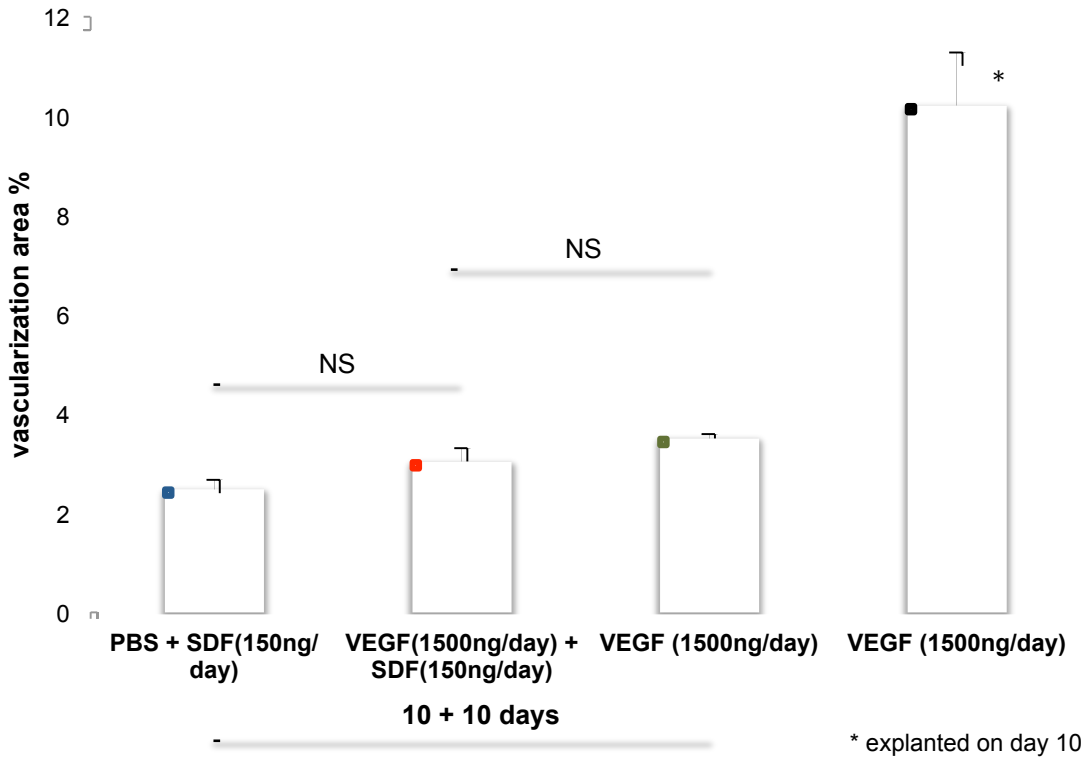

Fig.24. Immunohistochemical analysis of CD31+ vessels shows that the simultaneous delivery of VEGF-A and SDF-1 for 10 days has no synergistic effects on enhancing the stability of newly formed vessels. Immunohistochemical analysis revealed that the neovascularization at day 20 is not significantly different in neovascularization devices administered with VEGF alone.

observed, when VEGF and SDF-1 were delivered in tandem. As previously observed after delivering 1500ng/day VEGF for 10 days, growth-factor-induced neovessels had entirely regressed by day 20 (-236.6%, historical comparison).

4.3. Is regression of VEGF-induced neovasculature MMP-mediated?

Matrix metalloproteinases are critically involved in both the creation and remodelling of neovessels and in the degradation of immature vasculature[46,70-73,74]. MMPs have been described as potential contributors to neovascular regression[74,75], that may be targeted for therapeutic purposes. In three-dimensional collagen matrices Saunders et al. were able to show that suppression of EC-derived TIMP-2 and pericyte-derived TIMP-3 expression using siRNA resulted in capillary tube regression in an MMP-dependent manner[302]. These data directly implicated TIMP-2 and TIMP-3 in the pericyte-mediated enhancement of neovascular stability. Similar inhibition of regression was also observed with GM6001, an MMP-inhibitory small molecule.

In order to investigate a potential role of MMPs in vascular stability and the degradation of VEGF-induced neovasculature, GM6001 was delivered to block MMP activity after creation of the capillary bed. After delivering 1500ng VEGF/day over the course of 10 days, osmotic pumps were exchanged and GM6001 was administered at 2.5, 25 or 250mM, respectively, for an additional 10 days. The devices were harvested for histological analysis on day 20 and the vascularization area was assessed by immunohistochemical analysis with an antibody targeting CD31.

4.3.1. Results

Vessel ingrowth area after 20 days was 2.71±0.41%, 3.68±0.52% and 3.01±0.52% for GM6001 delivered at 2.5, 25 and 250mM, respectively (n=5-6, see Fig.25). No significant difference in vascularization was observed between the different dosages of GM6001 (p=0.36 25vs250mM; p=0.65 2.5vs250mM; p=0.2 2.5vs25mM GM6001). Furthermore, when compared with sole delivery of 1500ng VEGF/day vascularization measured on day 20 did not differ significantly at any dosage (VEGF 10+10: 3.5±0.09%, p=0.17 (GM6001 (2.5mM) vs. VEGF 10+10), p=0.78 (GM6001 (25mM) vs. VEGF 10+10), p=0.44 (GM6001 (250mM) vs. VEGF 10+10)). When compared to vessel ingrowth area induced by 1500ng VEGF/day around it's peak on day 10,

vascularization on day 20 was reduced by 276.4%, 177.2% and 238.8% after administration of GM6001 at 2.5, 25 and 250mM, respectively.

While this result cannot exclude an important role for specific MMPs in regulating the fate of immature vessels, it shows that broad inhibition of MMPs with GM6001 does not prevent unstable VEGF-induced vessels from regressing.

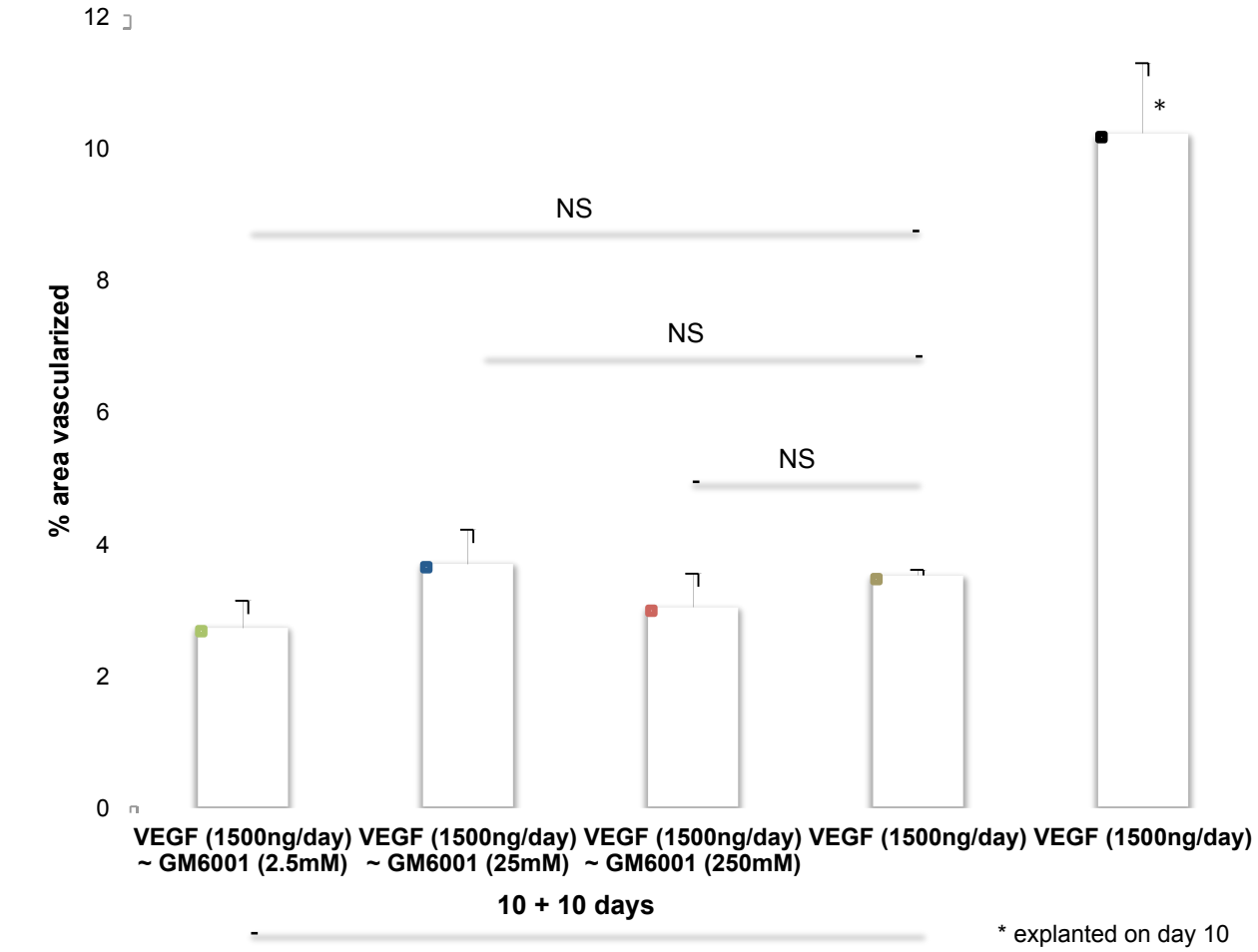

Fig.25. Vascularization area was assessed by analysis of CD31^{+}-vessels on day 20. VEGF-induced neovasculature is not stabilized by sequential delivery of the MMP-inhibitory small molecule (GM6001) at dosages ranging from 2.5 to 250mM.

4.4. Does PlGF create a more stable vasculature than VEGF?

Does the simultaneous delivery of VEGF-A, VEGF-C and PLGF promote vascular stability?

PlGF-induced vessels have been described as possessing a more stable phenotype than vessels created by VEGF delivery. A possible explanation offered has been the ability of PlGF to affect not only endothelial cells[127], but also smooth muscle cells, and macrophages, the three main cell types involved in the growth of collaterals[31,129]. While the simultaneous delivery of VEGF-A, VEGF-C and PlGF did not further promote short-term neovascularization in comparison with VEGF-A delivery alone, vascular stability may still be enhanced after concurrent stimulation of the lymphatic vasculature[285].

In order to investigate whether PlGF is superior in promoting vascular stability in comparison with VEGF, 1500ng PlGF/day were delivered for 10 days. After an additional 10 days, the neovascularization devices were explanted and neovessel stability was assessed by immunohistochemical staining for CD31.

To test whether the combinatorial delivery of VEGF-A, VEGF-C and PlGF induces a more stable vasculature, 150ng/day of each growth factor were delivered simultaneously over a period of 10 days, and after explanting the neovascularization devices on day 20, the effects on neovessel stability was determined by CD31 staining.

4.4.1. Results - PlGF

As previously shown, the delivery of 1500ng/day VEGF enhanced short-term neovascularization significantly more than the delivery of 1500ng/day PlGF (Fig.26). Vessel ingrowth area on day 10 after continuous growth factor delivery was 8.76±1.12% in neovascularization devices after VEGF delivery compared with 5.00±0.39% if PlGF was administered (p=0.013, n=4-6). When vascular stability of the induced neovasculature was assessed on day 20, 10 days after

termination of growth factor delivery, vessel ingrowth area for both treatments was not significantly different, as vascularization area for PlGF and VEGF-grafts was measured at 3.26±0.3 and 3.5±0.09%, respectively (p=0.55, n=4-6). While only 53% of neovessels seen on

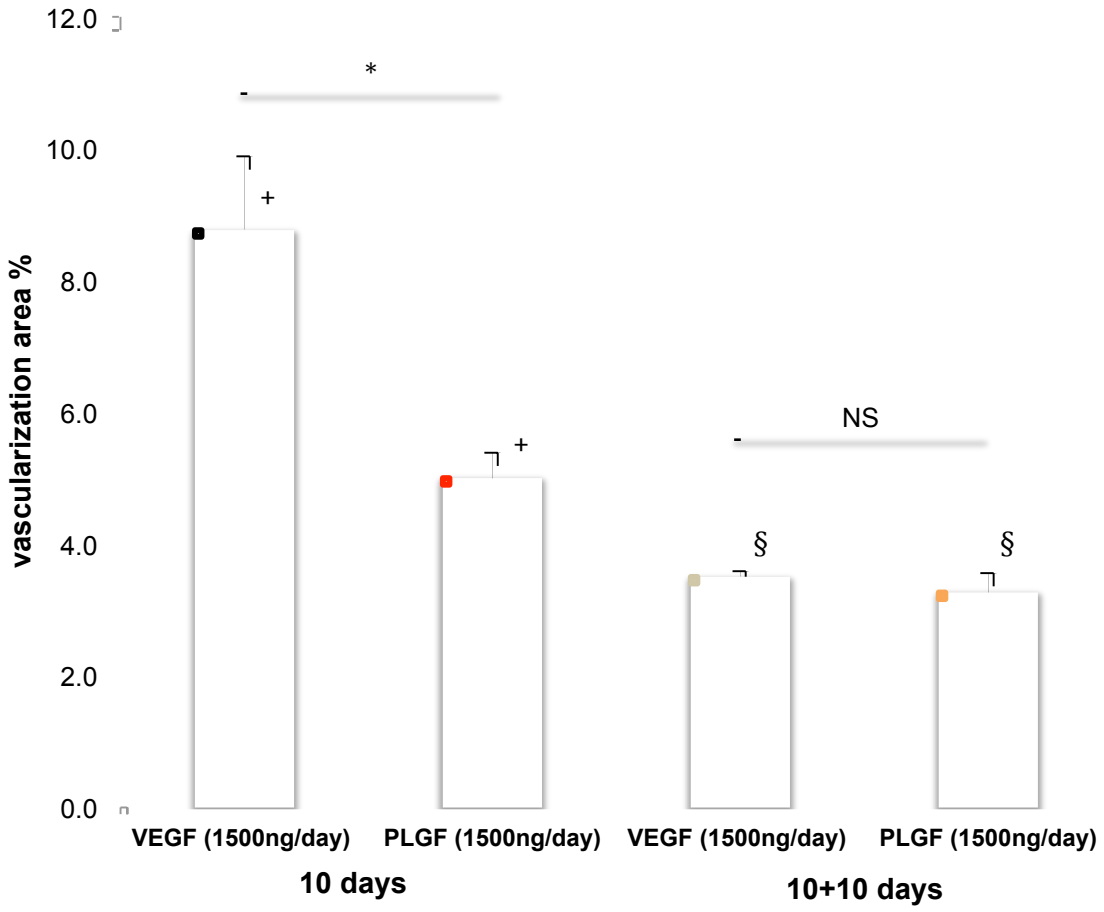

*Fig.26. Immunohistochemical analysis of CD-31^{+}-vessels after delivery of 1500ng/day PlGF or VEGF, respectively, was performed. On day 10 ($^{+}$), vascularization was significantly higher in neovascularization devices after VEGF administration in comparison with PlGF (*p<0.05). When devices were explanted on day 20, 10 days after termination of growth factor delivery (§), no significant difference was seen between the two treatment groups (p<0.05) and PBS controls (data not shown), indicating that neither VEGF nor PlGF can create a stable vasculature after delivered at high dosages.*

day 10 regressed after PlGF-administration, VEGF-grafts showed a three-fold higher regression of vessels on day 20 (-150%). Regardless, just as seen for VEGF, vessel ingrowth area measured on day 20 was not significantly different in PlGF-grafts when compared with PBS

controls (p=0.57, n=4-6, data not shown). Thus, when administered at high dosages (1500ng/day), PlGF did not promote a more stable neovasculature than VEGF.

4.4.2. Results – Simultaneous delivery of VEGF-A, VEGF-C, PlGF

Previous experiments had shown that when delivered continuously over 10 days, the simultaneous delivery of 150ng/day of VEGF-A, VEGF-C and PlGF did not further enhance short-term neovascularization in comparison with only delivering 150ng VEGF/day (6.39±0.87%

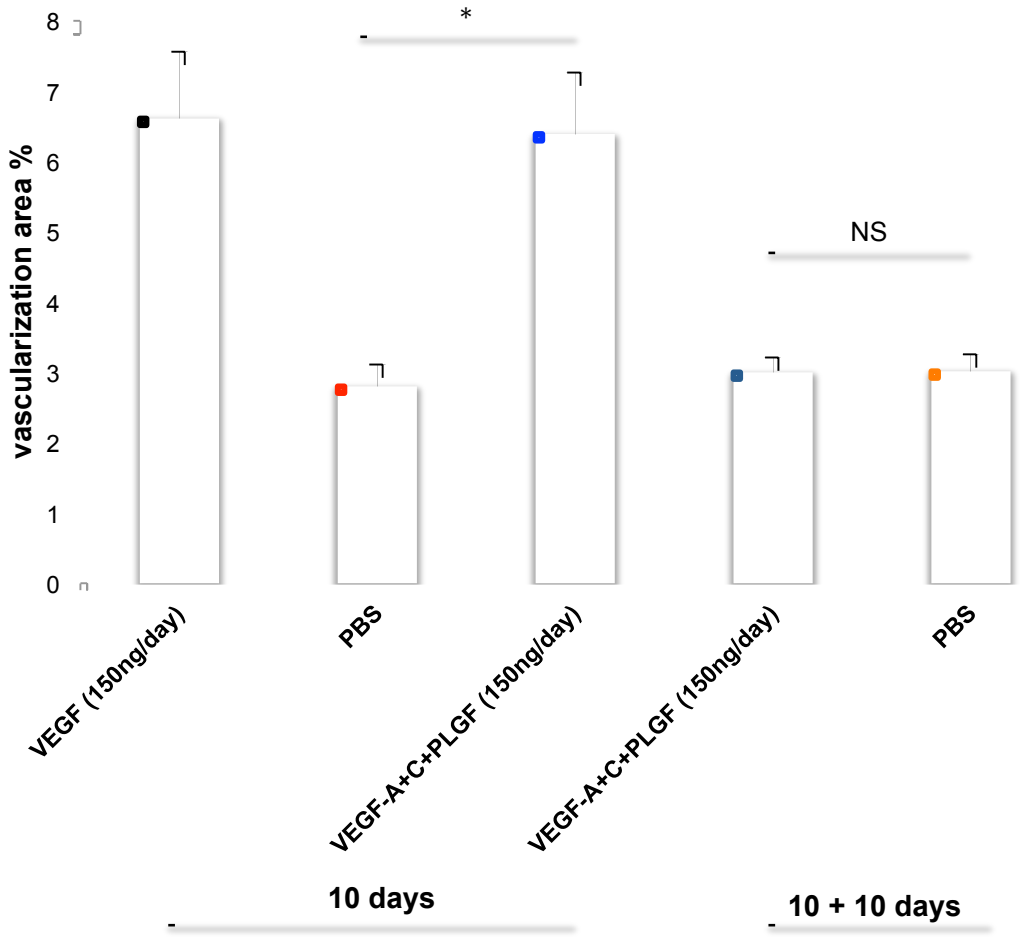

Fig.27. To assess the effects of simultaneous short-term delivery (10 days) of VEGF-A, VEGF-C and PlGF (150ng/day each), neovascularization devices were harvested 10 days after stoppage of growth factor delivery. Quantification of vessel ingrowth area showed that neovascular stability is not enhanced after combined delivery. Vessel regression was not prevented until day 20 and vascularization area was indistinguishable from PBS controls (p>0.05).

compared with 6.61±0.95%, respectively; p>0.05, n=6, see Fig.13). After stoppage of growth factor delivery on day 10 neovascularization devices were harvested on day 20 to assess the effects of simultaneously delivering VEGF-A, VEGF-C and PlGF on vessel stability. At this timepoint, 3.00±0.21% of the graft was vascularized, demonstrating that the combined short-term delivery of these three VEGF-family members does not promote vessel maturation and stability.

4.5. Discussion – Strategies to prevent regression of VEGF-induced neovasculature

A number of strategies to promote vascular maturation and long-term vascularization were previously described in the literature. Importantly, these previous studies were designed to test the potential of growth factors and combinations thereof to promote long-term neovascularization rather than examining factors that modulate maturation as opposed to regression in therapeutic angiogenesis after successful establishment of a new capillary bed. The potential of PlGF to promote vessel maturation and to create a stable vasculature has been described as superior in comparison with VEGF[31,127,129]. This finding was not observed using our angiogenesis assay (see Fig. 26). Again, timing and mode of delivery, growth factor dosage and tissue specificity are the most likely candidates that may explain this discrepancy. A strong case for the importance of growth factor dosage and the duration of growth factor administration can be made in light of previous findings. When testing the effects of short-term delivery of PlGF on vessel stability, a dosage of 1500ng/day PlGF was chosen. Findings from the more comprehensive investigation into the long-term stability of VEGF-induced neovasculature suggest that the high PlGF dosage may have been the underlying cause for this negative result. When PlGF was co-administered with VEGF-A and VEGF-C at 150ng/growth factor/day for 10 days, the neovasculature had also regressed by day 20 (see Fig.27). As VEGF-A successfully promoted long-term vessel stability when delivered at 150ng/day for 6 weeks, these experiments collectively suggest that short-term delivery (10 days) of the tested growth factors (VEGF-A, PlGF) is not sufficient to create a stable vasculature.

As the underlying mechanisms regulating vascular regression after pro-angiogenic therapy with high dosages of VEGF (1500ng/day) are currently not well understood, three independent hypotheses suggested in the literature were tested: a) that newly created capillary beds are dependent on continuous VEGF-supply[294,300]; b) that the stability of VEGF-induced vessels is SDF-1-dependent[84,246]; and c) that matrix metalloproteinases promote vascular regression after termination of VEGF-administration[74,75]. Neither one of these strategies did successfully prevent vessel regression, as vessel ingrowth area was indistinguishable from controls on day 20 (see Figs. 22-25). The nature of these findings is likely multifactorial as well. SDF-1 and GM6001 may not have reached therapeutic levels necessary to prevent the regression of VEGF-induced neovasculature; higher levels of VEGF could be necessary to promote EC survival in order to shift the balance between maturation and regression. Furthermore, a more complex in vivo setting may have contributed to prevent the successful inhibition of MMP-dependent capillary tube regression previously demonstrated in vitro[302].

Importantly, differences may exist between the regulatory mechanisms that control vascular stability and regression during physiological, pathological and therapeutic angiogenesis (depending on the growth factor regimen selected). Future therapeutic angiogenesis strategies will require the development of growth factor-specific assays that enable the identification of regulators determining vascular regression.

4.6. Identification of potential candidates that regulate the regression of VEGF-induced neovasculature

Factors contributing to an unstable vasculature (prone to regression) are largely unknown and the process of vascular regression remains incompletely understood. An observation in earlier experiments revealed that after 30 days of high VEGF delivery around 50% of the grafts were still highly vascularized, whilst neovessels in the other half of the grafts had completely regressed to levels comparable with PBS controls.

To identify factors that contribute to vascular stability and regression after VEGF delivery, a quantitative real-time PCR-based rat angiogenesis gene array was performed. Advanced primer design in the RT2 Profiler PCR Array System guarantees that every single q-RT-PCR reaction creates highly specific amplicons for each gene without co-amplifying non-specific byproducts. As each single reaction is optimized for standard condition, a panel of pathway-specific genes can be assayed simultaneously. Importantly the high reproducibility of these arrays has previously been demonstrated allowing comparison between samples run on different q-RT-PCR plates. 2 neovascularization devices per rat were implanted subcutaneously into 4 rats and VEGF was continuously delivered for 30 days at 1500ng/day. Vascularization devices were then harvested and RNA was isolated to allow the determination of the expression levels of angiogenic growth factors, growth factor inhibitors, adhesion molecules, proteases, and transcription factors.

4.7.1. Results - Immunohistochemistry

4 rats were used for this study. A total of 8 neovascularization devices were implanted. After harvest on day 30, the vascularization devices were cut in half. One half was used for RNA isolation, while the other one was processed for histological analysis of neovascularization by immunohistochemical analysis of CD31.

Image analysis confirmed the previous finding that continuous delivery of high VEGF dosages (1500ng/day) for 30 days results in neovascular regression 50% of the time (shown in Fig.28). Interestingly, this effect was rat-specific, as in each of the 4 animals both grafts were either highly vascularised or showed vascular regression to levels indistinguishable from controls.

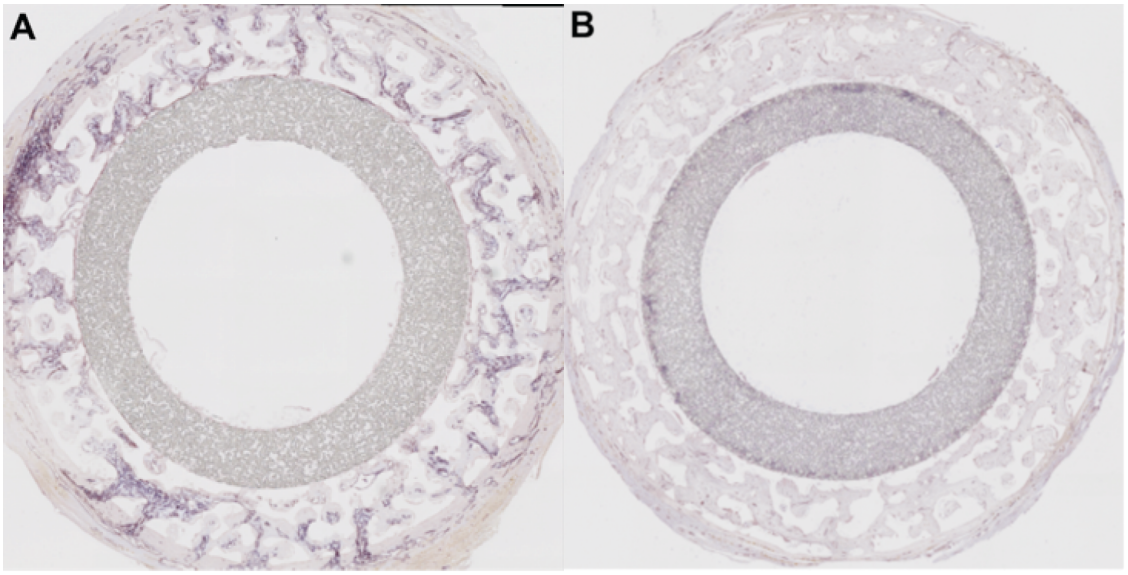

Fig. 28. Vascularization devices were harvested after 30 days of continuous VEGF delivery (1500ng/day). Immunohistochemical analysis of $CD31^{+}$-vessels confirmed that devices were either highly vascularised (4/8, 50%, Fig.28a) or showed postangiogenic vascular regression (4/8, 50%, Fig.28b).

4.7.2. RNA quality control

After isolation, high RNA quality was confirmed using a bioanalyzer at the Centre for Proteomic and Genomic Research (CPGR, located at the University of Cape Town), before proceeding with reverse transcription and sample preparation for the qRT-PCR-based gene array (see. Fig.29).

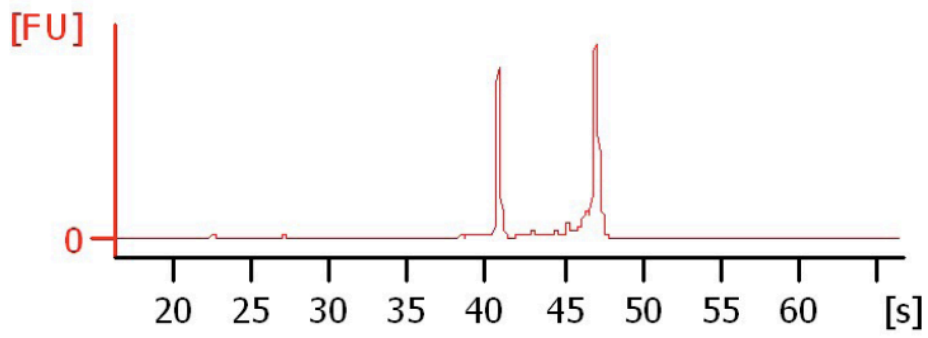

Fig.29. Representative electropherogram used to analyze the quality of RNA preparation is shown. Sharp peaks without shoulders for the 18S (left peak) and 28S (right peak) ribosomal RNA confirm high quality of total RNA.

4.7.3. Rat angiogenesis RT2 Profiler PCR Array

The expression profiles of 84 angiogenesis-related genes were determined. Significant differences were found for 24 genes when comparing neovascularization devices with a stable vasculature with grafts showing complete vascular regression ($p<0.05$, see table 1). Of these 24 genes, 17 were downregulated (14 by more than 2-fold) after vascular regression, while 7 genes were upregulated (6 by more than 2-fold). As expected, the regression of VEGF-induced neovasculature – from roughly 10% vascularization area to 2% (5-fold) – was concomitant with the significantly reduced expression of genes expressed by endothelial cells. Angiopoietin-2 (-4.35 fold), vascular endothelial cadherin (-3.35 fold), vascular endothelial growth factor receptor-1 (-4.23 fold), vascular endothelial growth factor receptor-2 (-5.46 fold), endothelial TEK tyrosine kinase (-4.35 fold), endothelial PAS domain protein 1 (-4.38 fold), endothelial differentiation gene 1 (-2.26 fold) and platelet/endothelial cell adhesion molecule 1 (-1.95 fold) were down-regulated. After neovascular regression, a significant up-regulation of Chemokine (C-X-C motif) ligand 2 (MIP-2, 12.17 fold), MMP3 (7.77 fold), Interleukin 1β (4.19 fold), TIMP1 (2.97 fold), Serpin F1/PEDF (2.89 fold), Ephrin A5 (2.56 fold) and Transforming growth factor β2 (1.97 fold) was observed. Levels of collagen type IV α3 (Tumstatin, 5.83 fold), collagen type XVIII α1 (Endostatin, 4.63 fold), laminin α5 (2.53 fold), transforming growth factor α (2.41 fold), jagged 1 (2.23 fold), fibroblast growth factor 1 (2.15 fold), plasminogen (2.05 fold), connective tissue growth factor (1.87 fold) and inhibitor of DNA binding 3 (1.71 fold) were significantly reduced. Trends towards a significantly reduced expression of fibroblast growth factor receptor 3 (-3.41 fold, $p=0.059$), vascular endothelial growth factor C (-2.53 fold, $p=0.068$), prostaglandin-endoperoxide synthase 1 (-2.38 fold, $p=0.097$), platelet-derived growth factor α (-2.39 fold, $p=0.13$) and platelet-derived growth factor β (-2.06 fold, $p=0.11$) were seen, while vascular endothelial growth factor A gene expression tended to be upregulated (+2.75 fold, $p=0.12$).

4.7.4. Discussion

Numerous angiogenic stimuli and factors controlling vascular stability have been identified, yet little is known about regulators that determine the fate of growth factor-induced neovessels. Two

prominent angiogenesis inhibitors were significantly upregulated in vascular grafts after neovascular regression, namely serpin F1 (better known as pigment epithelium-derived factor, PEDF, 2.89 fold up-regulation) and chemokine ligand 2 (CXCL2, also known as gro-β, 12.17 fold upregulation). Strong evidence exists supporting a critical interaction between VEGF and PEDF in regulating angiogenesis. Clinical studies have shown that loss of PEDF in combination with an increased expression of VEGF is a major stimulus for retinal angiogenesis[303]. Elevated levels of PEDF suppress VEGF-induced growth and migration of retinal endothelial cells while also inhibiting retinal neovascularization[304]. While this role for PEDF in inhibiting angiogenesis in the eye has been well established, PEDF has recently emerged as a critical regulator of microvascular density in prostate cells, pancreas[305] and the liver[306]. Counterbalancing VEGF levels after castration, PEDF was shown to critically regulate prostate regression, thereby establishing an interaction between PEDF and vascular endothelial growth factor in this organ. The most direct evidence implicating PEDF in the regression of VEGF-induced neovasculature, though, stems from a study showing that adenoviral delivery of PEDF induces regression of ocular neovascularization in rho/VEGF mice[307]. CXCL2, expressed by monocytes[308] that are highly present in granulation tissue, was shown to dose-dependently inhibit growth factor-induced capillary endothelial cell proliferation[309], and to inhibit angiogenesis in a chicken chorioallantoic membrane assay. Furthermore, CXCL2 delivery successfully slowed Lewis lung tumour growth by halting tumour-induced neoangiogenesis. MMP-3 and TIMP-1 upregulation (by 7.77 and 2.97 fold, respectively) may contribute to vascular regression by either modulating extracellular matrix turnover (and thereby releasing angiogenesis inhibitors) or by preferential splicing of vascular endothelial growth factor[310].

Growth factor interactions have long been known to significantly contribute to vascular stability[59,157,207]. Amongst others, fibroblast growth factor, angiopoietins and platelet-derived growth factor B have been shown to modulate long-term vascularization in concert with VEGF. Neovascular regression was coupled to significant reductions in gene expression levels of the pro-angiogenic factors FGF-1, connective tissue growth factor, jagged-1 and TGF-α. In addition the expression of EGF, PDGFα, PDGFβ, VEGF-C and FGFR3 was markedly reduced (albeit not

significant). These findings suggest that a lack of supporting growth factors or an impaired establishment of growth factor gradients may contribute to the untimely vascular regression. Another group of proteins that may contribute to the instability of VEGF-induced vasculature are the inhibitors of DNA binding 1 (Id 1) and 3 (Id 3). These proteins are highly expressed in endothelial cells of tumour infiltrating blood vessels[311] and it has previously been described that tumour growth and angiogenesis is impaired in Id1-Id3 double knockout mice[312]. In samples showing a regressed neovasculature, Id3 was significantly downregulated (-1.71 fold, $p<0.05$), while a strong trend was observed for Id1 (-2.1 fold, $p=0.098$). Interestingly, Id1 was recently identified as a selective marker of endothelial progenitor cells[313]. It is therefore intriguing to hypothesize that the number of endothelial progenitor cells contributes to the stability of VEGF-induced neovasculature. This draws further support from the finding that regression of VEGF-induced neovessels was a rat specific event, as in all 4 animals the neovascularization levels were similar in both implanted grafts.

Gene	AVG ΔC_t (Ct(GOI) - Ave Ct (HKG))		$2^{-\Delta C_t}$		Fold Difference	T-TEST	Fold Up- or Down-Regulation
	Test Sample	Control Sample	Test Sample	Control Sample	Test Sample /Control Sample	p value	Test Sample /Control Sample
Angpt2	7.35	5.23	6.1E-03	2.7E-02	0.23	0.0085	-4.35
Akt1	2.73	2.23	1.5E-01	2.1E-01	0.71	0.3831	-1.41
Angpt1	5.82	5.49	1.8E-02	2.2E-02	0.80	0.4881	-1.25
Anpep	2.49	2.36	1.8E-01	2.0E-01	0.92	0.6388	-1.09
Bai1_predicted	13.66	12.88	7.7E-05	1.3E-04	0.58	0.2543	-1.72
Ccl2	3.54	3.48	8.6E-02	9.0E-02	0.96	0.9292	-1.04
Cdh5_predicted	5.35	3.61	2.4E-02	8.2E-02	0.30	0.0126	-3.35
Col18a1	4.39	2.18	4.8E-02	2.2E-01	0.22	0.0037	-4.63
Col4a3	12.75	10.20	1.5E-04	8.5E-04	0.17	0.0248	-5.83
Ctgf	4.03	3.13	6.1E-02	1.1E-01	0.53	0.0339	-1.87
Cxcl1	5.50	6.73	2.2E-02	9.4E-03	2.34	0.2105	2.34
Cxcl2	2.27	5.87	2.1E-01	1.7E-02	12.17	0.0105	12.17
Cxcl9	5.43	5.21	2.3E-02	2.7E-02	0.86	0.8251	-1.17
Ecgf1	8.58	8.72	2.6E-03	2.4E-03	1.10	0.7351	1.10
Edg1	5.71	4.54	1.9E-02	4.3E-02	0.44	0.0017	-2.26
Ephrin A1	5.61	4.44	2.0E-02	4.6E-02	0.44	0.0689	-2.25
Ephrin A2	8.10	7.44	3.7E-03	5.7E-03	0.64	0.3994	-1.57
Ephrin A5	6.83	8.19	8.8E-03	3.4E-03	2.56	0.0271	2.56
Egf	14.49	11.75	4.3E-05	2.9E-04	0.15	0.2100	-6.68
Endoglin	2.40	1.61	1.9E-01	3.3E-01	0.58	0.1023	-1.72
Epas1	3.63	1.50	8.1E-02	3.5E-01	0.23	0.0024	-4.38
Epiregulin	9.87	11.76	1.1E-03	2.9E-04	3.69	0.2719	3.69
F2	5.98	6.92	1.6E-02	8.2E-03	1.92	0.5606	1.92
Fgf1	9.61	8.51	1.3E-03	2.7E-03	0.47	0.0000	-2.15
Fgf16	11.99	13.36	2.5E-04	9.5E-05	2.59	0.1733	2.59
Fgf2	11.98	12.70	2.5E-04	1.5E-04	1.65	0.6360	1.65
Fgf6	13.94	13.35	6.4E-05	9.6E-05	0.66	0.4813	-1.51
Fgfr3	10.35	8.58	7.7E-04	2.6E-03	0.29	0.0590	-3.41
Figf	6.83	7.52	8.8E-03	5.4E-03	1.61	0.3048	1.61
Flt1	7.78	5.70	4.5E-03	1.9E-02	0.24	0.0011	-4.23
Fibronectin 1	0.81	1.35	5.7E-01	3.9E-01	1.45	0.3017	1.45

Gene	AVG ΔC_t (Ct(GOI) - Ave Ct (HKG))		$2^{-\Delta C_t}$		Fold Difference	T-TEST	Fold Up- or Down-Regulation
	Test Sample	Control Sample	Test Sample	Control Sample	Test Sample /Control Sample	p value	Test Sample /Control Sample
Fzd5	7.98	8.12	4.0E-03	3.6E-03	1.10	0.7159	1.10
Hgf	5.54	6.08	2.1E-02	1.5E-02	1.46	0.3530	1.46
Hif1a	2.42	3.22	1.9E-01	1.1E-01	1.75	0.1161	1.75
Id1	5.71	4.64	1.9E-02	4.0E-02	0.48	0.0984	-2.10
Id3	3.28	2.51	1.0E-01	1.8E-01	0.58	0.0418	-1.71
Ifna1	14.49	14.01	4.3E-05	6.1E-05	0.71	0.7645	-1.40
Ifnb1	13.65	13.08	7.8E-05	1.2E-04	0.67	0.4091	-1.48
Ifng	10.93	11.84	5.1E-04	2.7E-04	1.88	0.3478	1.88
Igf1	1.87	3.77	2.7E-01	7.3E-02	3.73	0.5220	3.73
Il1b	2.33	4.39	2.0E-01	4.8E-02	4.19	0.0232	4.19
Il6	5.59	5.50	2.1E-02	2.2E-02	0.94	0.8824	-1.06
Itga5	5.18	4.02	2.8E-02	6.2E-02	0.45	0.0685	-2.24
Itgav_predicted	5.11	4.18	2.9E-02	5.5E-02	0.52	0.0813	-1.91
Itgb3	5.94	5.35	1.6E-02	2.4E-02	0.67	0.2066	-1.50
Jag1	5.03	3.87	3.1E-02	6.8E-02	0.45	0.0214	-2.23
Kdr	5.98	3.53	1.6E-02	8.6E-02	0.18	0.0116	-5.46
Lama5	6.47	5.13	1.1E-02	2.9E-02	0.40	0.0071	-2.53
Lect1	12.14	11.83	2.2E-04	2.7E-04	0.81	0.7694	-1.24
Lep	14.11	11.77	5.6E-05	2.9E-04	0.20	0.2124	-5.06
Mapk14	5.22	5.40	2.7E-02	2.4E-02	1.13	0.6523	1.13
Mdk	4.55	4.77	4.3E-02	3.7E-02	1.16	0.5000	1.16
Mmp19_predicted	3.55	3.27	8.6E-02	1.0E-01	0.83	0.6675	-1.21
Mmp2	4.03	4.42	6.1E-02	4.7E-02	1.31	0.6991	1.31
Mmp3	2.36	5.31	2.0E-01	2.5E-02	7.77	0.0080	7.77
Mmp9	4.64	4.58	4.0E-02	4.2E-02	0.96	0.9193	-1.05
Npr1	6.82	6.12	8.8E-03	1.4E-02	0.61	0.0766	-1.63
Nrp1	3.09	2.60	1.2E-01	1.7E-01	0.71	0.3516	-1.40
Nrp2	5.90	5.05	1.7E-02	3.0E-02	0.55	0.1345	-1.80
Pdgf1	9.11	7.85	1.8E-03	4.3E-03	0.42	0.1295	-2.39
Pdgfb	5.10	4.06	2.9E-02	6.0E-02	0.49	0.1120	-2.06
Pecam	3.72	2.75	7.6E-02	1.5E-01	0.51	0.0128	-1.95
Pgf	8.44	7.52	2.9E-03	5.4E-03	0.53	0.1834	-1.89
Plau	3.10	3.10	1.2E-01	1.2E-01	1.01	0.9873	1.01
Plg	12.41	11.37	1.8E-04	3.8E-04	0.49	0.0338	-2.05
Ptgs1	8.12	6.87	3.6E-03	8.6E-03	0.42	0.0972	-2.38
Serpinb5	14.49	14.45	4.3E-05	4.5E-05	0.97	0.9843	-1.03
Serpinf1	0.02	1.56	9.8E-01	3.4E-01	2.89	0.0025	2.89
Sphk1	8.43	7.90	2.9E-03	4.2E-03	0.69	0.2903	-1.45
Tbx4_predicted	12.72	14.12	1.5E-04	5.6E-05	2.64	0.3257	2.64
Tek	6.80	4.68	9.0E-03	3.9E-02	0.23	0.0046	-4.35
Tgf1	12.22	10.95	2.1E-04	5.1E-04	0.42	0.0434	-2.41
Tgfb1	3.81	3.09	7.2E-02	1.2E-01	0.61	0.0865	-1.64
Tgfb2	6.57	7.55	1.1E-02	5.3E-03	1.97	0.0245	1.97
Tgfb3	10.87	10.66	5.3E-04	6.2E-04	0.87	0.5651	-1.16
Tgfbr1	1.96	1.95	2.6E-01	2.6E-01	0.99	0.9756	-1.01
Thbs4	10.75	12.05	5.8E-04	2.4E-04	2.46	0.3428	2.46
Timp1	-0.60	0.97	1.5E+00	5.1E-01	2.97	0.0260	2.97
Timp2	2.03	2.38	2.4E-01	1.9E-01	1.27	0.3930	1.27
Timp3	2.98	2.40	1.3E-01	1.9E-01	0.67	0.3292	-1.49
Tnf	5.67	6.12	2.0E-02	1.4E-02	1.37	0.4076	1.37
Vegfa	5.14	6.59	2.8E-02	1.0E-02	2.75	0.1230	2.75
Vegfb	11.37	11.72	3.8E-04	3.0E-04	1.27	0.7535	1.27
Vegfc	6.05	4.71	1.5E-02	3.8E-02	0.39	0.0683	-2.53
Rplp1	-1.87	-1.59	3.7E+00	3.0E+00	1.22	0.1802	1.22
Hprt	3.09	3.00	1.2E-01	1.2E-01	0.94	0.7640	-1.06
Rpl13a	0.21	0.09	8.6E-01	9.4E-01	0.92	0.5949	-1.09
Ldha	0.85	0.93	5.6E-01	5.2E-01	1.06	0.6884	1.06
Actb	-2.28	-2.44	4.9E+00	5.4E+00	0.89	0.6463	-1.12

Table 1. Results from rat angiogenesis RT2 Profiler PCR Array

4.7.5. Conclusion

The results obtained from quantitative real-time PCR-based rat angiogenesis gene array studies implicate numerous factors in the regression of VEGF-induced neovasculature in our subcutaneous wound healing model and are of interest for further investigation. To substantiate these preliminary findings, these experiments need to be repeated to increase the number of replicates and protein levels of the differentially regulated genes need to be analysed by western analysis or immunohistochemistry to confirm the changes seen in gene expression levels. While these are clearly the confirmatory experiments needed, these studies were not performed due to time constraints.

5. SUMMARY: Angiogenesis chapter

Therapeutic angiogenesis has evolved into a promising strategy to treat ischemia-induced cell death, which underlies various cardiovascular pathologies. Developing strategies to create a mature and stable vasculature has been challenging due to a lack of suitable in vitro and in vivo models. Therefore a novel in vivo angiogenesis model that allows for characterization of stability and mural cell investment of newly created vessels was designed. Amongst a number of growth factors tested, vascular endothelial growth factor-A^{165} (VEGF) emerged as the most potent initiator of neovascularization in initial experiments. Subsequent studies showed that VEGF concentration plays a critical role in the nature and persistence of neovessels in a biomaterial scaffold. When VEGF was delivered at 150ng/day for 42 days, scaffold neovessels were found to be stable for up to 2.5 months after withdrawal of VEGF. At this timepoint, vessels induced by a 10-fold higher concentration of VEGF had regressed to levels comparable with PBS controls. Using the angiogenesis assay, a timeline was established illustrating that, when delivered at the highest dosage of 1500ng/day, termination of VEGF delivery resulted in diminished perfusion of the neovasculature within 48 hours, followed by rapid regression of the vascular network. A series of experiments testing the potential of PlGF and various growth factor combinations

(VEGF+SDF-1, VEGF-A+VEGF-C+PlGF) to promote neovascular stability and/or to prevent neovascular regression revealed that apart from the growth factor dosage, the duration of growth factor delivery is a critical determinant of long-term vessel stability. As previous strategies described to enhance vessel maturation did not prevent the rapid regression of the neovasculature induced by high VEGF dosages, a gene expression array was performed, identifying serpin F1, CXCL2, PEDF, and inhibitors of DNA binding as potential fate regulators of VEGF-induced neovessels. Their exact roles and underlying mechanisms will have to be tested in future experiments.

Overall, the major finding of the performed angiogenesis experiments was the identification of advantageous delivery conditions for VEGF to induce long-term therapeutic neovascularization. As myocardial ischemia remains one of the major pathologies hypothesized to benefit greatly from therapeutic neovascularization, the hypothesis that these findings might be applied in the setting of myocardial ischemia was tested next.

6. INTRODUCTION: Myocardial Infarction

An estimated 8 million Americans have previously suffered a myocardial infarct. According to recent statistics, 770 000 will present with a new coronary attack this year, an equivalent of 1 every 26 seconds, and about every minute someone will die from a MI[1]. Though early mortality after myocardial infarction has decreased over the past 20 years, the prevalence of heart failure is on the rise and studies have shown a close relationship between these two phenomena[2]. Today, 5.3 million Americans are suffering from heart failure[1], a syndrome characterized by reduced cardiac output, increased pressures in the venous system and various molecular abnormalities causing a progressive deterioration of the ailing heart[314,315].

Myocardial infarction is viewed as the most severe manifestation of ischemic heart disease (IHD), resulting in extensive cardiomyocyte death[316]. In more than 90% of cases, a reduced coronary blood flow due to atherosclerotic coronary arterial obstruction leads to a mismatch between supply of oxygenated blood and nutrients and demand of the heart [for oxygen and nutrients] and in parallel an inadequate removal of metabolites[316]. Acute myocardial infarction and unstable angina are commonly referred to as acute coronary syndromes, being frequently caused by a sudden plaque change[317]. These plaque changes, such as superficial erosion, ulceration, fissuring, rupture, or deep haemorrhage abruptly transform a stable atherosclerotic plaque to an unstable and life-threatening atherothrombotic lesion, putting at risk the cardiomyocytes downstream of the blocked artery.

6.1. Definition of myocardial infarction

Clinical features, electrocardiography, biochemical markers, imaging techniques and [histo]pathology are typically used to uncover myocardial necrosis and support the diagnosis of myocardial infarction[318]. In most cases, a myocardial infarct is preceded by longstanding atherosclerosis of a coronary artery. According to the response-to-injury hypothesis[319], this inflammatory process starts out as a reaction to endothelial dysfunction. A number of stimuli

are capable of damaging endothelial cells; amongst the more prominent are tobacco toxins[320], oxidized low density lipoprotein[321], reactive oxygen species[322] and high blood pressure[323]. The ensuing inflammatory process of the vascular wall promotes binding of circulating monocytes to the activated endothelial cells and their ensuing migration into the subendothelial layer[319]. Upon maturation to macrophages, these cells act as scavengers, taking up oxidized LDL and transforming into foam cells[319], which eventually rupture and deposit oxidized cholesterol onto the artery wall. The subsequent migration of smooth muscle cells from the media into the intima and their proliferation and fibrous transformation play a crucial part in rebuilding the plaque[319].

Atherosclerotic lesions range from fatty dots and streaks to fibroatheromas and complicated lesions. Whereas the vessel wall remodels outwards during the early phases, an expanding atherosclerotic plaque eventually results in the narrowing of the vessel lumen. The highest mortality from myocardial ischemia is typically seen in previously asymptomatic patients with acute plaque changes [before the plaque narrows the lumen] that lead to a complete obstruction of the coronary vessel, while the development of collateral vessels associated with recurrent minor ischemic episodes prior to myocardial infarction is associated with significantly lower in-hospital death and cardiogenic shock[324,325].

Myocardial ischemia is typically initiated by the change of an atherosclerotic plaque to an unstable lesion. Disruption of the plaque, e.g. by rupture, then leads to the activation of circulating thrombocytes and the coagulation cascade upon exposure of the highly thrombogenic subendothelial basement membrane and the lipid-rich centre of the plaque, thereby initiating the formation of an acute thrombus[326]. Within minutes the thrombus may then evolve and lead to the occlusion of a coronary artery and downstream myocardial ischemia. Contractility of the non-perfused segment of the heart is lost rapidly, within the first minute[327,328]. Irreversible cardiomyocyte death is first observed after 20 to 40 minutes[327,328]. In the case of a complete blockage of the coronary artery, the development of a transmural

myocardial infarct ensues with the necrosis stretching across the full thickness of the ventricular wall.

6.2. Course of events after acute myocardial infarction, compensatory mechanisms, post-infarction remodelling and progression to heart failure

Immediately after the coronary occlusion, there is a sharp drop in the contractility of the heart. Subsequently, less blood is ejected during the ensuing systole. A regular venous return thus produces an increased filling volume of the heart at the end of diastole. In agreement with the law of Starling, the higher end-diastolic volume, which corresponds to a higher preload, leads to an increase in contractility and subsequently to an increased stroke volume during the following systole[329].

In addition to the Frank-Starling mechanism, another important response to the hemodynamic changes that occur during MI is the activation of the neurohumoral system, aimed at upholding the blood pressure and thus ensuring the perfusion of vital organs[329]. At the root of the heart's short-term adaptive changes lies the activation of the sympathetic nervous system[330]. Increased adrenergic signalling and the stimulation of the renin-angiotensin-aldosterone system contribute to cardiac stimulation (increased inotropy, lusitropy, chronotropy and dromotropy), vasoconstriction (increased afterload) and fluid retention (increased preload). Secondly, the neurohumoral axis also initiates a proliferative response that promotes the initiation of a compensatory hypertrophy of the heart[315,330]. Collectively, the changes occurring on a molecular, cellular and structural level within the myocardium are known as ventricular remodelling. Together, they initially help a decreased number of cardiomyocytes, which are exposed to higher wall stresses according to the law of La Place, to carry an increased workload.

The ventricular remodelling occurring in the aftermath of a myocardial infarction has been suggested to be the result of a combination of increased pressure- and volume-load[331] and is characterized by thinning of the infarcted wall and an enlargement of the ventricular chamber.

The importance of this rebuilding process has emerged over the last 10 years, as various reports described that heart dimensions act as a meaningful surrogate marker for morbidity and mortality and have also proven their value in monitoring disease progression. Cardiac remodelling after a myocardial infarct is independently associated with a poor prognosis[332], and even fairly minor increases in ventricular volume are linked to a major independent increase in the risk of death in those patients[333]. Currently, the underlying mechanisms of this process on a cellular and molecular level are incompletely understood.

It has been suggested that early molecular and cellular changes in hypertrophied hearts that present compensatory mechanisms to adapt to elevated stresses/requirements post-MI depend on preferential activation of a set of signalling pathways promoting cell survival[334]. Cytoskeletal proteins have been linked to functioning as biomechanical sensors that transmit the increased loading conditions into a signal enhancing protein synthesis in cardiomyocytes[335,336]. The balance between adaptive mechanisms and detrimental changes, though, is fragile and not completely understood. During ventricular remodelling, the increase in cardiomyocyte size is not met by a comparable increase in capillary density, effectively increasing the distance between capillaries in the myocardium[337]. Furthermore, in the hypertrophied heart wall tension is elevated and higher metabolic demands need to be met[338,339]. Amongst other mechanisms responsible for pathological remodelling is a shift in the ratio of MMP´s and TIMP´s towards MMPs leading to an increased extracellular matrix turnover, which directly contributes to progressive LV dilation[340,341]. An enhanced formation of reactive oxygen species (ROS) and the activation of the neurohumoral pathway further increase the risk of cardiomyocyte death – in part via angiotensin II-mediated water retention and increased volume load on the heart which induce more stretch-induced abnormalities[342]. Eventually, the capacity of the infarcted heart to adjust to the combined volume- and pressure-load on non-infarcted areas of the myocardium is exhausted and leads to full onset of heart failure[331].

6.3. Mechanical properties of infarcted myocardium and their impact on ventricular function

The mechanical properties of the infarcted myocardium undergo characteristic changes after ischemic injury and 4 separate phases can be distinguished: a) acute ischemia (minutes to hours), b) the necrotic phase (hours to days 5-7), c) the fibrotic phase (between day 5 to 21) and d) the remodelling phase (21+ days)[343]. During acute ischemia, the infarcted myocardium loses its ability to generate force and contribute to systolic contraction, basically turning into a passive, viscoelastic material[328,344,345]. After a few hours, the infarct begins to stiffen[346,347] and the oedema responsible for that effect mainly controls the mechanical features until the end of the necrotic phase around day 7[348]. By increasing the stiffness, the oedema is hypothesized to prevent further expansion of the infarct. This theory is supported by studies showing that anti-inflammatory drugs like steroids[349,350], indomethacin[351,352] and ibuprofen[353], which reduce oedema, will lead to infarct expansion. Over the next month, during the fibrotic phase, collagen deposition[354-356] is the main influence on the mechanical characteristics of the infarcted area, further stiffening the infarct. During post-infarct remodelling, collagen crosslinking appears to be a critical variable affecting the infarct regions´ mechanical properties[357] and the scar remains stiffer than ischemic myocardium during the acute phase.

These changes in mechanical properties of the infarct region have a substantial impact on the remote areas of the heart and affect the function globally. Various scenarios may occur as a consequence, the most disastrous of which is myocardial rupture, which typically occurs during the first week[358,359]. Bulging or stretching of the infarct squanders some of the energy created by the viable myocardium. Stiff infarcts tend to show less systolic dysfunction[360] than compliant infarcts, which misuse a significant amount of energy[360-363], thereby reducing the heart´s efficiency and putting it at a higher risk of pump failure. The downside of overly stiff infarcts is that they may impact ventricular function by impairing[360] diastolic filling and restricting the ability to adjust left ventricular stroke volume by means of the Frank-Starling mechanism[364]. Another possible consequence after MI is infarct expansion[365] and dilation of

the ventricle. The mechanism underlying this complication is slippage of the diminished cardiomyocyte population[366]. As a result of ventricular dilation, a higher wall stress is necessary to achieve a given cavity pressure, since a smaller amount of the force generated by the cardiomyocytes is directed toward the centre of the ventricle. By continuously operating at a higher wall stress, the cardiomyocytes must perform additional internal work to stretch the heart, less external work is available for the ejection and cardiac efficiency is reduced. By being coupled to the infarcted region, adjacent myocardium is also affected and the functional border zone shows a decreased contractility despite normal perfusion during the acute phase of the infarct[367].

The relationship between regional myocardial contractility, wall stress and bioenergetics was recently described in a porcine model of myocardial infarction[368]. Increased wall stress in the infarct border zone was found to result in higher regional energy demand and bioenergetic abnormalities, leading to a decrease in myocardial bioenergetics efficiency[368]. As properties of the healing infarct influence mechanical variables (stress, strain, work) of the non-infarcted myocardium that give rise to adaptive stimuli[369] they are critical determinants for the remodelling of the ventricle that occurs after myocardial infarction[331]. Post-infarct ventricular remodelling may therefore precipitate the development of heart failure by driving the dilation of the cavity and the associated build-up in wall stress.

6.4. Current therapy for the prevention of heart failure – HF as a biomechanical model

Left-ventricular remodelling after myocardial infarction (MI) is a key component of heart failure and it has long been postulated that it may result from increased wall stress. While there have been advances in the medical therapy of heart failure, the only definite treatment currently known is heart transplantation, which suffers from a chronic shortage of organ donations. After early reperfusion, first line medical treatment of myocardial infarcts now consists of

angiotensin-converting enzyme (ACE)-inhibitors, angiotensin receptor blockers (ARB) and β-adrenergic antagonists (β-blockers). These medications break the vicious cycle of neurohumoral activation, vasoconstriction and water retention, decrease pre- and afterload and establish more favourable ventricular energetics. At least in part, the reduction of morbidity and mortality after myocardial infarcts by ACE-inhibitors, β-*blockers* and ARBs has been credited to the attenuation and partial reversal of the remodelling of the injured heart[370-378]. While heart failure can be stabilized using these treatment regimens, heart failure progresses in the majority of cases, even though this may occur more slowly[379]. The neurohumoral model of heart failure therefore does not entirely explain disease progression[380,381]. An increasing amount of evidence indicates that deterioration of HF may occur independently of activation levels of the neurohumoral axis. Thus, there is a high likelihood that a biomechanical component also drives progression of heart failure[382].

6.5. Biomaterials for treatment of ischemic myocardium

With the high prevalence of HF, substantial research has been devoted towards developing novel treatments with an emphasis on cell delivery. Questions have arisen as to whether the improved LV pump function observed in many cell delivery approaches has been solely a result of cellular paracrine signalling, causing myocardial regeneration, neovascularization[383] or decreased apoptosis[384], or whether changes found in ventricular function may purely or in part be a mechanical consequence of increasing the thickness of the LV wall [385,386]. Therefore the potential of biomaterial delivery into the ischemic heart to tackle post-infarct remodelling and progression into heart failure has begun to be explored.

Biomaterials have to meet numerous requirements to be considered potential candidates for tissue regenerative approaches. Most importantly, the materials need to be non-cytotoxic, non-immunogenic, non-infectious and when degradable, they must break down into non-toxic products[387]. Successful treatment of ischemic myocardium will further rely on selecting

biomaterials with adequate physical properties, such as mechanical strength, elasticity and viscosity. For additional protein delivery, non-covalent binding interactions and potential to control protein release will be of utmost importance.

Natural biomaterials such as collagen, fibrin, alginate and matrigel are amongst the materials used thus far to treat MI, and initial results have given reason for cautious optimism. Kofidis et al. reported that matrigel injections into an infarcted mouse heart increased wall/scar thickness and prevented deterioration of cardiac function. When delivered in combination with embryonic stem cells, matrigel injections significantly improved cardiac function[388]. In rats, collagen injections increased scar thickness and improved left ventricular stroke volume and ejection fraction[389]. Fibrin delivery was shown to increase the survival of co-delivered myoblasts, decrease infarct size and promote neovascularization[390]. In yet another report, alginate injections 7 days after myocardial infarction resulted in increased scar thickness and further attenuated left ventricular remodelling and cardiac dysfunction[391]. Furthermore, even after alginate injections into 60 day-old infarcts, an increase in scar thickness and functional improvement of the heart was observed[391-393]. In summary, increased wall/scar thickness[388,389,391], attenuation of adverse LV remodelling[391], decreased infarct size[390] and improvement of functional parameters[388,389,391] have all been described to result from treatment of MI by natural biomaterials.

Beneficial effects after synthetic biomaterial injections, which offer the advantage of enhanced control over characteristics such as degradation and mechanical properties, have also begun to be described. Performed concurrently with the work described in this thesis, studies showed that injection of self-assembling methoxy polyethylene glycol–poly (caprolactone)-(dodecanedioic acid)–poly(caprolactone)-methoxy polyethylene glycol (MPEG–PCL–MPEG) triblock polymer into rabbit and rat infarcts led to significant improvements in left-ventricular remodelling and function 4 weeks after treatment[394,395]. Reduced LV dilation and preserved contractility were reported after injection of a synthetic

thermoresponsive poly(NIPAAm-co-AAc-co-HEMAPTMC) hydrogel, up to 8 weeks after injection into 2-week-old infarcts[396].

While these initial results are promising, our current mechanistic understanding for the observed effects is insufficient. In a recent publication, Wall and colleagues used a finite element modelling approach in an attempt to shed light on some of the mechanisms responsible for LV improvement after material/cell injections into the heart[386]. They demonstrated that the injections help to normalize elevated wall stresses with stiffer materials showing greater benefit, improving ejection fraction and the stroke volume/end-diastolic volume relationship.

6.6. Polyethylene glycol (PEG) hydrogels

As novel synthetic biomaterials are being developed at a rapid rate, polyethylene glycol hydrogels have emerged as a frontrunner for the study of basic biologic processes and the development of tissue engineering-based therapies. A major advantage of synthetic biomaterials such as PEG over their natural counterparts is their easy purification, a reduced potential for immunogenicity and pathogen transmission and enhanced control over material properties allowing the tailoring to specific tissue requirements, and thus optimal exploitation of the injured tissue's regenerative potential. Important features of polyethylene glycol compared to other synthetic biomaterials include its high degree of inertness, which translates into superior biocompatibility and its lack of adhesiveness for cells, thus making it a prime candidate for the incorporation of bioactive molecules[397]. Furthermore, polyethylene glycol is easy to handle, allowing transformation from liquid to solid state in situ[398]. Due to the high water content of PEG hydrogels, their properties are comparable to soft tissue. The high water content is critically important in ensuring proper exchange of waste and nutrients and aids in preserving the bioactivity of hydrophilic drugs[399]. The high structural similarity of PEG hydrogels to extracellular matrix imitates a physiological environment for cells entrapped within the hydrogel, enabling three-dimensional organization, macromolecular transport and

playing an important role in promoting physiological cell differentiation. Collectively, these characteristics make polyethylene glycol an attractive candidate for in vivo tissue engineering.

Polyethylene glycol hydrogels have been developed that are formed by Michael-type conjugate addition reaction of PEG macromers with thiols[400-402]. [Based on chemistry, a variety of methods exist to initiate gelling[403]; as PEG hydrogels used for the ensuing studies were formed using Michael-type addition reaction, this method is explained in more detail.] Named after its discoverer, Arthur Michael, a Michael addition involves the formation of a chemical bond between a nucleophile, which donates a pair of electrons and is referred to as the Michael donor, and an electrophilic olefin, the Michael acceptor (an unsaturated chemical compound that contains one or more carbon-to-carbon double bonds). As the chemical reaction inducing PEG hydrogel formation uses non-enolate nucleophiles, namely thiols, as electron donors, this reaction is typically referred to as Michael-type addition reaction[404]. In biological systems, cysteine residues in proteins are taken advantage of, as the thiol group on the side chain of cysteine typically acts as the Michael donor. Hydrogel formation based on a Michael-type addition reaction between thiol and acrylate or vinylsulfone groups, respectively has often been described as ideally suited for biomedical applications, as thiols are absent in the bloodstream[404].

Due to advantageous condition reactions between thiols and acrylates or vinylsulfones, potential Michael addition reactions with amines are rare[404-406]. Importantly, the Michael-type addition reaction can be carried out at physiological pH without requiring organic solvents[402]. Upon mixing of PEG-macromers with a thiol-containing cross-linker, hydrogel formation of two takes place during gradual copolymerization. For studies carried out for this thesis, 20kD-8arm Vinyl sulfone (VS)-PEG macromers were used, functionalized with VEGF[165] for some studies. Crosslinking was either perfomed with dithiothreitol[402] or with thiol groups cysteine-containing peptides by conjugate addition, as previously described[400]. Gelling of PEG hydrogels is completed quickly without producing any toxic byproducts and most of its

degradation products are of neutral charge[399]. Generally, the molecular weight of degradation products is low enough to readily allow glomerular filtration and to prevent an immunological host response[399]. A major advantage of hydrogel formation via Michael-type addition reaction in terms of protein delivery is the lack of free radical formation, which potentially damages drugs and proteins bound to the hydrogel[399]. Apart from Michael-type addition reactions a wide range of crosslinking methodologies exist for PEG hydrogels that induce gel formation upon photopolymerization or after exposure to physiological temperatures. Increased free radical formation and more technically challenging crosslinking initiation, e.g. requiring a light source, make these techniques less suitable for in vivo tissue engineering[399]

Whilst biomaterial degradability is desired in most tissue engineering applications, a non-degradable hydrogel may be useful to provide mechanical support in tissues with low regenerative potential. Crosslinking VS-PEG with dithiothreitol (DTT) allows the formation of PEG hydrogels that are stable for up to 13 weeks after myocardial injection[407]. Crosslinking PEG-macromers with bis-cysteine peptides allows the integration of biological functionality into the hydrogel network[400]. The integration of cellular recognition sites, bioactive molecules and cell-responsive degradation sites allow the creation of an ECM-mimicking matrix[289,408]. Michael-type addition preserves the chemistry of protein drugs, as no potentially harmful basic catalyst or UV light is required during the hydrogel formation[402]. Additionally, incorporation of matrix metalloproteinase-sensitive sequences into PEG hydrogels has successfully been shown to regulate cell-invasion by MMP-secreting cells thus controlling the rate of hydrogel degradation[408,409]. Extending on these studies, it was shown that this principle could also be applied to allow for cell-demanded release of bioactive molecules[289]. Overall, the advanced interaction between host tissue and synthetic biomaterials, such as PEG, have significantly advanced the field of tissue engineering, effectively assuming the role of a transitional extracellular matrix that is gradually replaced by regenerating tissue, which subsequently restores tissue-specific physiological functions. PEG

crosslinking chemistry thus provides high flexibility in tailoring mechanical properties and drug release kinetics depending on target tissue[410,411].

In vitro experiments have established polyethylene glycol as a material widely used for 3D cell culture and, amongst others, pancreatic beta cells and neural cells have been successfully cultured and expanded in PEG hydrogels[412,413]. Despite mainly consisting of water (commonly more than 90%), polyethylene glycol hydrogels can be engineered to possess a mesh size in nanometer range[400], making the pore diameter of PEG hydrogels far smaller than that of either fibrin or collagen matrices, and smaller in magnitude than cellular migratory processes[414-416]. Therefore local (hydrolytic or proteolytic) breakdown of these gels dictates cellular migration. PEG hydrogels have thus emerged as model systems to study the effects of integrin-binding motifs and proteases on cellular migration by incorporating cell-binding sites such as RGD and by differentially crosslinking hydrogels with hydrolytically or proteolytically degradable peptide sequences[104,105]. The incorporation of proteolytic sequences (plasmin, MMPs) furthermore allows the introduction of an in vivo feedback system whereby the rate of hydrogel degradation and the release of incorporated proteins during tissue regeneration, is dictated by the secretion of proteinases from migrating host cells. Polyethylene glycol hydrogels have extensively been tested for their potential to deliver biologics and cells to promote tissue regeneration[417-419]. Lutolf et al. have previously shown that the incorporation of integrin-binding sites and MMP-degradable substrates allow invading inflammatory cells to dictate the release of bound bone morphogenetic protein-2[408]. In this study, PEG hydogels were shown to provide a temporary platform that promotes the regeneration of bony tissue by host cell activation (which participate in the generation of new ECM), resulting in complete closure of the rat cranium defect.

PEG hydrogels formed by Michael-type addition reaction have been used extensively for controlled, local delivery of drugs and therapeutics. These hydrogels allow spatial and temporal control over growth factor presentation and release[420-425], mimicking an important

role of the ECM, as some molecules are more effective when presented as a bolus, others when released slowly over time. Important aspects of controlling protein and drug release are the increased preservation of the therapeutics bioactivity and a decreased risk of adverse side effects[399]. In order to optimize targeted drug delivery a variety of different loading techniques, e.g. entrapment or tethering (covalent, enzymatic, hydrolytic) may be combined[399]. Affinity hydrogels that are based on the heparin-binding capability of numerous growth factors are an interesting alternative[422,423,426], as well as integration of biologics using the prodrug technique, whereby linker degradation hydrolytically[427,428] or enzymatically[289,429,430] releases the drug in its active form. Thus, PEG hydrogels are potentially well suited to deliver bioactive therapeutic molecules in the setting of myocardial infarction. Such delivery may be particularly useful in treating MI by stimulating therapeutic angiogenesis.

6.7. Therapeutic angiogenesis for myocardial ischemia

Therapeutic angiogenesis aims at establishing a stable, functional vascular network in tissues with an inadequate vasculature, thereby enhancing tissue perfusion and function[431]. Options for patients with ischemic heart disease (IHD) are limited and after myocardial infarction only directed towards restricting the damage. Medical treatment for IHD intends to reduce the oxygen demand of the myocardium[432]. Surgical options include revascularization by either angioplasty or coronary bypass grafting. While the promotion of angiogenesis with platelet-derived growth factor-BB (PDGF-BB) has been used to treat chronic wounds[433] in animals and translation to the bedside has been successful, therapeutic angiogenesis as a treatment option for ischemic vascular disease has suffered from repeated setbacks. A great deal has been learned from studying the biology of tumour angiogenesis, some of the molecular and cellular mechanisms of the angiogenic response have been elucidated, however therapeutic neovascularization has yet to demonstrate the functional benefits previously shown in numerous animal experiments[16,17,434]. The inability to promote vessel maturation[76] followed by the subsequent regression of neovessels

induced by angiogenic therapy has been identified as a major obstacle that therapeutic angiogenesis has yet to overcome to allow clinical translation.

The original study showing that in a canine model of myocardial infarction the intracoronary delivery of basic FGF (bFGF) successfully increased neovascularization, improved the systolic function of the heart and limited infarct size was carried out by Yanasigawa-Miwa and colleagues[16]. Subsequently, numerous reports validated the theory that enhancing the angiogenic response by delivering a single growth factor is possible. Using a rabbit hind limb ischemia model, Takeshita et al. demonstrated that a single intra-arterial bolus injection of recombinant VEGF leads to a significant increase in capillaries and augmentation of collateral vessels and as a result an improved perfusion compared to controls[17]. The intramuscular injection of naked plasmid DNA encoding vascular endothelial growth factor[165] (VEGF[165]), VEGF-C and recombinant hepatocyte growth factor (HGF) in the same model yielded similar results[435,122,253]. Banai and colleagues reported increased angiogenesis in the ischemic myocardium after intracoronary administration of VEGF[434]. Work showing that an intracoronary injection of a recombinant adenovirus expressing human fibroblast growth factor-5 (FGF-5) ameliorated blood flow abnormalities and restored function in an ischemic pig heart added more evidence supporting the hypothesis that the delivery of a single growth factor might be sufficient for therapeutic angiogenesis[436].

Despite the likelihood that any single factor would not induce the optimal angiogenic response, these early results were encouraging and warranted the first clinical trials for patients not eligible for traditional revascularization.

6.8. Clinical trials for therapeutic angiogenesis

To date bFGF and VEGF are the only growth factors tested in clinical trials for their potential to promote biological revascularization. The initial report was published by Jeffrey Isner´s group in 1996. Delivery of 2000 micrograms of human plasmid phVEGF[165] via the hydrogel

polymer coating of an angioplasty balloon in a patient with severe peripheral vascular disease led to an increase in collateral vessels after 4 and 12 weeks, which was accompanied by increased resting and maximum flows[437]. 2 years later, Schumacher and colleagues reported that the injection of recombinant FGF-1 during coronary artery bypass surgery promoted angiogenesis in the setting of coronary artery disease[438]. In a control group injected with inactivated FGF-1, neovascularization was not evident. Several phase I studies followed, reporting improved stress perfusion detected with magnetic resonance imaging (MRI) or single photon emission computed tomography (SPECT) after treatment with recombinant FGF-2[184,439,440] and VEGF[441,442] and proving that the treatment was well tolerated. Phase I studies evaluating the potential use of plasmids[443] and adenoviruses[444] to deliver VEGF or FGF-4[445] also demonstrated that the approach is safe. Larger Phase II trials further testing the potential of recombinant FGF-2[185] and VEGF[446] as well as adenoviral delivery of FGF-4[447] confirmed the safety of pro-angiogenic therapy, but these studies failed to show significant improvements in the treatment groups. Instead they revealed the presence of a large placebo effect and emphasized that randomized, controlled studies are needed. Possible explanations offered for the negative results included a diminished response by the diseased vasculature in no-option patients to an angiogenic stimulus, short exposure times to the respective growth factors that promote vascular stability and prevent rapid neovascular regression, and a limited capability to detect treatment effects due to technical limitations[76].

6.9. Cell delivery to promote therapeutic angiogenesis

After disappointing results in molecular strategies for therapeutic angiogenesis in clinical trials, cell therapy strategies gained attention. While initially intended to replace irreversibly damaged cardiomyocytes, proof of substantial cardiac regeneration by cellular therapy remains elusive. Since the initial studies, functional improvements after cell injections have largely been attributed to paracrine effects, such as promoting angiogenesis. Skeletal muscle myoblasts were the first proposed as surrogate cells for cardiac repair[448-450]. After extensive testing in animal models proving the beneficial effects of cell transplantation after myocardial

infarcts[451-453], initial human trials were started in 2000[454]. The early trials for chronic ischemic disease proved the feasibility of cell transplantation and some long-term engraftment of myoblasts[455,456] was shown. It also became apparent that improving cell retention and survival of transplanted cells in the hostile host environment constitutes one of the major challenges. While patients showed improved symptoms, ejection fraction and regional contractility[454,457,458], definite conclusions regarding the efficacy of the treatment could not be shown due to the lack of control groups.

After myoblasts had paved the way, the field quickly moved forward focusing on bone marrow[459-462] and endothelial progenitor cells[463] for cardiac repair due to their suggested additional benefits. Bone marrow cells had previously been shown to contain a subpopulation of progenitor cells, including hematopoietic stem cells[464,465], mesenchymal stem cells[466] and multipotent adult progenitor cells[467]. These were hypothesized to contribute to an enhanced neovascularization by incorporating into the newly formed vessels and also by secreting pro-angiogenic factors in a paracrine way. Originally believed to generate new myocardium by either differentiating into cardiac cells or by means of cell fusion[468], hematopoietic stem cells and bone marrow mesenchymal stem cells are now thought to exert their effects mainly via their non-cardiogenic mechanisms[469]. Indeed, the formation of cardiomyocytes from hematopoietic stem cells seems to be an extremely rare event caused by cell fusion[470-473]. Initial clinical trials for acute myocardial infarction with both bone marrow cells[459,462,474] and cardiac progenitor cells[460,475] yielded comparable results: improved contractility, perfusion and significantly reduced end-systolic left ventricular volumes. The outcome of the following larger, randomized studies was somewhat more controversial and emphasized the importance of choosing the right cell population. In the same issue of the New England Journal of Medicine, Schächinger and colleagues reported that in the setting of acute myocardial infarction the injection of progenitor cells isolated from bone marrow cells significantly improved left ventricular ejection fraction[476] while Lunde et al.[477] described that no significant difference had been found between treatment and control group after the

delivery of unselected bone marrow mononuclear cells. Bone marrow progenitor cell transplantation for patients with stable ischemic heart disease was linked to a moderate but significant improvement in left ventricular ejection fraction after 3 months[478].

This second phase of therapeutic angiogenesis trials focusing on cell therapy again underlined the need for large randomized placebo-controlled Phase III trials to prove the efficacy of this novel therapy. Amongst the important lessons learned from experimental and clinical cell transplantation were that an improvement in function is not synonymous with definite myocardial regeneration and that effects seen with cell therapy thus far likely result from promoting angiogenesis, reducing ventricular remodelling or mediating pro-survival signals[468].

In summary, recent evidence suggests that clinical trials to promote neovascularization and the recovery of ischemic tissues after injury have been hampered by the inability to create a stable vascular network. Developing more efficient approaches will likely depend on acquiring a deeper understanding of the mechanisms involved in both promoting a mature vascular phenotype and governing neovascular regression.

6.10. Biomaterials as vehicles for prolonged and sequential growth factor delivery to enhance therapeutic angiogenesis

Prolonged growth factor delivery from biomaterials holds great promise for therapeutic angiogenesis. In many tissues, the development of a stable neovasculature is dependent on continuing growth factor exposure, as single bolus injections show little to no effect partly due to rapid clearance from the target site or insufficient delivery[479,480]. Furthermore, many potent angiogenic growth factors induce adverse side effects. Particularly VEGF levels need to be highly controlled as high dosages may lead to vascular permeability, leakage and hypotension[481,482]. Repeated drug injections into remote tissues (e.g. myocardium) is also

technically challenging, impractical and generally considered unsafe[481,483]. Previously, in collaboration with our laboratory, Jeffrey Hubbell's group has shown that the integration of integrin binding sites and VEGF into MMP-sensitive PEG hydrogels leads to the complete replacement of the hydrogel by newly formed blood vessels in a subcutaneous wound healing model, providing the first in vivo evidence that PEG hydrogels are suitable candidates to promote therapeutic angiogenesis in the ischemic myocardium[289]. In this study, $VEGF^{121}$ and $VEGF^{165}$ were bound to the PEG matrix by Michael-type addition reaction. Formation of the hydrogel was subsequently performed with a MMP-sensitive crosslinker-sequence that allowed for VEGF release upon cellular invasion, thus establishing a feedback mechanism between the implanted PEG matrix and the host tissue. Integration of VEGF into PEG chains was shown by semi-quantitative SDS-PAGE and the bioactivity of PEG-bound VEGF was confirmed in HUVEC proliferation assays, as matrix-bound, VEGF released from the hydrogel after MMP2-administration and unmodified VEGF induced identical dose-response curves. VEGF-functionalized PEG-peptide hydrogel matrices were then shown to promote HUVEC migration and to effectively stimulate vascularization in the CAM assay and after subcutaneous implantation into porous polyurethane discs in rats. Matrix functionality was thus shown by the authors to be essential to support endothelial cell survival, migration and angiogenesis. It is important to note that, since vascular regression is a major obstacle for successful therapeutic angiogenesis, no immature vessels were detected after prolonged delivery of $VEGF^{165}$ from PEG hydrogels. This suggests that while successful long-term establishment may be coupled to the development of a physiological oxygen load[484], sustained VEGF release from PEG matrices successfully prevented the rapid regression of newly formed vessels. Therefore delivery of VEGF-conjugated PEG hydrogels may be a promising strategy to induce long-term neovascularization of ischemic tissues.

Some of the mechanisms that contribute to enhanced long-term neovascularization are also beginning to emerge. Long-term exposure to angiogenic growth factors has been demonstrated increase the efficacy of therapeutic angiogenesis through enhanced homing of

progenitor cells that contribute to angiogenesis and neovascular maturation[468]. Subsequently, it was shown that beneficial effects on cardiac performance and the accompanying increase in neovasculature rely heavily on the continued physical incorporation and presence of pro-angiogenic cells[485]. Survival of pro-angiogenic peripheral blood derived mononuclear cells transplanted into the heart was directly responsible for increased long-term neovascularization and improved cardiac function[485]. This adds evidence that long-term exposure to pro-angiogenic treatments has substantial impact on the therapeutic outcome. Likewise, sustained local delivery of protease-resistant stromal derived factor-1 via self-assembling peptides was shown to drive stem-cell homing into the injured myocardial tissue, thereby enhancing neovascularization and cardiac function. As simultaneous release of VEGF and PDGF-BB from poly(lactide-co-glycolide) has been shown to significantly increase the vascular density and induce a more mature vasculature in vivo in comparison with delivering of either VEGF or PDGF alone[288], the simultaneous delivery growth factors should also be strongly considered for therapeutic angiogenesis.

While more sophisticated delivery vehicles have contributed to the continued evolvement of novel strategies for therapeutic angiogenesis therapies, recent findings emphasize the complexity of engineering a stable neovasculature in ischemic tissues. Thus, translational success will likely depend on simultaneously targeting a variety of vasculogenic cell populations and creating a local microenvironment conducive for tissue regeneration using smart biomaterials that interact with host tissue and help limit damage sustained from ischemia[486].

7. Hypothesis MI chapter

Collectively, a large body of work has shown that promoting neovessel formation after myocardial infarction can effectively be used to limit detrimental effects of MI in animal models. Polymeric delivery systems that allow for sustained growth factor supplementation to the ischemic tissue have been demonstrated to more efficiently promote long-term

neovascularization and improve cardiac function after MI than injecting a single bolus of a growth factor. The central finding from the subcutaneous angiogenesis model study suggests that the growth factor dosage delivered critically regulates the development of a stable neovasculature. Recently developed smart hydrogels allow advanced control over growth factor release through modification of degradation kinetics, thus enabling prolonged growth factor delivery to target tissues that are less accessible, such as the heart. Amongst smart biomaterials, PEG hydrogels, which have previously been extensively studied in our laboratory, have proven their value for therapeutic angiogenesis. Enzymatically degradable VEGF-^{165}-conjugated PEG hydrogels crosslinked by Michael-type addition were shown to promote angiogenesis and prevent vascular regression in a subcutaneous in vivo angiogenesis assay.

While their use as a delivery matrix has long been described, synthetic biomaterials have recently gained attention as stand-alone therapies after myocardial ischemia, as the injection of hydrogels themselves was shown to have beneficial effects on heart function post-MI. Collagen, fibrin, alginate and matrigel hydrogel injections all yielded beneficial results ranging from increased angiogenesis to improved myocardial contractility and function[388-391].

Combining these recent findings, this thesis tests the following hypothesis:

1. Prolonged delivery of VEGF^{165} dosages - that promoted long-term neovascularization in the subcutaneous wound healing assay – from enzymatically degradable polyethylene glycol hydrogels results in increased angiogenesis and the formation of a more stable neovasculature in the heart, resulting in enhanced functional recovery and/or improved heart remodelling.
2. When used as stand alone therapy, polyethylene glycol hydrogel injections into the ischemic myocardium ameliorate left ventricular dysfunction and remodelling after myocardial infarction.

As a necessary step towards investigating the above, a rat myocardial ischemia model was established.

8. Results MI chapter

8.1. Establishment of a rat myocardial infarct model

The aim of an initial pilot study was to show successful induction of myocardial infarcts in rats by ligation of the left anterior descending (LAD) coronary artery. An important technical objective of this study was to determine whether a correlation between a decrease in fractional shortening and infarct size can be achieved in our rat model. In 12 rats a myocardial infarction was induced by ligation of the LAD (see 10.2.5). 10 rats serving as control animals (sham group) underwent a thoracotomy without LAD ligation. The success of a ligation was confirmed by ST-elevation, which was recorded by 2-lead ECG (see Fig.30). Additional markers that were monitored during the surgery were the appearance of a pale demarcated zone and dyskinesia of the left-ventricular wall, the area typically supplied with blood by the left anterior descending coronary artery.

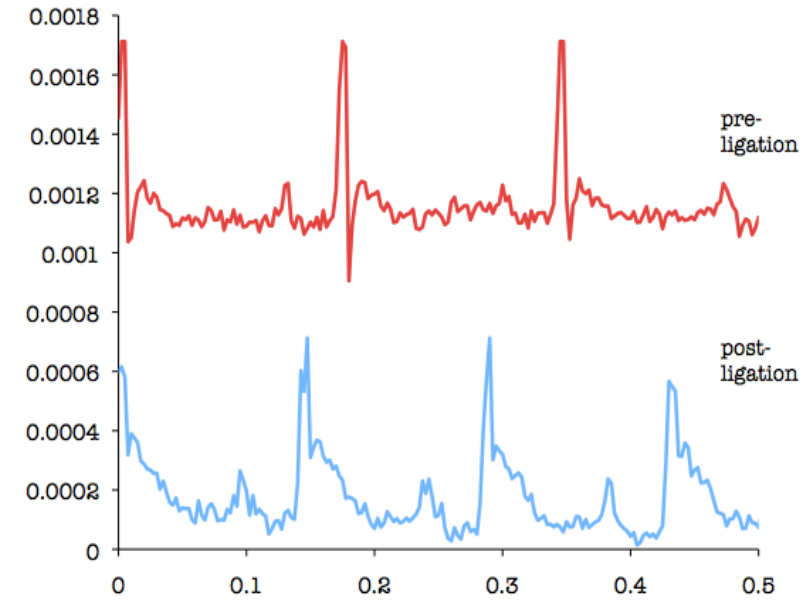

Fig.30. 2-lead electrocardiograms before (red) and after successful ligation of the left anterior descending coronary artery (blue) are shown. ST-elevation characteristic of myocardial ischemia, namely, was observed.

Left-ventricular function of the animals was assessed both at days 14 and 28 post surgery by transthoracic echocardiography. Left-ventricular diameters at the end of systole and diastole were obtained in both 2D-mode and m-mode (representative images **are shown in figure**)[407]. Both 2D and m-mode measurements were included to obtain the final data. Animals were sacrificed on day 29 and the explanted hearts were processed for histological analysis. To determine infarct volumes heart sections were stained with modified Masson's trichrome.

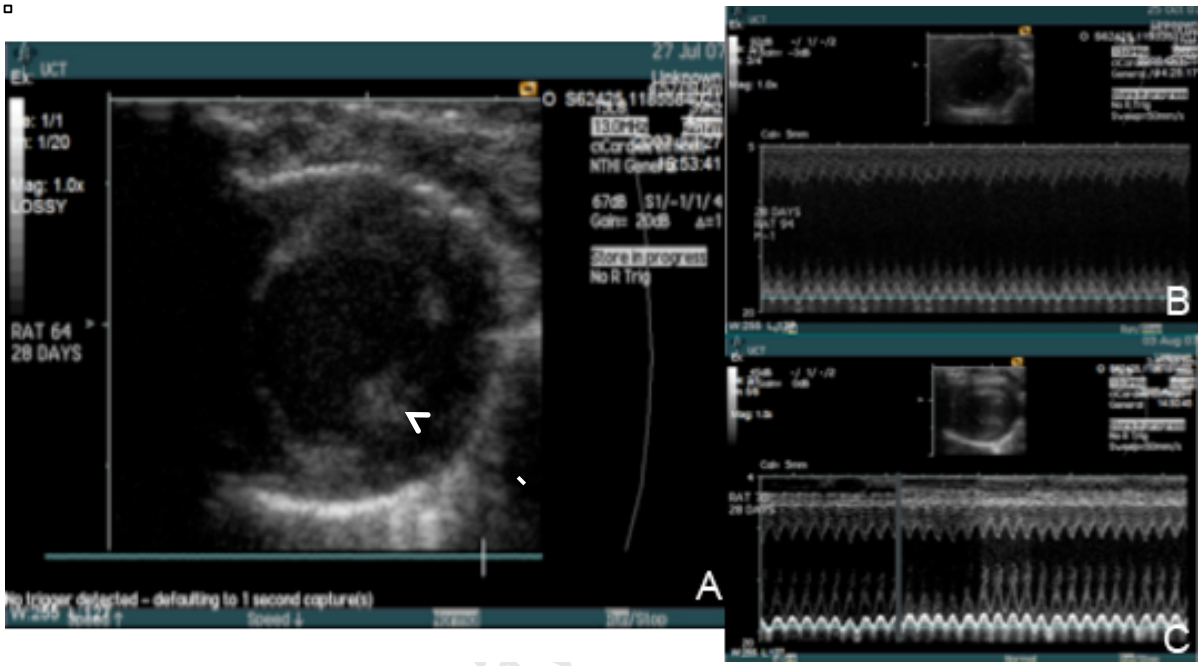

Fig.31. Representative echocardiographic images obtained on day 28 post surgery for analysis of cardiac function and ventricular remodelling. A 2D image (Fig.31A), and M-mode images of a large (Fig31.B) and small infarct (Fig31.C) taken on the level of the papillary muscle (white arrow in Fig 31.A) are shown.

8.1.1. Echocardiographic analysis, day 14

As early as day 14, a highly significant 17.29% decrease in fractional shortening in the myocardial infarction group (31.7±2.95%, n=11, $p<0.001$) was observed in comparison with sham-operated animals (shown in Fig.32).

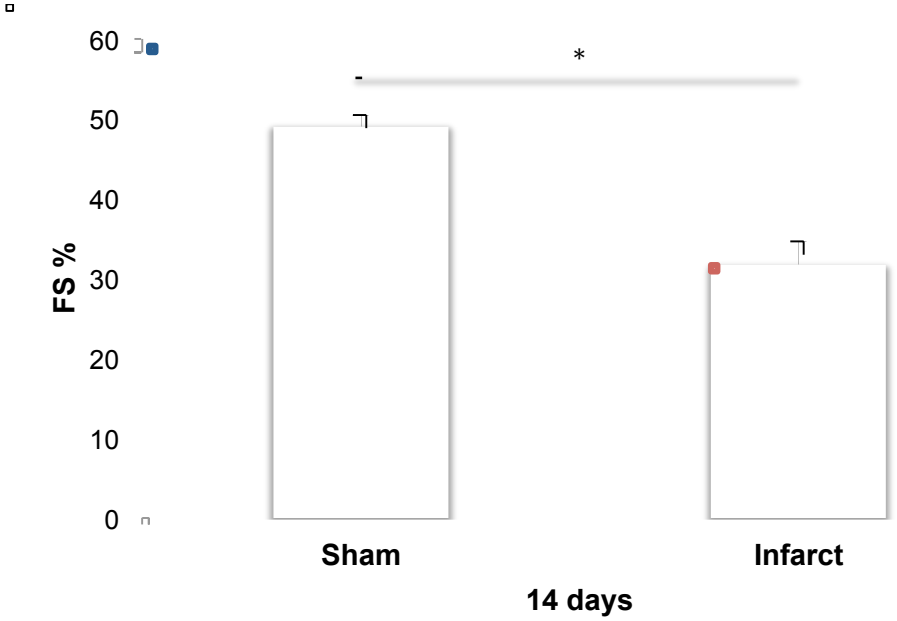

*Fig.32. Echocardiographic analysis was performed on day 14. Myocardial infarction induced by permanent ligation of the left anterior descending coronary artery (LAD) led to a significant reduction in fractional shortening 14 days after surgery (*p<0.001, -17.29%).*

Similar results were observed for both the 2D and M-modes as stand alone measurements (see Fig.33).

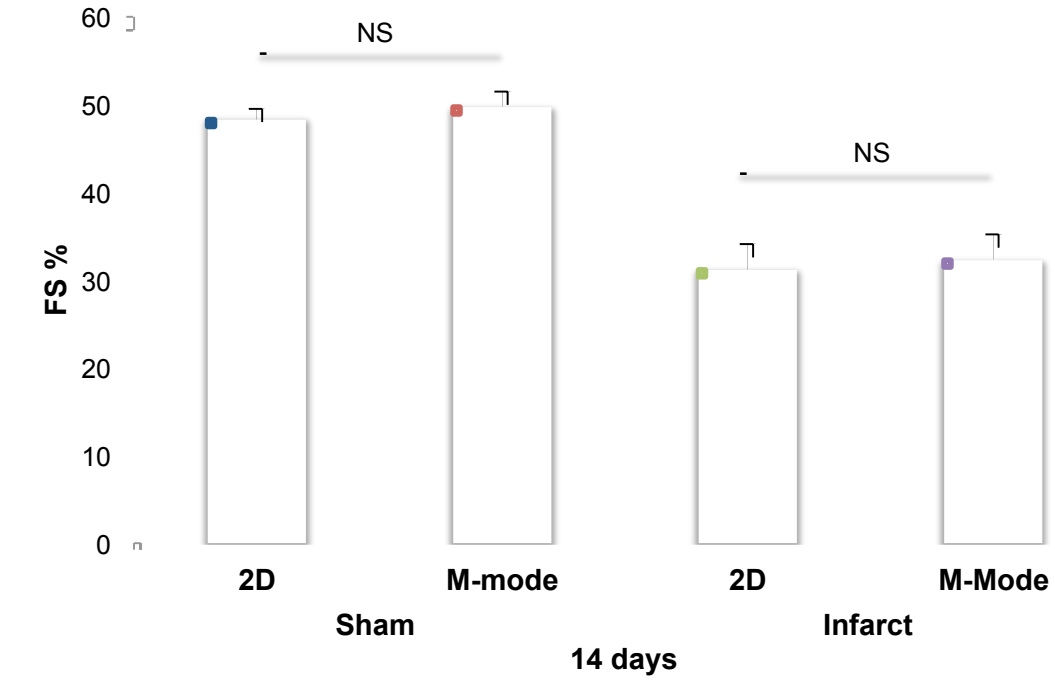

Fig.33. Independent assessment of cardiac function was performed for echocardiographic images acquired in 2D-mode and M-mode, respectively. No significant difference was observed after comparing 2D and M-mode measurements, confirming a significant reduction in fractional shortening after experimental myocardial infarction.

8.1.2. Echocardiographic analysis, day 28

The results obtained from echocardiographic analysis at day 28 were almost identical when compared to the day 14 timepoint. At 4 weeks, myocardial infarction surgery significantly reduced fractional shortening by 20.05% in comparison with sham-operated animals (n=11, p<0.001). This confirmed that the main loss of left-ventricular function in the MI group had occurred over the initial 2 week-period after experimental coronary artery ligation.

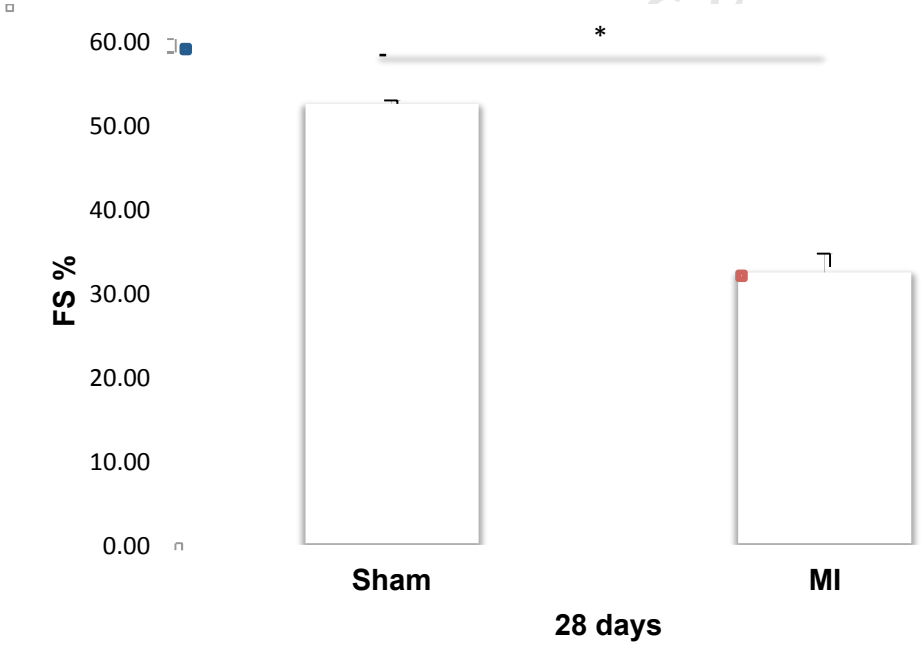

*Fig.34. Combined echocardiographic analysis for images acquired in 2D and M-Mode. Significant loss of cardiomyocyte contractility after LAD coronary artery ligation is confirmed at day 28 (*p<0.001).*

8.1.3. Histological analysis – Infarct volume

Immediately after sacrifice, the hearts were explanted and evaluated macroscopically. Extensive scar formation in the left-ventricular area indicated successful LAD ligations in the myocardial infarction group (a representative photograph is shown in Fig.35).

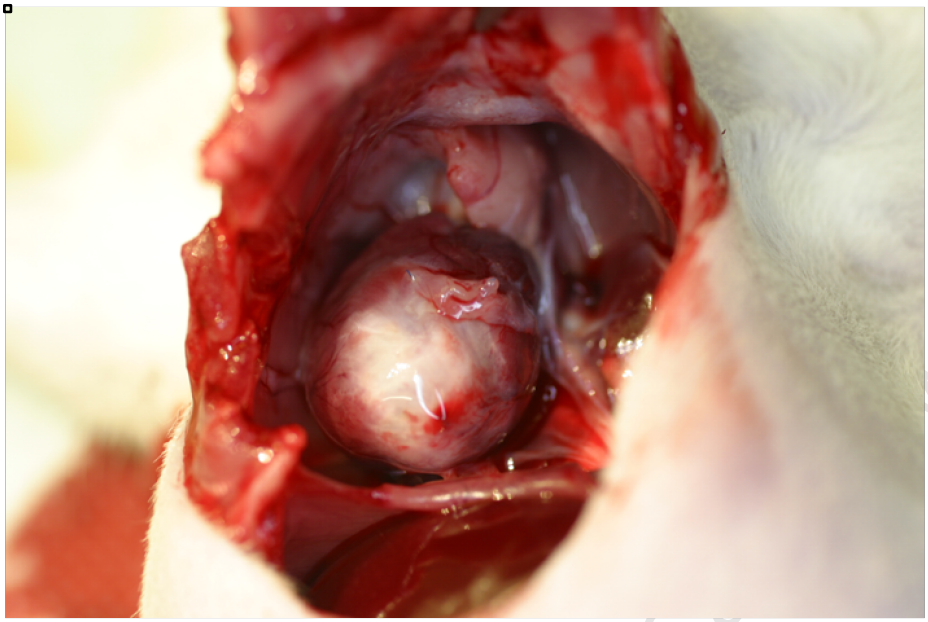

Figure.35. Macroscopic picture of a rat heart explanted 29 days after induction of myocardial infarction. Extensive scar formation (white) is seen in the left-ventricular region of the heart.

After fixation and staining with modified Masson's Trichrome, histologic sections were photographed and analysed using Visiopharm Integrator System (VIS, as seen in Fig.36). Sham-operated animals looked healthy and did not show any signs of scar formation (data not shown). On the contrary, extensive scar formation was observed in animals subjected to coronary artery ligation. The average infarct volume in animals after myocardial infarction was 22.48±3.54%.

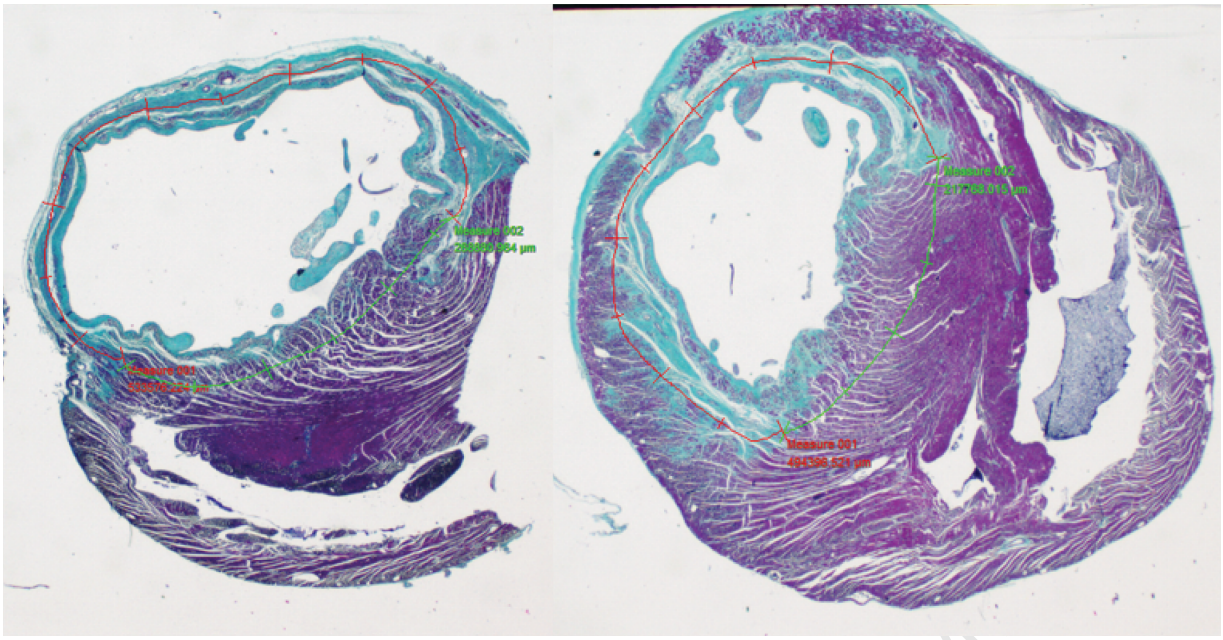

Figure.36. Modified Masson's Trichrome stains of two cross sections of infarcted rat hearts are shown. The micrograph includes the Visiopharm Integrator Systems (VIS) image analysis tracings of infarcted (in red) and non-infarcted (in green) left-ventricular circumference, which were subsequently used for calculations of infarct volume.

After plotting infarct size against fractional shortening for each animal that had undergone permanent LAD occlusion a significant correlation (p=0.023) between the volume of the infarcted left ventricle and the decrease in left-ventricular function was revealed (shown in Fig.37.) revealed. This finding confirmed successful establishment of the rat myocardial infarction model.

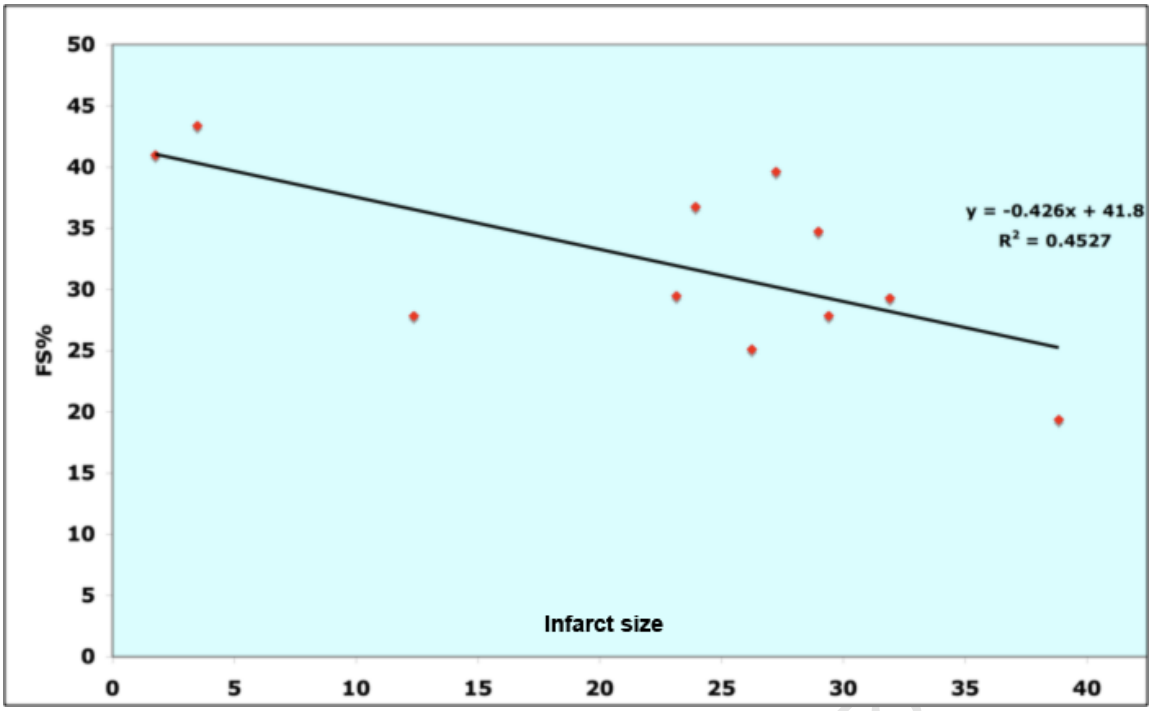

Figure.37. After analysis, parameters for cardiac function (fractional shortening) and infarct size were plotted against each other. Increased infarct size significantly correlated with an increased drop-off in cardiac contractility (p=0.023).

8.2. Pilot PEG injections

8.2.1. Rationale

Polyethylene glycol (PEG) hydrogels exhibit a range of properties that render them suitable for a variety of in situ applications[409,487]. They gel within a few minutes at physiological temperature and pH, do not require the addition of initiators, produce no by-products, have very low reactivity toward tissue, and are considered to be very biocompatible[488]. Furthermore physical properties of PEG hydrogels may be varied by choice of molecular mass, functionality and crosslinker type, and protein, carbohydrate and therapeutic agents may be readily coupled and released from the gels, either with or without degradation of the gel itself. As PEG hydrogels represent a promising class of biomaterials for myocardial tissue

engineering, pilot experiments were designed to demonstrate that polyethylene glycol (PEG) hydrogels can successfully be injected and permanently implanted into infarcted rat hearts. One of the major concerns associated with hydrogel injections into the heart is the short time window after injection of the solution, before the gelling process is completed. During this timespan, a substantial proportion of the injected monomeric gel components may be washed out of the beating heart into the circulation. This may lead to the formation of foreign body emboli, which subsequently can cause ischemic events such as strokes.

8.2.2 In vitro gel formation

To generate stable polyethylene glycol hydrogels dithiothrietol was used to initiate gel formation of 20kD-8arm Vinyl sulfone-PEG-hydrogels. After the addition of the crosslinker dithiothrietol (DTT), non-degradable polyethylene glycol hydrogels completely gelled within 2 minutes in vitro.

8.2.3. Surgery and in vivo injections of PEG hydrogels

To allow for easier detection after in vivo injections, PEG hydrogel solutions were labelled with a covalently attached far-red fluorescent marker (described in Chapter 10.2.2). Experimental myocardial infarcts were then induced in 3 rats by ligation of the LAD, and 100 µl of the non-degradable polyethylene glycol hydrogel solution were immediately injected into the infarcted area. As previously detected in vitro, in situ gelling of PEG hydrogels was completed within 2 minutes. All animals (n=3) survived the initial surgery and PEG injection, suggesting that in vivo gelling times were rapid enough to prevent PEG from entering the circulation and forming foreign body thrombi. To detect PEG retention and distribution within the left ventricle, the animals were sacrificed and hearts harvested 4, 24 and 48 hours post surgery.

8.2.4. Detection of PEG hydrogels

In all animals, after 4, 24 and 48 hours, respectively, PEG hydrogels were readily detected by fluorescent microscopy of the attached far-red fluorescent label. The rapid gelling time likely aided in the retention of the hydrogel within the myocardial wall. PEG hydrogels were evenly distributed around the injection sites at all timepoints (see representative image in Fig.38).

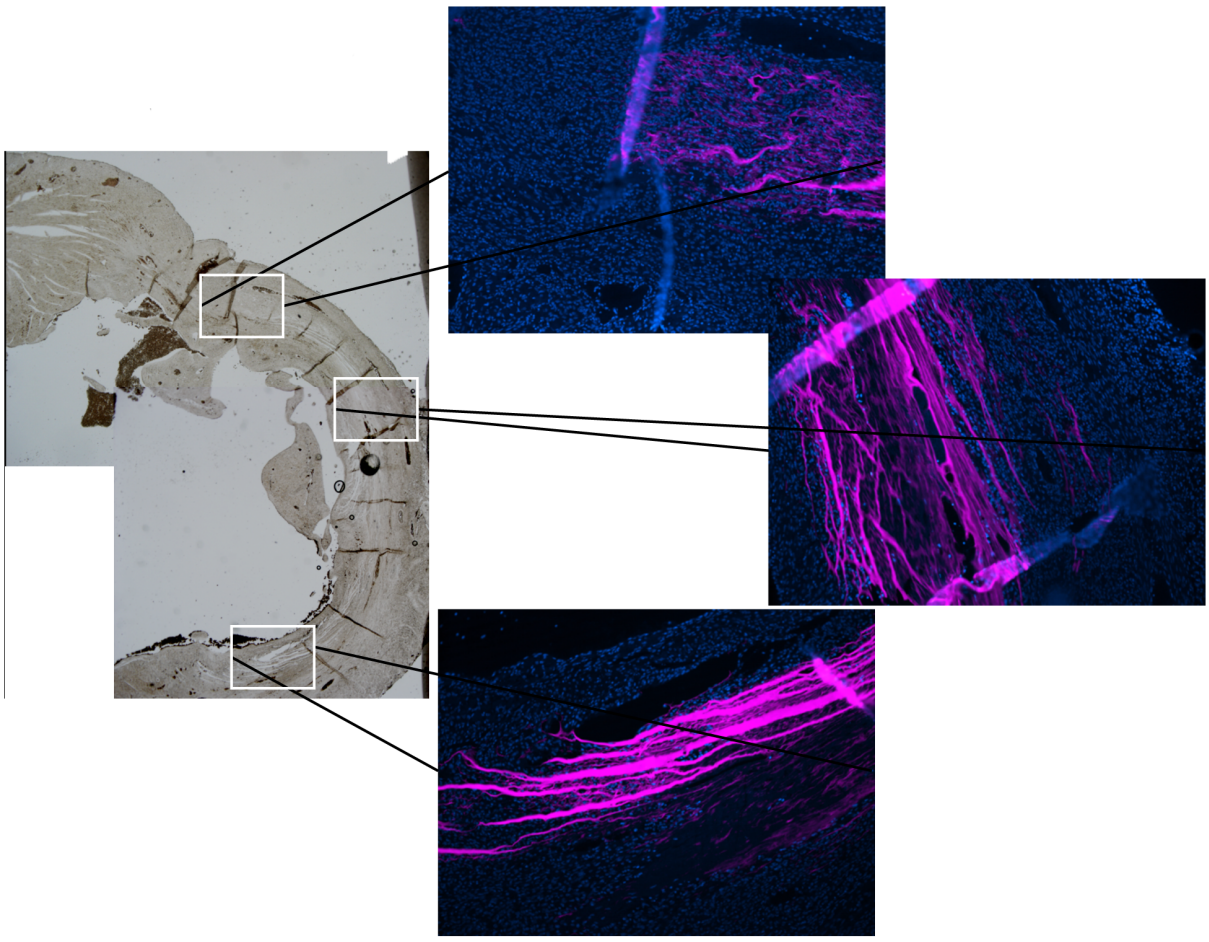

Fig.38. A covalently attached far-red fluorescent marker allows easy identification of PEG hydrogels on histological sections. Around the injection sites, PEG hydrogels (shown in purple) are maintained in the left-ventricular wall after in vivo injection for at least 48 hours.

8.2.5. Conclusion

Pilot experiments confirmed successful PEG hydrogel implantation after permanent left anterior descending coronary artery occlusion. PEG hydrogels were detected throughout the left ventricle and retained within the myocardial wall for 48 hours.

Next, the effects of polyethylene glycol hydrogels on ventricular function and architecture after myocardial ischemia were explored.

8.3. The effects of a non-degradable polyethylene glycol hydrogel on post-infarct left ventricular function and remodelling

8.3.1. Rationale

Over the last few years a number of animal studies have shown that biomaterial injections may attenuate left-ventricular dysfunction after ischemia. Wall and colleagues have used a finite element modelling approach to show that biomaterial injections into the heart help normalize wall stresses thereby contributing to an improvement in LV function[386], with stiffer materials showing a greater benefit. While the materials used thus far have all been degradable, it has recently been proposed that an injectable polymer that is non-degradable may be needed for long-term beneficial effects on heart remodelling [489]. To overcome handling problems, potential immunogenicity and limited engineerability of natural polymers that limit their potential for clinical application[409], a synthetic, non-degradable, polyethylene glycol based hydrogel was chosen for this study. Polyethylene glycol's mechanical properties are well suited for myocardial injections, as it ranks amongst the stiffest materials mentioned in Wall´s paper and remains amongst the most inert synthetic biomaterials to date[490].

The aim of the study was to determine short- and long-term effects of permanent mechanical reinforcement on post-infarction ventricular remodelling in an attempt to answer whether or not the presence of a synthetic biomaterial produces some of the same benefits as cell

transplantation, namely wall thickening, beneficial LV remodelling and functional improvement.

After permanent ligation of the left anterior descending artery, PEG gel reagents were injected into the infarcted region and polymerised in situ. Ventricular function and heart dimensions were assessed at 2, 4 and 13 weeks. Histological analyses to determine post-mortem infarct volume and scar thickness were performed at 4 and 13 weeks.

8.3.2. Survival

A total of 91 rats were used in this study. The survival in the 28-day experiment was 100 % (42 rats, n=10-11). In the 3-month study one rat died due to fibrillation, immediately after the thoracotomy was performed. The remaining 48 animals survived (97,96 %; 48 rats, n=10-14). The overall survival rate for the study was 98,9 %.

8.3.3. Durability of PEG-gel in rat hearts

Distribution of injected PEG-hydrogel was assessed at 4 and 13 weeks by detection through fluorescent microscopy of a covalently attached far-red fluorescent label. The label was easily detected at both time points and the hydrogels had very similar signal intensities (Figure 39). PEG hydrogel was found distributed throughout the infarcted region and its border zones at 4 and 13 weeks with the amount of gel appearing to remain constant.

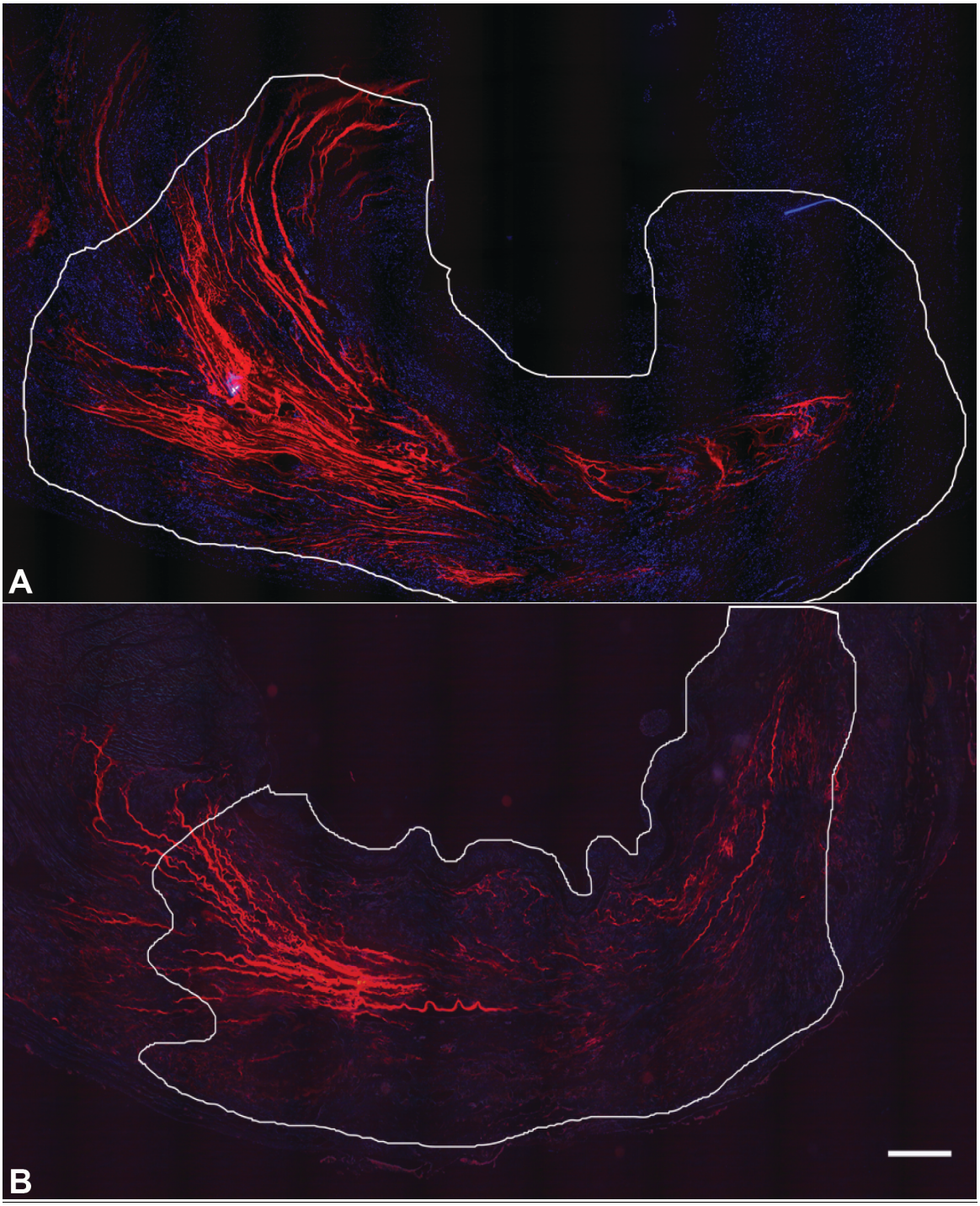

Figure.39. Assessment of polyethylene glycol (PEG) gel distribution in an infarcted rat heart. Representative micrographs of Alexa Fluor 660 labeled PEG (red) at (A) 4 and (B) 13 weeks. The white line delineates the infarcted regions. Nuclei are stained blue with DAPI. Bar represents 500 µm.

8.3.4. Echocardiographic analysis

The fractional shortening was not significantly different between saline and PEG hydrogel injected hearts at 2, 4 and 13 weeks (Table 2). The dimensions of the PEG hydrogel injected hearts were significantly reduced at end diastole at 2 and 4 weeks as compared to the saline controls (Table 2, Figure 40). The increase in heart size that was induced by infarction was reduced by 33% at 2 weeks and 43% at 4 weeks ($p \leq 0.05$) for the PEG hydrogel injected heart relative to the saline control. The dimension changes at end systole showed a similar but non-significant trend, whereby the infarction induced increase was reduced by 22% and 23% in the PEG gel-injected hearts at 2 and 4 weeks respectively ($p=0.25$ and 0.19).

Weeks	Parameter	Sham	Sham plus PEG	Infarct plus saline	Infarct plus PEG
2	FS%	48.99±1.43	47.56±1.26	34.99±1.29	36.55±2.58
	ESD	3.52±0.13	4.25±0.17[δ]	5.55±0.22	5.09±0.31
	EDD	6.89±0.10	8.07±0.15[δ]	8.51±0.19	7.98±0.18*
4	FS%	52.27±0.42	48.29±0.84[δ]	34.42±1.63	35.51±2.75
	ESD	3.60±0.04	4.04±0.16[δ]	6.07±0.30	5.49±0.31
	EDD	7.54±0.09	7.79±0.20	9.2±0.24	8.48±0.16*
13	FS%	48.35±0.61	34.73±1.24	26.48±1.53	26.11±2.53
	ESD	4.36±0.10	5.76±0.20[δ]	7.54±0.32	7.66±0.45
	EDD	8.44±0.14	8.81±0.16	10.20±0.26	10.24±0.30

Table 2: Echocardiography at 2, 4 and 13 weeks

The initial partial preservation of heart dimensions obtained by synthetic hydrogel injection was however lost at 13 weeks with the ESD and EDD being equivalent for both saline and PEG hydrogel injected hearts (Table 2, Figure 40).

The injection of PEG hydrogel into sham-operated hearts did not affect fractional shortening at 2 weeks but there was a small but significant reduction at 4 weeks relative to sham-operated hearts with no PEG injection (Table 2). By 13 weeks, there was a further marked deterioration in fractional shortening associated with PEG injection in sham animals. At 2 weeks both EDD and ESD were significantly increased relative to the sham for PEG gel injected hearts, but by 4 weeks only the ESD was significantly increased, a difference that was amplified at 13 weeks.

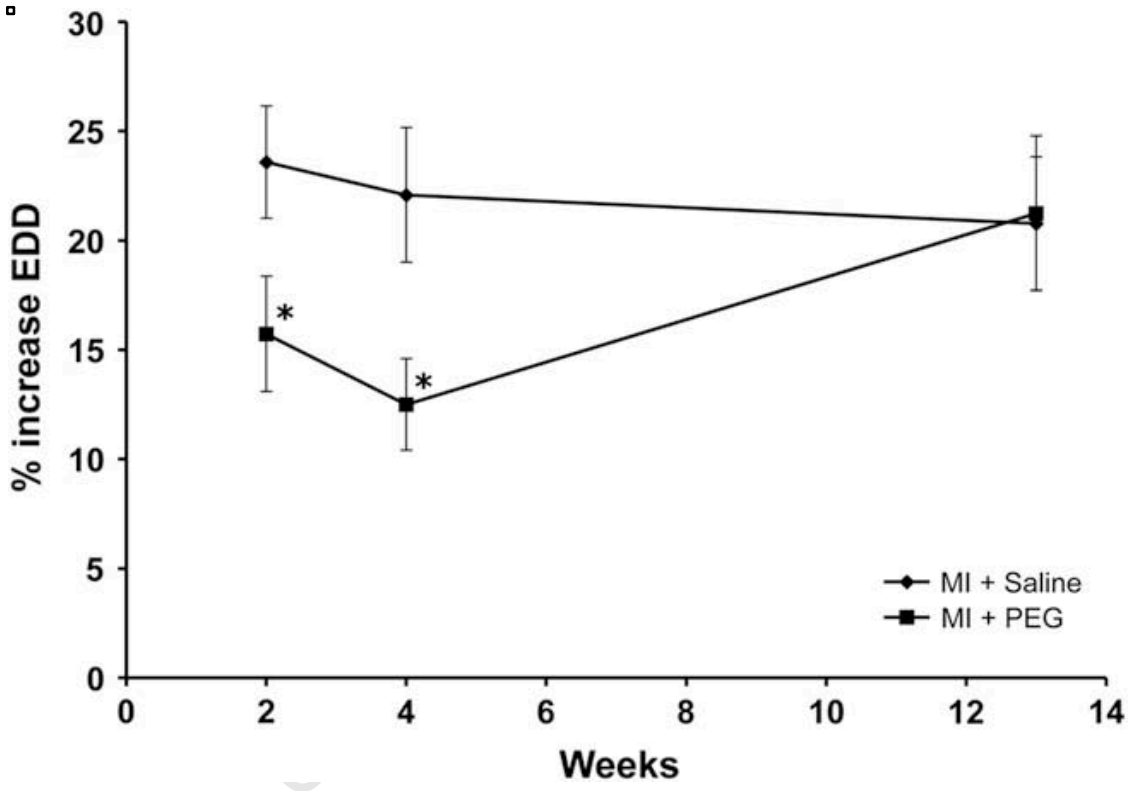

*Fig. 40. Polyethylene glycol (PEG) hydrogel injections reduce infarct induced diastolic dilation over the medium-term. The change in diastolic dimensions over time is presented as a percentage increase relative to sham diastolic dimensions. There was a significant reduction at 2 and 4 weeks (*p=0.05 and 0.02 for 2 and 4 weeks, respectively).*

8.3.5. Post-mortem infarct volume and scar thickness

Infarct volume at 4 weeks in the saline group was 21.96±11.84 % and was not significantly different in the PEG hydrogel injected hearts (22.37±9.85 %). Likewise at 13 weeks the infarct volumes were similar with infarcts occupying 22.55% and 27.87% of the left ventricle volume for saline and PEG hydrogel injected hearts respectively.

Animals in the PEG hydrogel injected group had a significantly thicker scar at 4 weeks relative to the saline injected group, 2.96 mm and 1.66 mm respectively ($p<0.01$). While saline-injected rats showed a 36% decrease in wall/scar thickness, PEG hydrogel injection completely prevented thinning of the scar compared to the sham group at 4 weeks (Figure 41). At 13 weeks the scar in the PEG hydrogel group had thinned relative to the wall of the sham group. Though there was still a trend towards an increased scar thickness as compared to the saline, it was no longer significant (30% increase $p=0.069$).

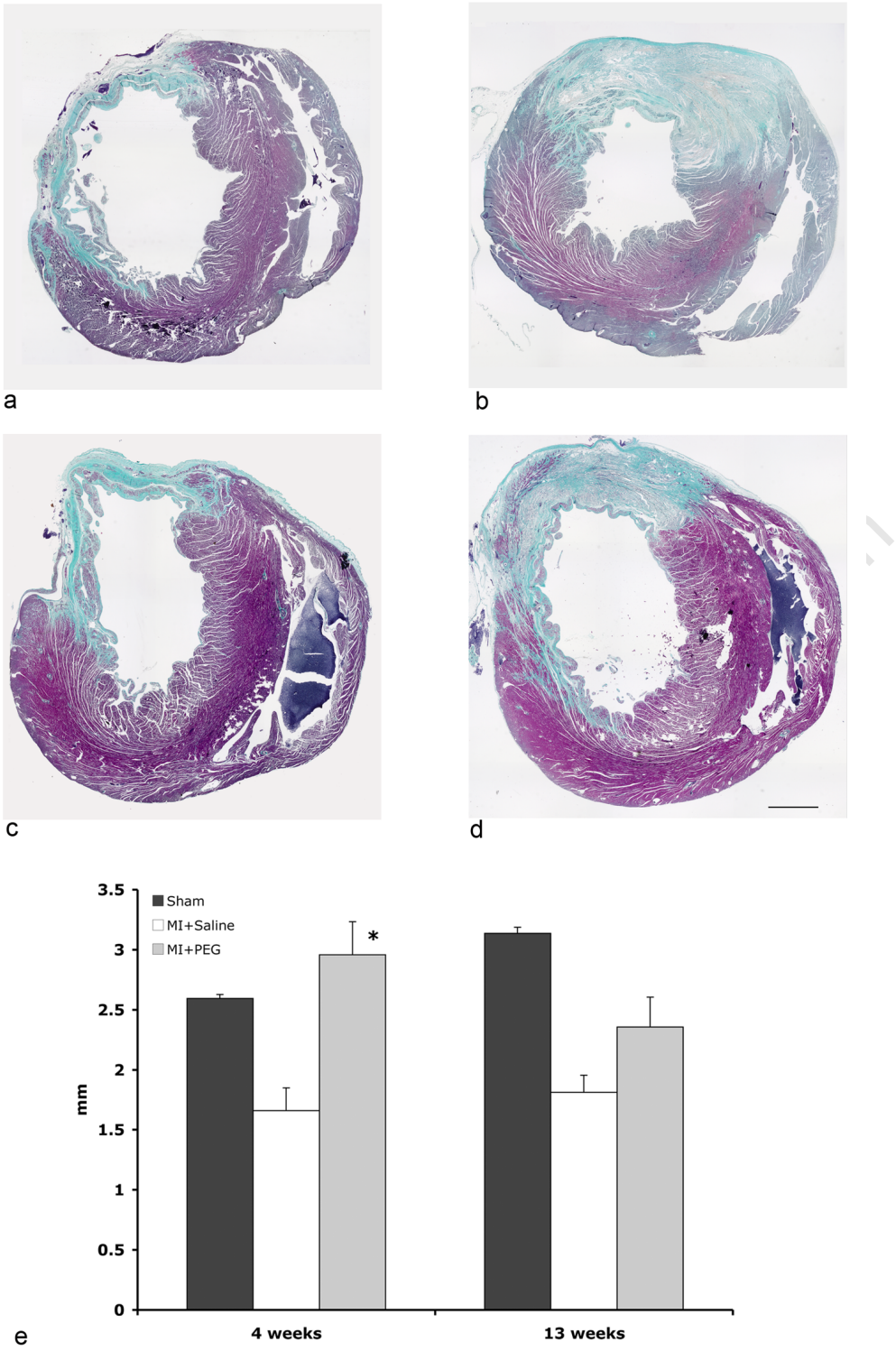

*Fig. 41. Polyethylene glycol (PEG) hydrogel injections preserve wall thickness in the medium-term. Micrographs of Masson's trichrome-stained infarct scars of at 4 weeks (a, b) and 13 weeks (c, d) for saline (a, c) and PEG hydrogel injected hearts (b, d). Bar represents 2 mm. The wall thickness was quantified by image analysis (e). The wall thinning was prevented at 4 weeks (*P <0.01).*

8.3.6. Inflammatory reaction

As a non-degradable hydrogel was being delivered into heart tissue, the inflammatory reaction was assessed by immunohistochemical detection of macrophages. At 4 weeks there was a clear and pronounced macrophage response to the hydrogel that persisted out to 3 months (Figure 42).

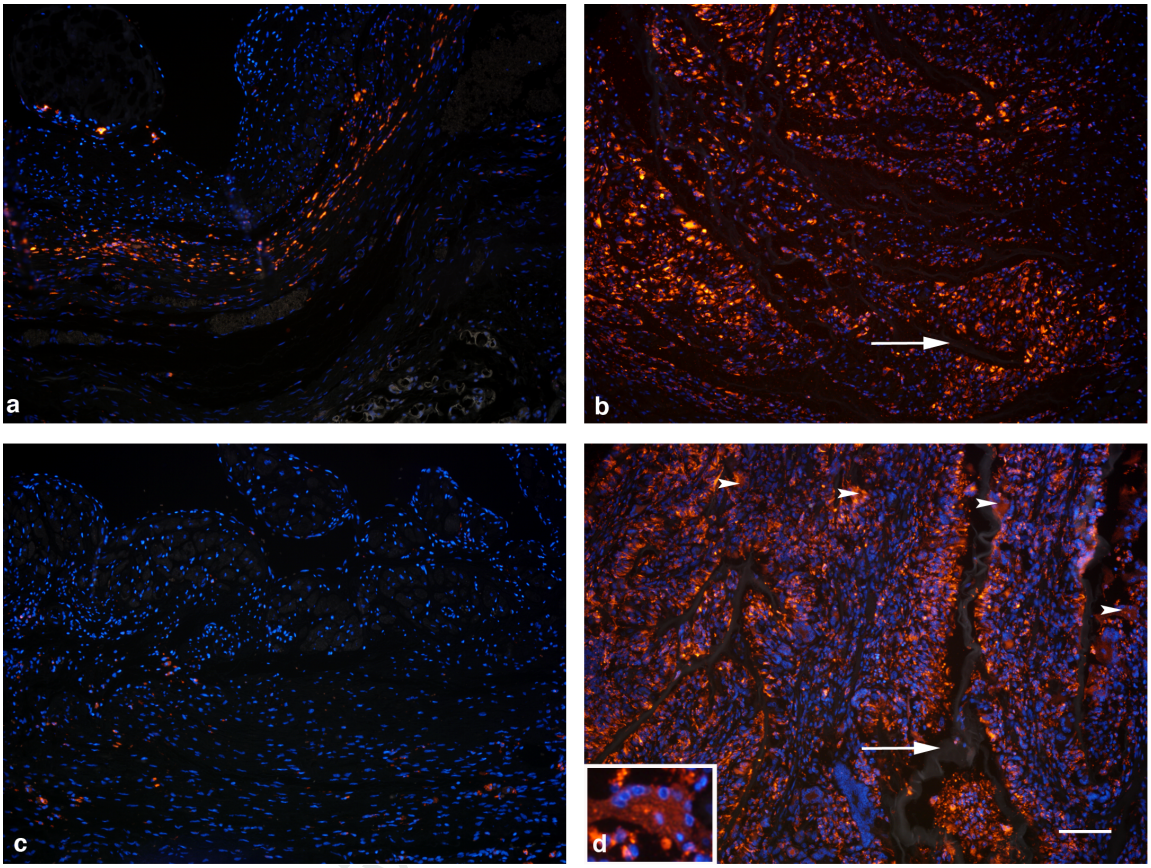

Fig. 42. Inflammatory reaction to polyethylene glycol (PEG) hydrogel. Macrophages were identified by staining for ED-1 (red). Saline injected hearts at 4 and 13 weeks (a, c) and PEG hydrogel injected hearts at 4 and 13 weeks (b, d). Foreign body giant cells were identified by their clustered nuclei (DAPI: blue) at 13 weeks in PEG hydrogel injected hearts (arrowheads). Inset in (d) shows a higher magnification of the cell identified by the rightmost arrowhead clearly demonstrating the characteristic multiple nuclei present within the singular ED1 positive cytoplasm. The PEG hydrogel is visible on the micrograph (arrows) as light gray material. This identification was confirmed by examination of adjacent serial sections for presence of Alexa Fluor 660 label, as the label was lost during the immunohistochemical staining procedure (data not shown). Bar represents 100 μm.

The macrophages were relatively evenly distributed in the PEG hydrogel infiltrated regions. By 13 weeks, a low number of putative foreign body giant cells were observed on the borders of the hydrogel strands.

8.3.7. DISCUSSION

These studies showed for the first time that the injection of a synthetic non-degradable PEG based hydrogel into ischemic myocardium is feasible and leads to a retardation of post-infarct left-ventricular dilatation. A non-degradable form of a PEG-hydrogel gel was utilized to investigate whether a permanent support of the heart is needed to maintain beneficial effects on post-MI remodelling.

It has been suggested previously that in order to maximize the attenuation of remodelling, limit deterioration of cardiac function and progression into heart failure when using injected polymers as a stand-alone treatment, stiffer materials should be used[386,489]. The proposed mechanism for the efficacy of such materials - that they impart an increased mechanical strength to the infarct, providing stress-relief for the cardiomyocytes - draws support from a recent clinical study: Sabatine et al. showed that high baseline levels of ST2, a marker for biomechanical strain, correlated significantly with higher incidences of cardiovascular death and heart failure after myocardial infarcts[491]. PEG-based hydrogels are mechanically more stable than natural hydrogels such as fibrin, collagen and alginate and rank amongst the stiffest hydrogels[386]. Furthermore, many of the natural biomaterials that have been used in similar approaches (fibrin, alginate, matrigel) are known to also enhance angiogenesis, making it challenging to separate effects mechanical strengthening of the infarcted wall might have from a paracrine effect[492,493].

PEG-injected hearts showed reduced adverse remodelling 2 and 4 weeks after myocardial infarction with a complete prevention of wall thinning and significant 33,3% and 43,3% reductions in end-diastolic diameter increase at 2 and 4 weeks, respectively. PEG-injected

hearts also showed a similar trend towards reduced end-systolic dilation. Taken together, the increased scar thickness and decreased heart dimensions should help lessen elevated cardiomyocytes stresses in accordance with Laplace´s law. Indeed at 1 month, delivery of PEG hydrogel resulted in comparable effects to the ACE-inhibitor Lisinopril, namely beneficial remodelling consisting of a significantly decreased EDV and a non-significant decrease in ESV, without improving the ejection fraction after ischemic myocardial injury[494]. However, 3 months after the ischemic event, the remodelling caught up in the PEG-treated group. Luminal dimensions were virtually identical with only the wall thickness in the PEG-group somewhat preserved. To what degree the inflammatory reaction (foreign body reaction) at three months is responsible for the late adverse remodelling is not clear. The continuous inflammation might rather reflect the non-degradability of the material and not the material itself. What speaks against inflammation being the sole reason for the late remodelling in the PEG-treated group is that although long-term implants of non-degradable PEG did damage the non-infarcted heart as confirmed by a substantially decreased fractional shortening at 3 months, the injection of PEG into sham operated hearts did not lead to increased diastolic dimensions at this time.

A possible explanation for the late remodelling in the treatment group might be a delayed build up of cardiomyocyte stresses (in the border zone) above a threshold level. [PEG might act as a buffer for stresses initially – permanently but insufficiently reducing stresses. As the hearts grow bigger, stresses may well increase slowly, ultimately leading to apoptosis, late adverse remodelling and ultimately to a common endpoint in the treatment and control group]

8.3.8. Conclusion

While the experiments showed that the injection of non-degradable synthetic gel was effective in ameliorating pathological remodelling in the medium-term after infarction they also revealed that the injections were unable to prevent long-term dilation, a likely explanation being the inflammatory reaction caused by the non-degradability of the gels.

One of the major advantages of PEG hydrogels is that the engineerability afforded by this gel allows for controlled degradability, potentially reducing inflammation. Therefore the potential of degradable PEG hydrogels for myocardial therapy was investigated next. Degradable hydrogels may overcome the inflammatory issue whilst still providing mechanical support for an extended period of time.

8.4. Enzymatically degradable polyethylene hydrogels for myocardial injection

Enzymatically degradable PEG hydrogels are a potentially important alternative therapy to the non-degradable gel as they will disappear over time and may not induce as pronounced an inflammatory response. The feasibility of crosslinking PEG hydrogels with enzymatically degradable peptides has previously been shown[400].

The main purpose of the following set of experiments was to determine whether controlling the degradability does allow a reduction or even lead to the prevention of the inflammation related to non-degradability. For these studies, hydrogel formation was achieved by Michael-type addition reaction between 20kD-8arm-vinyl sulfone PEG macromers and the thiol groups of cysteine-containing MMP-sensitive peptides. An observation previously made in the laboratory was that PEG hydrogels crosslinked with two different matrix-metalloproteinase sensitive sequences, a highly degradable sequence modified from MMP-1 (GCREGPQGIWGQERCG)[400] or MMP-9 (GCREKGPRQITERCG), respectively, exhibit different degradation times in vitro (personal communication, Mona Bracher).

Therefore a second aim was to determine whether these differences in degradation times between hydrogels crosslinked with MMP1-sensitive (MMP1s) or MMP9s-sequences [from here on referred to as either PEG-MMP1s or PEG-MMP9s] also persist in vivo, as these differences may potentially be exploited for local sustained delivery of cardioprotective factors.

A minor objective of these studies was to assess whether the gelling times of enzymatically degradable PEG hydrogels allowed for efficient delivery to the beating heart. A potential issue previously identified was the increased gelling time compared with non-degradable PEG hydrogels crosslinked with DTT, which may interfere with hydrogel retention in the beating heart.

8.4.1. In vivo gelling times, retention and distribution of enzymatically degradable PEG hydrogels

In vitro gelling times for the enzymatically degradable PEG hydrogels were comparable. MMP-1s crosslinked hydrogels gelled within 13.5 minutes, while it took MMP-9s-crosslinked hydrogels 11.5 minutes to gel under physiological conditions (37°C).

To assess retention and distribution of PEG-MMP1s and PEG-MMP9s, 100 µl of PEG-MMP1s or PEG-MMP9s were injected into the left ventricular region of rat hearts and polymerised in situ. Histological analysis of hears harvested 60 minutes after hydrogel injections revealed successful retention of hydrogels crosslinked with MMP-1- and MMP9-sensitive sequences in beating rat hearts. Both MMP1s and MMP9s-crosslinked hydrogels were retained well within the myocardium and showed similar distributions 60 minutes after the injections (representative image for PEG-MMP1s is shown in Fig.43). Overall the enzymatically degradable hydrogels seemed to integrate better into the myocardial tissue than non-degradable PEG hydrogels (see Fig.43c-d). The hydrogels were dispersed over a larger area than non-degradable polyethylene glycol hydrogels and appeared more fibrillar in nature. Due to the slower gelling times of enzymatically degradable hydrogels, the possibility of gelling as a globule within the heart should be reduced. This in turn may explain the increased homogeneity in distribution between cardiomyocytes (see Fig.43c-d).

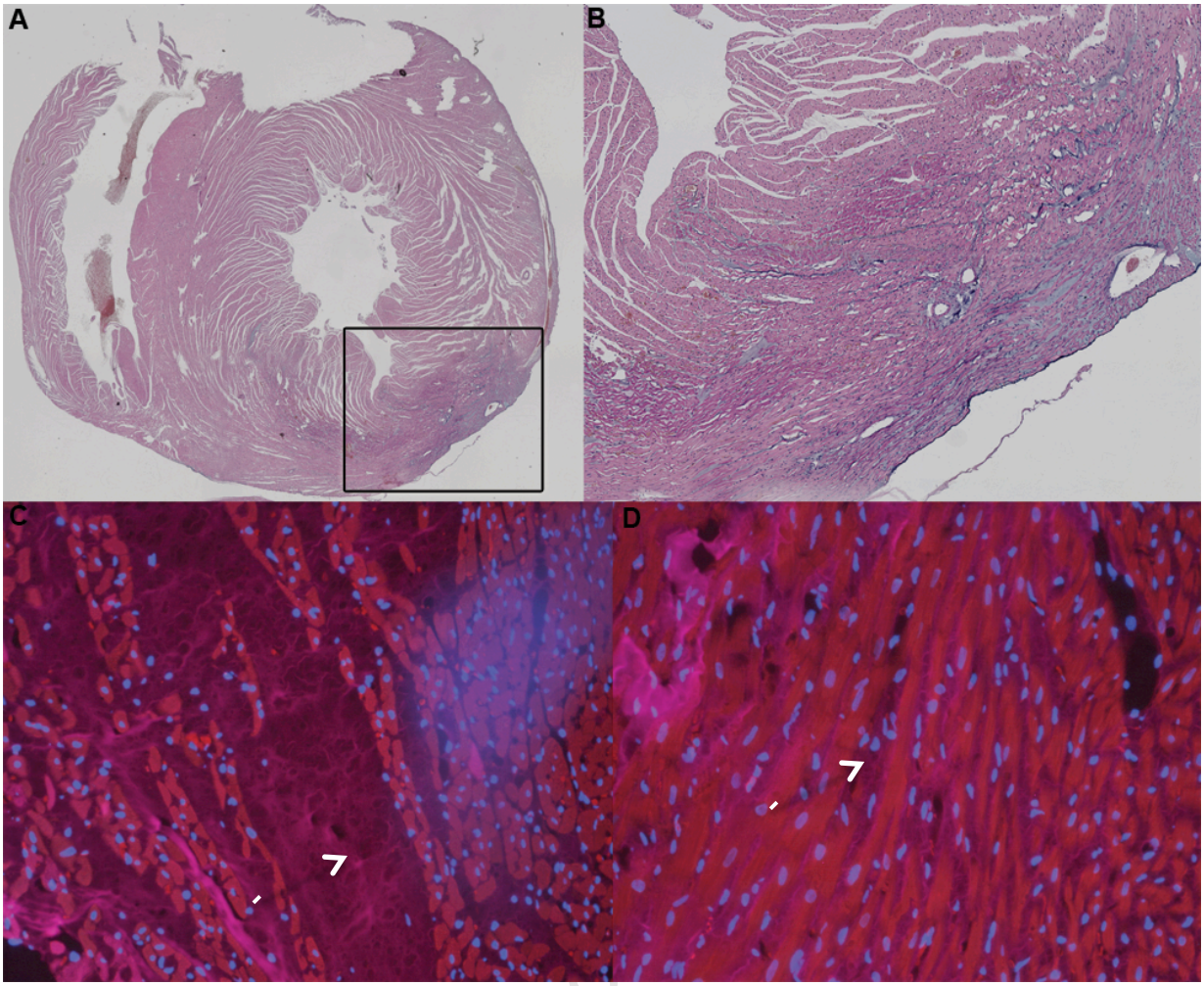

Figure.43. Micrographs of degradable PEG-MMP1s implants 1 hour after myocardial injection. H&E scan showing entire cross section with extent of PEG dispersion indicated (black frame), 2x magnification (A). H&E 10x magnification (B). Fluorescent micrograph showing fibrillar nature (PEG in pink (arrows), cardiomyocytes red due to autofluorescence, Nuclei counterstained with DAPI in blue, 200x magnification (C). Micrograph showing even dispersion of PEG between cardiomyocytes, 200x magnification (D).

8.4.2. In vivo degradability of PEG-MMP1s and PEG-MMP9s hydrogels

To assess the degradation rates of and the inflammation provoked by PEG-MMP1s and PEG-MMP9s, hearts were again injected with 100µl of the respective PEG hydrogels. Distribution of PEG-hydrogels was then assessed 60 minutes, 1, 2 and 4 weeks after

intramyocardial injection by detection through fluorescent microscopy of the covalently attached far-red fluorescent label (n=2 for each timepoint).

Hearts harvested 60 minutes after myocardial injection showed that hydrogel distribution was similar for PEG-MMP1s and PEG-MMP9s, demonstrating successful in vivo delivery after crosslinking with either sequence (see Fig.44)

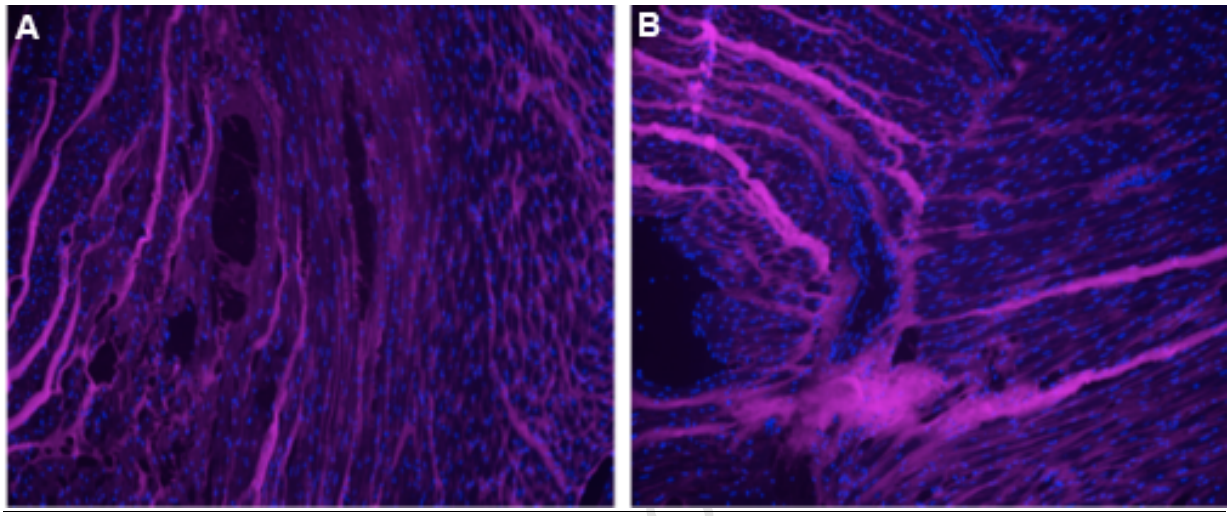

Fig.44. To confirm successful delivery, distribution of PEG hydrogels crosslinked with a MMP1-sentitive (A) or a MMP-9-sensitive sequence (B) was analyzed 60 minutes after cardiac injection and was shown to be similar in both treatment groups.

After successful implantation, PEG-MMP1s degradation occurred at a much more rapid pace in comparison with PEG-MMP9s hydrogels (Fig.45). 7 days after intramyocardial injection a majority of the hydrogel had been degraded (see Fig.45a). In histological section obtained from hears harvested after 14 and 28 days, respectively, only traces of remaining hydrogel were found [Fig.45c (14 days) and Fig.45e (28 days)], suggesting that degradation is essentially completed between day 7 and 14 after intramyocardial injection. PEG-MMP9s hydrogels on the other hand were found throughout the left-ventricle at all timepoints [shown in Fig.45b (7 days), d (14 days), f (28 days)]. PEG distribution was similar between the 60-minute and the 28-day timepoint suggesting that PEG-MMP9s hydrogels are stable for up the first month after cardiac implantation into sham-operated rat hearts.

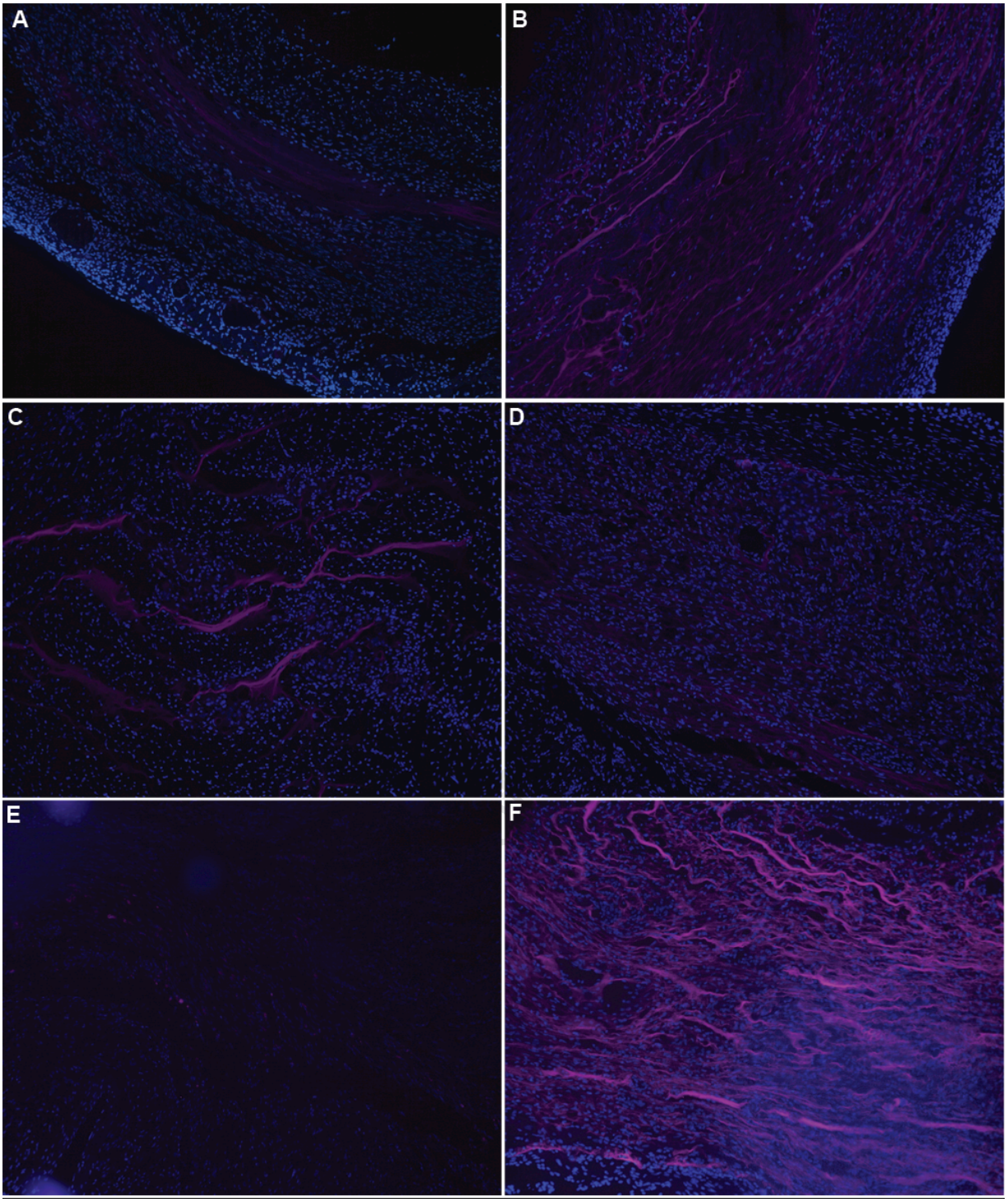

Fig.45. Left-ventricular distribution of PEG-MMP1s and PEG-MMP9s 7, 14 and 28 days after intramyocardial injection was assessed. PEG-MMP1s hydrogels degraded faster in vivo [7 days (A), 14 days (C), 28 days (E)] than PEG hydrogels crosslinked with a MMP9-sensitive peptide sequence [7 days (B), 14 days (D), 28 days (F)]

8.4.3. Discussion

Differential degradation rates between PEG-MMP1s and PEG-MMP9s hydrogels had been expected prior to conducting these experiments. The MMP1-derived MMP1s-sequence used to form PEG-MMP1s hydrogels had previously been engineered to be highly degradable[400]. Furthermore in vitro experiments had revealed faster degradation rates of PEG-MMP1s hydrogels when compared with PEG-MMP9s hydrogels (personal communication M.Bracher). The current study thus confirmed these previous findings in vivo after myocardial injection.

Since it was hypothesized that the prolonged inflammatory reaction observed in previous studies was correlated to the non-degradability, the next objective was to assess the inflammatory response triggered by enzymatically degradable PEG hydrogel at the 7-, 14- and 28 day-timepoints.

8.4.4. Inflammatory response after cardiac injection of enzymatically degradable PEG hydrogels

At day 7, the inflammation assessed by immunohistochemical analysis of ED-1, a marker for rat macrophages, was similar in hearts injected with PEG-MMP1s and PEG-MMP9s (see Fig.46A and 46.B respectively). By day 14, as PEG-MMP1s hydrogels had almost entirely degraded, the inflammatory response had also mostly resolved (see Fig.46C). Samples obtained on day 28 confirmed this trend as inflammation was remarkedly reduced after PEG-MMP1s degradation (Fig.46E). In PEG-MMP9s hydrogels ED-1 staining revealed similar amounts of inflammation at all timepoints [Fig.46B (7 days), 46.D (14 days) and 46.F (28 days)]. This result suggests that the rate of PEG degradability is linked to the degree of inflammation induced after myocardial injection.

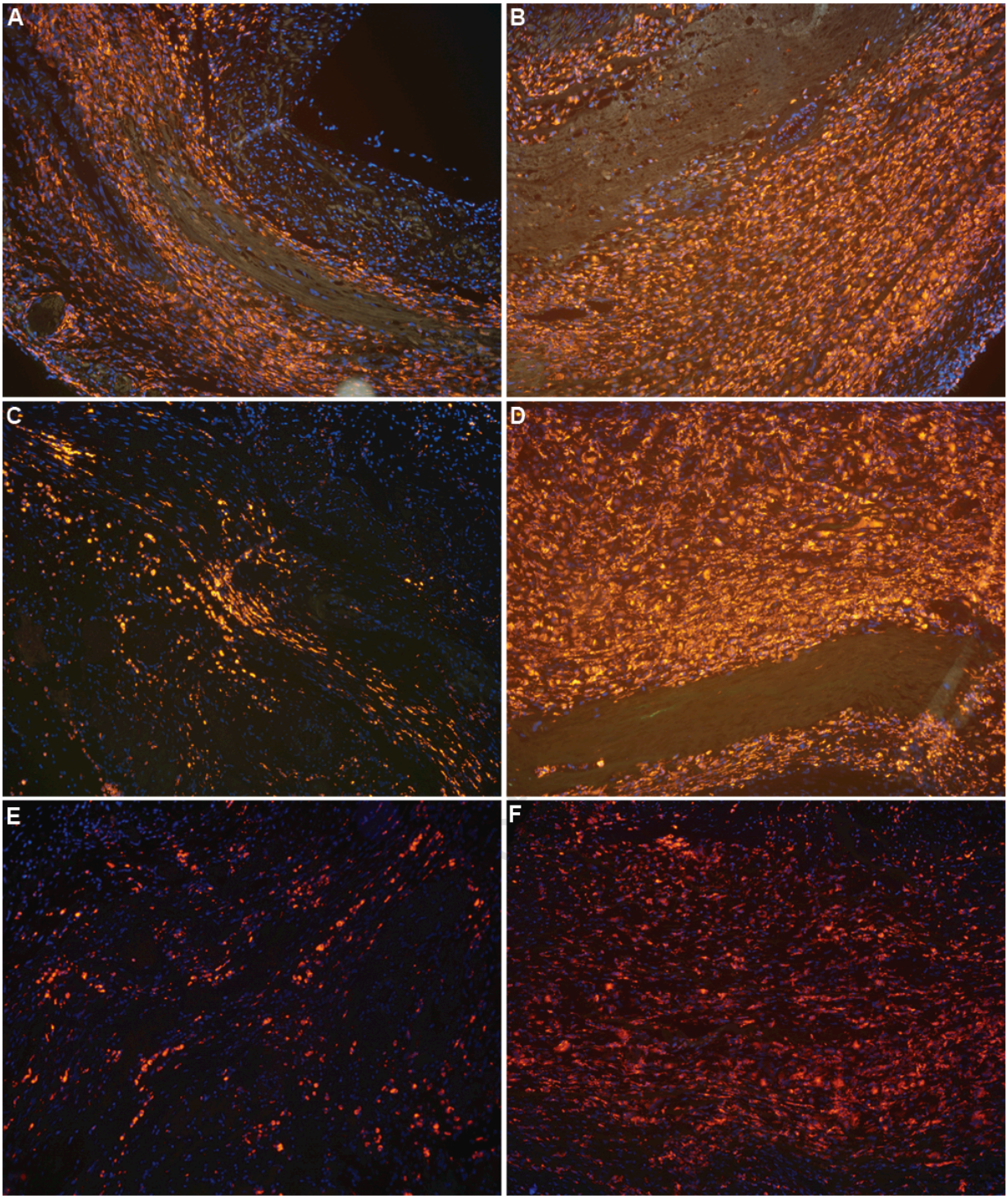

Fig.46 Immunohistochemical analysis of ED-1^{+}-cells was performed to determine the inflammatory response present 7, 14 and 28 days after injection of PEG-MMP1s and PEG-MMP9s, respectively. In accordance with a faster degradation of PEG-MMP1s hydrogels (shown in Fig.45) inflammation was markedly reduced at later timepoints [7 days (A), 14 days (C), 28 days (E)]. PEG-MMP9s hydrogels illicited an inflammatory response that remained constant over the course of the study [7 days (B), 14 days (D), 28 days (F)].

8.4.5. Conclusion

Characterization of hearts injected with both PEG-MMP1s and PEG-MMP9s hydrogels revealed that in situ polymerisation and retention of enzymatically degradable hydrogels within the beating heart is feasible. Importantly, degradation times differed between PEG hydrogels crosslinked with MMP1s and MMP9s, as PEG-MMP1s hydrogels had almost entirely degraded after 14 days, while PEG-MMP9s hydrogels remained stable for the duration of the study. This finding suggests that hydrogel formation with varying protease-sensitive peptide sequences allows control over the rate of hydrogel degradation in vivo. This in turn could be exploited to modulate the release of bioactive molecules for therapeutic angiogenesis.

Furthermore, these experiments revealed that the inflammation observed after cardiac PEG hydrogel injection is linked to their degradation rate, as the induced inflammatory response resolved faster after injection of quickly degrading PEG-MMP1s hydrogels.

Since it was hypothesized that the prolonged inflammatory reaction observed in previous studies with DTT-crosslinked PEG hydrogels was a result of the non-degradability leading to a reduction in cardiac function, the next objective was to investigate the biocompatibility of enzymatically degradable polyethylene hydrogels (PEG-MMP1s and PEG-MMP9s) after intramyocardial injection into healthy hearts.

8.5. Biocompatibility of enzymatically crosslinked PEG-hydrogels in rat hearts

To determine the biocompatibility of PEG hydrogels cross-linked with either the MMP1 or MMP9-sensitive peptide sequence, 100 µl of PEG hydrogels was injected into the heart after a thoracotomy (n=8). Saline injected rat hearts served as control animals (n=8). Echocardiographic analysis was performed 2 and 4 weeks post surgery. The animals were

sacrificed on day 29 and histological analysis to investigate a potential inflammatory reaction was performed.

8.5.1. Survival

A total of 24 rats (n=8) were used in this study. All animals survived for the duration of the study period.

8.5.2. Echocardiographic analysis

Left-ventricular function was assessed at days 14 and 28. After 2 weeks, animals injected with polyethylene hydrogels crosslinked with either an MMP1-sensitive or an MMP9-sensitive peptide sequence had an ejection fraction of 43.01±2.58% and 47.16±0.49%, respectively, and did not differ significantly from saline-injected control animals (46.3±1.03%, n=8, NS, see Fig.47).

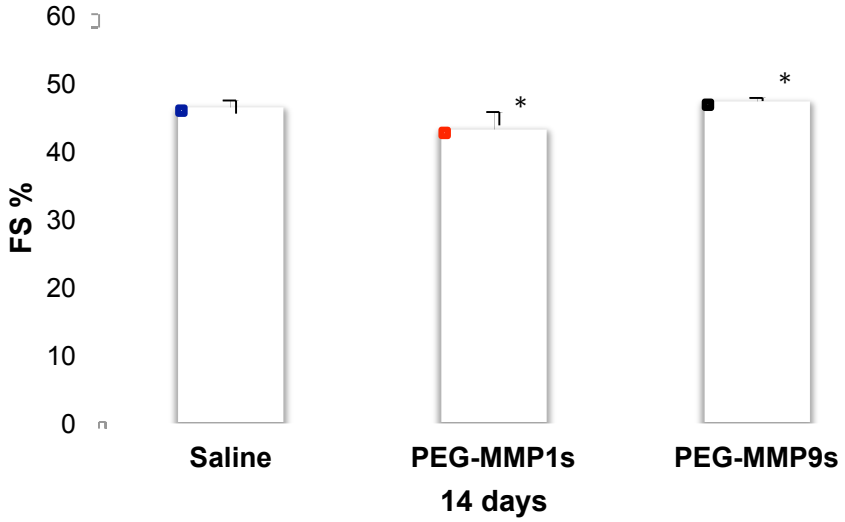

*Fig.47. Echocardiographic evaluation of cardiac function was performed 14 days after intramyocardial injection of enzymatically degradable PEG hydrogels into sham-operated hearts. No significant changes were observed after treatment with PEG-MMP1s or PEG-MMP9s in comparison with saline controls (*p>0.05).*

Myocardial contractility was again evaluated 4 weeks after PEG-MMP1s and PEG-MMP9s injections into the heart. As seen on day 14, no adverse effects on left-ventricular function resulted from injection of enzymatically degradable PEG hydrogels (n=8, p>0.05, see Fig.48). Fractional shortening after PEG-MMP1s injections was 44.18±2.47% at the 4 week-timepoint, while animals injected with PEG-MMP9s had an ejection fraction of 47.15±1.19%. These results were not significantly different in comparison with saline-injected controls (46.49±0.94%).

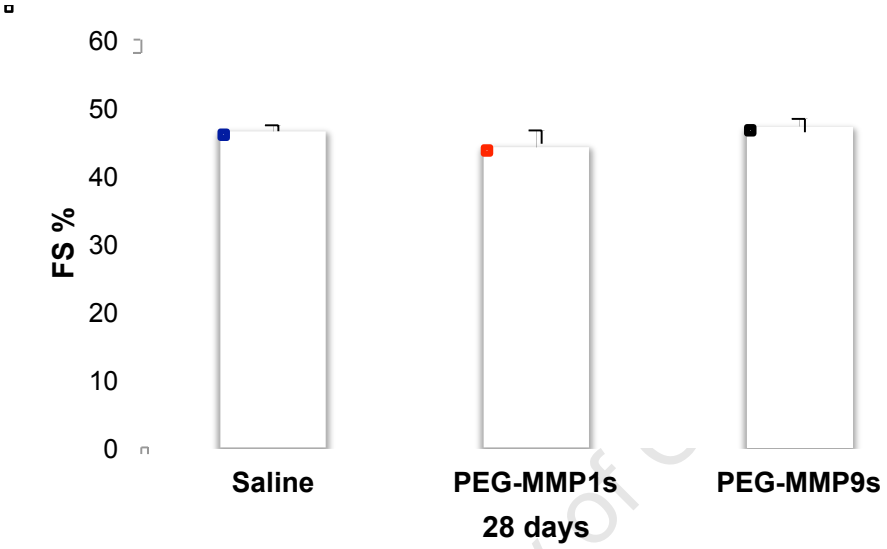

*Fig.48. Graph shows results from echocardiographic analysis of cardiac function on day 28. Injections of PEG-MMP1s and PEG-MMP9s did not adversely affect cardiac contractility at this timepoint (*p>0.05 vs saline injected controls).*

8.5.3. Histological analysis – Masson's Trichrome

To determine, whether injections of PEG-MMP1s and PEG-MMP9s is associated with scar formation within the left-ventricular wall, hearts sections obtained after sacrifice on day 29 were stained with modified Masson's Trichrome. No differences with saline-injected control hearts were observed. Neither the faster degrading PEG-MMP1s hydrogels nor the more stable PEG-MMP1s hydrogels induced scar formation 4 weeks after intramyocardial injection, confirming a superior biocompatibility in comparison with PEG-DTT hydrogels (see Fig.49).

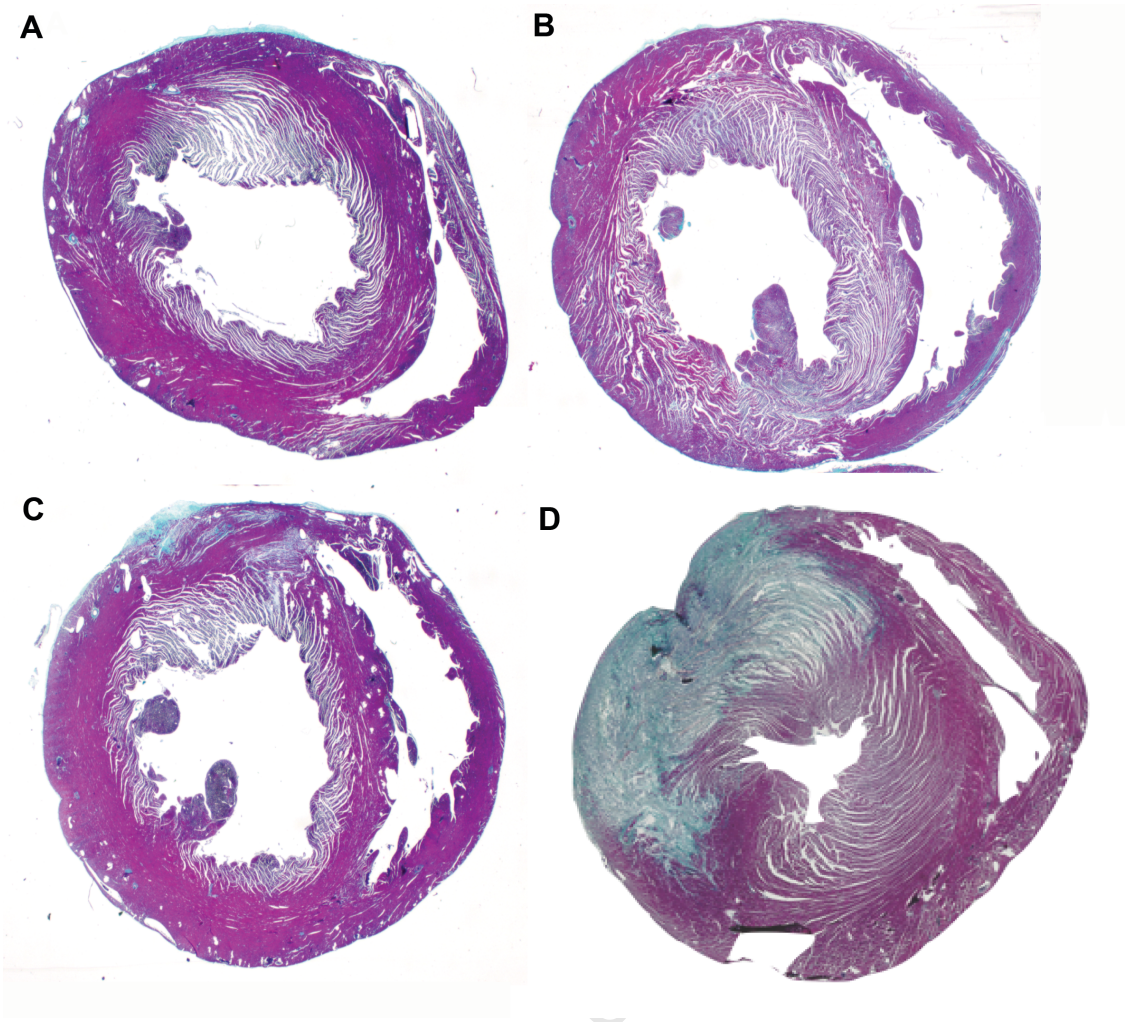

Fig.49. Masson's Trichrome images of sham-operated hearts injected with saline (A), PEG-MMP1s (B), PEG-MMP9s (C), and non-degradable PEG-DTT (D) are shown. At day 29, no traces of scar formation are found around the injection sites of enzymatically degradable PEG hydrogels while PEG-DTT injections resulted in extensive scarring of the LV at this timepoint.

8.5.4. Inflammation (not shown, see Fig.46)

Immunohistochemical staining for macrophages in hearts injected with PEG-MMP1s and PEG-MMP1s was performed to determine the extent of inflammation at day 29. As found in the previous study (see.Fig.46), the injection of MMP9s-crosslinked hydrogels caused a more pronounced inflammatory reaction in comparison with the faster degrading MMP1s-crosslinked gels at day 29.

8.5.5. Conclusion

Myocardial injections of enzymatically crosslinked PEG-MMP1s and PEG-MMP9s hydrogels had no adverse effects on ventricular function at days 14 and 28. On the contrary, after injection of DTT-crosslinked hydrogels, a slight, but significant decrease in myocardial contractility had been observed on day 28 in comparison with saline controls (see Table 2, 8.3.4.).

When investigating the amount of inflammation present at day 29, an increased inflammatory reaction directed against PEG-MMP9s hydrogels was observed in comparison with PEG-MMP1s or saline injected hearts. Yet, this did not have an effect on myocardial performance (see Fig.48). Time constraints did not allow for additional long-term experiments to definitively exclude an adverse effect of PEG-MMP9s hydrogels on cardiac function at a later timepoint. However, the significant reduction seen after injection of the highly degradable PEG-MMP1s suggests, that once degradation of the gels sets in, the inflammation present around the hydrogels quickly resolves. Collectively these results indicate that degradable polyethylene glycol hydrogels are more suitable for intramyocardial injections in comparison with non-degradable PEG-hydrogels and present a promising platform for in vivo targeted delivery of bioactive molecules. Whether transient support by PEG-MMP1s and PEG-MMP9s hydrogels is sufficient to ameliorate left ventricular remodelling after myocardial infarction, though, is unknown. Thus, the effects of enzymatically degradable PEG-MMP1s and PEG-MMP9s hydrogels on post-infarct left-ventricular function and remodelling were tested next.

8.6. Effects of enzymatically-degradable polyethylene glycol hydrogels on post-infarct left ventricular function and remodelling

8.6.1. Rationale

After confirming that myocardial injections of enzymatically-degradable polyethylene glycol hydrogels do not have adverse effects left-ventricular function up to 28 days after myocardial injection, the next objective was to test whether a transient support of the left ventricle after

myocardial infarction is sufficient to ameliorate infarction-associated left ventricular remodelling and whether the implantation of degradable hydrogels has beneficial effects on heart function post MI.

Immediately after permanent ligation of the left anterior descending artery, PEG-MMP1s or PEG-MMP9s hydrogels were injected into the infarcted region and polymerised in situ. Ventricular function and heart dimensions were assessed at 2 and 4 weeks. Histological analysis to determine post-mortem infarct volume and scar thickness was performed subsequent to sacrifice of the animals at day 29.

8.6.2. Survival

A total of 35 rats were operated for this study. Two animals died within 30 minutes of the surgery. An additional animal died 3 weeks post operation. The overall survival rate for the study was 91.43% (32 rats, n=9-12).

8.6.3. Echocardiographic analysis

Echocardiographic analysis did not reveal any significant differences between the treatment and control groups at both days 14 and 28. Saline injected animals had a fractional shortening of 31.71±1.78% at day 14 (n=10), which was similar to animals treated with either PEG-MMP1s (31.86±1.89%, n=11, p=0.95) or PEG-MMP9s (30.26±1.8, n=12, p=0.58), respectively (see. Fig.50).

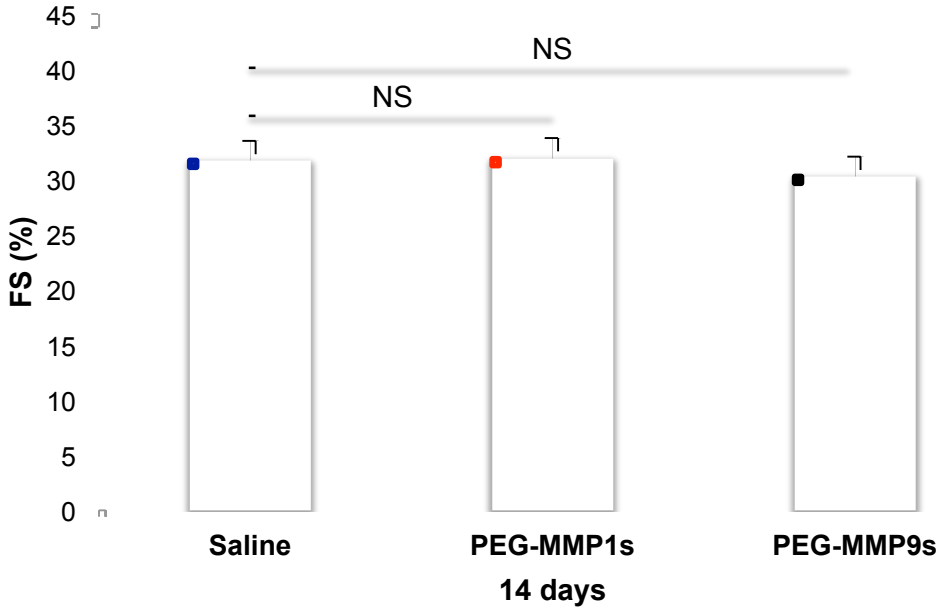

Fig.50. Echocardiographic analysis of cardiac function was performed 14 days after experimental myocardial infarction. Injections of ezymatically degradable PEG-MMP1s or PEG-MMP9s hydrogels did not improve fractional shortening in comparison with saline-injected controls (p>0.05).

Ventricular function slightly decreased in all groups between days 14 and 28. At day 28 the fractional shortening of saline injected animals was 28.98±1.95% (n=9) and did not differ significantly from animals treated with either PEG-MMP1s (29.81±1.99%, n=11, p=0.77) or PEG-MMP9s (28.43±1.95, n=12, p=0.85), respectively.

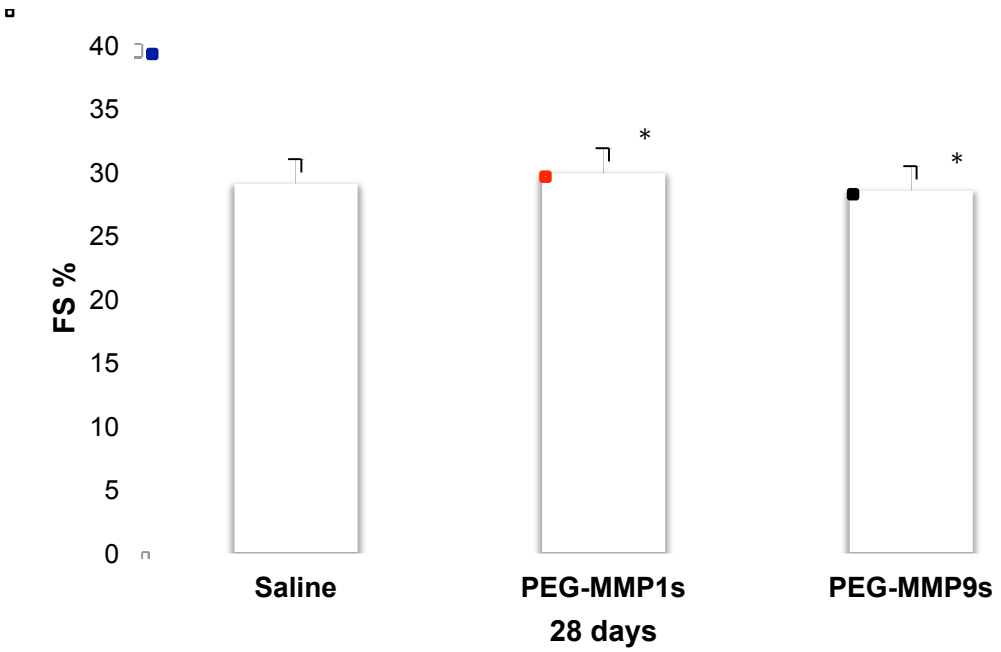

*Fig.51. Cardiac contractility was again assessed 28 days after MI. Neither PEG-MMP1s nor PEG-MMP9s significantly affected fractional shortening at this timepoint (*p>0.05 compared to saline).*

8.6.3.1. Heart dimensions

To determine whether enzymatically degradable PEG hydrogels affect post-infarct heart remodelling, left-ventricular end-systolic (ESD) and end-diastolic (EDD) dimensions were measured using echocardiography at 14 and 28 days. 14 days after experimental myocardial infarction ESD was 574.35±31.72μm in saline-injected hearts (n=10). PEG-MMP1s and PEG-MMP9s injections did not significantly change ESD in comparison with controls at this time and were 573.97±31.49μm (n=11) and 581.71±26.90μm (n=12), respectively (see Fig.52).

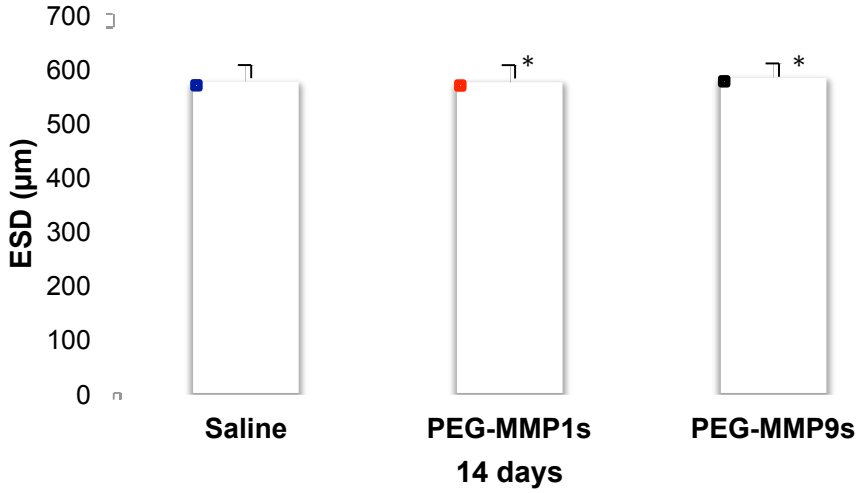

*Fig.52. 14 days after having undergone experimental myocardial infarction, end-systolic diameters were measured during echocardiographic evaluation to determine post-infarct left ventricular remodelling. No significant effects were seen after injection of either PEG-MMP1s or PEG-MMP9s (*p>0.05 vs. saline controls), respectively.*

EDD measured 14 days after injection of saline (836.50±28.41µm, n=10), PEG-MMP1s (836.20±25.21µm, n=11) or PEG-MMP9s (830.39±19.13µm, n=12), respectively, were almost identical and did not statistically differ (p>0.05, shown in Fig.53).

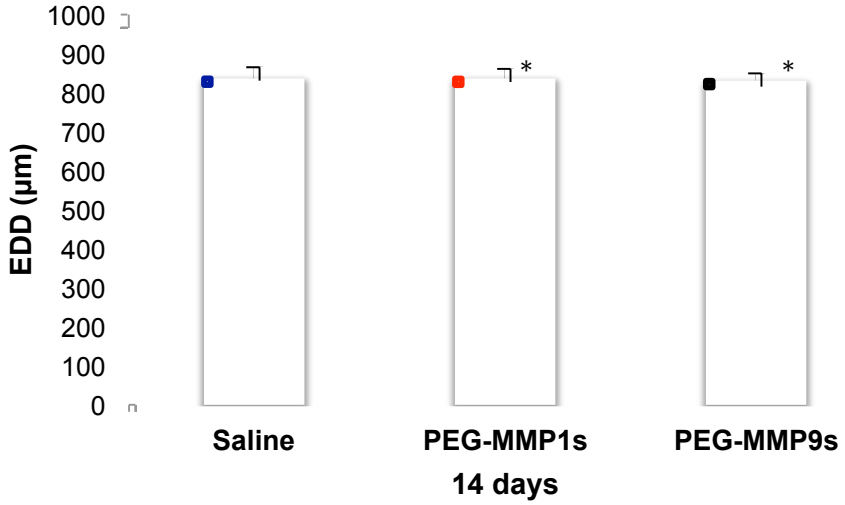

*Fig.53. Echocardiographic measurement of end-diastolic diameters revealed no significant differences between hearts injected with saline, PEG-MMP1s and PEG-MMP9s (*p>0.05, compared to saline) 14 days after myocardial infarction.*

As seen on day 14, left ventricular diameters were not significantly different 28 days after intramyocardial injection between the three treatment groups. ESD was 625.15±36.62µm (n=9), 623.53±34.69µm (n=11), and 634.70±38.31µm (n=12) after administration of saline, PEG-MMP1s and PEG-MMP9s (see Fig.54).

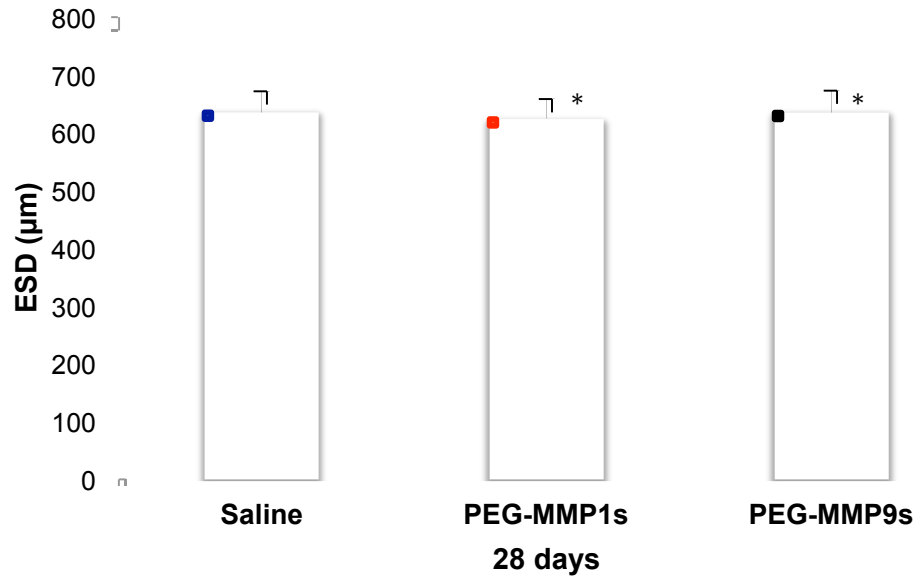

*Fig. 54. Graph shows end-systolic diameters 28 days after myocardial infarction. A significant difference after saline, PEG-MMP1s or PEG-MMP9s-delivery was not seen (*p>0.05 vs. saline).*

At day 28, left ventricular diameter at the end of diastole was 888.06±28.49µm (n=9), 881.83±26.13µm (n=11), and 879.81±28.18µm (n=12) hearts injected with saline, PEG-MMP1s and PEG-MMP9s, respectively (see Fig.55).

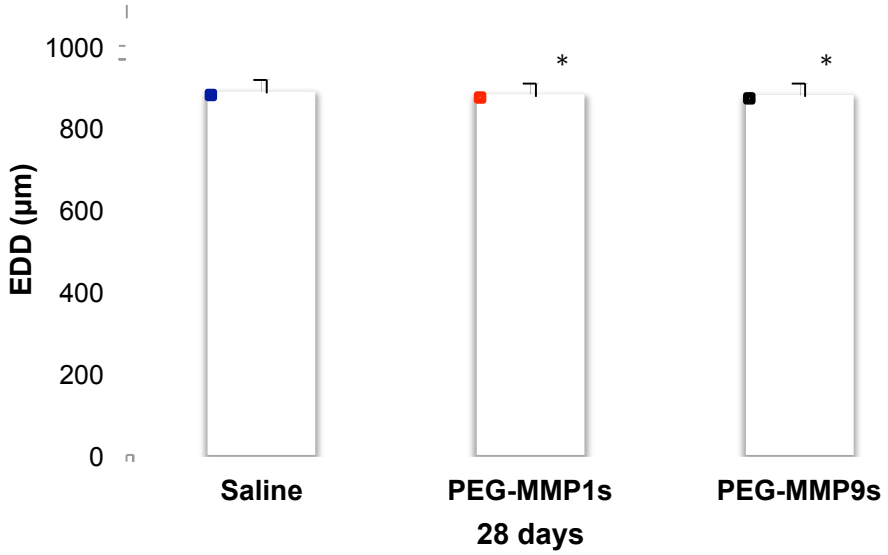

*Fig.55. No significant difference in end-diastolic diameter as measured by echocardiography was found (*p>0.05 vs. saline controls) between the three treatment groups at day 28 after MI.*

8.6.4. Post-mortem scar thickness and infarct volume

To determine whether the injection of PEG-MMP1s or PEG-MMP9s leads to successful prevention of left ventricular wall thinning or a reduction in infarct volume, heart sections were stained with Masson's Trichrome.

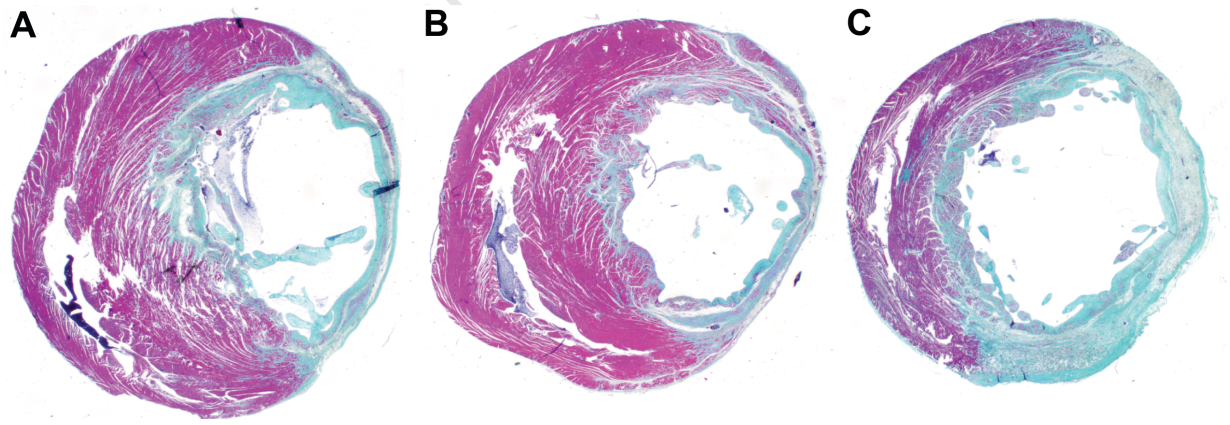

Fig. 56. Masson's Trichrome staining of histological sections from hearts explanted on day 28 was performed to assess myocardial infarct scar thickness. Representative images for hearts treated with saline (A), PEG-MMP1s (B) and PEG-MMP9s (C) are shown.

Image analysis revealed that the average thickness of the scar spanning the left ventricular wall after MI was 907.75±80.02µm in hearts injected with saline. Injections of both enzymatically degradable PEG-hydrogels resulted in a non-significant decrease in wall thinning after myocardial infarction (see Fig.56+57). Scars stemming from MI were 17.6% thicker after PEG-MMP1s hydrogel injections on day 28 and were measured at 1067.90±131.92µm (p=0.36 vs. saline). PEG-MMP9s injections preserved the thickness of the left-ventricular wall best. There was a strong trend towards a significant increase in scar thickness in comparison with saline injected control hearts (p=0.16), as the treatment of PEG-MMP9s resulted in an average scar thickness of 1126.73±108.32µm (a 24.12% increase over saline controls, see Fig.57). The fact that PEG-MMP9s injections resulted in the biggest increase in scar thickness/lowest decrease in wall thickness post MI is in accordance with the previous finding that these hydrogels were more stable and degraded slower after intramyocardial injections in comparison with PEG hydrogels crosslinked with the MMP1-sensitive sequence.

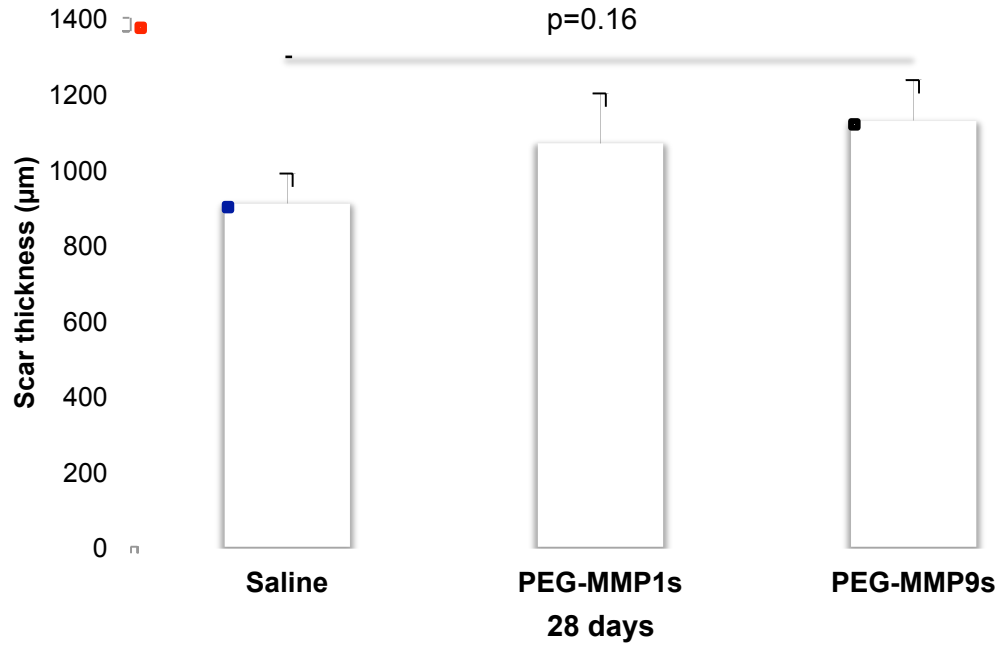

Fig.57. Quantification of scar thickness revealed no significant differences in scar thickness between treatment groups and saline injected controls. A trend towards decreased wall thinning was observed after injection of slower degrading PEG-MMP9s hydrogels (p=0.16).

A potential effect of enzymatically degradable PEG-hydrogels on limiting the extent of the myocardial infarct was investigated next. Infarct volume in hearts treated with saline was 27.85±2.37% 28 days after permanent LAD occlusion. In comparison, infarct volumes measured after PEG-MMP1s and PEG-MMP9s injections were 26.75±3.55% and 33.23%, respectively and not significantly different (see Fig.58). While there appears to be a trend towards increased infarct volumes in PEG-MMP9s injected hearts, this likely represents an artefact due to the increased wall thickness present after treatment in this group (p=0.18 vs. saline, p=0.16 vs. PEG-MMP1s).

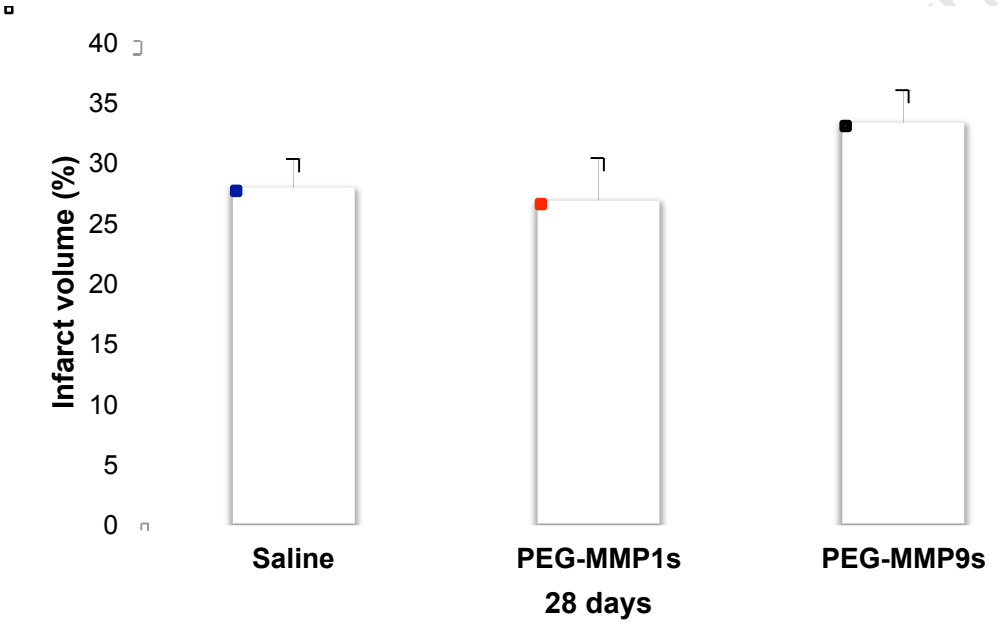

Fig.58. Quantification of infarct volume was performed on heart sections stained with Masson Trichrome is shown. On day 28, no significant differences were seen after treatment of infarcted hearts with saline, PEG-MMP1s or PEG-MMP9s, respectively.

8.6.5. Discussion

While the injection of non-degradable polyethylene glycol hydrogels significantly slowed down heart remodelling over the first 4 weeks after myocardial infarction, enzymatically degradable polyethylene glycol hydrogels were not effective in ameliorating post-infarction left ventricular

remodelling during this period of time. The results of this study thus confirm that degradable PEG-MMP1s and PEG-MMP9s hydrogels used in this study are not an effective alternative to non-degradable polyethylene glycol hydrogels. Currently a lack of long-term data exists determining whether beneficial effects seen after biomaterial injections persist over extended periods of time[495]. Collectively the data obtained after injection of non-degradable DTT-crosslinked and enzymatically degradable PEG-MMP1s and PEG-MMP9s hydrogels suggest that permanent support is necessary to maintain beneficial effects on cardiac remodelling. Yet, many degradable natural biomaterials such as fibrin and collagen have been previously reported to limit infarct size, cardiac remodelling and to promote cardiac function up to 5 weeks after MI[388,390,393]. A number of potential explanations for this finding exist, including differences in MI model (chronic MI vs. ischemia-reperfusion), differences in infarct size, and timing and volume of biomaterial injections. In part the differential outcome may also be a result of the pro-angiogenic potential of natural biomaterials[393]. A comprehensive comparison between natural and synthetic biomaterials using standardised protocols would yield valuable information to gain a better understanding into the mechanisms underlying beneficial effects on post-MI remodelling after biomaterial injections. A shortcoming of the current study is the lack of data on ventricular remodelling prior to the 2-week time-point. Thus it remains unclear whether the degradable hydrogels used in this study retarded LV remodelling at any point prior to 2 weeks. Consequently, no definitive conclusion can be drawn as to whether mechanical support by hydrogels exerts its main beneficial effects within the first minutes after myocardial infarction or whether ventricular remodelling proceeds after rapid degradation of the hydrogel. As gelling times in non-degradable hydrogels were shorter, an increased benefit would be expected, if immediate support after coronary occlusion is the most crucial variable. While slower gelling times allow for a more homogeneous distribution of the enzymatically degradable hydrogels, this may also result in inferior mechanical characteristics of degradable hydrogels in comparison with non-degradable hydrogels. Therefore it is possible to hypothesize that insufficient stress relief for surviving cardiomyocytes provided by degradable hydrogels in the first minutes to hours after

myocardial infarction explains the different outcomes. Additional studies to determine mechanical characteristics of hydrogels crosslinked with enzymatically degradable peptide sequences in comparison with DTT (to form non-degradable hydrogels) should be performed in the future. Alternatively, if lack of initial mechanical support is not the underlying mechanism for the negative result of this study, an early benefit could have been lost after partial degradation of the enzymatically degradable hydrogels. One of the main benefits after injection of non-degradable PEG hydrogels, a prevention of wall thinning, was somewhat preserved after injection of the more slowly degrading PEG-MMP9s hydrogels, as a 24.12% increase in scar thickness was observed on day 28 in comparison with saline controls ($p=0.16$). This points towards hydrogel degradability being the main reason responsible for the lack of positive effects of post-infarct heart remodelling. As - due to the limited regenerative potential of the myocardium - degrading hydrogels are mainly replaced by scar tissue, rapid degradation of the enzymatically polyethylene hydrogels may not allow sufficient time for proper scar formation thereby eradicating an initial benefit.

8.6.6. Conclusion

Enzymatically degradable hydrogels did not effectively reduce LV remodelling after myocardial infarction. Even after injection of PEG-MMP9s hydrogels, which degrade more slowly in vivo, only a non-significant increase in scar thickness compared with saline injected controls was seen. Importantly, though, it was shown that the host inflammatory response after myocardial injection was dramatically reduced as hydrogel degradation progressed, suggesting that no adverse long-term effects result from local delivery of enzymatically degradable PEG-hydrogels to the myocardium. Thus, these synthetic hydrogels still have a great potential for use as slow delivery matrix for therapeutic angiogenesis.
Consequently, the potential of enzymatically degradable PEG hydrogels to act as long-term delivery matrix to promote therapeutic angiogenesis after MI, was tested next. As an increased scar thickness and slower degradation in vivo (over 4 weeks instead of 7-14 days with PEG-MMP1s) was observed after PEG-MMP9s hydrogel injections, it was hypothesized

that PEG-MMP9s hydrogels may be more suitable for sustained delivery of angiogenic growth factors such as VEGF than PEG-MMP1s hydrogels, while still exerting a limited beneficial effect on wall stress reduction. Therefore PEG-MMP9s hydrogels were chosen for the following experiment.

8.7. Targeted delivery of VEGF from enzymatically degradable PEG-MMP9s hydrogels to promote therapeutic angiogenesis after myocardial infarction

8.7.1. Rationale

Myocardial infarction remains one of the pathologies hypothesized to be most effectively treated via therapeutic angiogenesis. More effective therapeutic angiogenesis regimens centering on the prolonged targeted delivery of growth factors from polymeric delivery systems to promote long-term neovascularization have recently been developed. The increased long-term benefit is hypothesized to stem from overcoming rapid neovascular regression by promoting neovascular stability. PEG hydrogels are amongst a group of synthetic biomaterials that allow feedback dependent release of bound biologics. The chemistry utilized in forming PEG hydrogels employed in the previously described studies, Michael-type addition reaction, also allows for the covalent attachment of growth factors and other bioactive moieties[409]. In concert with Jeff Hubbell's laboratory, our group has previously shown that these synthetic hydrogels can effectively be used to release bioactive VEGF as they degrade, promoting angiogenesis and preventing vascular regression in vivo[289]. In addition, previous studies showed that when injected as stand-alone treatment after myocardial infarction, PEG hydrogels ameliorated post-infarct left ventricular remodelling. Therefore, this type of gel may not only be used to provide mechanical strength for the critical early stages of the infarct, but also to deliver paracrine type signals in a well-defined manner.

The objective of the following study was to test whether a synergistic beneficial effect can be achieved by providing initial mechanical support for the ischemic heart in combination with

sustained delivery of the pro-angiogenic growth factor VEGF. PEG hydrogels crosslinked with the MMP9-sensitive peptide sequence showed a slower degradation rate in vivo compared to hydrogels crosslinked with the MMP1-sensitive peptide. Furthermore, when injected after MI, a strong trend towards better preventing wall thinning was seen after PEG-MMP9s delivery. It was therefore hypothesized that PEG-MMP9s hydrogels would provide extended mechanical support in comparison with MMP1s-crosslinked hydrogels while also allowing extended release of vascular endothelial growth factor.

In the long-term angiogenesis study performed in the subcutaneous wound-healing model, the medium dosage of VEGF (150ng/day for 42 days) promoted vascular stability up to 80 days after termination of growth factor delivery. Earlier experiments showed that when injected immediately following permanent LAD occlusion, PEG-MMP9s hydrogels had almost entirely degraded 4 weeks after myocardial infarction. Accordingly, to test whether the VEGF dosage that most efficiently increased the neovasculature at 4 months in our subcutaneous angiogenesis model would impart functional benefit in the setting of MI, a total amount of 4.675μg of VEGF was delivered per intramyocardial injection for this study, corresponding to 150ng/day over a period of 31 days.

8.7.2. Procedure and VEGF dosage

After permanent ligation of the left anterior descending artery, rats were randomly selected to receive 100 μl injections of saline, 4.675μg VEGF as a single bolus injection, 10% PEG-MMP9s or 100μl of 4.675μg VEGF incorporated into 10% PEG-MMP9s. Ventricular function and heart dimensions were assessed at 1, 2, 4 and 10 weeks. Histological analysis to determine post-mortem infarct volume, scar thickness and vascular density was performed subsequent to sacrifice of the animals after 10 weeks.

8.7.3. Survival

A total of 62 rats were operated on for this study. 6 animals died within 48 hours of the surgical procedure, resulting in an overall survival rate of 90,3 % (n=10-13 per experimental group).

8.7.4. Echocardiographic analysis

8.7.4.1. Cardiac function

To assess potential benefits on cardiac function, echocardiographic analysis was performed at 1, 2, 4 and 10 weeks. Compared to sham-operated animals (47.94±0.66%) a significant drop-off in fractional shortening was seen in all groups that underwent permanent LAD occlusion as early as 1 week after surgery (saline, PEG-MMP9s, VEGF, PEG-MMP9s+VEGF; $p<0.05$ vs. sham). Fractional shortening was 26.94±1.66, 23.65±1.79, 27.77±2.07 and 26.2±2.8 after treatment with saline, PEG-MMP9s, VEGF and PEG-MMP9s-VEGF, respectively; no significant difference between the treatment groups was seen at this timepoint (see Fig.59).

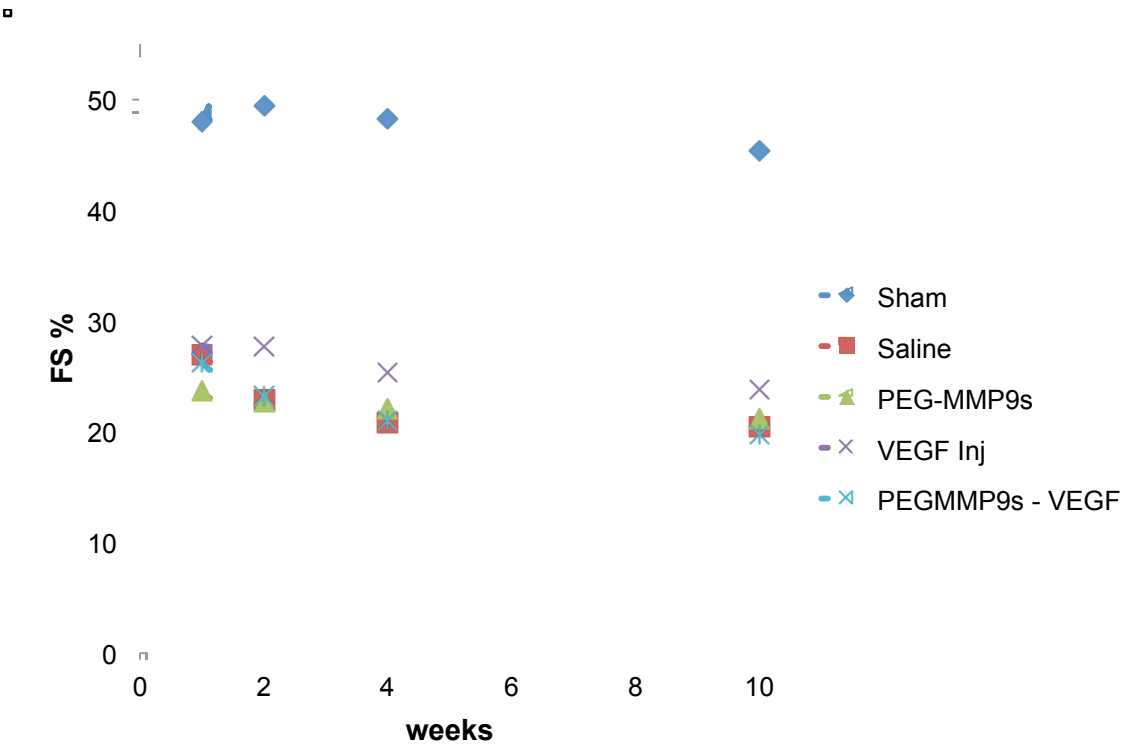

Fig.59. The effects of single bolus and prolonged delivery of VEGF on cardiac function were evaluated using echocardiographic analysis of fractional shortening 1, 2, 4, and 10 weeks after experimental myocardial infarction. Significant differences between treatment groups were not found.

Echocardiographic evaluation at the later timepoints, at 2, 4 and 10 weeks, respectively, also did not reveal any significant differences between the treatment groups (see Fig.59, Table 3). Neither single bolus nor prolonged delivery of vascular endothelial growth factor via PEG hydrogels led to an improved functional recovery from myocardial ischemia (see table). Interestingly, single bolus injections of VEGF, and not prolonged delivery of VEGF from PEG-MMP9s hydrogels, showed a non-significant trend towards increased fractional shortening in comparison with saline injected control hearts at 2, 4, and 10 weeks (p=0.16 at 2 weeks, p=0.14 at 4 weeks, p=0.22 at 10 weeks vs. saline). A trend towards increased cardiac function seen subsequent to PEG-MMP9s treatment at 1 week (p=0.19 vs. saline), but was lost over the course of week 2 (p=0.96 vs. saline at the 2-week-timepoint).

Weeks	1	2	4	10
Sham (n=10)	47.94±0.66	49.38±0.74	48.25±0.85	45.35±0.8
Saline (13)	26.94±1.66	22.85±2.09	20.79±1.84	20.41±1.77
PEG-MMP9s (11)	23.65±1.79	22.72±1.75	22.07±2.08	21.17±1.79
VEGF (11)	27.77±2.07	27.67±2.69	25.37±2.54	23.8±2.12
PEGMMP9s – VEGF (11)	26.2±2.8	23.22±2.76	21±3.12	19.75±2.75

Table 3. Ejection fraction measured by echocardiography 1, 2, 4, and 10 weeks after MI.

8.7.4.2. Left-ventricular remodelling

To determine whether single bolus or prolonged delivery of VEGF has beneficial effects on post-infarct remodelling, left ventricular end-systolic and end-diastolic diameters were measured, 1, 2, 4, and 10 weeks after MI. Over the course of the study, a steady increase in both left-ventricular end-systolic and end-diastolic diameter was observed (shown in Fig.60-61).

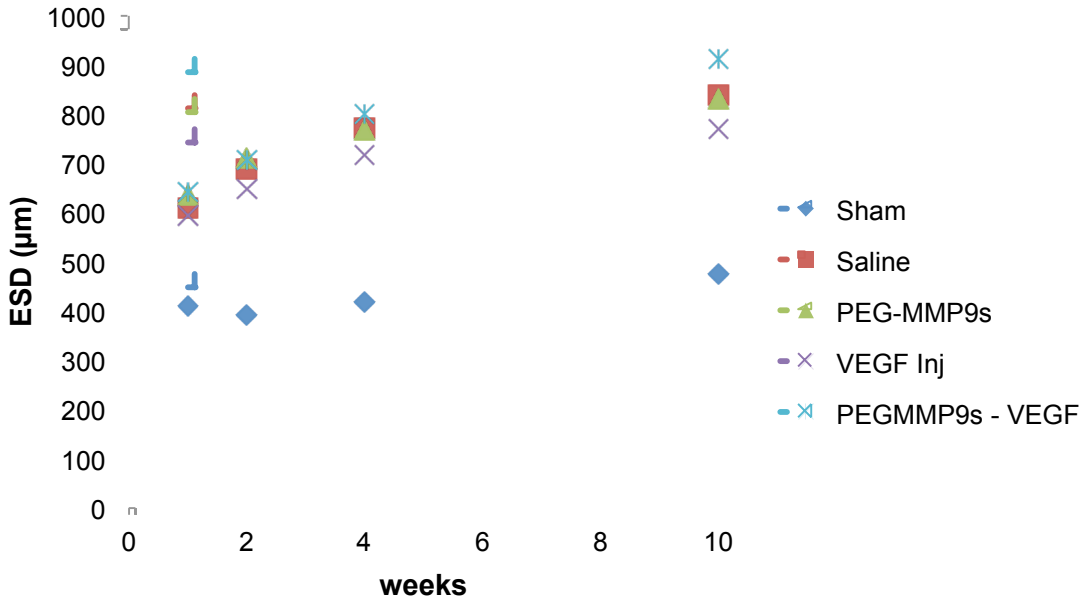

Fig.60. Echocardiographic measurements of left-ventricular diameters were taken 1, 2, 4, and 10 weeks after experimental MI. At the 10-week-timepoint, a strong, non-significant trend towards increased left-ventricular dimensions at the end of systole was seen when comparing single bolus VEGF injections (purple) with PEG-MMP9s-VEGF injections (turquoise), p=0.07.

Subsequent to myocardial infarction, a significant increase in both ESD and EDD occurred in the saline, PEG-MMP9s, VEGF and PEG-MMP9s-VEGF groups ($p<0.05$, see Fig.60-61). Up to 4 weeks after MI, ventricular dimensions between the experimental treatment groups remained similar.

ESD (in µm)				
Weeks	**1**	**2**	**4**	**10**
Sham (n=10)	410.13±10.02	391.38±8.37	419.24±10.19	475.65±10.77
Saline (13)	609.04±22.29	689.05±27.25	771.56±30.52	839.29±31.66
PEG-MMP9s (11)	831.41±39.63	711.56±34.20	768.88±40.92	831.41±39.63
VEGF (11)	594.78±26.41	648.55±37.09	717.09±42.84	769.80±43.40
PEGMMP9s – VEGF (11)	641.88±38.98	707.52±48.42	799.80±58.37	912.66±60.77

Table 4. Left-ventricular end-systolic diameters measured by echocardiography.

While ESD in the VEGF, PEG-MMP9s and PEG-MMP9s-VEGF groups measured at 10 weeks did not significantly differ from saline-injected controls (VEGF vs. saline p=0.2; PEG-MMP9s-VEGF vs. saline p=0.27), a strong trend towards an increase was measured when comparing VEGF and PEG-MMP9s-VEGF treatments (VEGF: 769.80±43.40µm; PEG-MMP9s-VEGF: 912.66±60.77; p=0.07; see Fig.60, table 4).

Analysis of EDD at the 10-week-timepoint revealed a significant increase in the PEG-MMP9s-VEGF group when compared to hearts injected with a single VEGF bolus (see Fig. 61, table 5, p=0.03) and a trend when compared with saline-injected controls (p=0.12). Interestingly, at this time, a non-significant reduction in EDD was observed after administration of VEGF as a single bolus when compared to saline-controls (p=0.17)

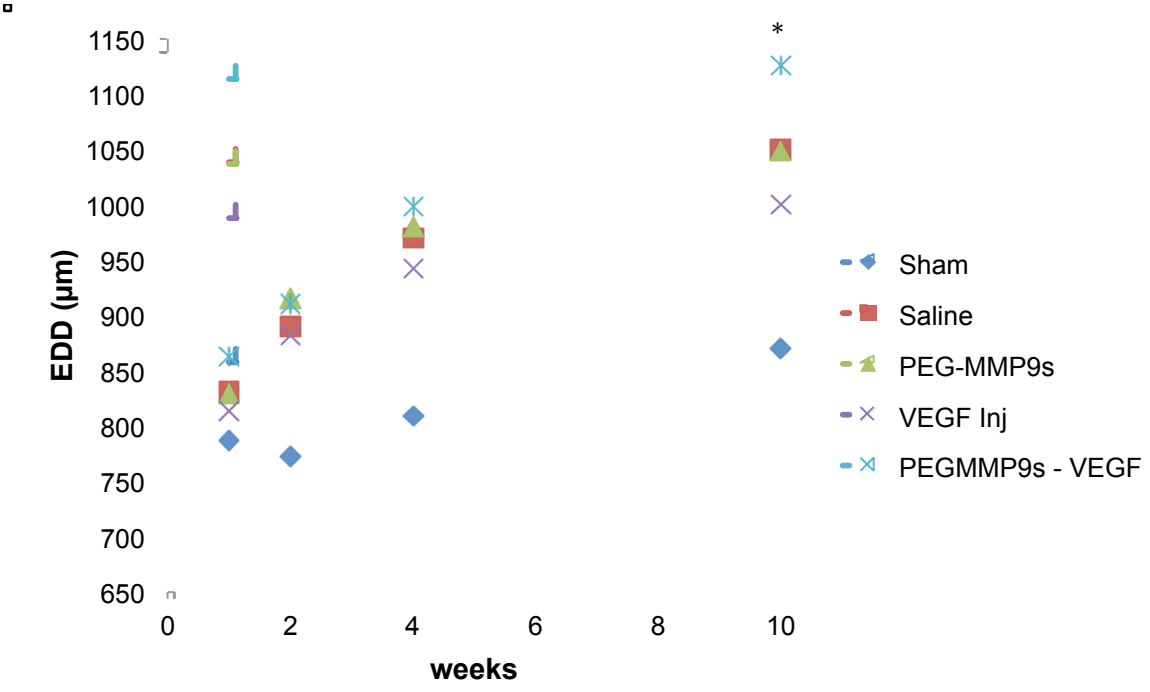

*Fig.61. Post-infarct remodelling was assessed via echocardiography at 1, 2, 4, and 10 weeks. 10 weeks after MI, a significant increase in EDD was observed in hearts injected with PEG-MMP9s-VEGF (turquoise) when compared with single bolus VEGF injections (purple), *p=0.03.*

EDD (in µm)				
Weeks	**1**	**2**	**4**	**10**
Sham (n=10)	787.06±12.11	772.86±10.91	809.42±8.79	869.87±9.93
Saline (13)	831.12±16.90	890.00±14.90	970.40±20.45	1050.66±20.06
PEG-MMP9s (11)	1049.08±26.43	915.93±25.53	979.74±27.63	1049.08±26.43
VEGF (11)	813.69±13.79	882.02±18.43	942.32±27.26	1000.14±30.36
PEGMMP9s – VEGF (11)	863.14±21.89	910.79±30.94	998.67±37.09	1125.89±44.20

Table 5. Left-ventricular end-diastolic diameters measured by echocardiography 1, 2, 4, and 10 weeks after MI.

8.7.5. Post-mortem infarct volume and scar thickness

To evaluate the effects of VEGF delivery on the extent of the infarcted left ventricular area, image analysis of Masson's Trichrome stained sections was performed at 10 weeks.

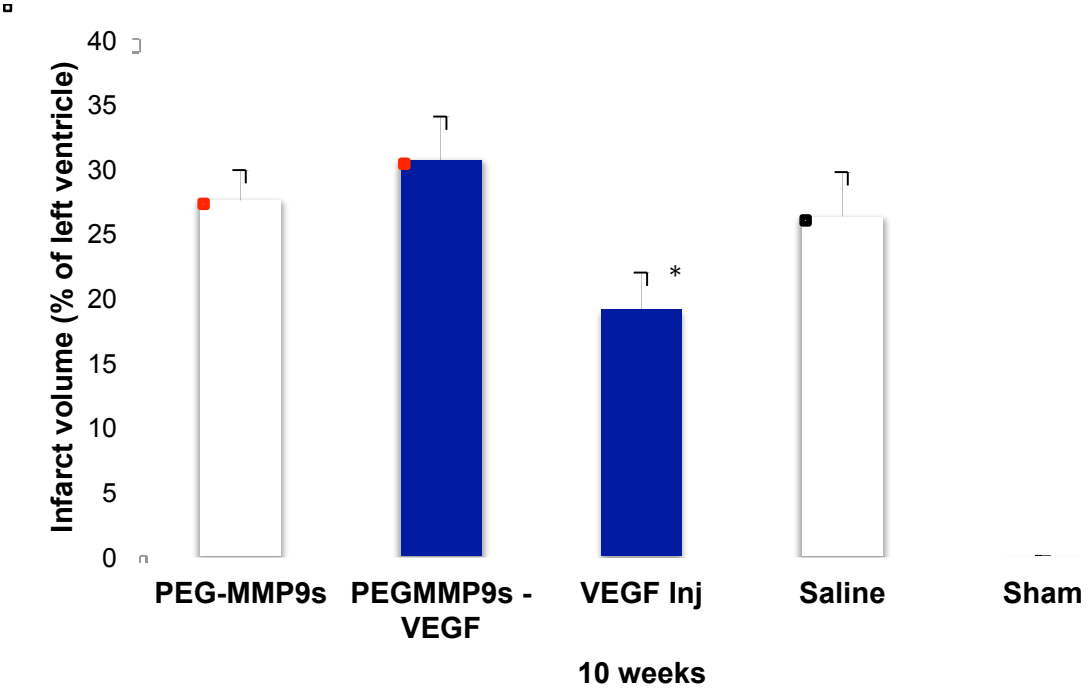

*Fig.62. Morphometric analysis of infarct volume is shown. A significantly reduced infarct volume was observed after single bolus VEGF administration in comparison with PEG-MMP9s-VEGF treatment (*p=0.04).*

No scar formation was observed in sham-operated animals. In saline-injected animals, infarct volume was 26.22±3.48% of the left-ventricle. PEG-MMP9s, VEGF and PEG-MMP9s-VEGF treatment resulted in infarct volumes of 27.5±2.36, 19.06±2.87, and 30.6±3.4%, respectively (see Fig.62).

In comparison with saline-injected control, neither VEGF bolus injections, PEG-MMP9s injections nor local PEG-MMP9s-VEGF delivery, led to significant changes in infarct volume at week 10. Nevertheless, a trend towards a reduction in infarct volume was observed in VEGF bolus-injected animals (p=0.23 VEGF vs. saline). When prolonged VEGF delivery was compared with single bolus VEGF injections, though, a significantly reduced infarct volume was found in the latter group (p=0.04, see Fig.62).

To determine whether PEG-MMP9s, single bolus VEGF or PEG-MMP9s-VEGF effectively prevent left ventricular wall thinning after MI, the thickness of the MI scar was measured.

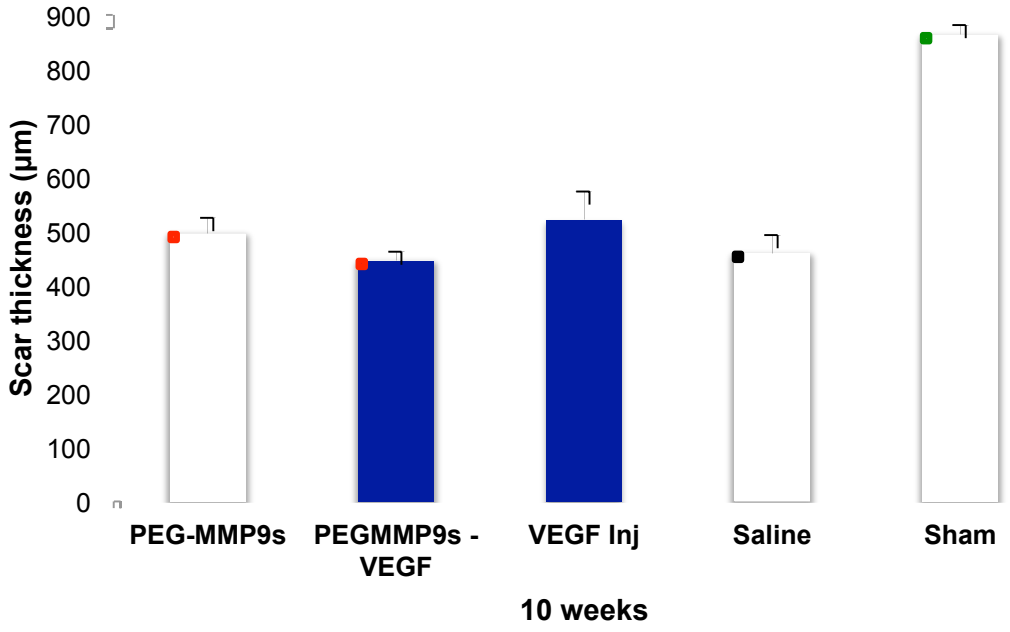

Fig.63. The potential to prevent wall thinning subsequent to MI was determined by measuring the thickness of the infarct scar 10 weeks after treatment. Significant differences were not observed between the groups.

Scar thickness 10 weeks post-MI did not significantly differ between the treatment groups and the saline injected control animals (see Fig.63). Surprisingly, when comparing scar thickness after PEG-MMP9s (495.37±29.26µm) and single bolus VEGF treatment (521.23±52.55µm) with combined PEG-MMP9s-VEGF delivery (445.51±16.97µm) trends towards an increase in scar thickness were seen (PEG-MMP9s vs. PEG-MMP9s-VEGF p=0.16; VEGF vs. PEG-MMP9s-VEGF p=0.19).

8.7.6. Vascularization area and vessel density in the LV infarct area

Quantification of vWF^+-vessels was carried out to assess the effects of prolonged VEGF delivery on long-term neovascularization. Vessel density, as vessels per mm^2, and vascularization area, as a percentage of the infarcted left ventricle, were measured (Fig.64).

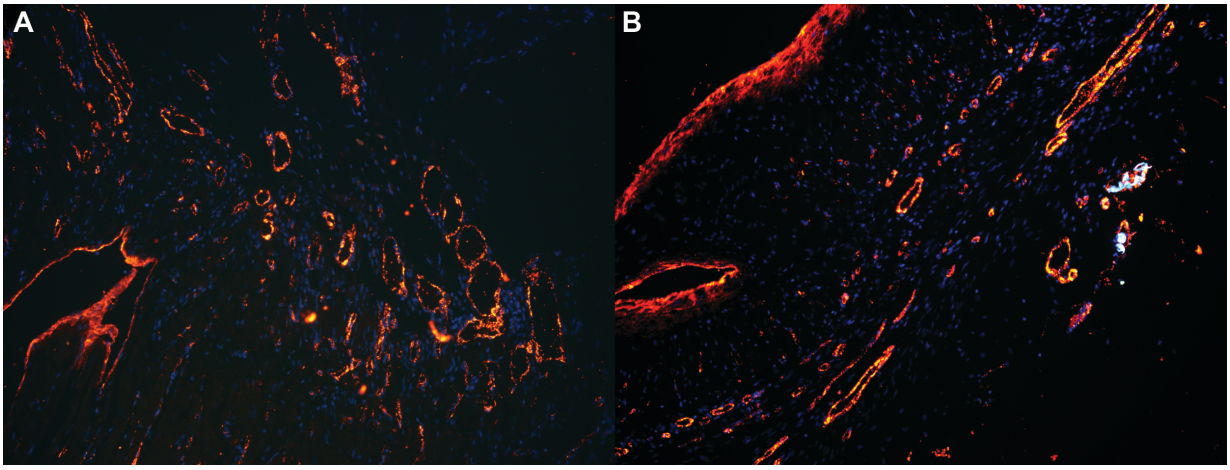

Fig.64. Immunoflurescent staining for vWF^{+}-vessels 10 weeks after MI was performed to evaluate vascularization of the left ventricle. Images were acquired at 80x magnification (A, B), before automated image analysis with VIS was carried out.

No statistically significant long-term effects of single bolus or prolonged VEGF delivery on neovascularization were seen 10 weeks after experimental myocardial infarction. Vascularization area was 5.13±0.59, 5.18±0.86, 4.98±0.65 and 5.28±0.53% after administration of saline, PEG-MMP9s, VEGF and PEG-MMP9s-VEGF, respectively (see Fig.65).

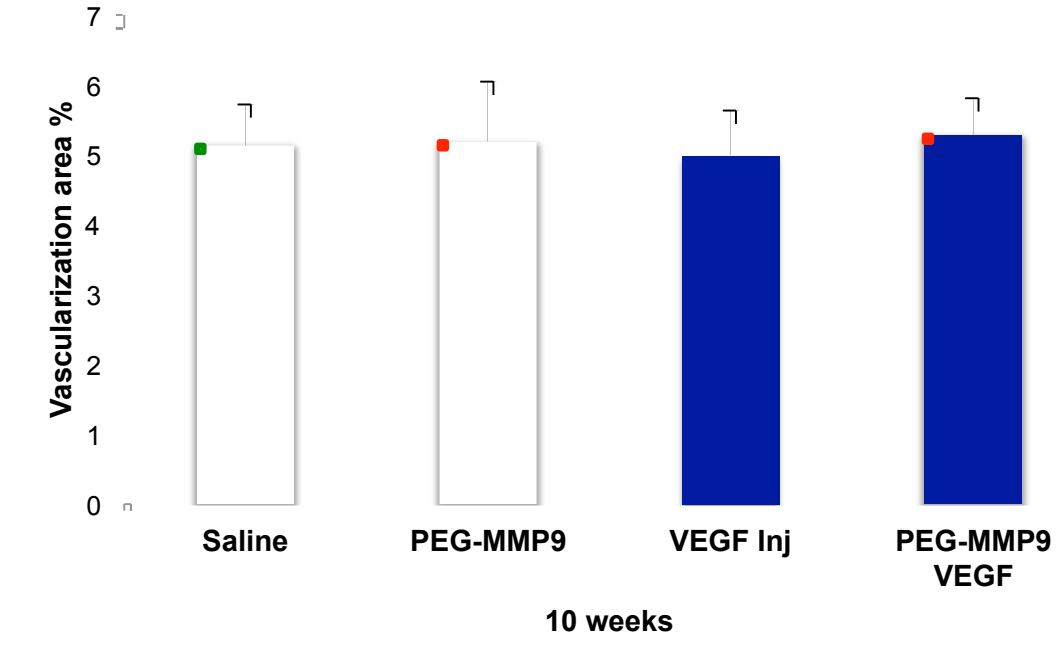

Fig.65. Immunofluorescent staining for vWF was performed to quantify the vascularization area 10 weeks after MI. No significant differences were seen between treatment groups and saline-injected controls.

A non-significant increase in vessel density was seen in all treatment groups in comparison with saline-injected control hearts (see Fig.66). The strongest trend towards an increase in vessel density at 10 weeks was seen after prolonged delivery of VEGF (p=0.16 PEG-MMP9s-VEGF vs. saline-injected heart, p=0.34 PEG-MMP9s vs. saline, p=0.54 VEGF vs. saline).

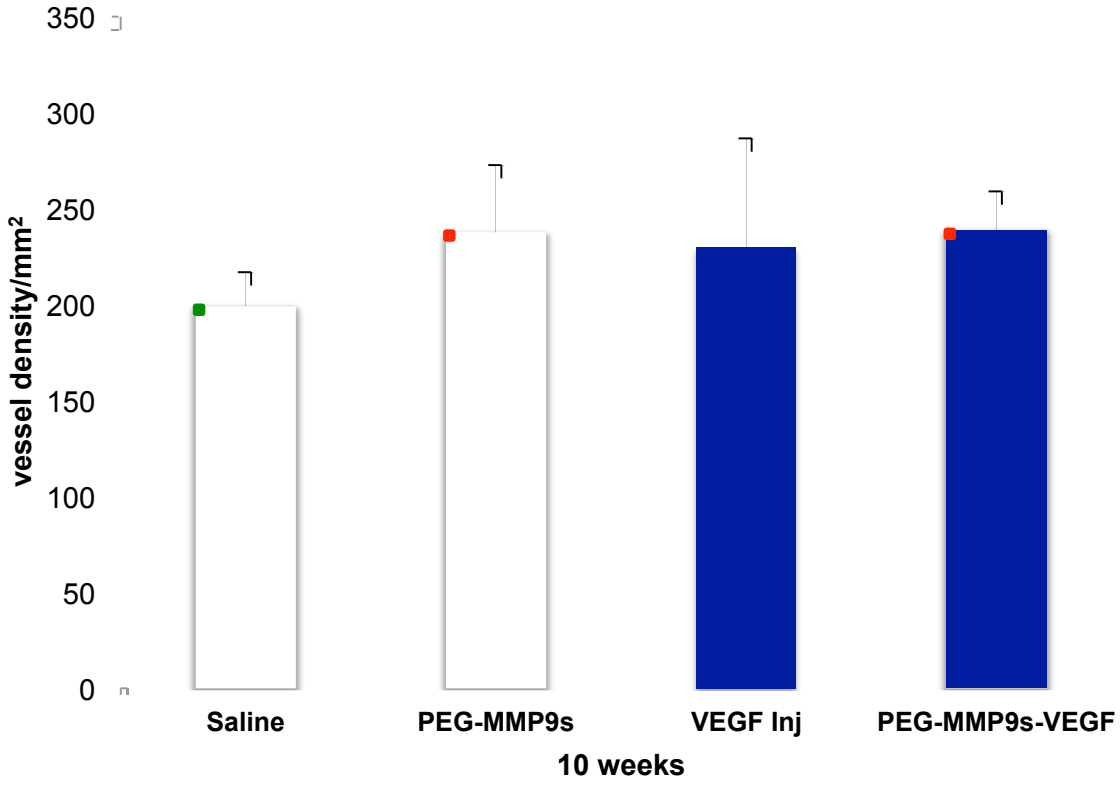

Fig.66. Capillary density was assessed by immunofluorescent staining of vWF. 10 weeks after experimental myocardial infarction, non-significant increases were observed after treatment with PEG-MMP9s, VEGF and PEG-MMP9s-VEGF.

8.7.7. Discussion + Conclusion

In the current study, the potential of sustained VEGF-delivery from enzymatically degradable PEG hydrogels for the stimulation of therapeutic angiogenesis in the setting of MI was tested. Previous work had shown that PEG hydrogels successfully ameliorate left-ventricular remodelling post-MI and that these smart hydrogels can be used to successfully promote angiogenesis in vivo. By combining the mechanical support provided by PEG hydrogels with the sustained delivery of VEGF to establish a stable vascular network, a synergistic beneficial effect on post-MI remodelling and cardiac function was expected. The only positive result seen after PEG-MMP9s-VEGF administration, though, was a statistically non-significant increase in capillary density 10 weeks after MI. Further, single bolus administration of VEGF appeared to be the superior treatment option, as adverse left-ventricular remodelling was reduced in comparison with the PEG-MMP9s-VEGF group, a significantly smaller infarct volume was observed and cardiac function was better preserved over the course of the 10-week study. As successful in-vitro release of bioactive VEGF from PEG hydrogels and in vivo functionality was previously shown in a collaborative effort with Jeff Hubbell's laboratory[289], further experiments to characterize in vivo-release in the heart were not pursued due to their technically challenging nature. While insufficiently high VEGF levels may have contributed to the negative results of the study, it is impossible to exclude a potential increased pro-angiogenic effect induced by prolonged VEGF delivery earlier during the study, due to the lack of additional time-points to assess neovascularization. Nevertheless, with the current protocol, no improvement in long-term neovascularization was seen 10 weeks after MI. As the single bolus delivery of VEGF repeatedly outperformed treatment with PEG-MMP9s and PEG-MMP9s-VEGF, the suitability of these hydrogels for targeted delivery to the myocardium after MI has to be questioned, despite the fact that a detailed comparison between PEG-MMP9s treatment groups and saline-injected controls up to 10 weeks suggests no adverse long-term effects after cardiac injection of enzymatically degradable hydrogels.

As the continued inflammatory reaction against non-degradable PEG hydrogels limits their usefulness as in vivo therapy, future experiments need to identify the ideal crosslinking

chemistry (e.g. using multiple different protease-sensitive peptide sequences) that strikes a balance between optimal mechanical support and growth factor release for the ischemic heart, while ensuring sufficient degradability to prevent prolonged inflammation that potentially damages the heart.

9. CONCLUSION

9.1. THERAPEUTIC ANGIOGENESIS

In recent years enhancing neovascularization in ischemic tissues has emerged as a novel therapeutic concept. While many pro-angiogenic factors have been identified, the instability of growth factor-induced neovasculature remains a major obstacle that has yet to be overcome. A novel in vivo angiogenesis assay was designed as a part of this thesis that allows delivery of defined dosages of pro-angiogenic growth factors into a scaffold of well-defined porosity and the complete termination thereof, thereby allowing investigations into the stability and mural cell investment of newly created vessels. While a number of growth factors tested in this assay significantly increased angiogenesis (PlGF, BDNF), $VEGF^{165}$ emerged as the most potent pro-angiogenic factor tested. Subsequent experiments revealed that depending on dosage and duration of $VEGF^{165}$ delivery, a single growth factor is sufficient to create a long-term stable vasculature for therapeutic angiogenesis. The medium dosage of $VEGF^{165}$ tested (150ng/day for 42 days) significantly enhanced neovascularization up to 80 days after termination of $VEGF^{165}$ delivery, and this increased vessel stability was shown to correlate with an increase in mural cell investiture. With increased incidence as time went on, the continuous delivery of $VEGF^{165}$ at 10-fold higher concentrations (1500ng/day) was shown to lead to rapid vascular regression in the presence of VEGF as early as 20 days after the initiation of pro-angiogenic therapy. This finding was taken advantage of to establish an assay that allows for the identification of underlying mechanisms contributing to the regression of $VEGF^{165}$-induced neovasculature. As early as day 2 after discontinuation of $VEGF^{165}$-delivery (at 1500ng/day), perfusion of the newly created vessels highly diminished and was followed by neovascular regression. A number of strategies

were tested to increase neovessel stability based on previous reports in the literature. Neither SDF-1, inhibition of MMPs, nor simultaneous delivery of stabilizing growth factors successfully prevented the regression of $VEGF^{165}$-induced vessels. Finally a gene array was performed to identify future targets implicated in the regulation of $VEGF^{165}$-induced vessel stability revealing serpin F1, CXCL2, PEDF, and inhibitors of DNA binding as potential candidates.

9.2. PEG HYDROGELS FOR MI THERAPY

Smart hydrogels represent a novel class of biomaterials that have been identified as promising technologies for in vivo tissue engineering. Previous work has demonstrated that feedback-dependent release of therapeutic proteins from bioactive biomaterials can successfully promote angiogenesis and enhance tissue regeneration[289,496]. Collectively, the work described in the second part of this thesis presents the first steps to establish PEG hydrogel implantation as a novel therapy for myocardial ischemia. Pilot experiments confirmed successful PEG hydrogel delivery and retention after permanent left anterior descending coronary artery occlusion. As stand-alone therapy, the injection of non-degradable PEG hydrogels was shown to effectively limit pathological remodelling in the early stages after MI. Most likely due to an enhanced inflammation elicited by non-degradable hydrogels, though, the injections were unable to prevent long-term left ventricular dilation. Subsequently the potential of enzymatically degradable PEG hydrogels for myocardial therapy was assessed. Cardiac injections of PEG-MMP1s and PEG-MMP9s hydrogels were shown to have no detrimental effects on cardiac function as opposed to non-degradable hydrogels. Breakdown of the degradable hydrogels in vivo resulted in a rapid resolution of the inflammatory response present after initial hydrogel injection. However, unlike non-degradable PEG hydrogels, local injections of PEG-MMP1s and PEG-MMP9s into the heart did not effectively retard LV remodelling after myocardial infarction. Finally, as the long-term goal remains the simultaneous exploitation of mechanical support provided by PEG hydrogels and sustained local delivery of therapeutics, the potential of enzymatically degradable PEG hydrogels to locally promote long-term neovascularization after MI was tested. According to

the successful establishment of a long-term stable vasculature in the subcutaneous in vivo assay and previous characterization of PEG-MMP9s degradation, an amount of VEGF sufficient to result in the release of 150ng/day was attached to the PEG gel. While the outcome of this study was negative, as no significant increase in vascularization was seen 10 weeks after MI, these experiments confirmed the potential usefulness of enzymatically degradable PEG gels for cardiac therapy, as no detrimental effects on cardiac function were observed up to 10 weeks after injection.

To fully explore the potential of bioactive PEG hydrogels, future studies will be needed to deepen our understanding of the mechanisms that underlie the beneficial effects on cardiac remodelling seen after injection of non-degradable PEG hydrogels. The timing of hydrogel injection (hours, days, weeks after MI) may for instance be a crucial variable that determines the successful outcome of this therapy. Additionally to establish PEG hydrogels as a technological platform to promote therapeutic angiogenesis, the ideal crosslinking conditions need to be identified to optimize hydrogel degradation and release kinetics of the attached biologics.

10. MATERIALS & METHODS

10.1. ANGIOGENESIS

10.1.1. Porous polyurethane scaffold fabrication

Porous polyurethane tubes were produced as described earlier [497]. Briefly, the interstices in an annular column of spherical gelatin beads (150-180μm sieve size), contained between a glass tube (3.7x8.0x150mm: IDxODxLength) and a central stainless steel mandrel (2.7x175mm), were infiltrated with a polyurethane solution (20% in N-methylpyrrolidone (Sigma-Aldrich, Steinheim, Germany) and subsequently demolded. The polyurethane was precipitated by immersion in ethanol (96%, 24h, RT), the porogens extracted by extensive washing in deionized water (60 ºC, 5 days), and the resulting structures dried and cut to 19mm lengths.

Each device (shown in Figure 1) was assembled from a porous PU tube (2.4x3.4x19mm, 150μm pores with 70μm interconnecting windows), an ePTFE barrier (1.8x2.4x19mm, 20±4μm internodal distance, (Zeus Inc., Orangeburg, SC, USA) to prevent cell penetration into the lumen, a distal PTFE plug (1.2x1.8x3mm), and a polyethylene (PE/4 and PE/8 (Scientific Commodities Inc., Lake Havasu City, AZ, USA) feeder tube assembly, tied down with 4/0 silk ligatures.

10.1.2. Production of human VEGF^{165} in E. coli

The cDNA of human VEGF^{165} was cloned into the expression plasmid pRSET T7 (Novagen, Madison, WI, USA) between restriction sites Nde1 and BamHI. The pRSET-VEGF^{165} was introduced into the *E.coli* expression host BL21 (DE3) pLysS. Once the transformed bacteria had reached an OD600 of 0.8, isopropyl-β-D1-thiogalactopyranoside was added to 1 mM to induce protein expression for 3 hrs. The bacterial cells were pelleted, frozen at –20°C and then resuspended in a tenth of the original culture volume in 50 mM Tris, PH 7.5, 150 mM

NaCl, 5 mM EDTA, followed by incubation with lysozyme at 0.1 mg/ml suspension for 20 min at room temperature. Benzonaze (Merck KGA, Darmstadt, Germany) was then added at 50 units/ml suspension, and incubated overnight at 4°C. Inclusion bodies were then collected by centrifugation at 30 000*g* for 30 min and then washed in 4 M urea, 20 mM Tris, pH 8.0, 150 mM NaCl, 2 mM EDTA overnight at 4°C. They were then solubilised in 8 M urea, 20 mM Tris, pH 8.0, 150 mM NaCl, 10 mM dithiothreitol at 4°C. The supernatant was then dialysed sequentially for 24 hrs against 6, 4 and 2 M urea in 20 mM Tris, pH 8.0, 150 mM NaCl, 2mM EDTA at 4°C. The monomeric proteins were then dimerized over a period of 48 hrs at 4°C in the presence of oxidised and reduced glutathione (Sigma-Aldrich, Steinheim, Germany) at 0.5 and 5 mM respectively. The dimerized solution was then dialysed against 20 mM Tris, pH 8.0, 150 mM NaCl, 2mM EDTA at 4°C and passed over a heparin agarose column (Applichem, Darmstadt, Germany). The column was washed with 150 mM NaCl, 20 mM Tris pH 8.0, and the bound VEGF eluted with 0.75 M NaCl, 20 mM Tris, pH 8.0. The eluted VEGF was then dialysed against 150 mM NaCl, 20 mM Tris, pH 8.0.

10.1.3. In vivo angiogenesis assay

Osmotic pumps (Alzet, Cupertino, CA, USA) with a nominal pump rate of 0.25 µl/hr were filled under sterile conditions with the respective growth factor, growth factor combination or PBS. The nominal pump rate was used to calculate the dosage per day. After sterilizing the tubular polyurethane devices with 70% ethanol (Sigma, Steinheim, Germany), they were flushed with 10 ml of 99.7% ethanol to make them permeable and subsequently attached to the osmotic pump. The whole construct was then put into distilled water and placed into an incubator for 24 (Alzet 1002 model) or 48 (2004 model) hours at 37^{o}C. Animals were anaesthetized using 100 µl of a ketamine (64,3 mg/ml) and xylazine (7,14 mg/ml) mix i.m. and 100 µl i.m. of buprenorphine (Temgesic®, Schering-Plough LTD, Woodmead, SA). Two 1cm skin incisions were made in the dorsal paramedian region of the skin and two tissue pockets were dissected bluntly. The entire construct was then placed into the pocket before the skin was

closed up using a 4-0 Prolene suture (Ethicon, Johnson&Johnson, Halfway House, SA). Pump exchanges and removal were performed under anaesthesia. After pump removal the catheter tubing was sealed using a LT 200 liga clip (Ethicon) before the skin incision was closed as described above. The rats were sacrificed using carbon dioxide and the devices explanted at the end of the study period. For a comprehensive list of the detailed experimental protocol see table 6.

TIMELINE for osmotic pump experiments				
Experiment	Construct implant	Pump change	Pump explant	Graft explant
5	0	N/A	5	5
10	0	N/A	10	10
10+1	0	N/A	10	11
10+2	0	N/A	10	12
10+4	0	N/A	10	14
10+10	0	N/A	10	20
10+10	0	10		20
10+20	0	N/A	10	30
20	0	N/A	20	20
30	0	N/A	30	30
42	0	N/A	42	42
42+80	0	N/A	42	122
Day				

Table 6. Timetable shows different experimental protocols for the assessment of angiogenesis in the neovascularization devices. Time of pump exchange, pump explant and neovascularization device harvest was measured from time of subcutaneous implantation (=day 0).

The animal study protocol had been approved in writing by the University of Cape Town Animal Ethics Committee. All animal studies were performed in accordance with the National Health Institute (NIH, Bethesda, MD USA) guidelines.

10.1.4. Vascular perfusion with *Lycopersicon esculentum*

Patency and blood flow were assessed in the various implants by perfusion of the vasculature with *lycopersicon esculentum* lectin, which was essentially done as previously described[498]. In brief, prior to explantation of the device, the rat was anaesthetized with a 400µl intramuscular injection of ketamine/xylazine. The animal was then placed onto a heating pad, a skin incision was made above the groin, the femoral vein was visualised and dissected under a Leica MS 5 microscope (Leica, Wetzlar, Germany) and 500 µl of biotinylated *l. esculentum* lectin (1 mg/ml, Vector Laboratories, Burlingame, CA, USA) in 0.9% NaCl were injected into the vein. After two minutes of perfusion, the chest was opened and the vasculature was perfusion fixated with 250 ml 1% paraformaldehyde (Saarchem, Kruegersdorp, South Africa) in PBS at 37°C at 120 mmHg via an 18-gauge cannula inserted into the ascending aorta through the left ventricle. The right atrium was incised to allow for the exsanguination of the animal while the circulatory system was perfused. The device was explanted and placed in zinc fixative (2.8 mM calcium acetate (Merck KGA, Darmstadt, Germany), 2.3 mM zinc acetate (Merck KGA, Darmstadt, Germany), 3.7 mM zinc chloride (Sigma-Aldrich, Steinheim, Germany) in 0.1 M Tris. HCl pH 6.75 (Sigma-Aldrich, Steinheim, Germany)[499] for 24 hours.

10.1.5. VEGF Stability

To determine the stability of VEGF over the maximum period of delivery, VEGF (250 µg/ml PBS) was incubated at 37°C for 42 days. The concentration of VEGF remaining after incubation was quantified using a human VEGF ELISA (Catalog Number: DY293, R&D, Minneapolis, MN, USA) as per manufacturer's instructions. In order to measure the amount of

VEGF in an implanted device, constructs were explanted at days 10 and 42. They were then cut in half and rotated at 50 rpm in 2 ml of a protease-inhibitor mix (1µg/ml leupeptin, 25µM benzamidine, 1 mM EGTA, 1mM phenylmethylsulfonyl fluoride, 1µg/ml aprotinin in PBS) for 1 hour @ 4°C and the VEGF content was assayed with a human VEGF ELISA.

Briefly, after the capture antibody was diluted to the working concentration in PBS, a 96-well microplate was immediately coated with 100 µl per well of the diluted antibody. The plate was then sealed and incubated overnight. The next morning, each well was aspirated and washed three times with 400 µl the freshly made up wash buffer. After the final wash remaining wash buffer was removed by inverting the plate and blotting it against a clean paper towel. 300 µl of block buffer was added to each well, the plate was sealed and incubated at room temperature for 1 hour. Again, each well was aspirated, washed three times with 400µl wash buffer and after the third wash the remaining wash buffer was removed by inverting the plate and blotting it against a clean paper towel. Subsequently, 100 µl of sample or standard diluted in reagent diluent, was added per well, the plate was covered with an adhesive strip and incubated for 2 hours at room temperature. Yet again, the wells were aspirated, washed three times and remaining buffer removed. After adding 100 µl of the detection antibody, diluted in reagent diluent, to each well, the sealed plated was incubated for 2 hours at room temperature. The aspiration/wash step was repeated and 100 µl of the working dilution of Streptavidin-HRP was added to each well. The plate was covered and incubated for 20 minutes at room temperature and careful attention was paid to avoid placing the plate in direct light. After another aspiration/ wash step, 100 µl of substrate solution were added to each well and in a light-protected place, the plate was incubated for 20 minutes at room temperature. Next, 50 µl of stop solution (H_2SO_4) was added to each well and the plate was gently tapped to ensure thorough mixing. The optical density of each well was measured immediately using a Benchmark® Microplate Reader (Biorad, Japan) set to 450 nm. Wavelength correction was set to 540 nm to correct for optical imperfections in the plate.

The bioactivity of the incubated VEGF was assessed in an endothelial cell proliferation assay. Briefly, human saphenous vein endothelial cells (passage 2) were cultured at 2000 cells/cm2 in MCDB131 medium (Sigma-Aldrich, Steinheim, Germany), 2% fetal calf serum (Invitrogen, Carlsbad USA) and 1 ng/ml VEGF for 2 days. The number of cells was then quantified using a Cell Titre Glo assay (Promega, Madison, USA) as per manufacturer's instructions. The number of cells determined for the incubated VEGF was compared to cells cultured in MCDB131, 2% FCS plus/minus fresh 1 ng/ml VEGF.

Briefly, CellTiter-Glo® Buffer and lyophilized CellTiter-Glo® Substrate were allowed to equilibrate to room temperature prior to use. To form the CellTiter-Glo® Reagent CellTiter-Glo® Buffer was added to CellTiter-Glo® Substrate to reconstitute the lyophilized enzyme/substrate mixture and vortexed to obtain a homogeneous solution. The cultured human saphenous vein endothelial cells were transferred onto opaque-walled multiwell plates, covered with 100µl culture medium per well. To obtain a value for background luminescence, control wells containing medium without cells were prepared. Plate and its contents were allowed to equilibrate to room temperature for approximately 30 minutes before adding a volume (100 µl) of CellTiter-Glo® Reagent equal to the volume of cell culture medium present in each well. Contents were then mixed for 2 minutes on an orbital shaker to induce cell lysis and the plate was allowed to incubate at room temperature for further 10 minutes to stabilize the signal, before luminescence was recorded.

10.1.6. HISTOLOGY

10.1.6.1. Lectin

Sections fixed in 4% paraformaldehyde were dewaxed in xylene. To remove the polyurethane, sections were incubated with cyclohexanone (2x 30 min). Sections were cleared in alcohol baths, thoroughly washed in H2O and then placed in TBS for 10 minutes. Lectin was detected by overnight incubation at 4°C with a 1:3500 dilution of Cy3 conjugated streptavidin (Jacksons Immunoresearch, West Grove, PA, USA).

The next morning, after a wash in TBS (2x10 min @ RT), sections were counterstained with DAPI using Vectashield® mounting medium (Vector Laboratories, Burlingame, CA).

10.1.6.2. H&E

Histological slides were dewaxed using Xylene or Trimethylpentane (for PU) before the sections were cleared in alcohol baths, thoroughly washed in H2O and placed in TBS. The sections were then incubated in Haematoxylin for 5 minutes. After a 5 wash in running tap water, the slides were placed in Eosin for 30 seconds, dipped in distilled water, dehydrated through the alcohols, before being mounted with Entellan (Merck, Darmstadt, Germany).

10.1.6.3. CD31

PU-grafts were fixed in zinc-fixative for 24 hours before being processed through graded alcohols and embedded in wax. 5 µm sections were cut onto uncoated slides and incubated at 37°C overnight. Sections were then dewaxed using 4 changes of 2,2,4 tri-methylpentane and 2 changes of cyclohexanone before being taken through graded alcohol to water. After rinsing for 10 min with 0.1% tween in PBS the primary antibody mouse anti-rat from RDI-RTCD31 (RDI Research Diagnostics Inc., Flanders, NJ) was applied at a 1:50 dilution in 1 % BSA in PBS for 40 minutes. Sections were rinsed twice for 10 minutes each with 0.1 % tween in PBS prior to using the alkaline phosphatase Biocare Medical kit. Sections were incubated with the Rodent body for 30 minutes, followed by two 10-minute washes with TBS. The Mouse on Rat alkaline phosphatase polymer was subsequently added for 30 min, followed by 2 washes with 0.1 % tween in PBS. Finally, sections were incubated with the substrate BCIP/NBT DAKO (DAKO, A/S, Glostrup, Denmark) until colour development was complete. After a rinse with running tap water, the sections were dehydrated, cleared in 2,2,4 trimethylpentane, and mounted with Entellan (Merck, Darmstadt, Germany).

10.1.6.4. CD31/Desmin (fluorescent)

After fixation in zinc fixative, all samples were processed through graded alcohol and xylene (tissue processor), and then embedded in paraffin wax. 3 µm thick cross-sections from the mid-region of the device were dewaxed with xylene. To remove the polyurethane, sections were incubated with cyclohexanone (2x 30 min). Sections were cleared in alcohol baths, thoroughly washed in H2O and then placed in TBS. To reduce background staining, sections were incubated with Rodent Block (Biocare Medical) for 1 hour. Pericytes and their associated vessels were detected by incubation with a 1:400 dilution of rabbit polyclonal anti-desmin antibody (Abcam, Cambridge UK) and a 1:25 dilution of mouse anti-rat CD31 primary antibody (RDI Research Diagnostics Inc., Flanders, NJ, USA) in 1% bovine serum albumin (BSA, Jacksons Immunoresearch, West Grove, PA, USA)/PBS for 2 hours at room temperature (RT). Next, sections were incubated with a 1:250 dilution of a biotinylated donkey anti-mouse IgG antibody (Rockland, Gilbertsville, PA, USA) for 30 minutes. Thereafter, the former was detected by incubating with a 1:3500 dilution of Cy3 conjugated streptavidin (Jacksons Immunoresearch, West Grove, PA, USA) and the anti-desmin antibody was detected with a 1:50 dilution of an Alexa 488 conjugated goat anti-rabbit IgG antibody (Invitrogen, Carlsbad, CA, USA) for 2 hours at RT. After a wash in TBS, sections were counterstained with DAPI using Vectashield® mounting medium (Vector Laboratories, Burlingame, CA).

10.1.7. Image analysis of immunostained sections for quantitative assaying of neovascularization

CD31-stained samples were loaded into a Nikon Coolscope (Nikon Corp., Tokyo, Japan), and an image of the complete cross-section was acquired at a 100x magnification. All of the ensuing analysis was performed with Visiopharm Integrated Systems (VIS) (Visiopharm A/S, Hørsholm, Denmark). Briefly, the software was trained to automatically detect CD31 positive structures; all analyses were assessed by an observer for accuracy and, if necessary, manually corrected. Vessel area and cross-sectional tissue ingrowth area of the graft were

calculated and the vascular density was obtained by dividing vessel area through cross-sectional area. The average vessel diameter was calculated from the average vessel area with the assumption of vessel circularity.

4 random images were acquired with a Nikon 90i fluorescence microscope (Nikon Corp., Tokyo, Japan) at 200 X magnification of each desmin/Cd31 stained cross-section. The interface length between desmin positive cells and CD31 positive vessels was calculated for those desmin positive cells that had greater than 15% of their circumference in direct contact with a vessel using VIS. The total of all interface lengths was divided by the total of all vessel circumferences to obtain vessel coverage.

10.1.8. Rat angiogenesis RT2 Profiler PCR Array

10.1.8.1. RNA Isolation (Preparation & Quality Control)

RNA was isolated using a RNeasy® Plus kit from Qiagen (Qiagen N.V., Venlo, The Netherlands) as per manufacturer´s instructions. Briefly, a 2,5 mm section of the frozen PU-graft with approximately 20-30g of tissue was placed in liquid nitrogen, then disrupted and homogenized using a pestle and mortar. Careful attention was being paid to not allow the sample to thaw by repeatedly adding small amounts of liquid nitrogen. The tissue powder was then transferred to an empty 2ml microcentrifuge tube, the remaining liquid nitrogen was allowed to evaporate and 600 µl of RLT-buffer was immediately added. After vortexing thoroughly, the lysate was pipetted into a QIAshredder spin column placed in a 2ml collection tube and centrifuged for 2 minutes at 13200 RPM. The lysate was centrifuged for another 3 minutes at 13200 RPM before the supernatant was carefully removed by pipetting and transferred to a gDNA Eliminator spin column placed in a 2 ml collection tube. After centrifugation for 30 seconds at 10600 RPM, the column was discarded and the flow-through saved. An equal volume of 70% ethanol was added to the flow-through and mixed well by pipetting, before the sample was transferred to an RNeasy spin column placed in a 2ml

collection tube. After a 15 second centrifugation at 10600 RPM, the flow-through was discarded. Then 700 µl of RW1 Buffer was added to the RNeasy spin column and centrifuged for 15 seconds at 10600 RPM to wash the spin column membrane. Again, the flow-through was discarded. 500 µl of Buffer RPE was added to the RNeasy spin column and centrifuged for 2 minutes at 10600 RPM, thereby washing the spin column membrane, once again. The RNeasy spin column was subsequently placed into a new 2 ml collection tube and centrifuged at 13200 RPM for 1 minute to eliminate any possible carryover of Buffer RPE. After that the RNeasy spin column was transferred into a new 1.5 ml collection tube, 30 µl of RNAse-free water was added to the spin column membrane and centrifuged for 1 minute at 10600 RPM. Since we expected a RNA yield of more than 30 µg, we repeated the last step, adding another 30 µl of RNAse-free water to the spin column membrane before centrifuging for 1 minute at 10600 RPM. The eluate was then aliquoted, snap frozen and stored at -80°C until experiments were carried out. RNA quality control was assessed at the Centre for Proteomic and Genomic Research (CPGR) at the University of Cape Town.

10.1.8.2. RT2 First Strand cDNA Synthesis

Genomic DNA Elimination mixture was prepared by adding 2.0 µl GE (5x gDNA Elimination Buffer) and RNAse free H2O to 0.5 µg of total RNA for a final volume of 10 µl. The contents were gently mixed with a pipettor and briefly centrifuged. Samples were then incubated at 42°C for 5 minutes and immediately thereafter chilled on ice for 1 minute.

10 µl of RT Cocktail (1 reaction: 4 µl BC3 (5x RT Buffer 3) + 1 µl P2 (Primer & External Control Mix) + 2µl RE3 (RT Enzyme Mix 3) + 3 µl RNase free H_2O) was added to each 10µl Genomic DNA Elimination mixture and mixed well with a pipettor. Samples were then incubated at 42°C for exactly 15 minutes, after which the reaction was immediately stopped by heating at 95°C for 5 minutes. 91 µl of double distilled water (ddH_2O) were subsequently added to each 20 µl of cDNA synthesis reaction. The finished First Strand cDNA Synthesis Reaction was kept on ice until Real-Time PCR was performed.

10.1.8.3. Quantitative Real-Time Polymerase Chain Reaction

The experimental cocktail was prepared by mixing 102 µl of the First Strand cDNA Synthesis Reaction, 550 µl of 2x SuperArray RT2 qPCR Master Mix and 448 µl ddH2 for a total volume of 1100 µl. Samples were kept on ice. Samples were loaded using an automated liquid handling system at the CPGR and quantitative real-time PCR was performed using an ABI 7900HT.

10.2. MYOCARDIAL INFARCTION

10.2.1. PEG derivatization

Vinyl sulfone derivatized polyethylene glycol was prepared by methods similar to those employed by Lutolf et al.[408]. Briefly, a 5% polyethylene glycol (20kDa, 8-arm, hydroxyl-terminated: 20PEG-8OH, Shearwater/Nektar) solution in dry dichloromethane (DCM) was reacted with 5x molar excess of NaH followed by 50x molar excess of divinyl sulfone (DVS) under inert atmosphere for 48hr. After neutralization of the remaining NaH with glacial acetic acid and removal of the precipitated NaOAc salt through centrifugation and vacuum filtration, reduction of the volume by rotary evaporation, and precipitation in 10X excess cold diethyl ether (DEE), the product was dried (RT, 24hr, reduced pressure). Purification of the product (20PEG-8VS) was achieved through 3x re-precipitation from DCM in DEE and drying. PEG-$[O\text{-}(CH_2)_2\text{-}SO_2\text{-}C\mathbf{H_a}\text{-}C\mathbf{H_{cis}H_{trans}}]_8$. Yield = 65%. ^{1}H NMR, 400MHz, $CDCl_3$, δH 6.1 (H_{cis}), 6.4 (H_{trans}), 6.8 (H_a). Complete conversion was shown by the absence of the –$\mathbf{C}H_2$-OH peak in the ^{13}C spectrum of the derivatized product (62ppm in the unmodified PEG-OH) and a 97% conversion calculated from integration of the ^{1}H peaks.

10.2.2. Labelling and formation of non-degradable PEG hydrogels

40ng of Alexa Fluor® 660 C2 maleimide (Invitrogen, Carlsblad, California) was added to 50µl of 12mg/ml dithiothrietol (DTT, Sigma-Aldrich, Steinheim, Germany) in phosphate buffered

saline (PBS 0.15M, pH=7.4) and reacted for 30 minutes at 37°C. Gels of 10% (m/v) nominal concentration were prepared by dissolving 10mg of 20PEG-8VS in 50 µl PBS, and then adding 50 µl of the above labelled DTT solution, vortex mixing, immediately aspirating the admixture into a syringe, and injecting the contents into the myocardium.

10.2.3. Labelling and formation of MMP-1/MMP-9 degradable PEG hydrogels

10mg of 20PEG-8VS were dissolved in 50 µl PBS before adding 40ng of Alexa Fluor® 660 C2 maleimide (Invitrogen, Carlsblad, California). After reacting for 30 minutes at 37°C, gels of 10% (m/v) nominal concentration were prepared by adding 50µl of a peptide crosslinker sequence (MMP-1s or MMP9s), sensitive to cleavage by either MMP-1 (GCREGPQGIWGQERCG; 3.45mg/gel) or MMP-9 (GCREKGPRQITERCG; 3.65mg/gel). After mixing, the admixture was immediately aspirated into a syringe, and the contents were injected into the myocardium.

10.2.4. Attachment of Growth factors to the PEG hydrogel (PEGylation of VEGF)

To allow attachment of the respective growth factors, 20kDaPEG-8arm vinylsulfone was dissolved in PBS containing recombinant VEGF and incubated at 37°C for 30 minutes. Formation of growth factor containing PEG hydrogels was performed using a peptide crosslinker sequence sensitive to cleavage by MMP-9 (GCREKGPRQITERCG; 3.65mg/gel), as described above.

10.2.5. Induction of myocardial infarction and injection of PEG hydrogels

Myocardial infarction was produced in male Wistar rats weighing approximately 180-220g as previously described[249]. Briefly, rats were anaesthetized with a 5% isoflurane (Safeline Pharmaceuticals (PTY) LTD, Johannesburg, RSA) /oxygen mix, placed on a rodent work stand (Braintree Scientific Inc., Braintree, MA, USA) and the vocal cords were visualized

using a Welch Allyn LI ION Otoscope equipped with a specially designed and molded, autoclavable intubation speculum (Braintree Scientific Inc.). After tracheal intubation with an 16 G i.v. indwelling cannula (Braun, Melsungen, Germany), the animals were placed on a heated Deltaphase® operating board (Braintree Scientific Inc.). During the surgery, animals were ventilated at 110 BPM with a small animal ventilator (Harvard apparatus, Holliston, MA, USA) and the anaesthesia was maintained with 1,5% isoflurane/oxygen. A 2 cm skin incision was made above the 4th intercostal space. With a cotton earbud the pectoral muscles were dissected bluntly and the hearts were exposed via left thoracotomy. An eyelid retractor was used to retract the ribs and ensured optimal vision of the operating field. Following a pericardiotomy, a myocardial infarct was induced by permanently ligating the left anterior descending (LAD) artery 2 mm below the left atrial appendix with a 6-0 prolene suture. MI was confirmed by ECG, colour change and dyskinesis of the left ventricular wall. After successful ligation animals were randomized to either receive 100 µl injections of treatment or control. For the sham operation only a thoracotomy and pericardiotomy were performed. Via 2-3 injections a total of 100µl of treatment/control was delivered to the infarct area within 2 minutes of coronary artery ligation. 4-0 silk sutures (Ethicon) were used to close ribs, muscle layer and the skin. For analgesia, i.m. buprenorphine (Temgesic ®, Schering-Plough LTD, Woodmead, RSA) was given during the first 48 hours after surgery. At the end of the study period, animals were anaesthetized with a mix of 100 µl Pentobarbitol and 200 µl Heparin (1000 I.U. per ml). The abdominal cavity was opened, the tip of the heart visualized, the needle was advanced through the diaphragm into the left ventricle and the animals were sacrificed by injecting 500 µl saturated KCl (Sigma-Aldrich, Steinheim, Germany), thereby arresting the heart in diastole.

The animal study protocol had been approved in writing by the University of Cape Town Animal Ethics Committee. All animal studies were performed in accordance with the National Institutes of Health (NIH, Bethesda, MD USA) guidelines.

10.2.6. Echocardiography

A 5%isoflurane/oxygen mix was used for the induction of the anaesthesia. The rats were placed on a Deltaphase® operating board in a left lateral decubitus position. Anaesthesia was maintained with mixture of 1,5% isoflurane/oxygen. Images acquired with a Siemens Acuson Sequoia 512 Ultrasound system and a 15L8 transducer (both Siemens, Berlin, Germany) were analysed at the time of acquisition. Short-axis 2D and m-mode measurements of the left ventricular diameters were taken at the level of the papillary muscle and all measurements were averaged over 3 consecutive cardiac cycles.

Left ventricular fractional shortening (in percent) was calculated as following: (EDD-ESD)/EDD * 100, where EDD is end-diastolic diameter and ESD end-systolic diameter. Depending on the experimental protocol, echocardiography was performed at 7, 14, 28 days, 10 weeks and 3 months after experimental myocardial infarction by an examiner blinded to the treatment groups.

10.2.7. Infarct size measurement

Explanted hearts were flushed with 10 ml 1% paraformaldehyde, fixed in 4% paraformaldehyde (Sigma-Aldrich) for 24 hours, cut into 4 equally sized parts and embedded in paraffin. After obtaining a 3µm section, the 4 parts were trimmed and a second 3µm section was cut 250 µm deeper. All 8 sections were stained with Masson´s Trichrome stain, and then captured using a Nikon E1000M (Nikon, Tokyo, Japan) with a 0,5x magnification lens. The infarct size derived from midline length measurements was calculated by dividing the sum of midline infarct lengths, acquired with Visiopharm Integrator Systems (Visiopharm, Hørsholm, Denmark), from all sections by the sum of midline circumferences from all sections and multiplying by 100, as previously described[500].

10.2.8. Scar Thickness

Scar thickness measurements were taken in 1 mm intervals from all 8 Masson's Trichrome sections. The measurements were then added and divided by the number of measurements taken for every single sample to calculate the average thickness of the scar. For sham-operated animals, the thickness of the wall was measured in the corresponding region and quantified in similar fashion.

10.2.9. HISTOLOGY

10.2.9.1. PEG-Alexa fluor® 660 detection

3 µm myocardial tissue sections were dewaxed, hydrated and mounted with DAPI. Stitched images were acquired with a Nikon 90i fluorescence microscope.

10.2.9.2. Modified Masson's Trichrome stain

After fixation in 4% paraformaldehyde (Sigma-Aldrich, Steinheim, Germany), all samples were processed through graded alcohol and then embedded in paraffin wax.

3 µm tissue sections were heat fixed on a hotplate at 60°C, dewaxed with xylene and taken through alcohol followed by a wash in running tap water. The sections were then flooded with 0.5% acid fuchsin (5 min) (Merck, Gauteng, South Africa), followed by 1% phosphomolybdic acid (5 min) (Sigma-Aldrich, Steinheim, Germany) to remove excess acid fuchsin. A 2% light green (2 min) (Sigma-Aldrich, Steinheim, Germany) solution was used as a counter-stain.

10.2.9.3. ED1 (anti-rat cd68)

3 µm myocardial tissue sections were dewaxed, hydrated and pre-treated with a ready to use proteinase k solution (Dako, California, USA) for 10 minutes. After washing in TBS for 5 minutes, sections were blocked with 1% bovine serum albumin/or rodent block (BSA, Jacksons Immunoresearch, West Grove, PA, USA) for 20 minutes and then incubated with a

1:100 dilution of mouse anti rat ED1/CD68 primary antibody (Serotec, Kidlington, Oxford, UK) in 1% BSA in PBS for 1 hour. Sections were again washed in TBS for 5 minutes and subsequently the primary antibody was detected by incubating with a 1:1000 (1:500 after freezing with glycerol) of a CY3 donkey anti-mouse IgG antibody (Jackson Immuno Research Lab, West Grove, USA) for 1-2 hours. During the incubation period with the secondary antibody and the following 5-minute wash in TBS, slides were kept in the dark. Slides were finally counterstained and mounted with DAPI (Vector laboratories, Burlingame, CA) and the coverslip was sealed with nail polish. Images were acquired with a Nikon 90i fluorescence microscope (Nikon Corp., Tokyo, Japan)

10.2.9.4. Von Willebrand Factor

Cross-sections were dewaxed in xylene (3x), cleared in alcohol (3x) and washed with H2O. After a 20 minute incubation step (at 37°C) with proteinase K (Dako, Glostrup, Denmark), sections were washed with H2O and placed in TBS. Next, slides were incubated with 10% goat serum for 15 minutes at RT, before being incubated with a 1:400 dilution of primary rabbit anti-rat von Willebrand factor antibody (ab6994, ABCAM, Cambridge, UK) in 1 % BSA in PBS overnight at 4°C. The next morning, sections were washed in TBS, and the primary antibody was detected by a 2 hour 30 minute incubation with a 1:500 dilution of Cy3 donkey anti-rabbit antibody (Jacksons Immunoresearch, West Grove, PA, USA). After a wash in TBS (in the dark), sections were counterstained with DAPI (Vectashield® mounting medium, Vector Laboratories, Burlingame, CA).

10.2.9.4.1. Quantification of vascularisation area and vessel density in infarcted hearts

4 random images were acquired with a Nikon 90i fluorescence microscope (Nikon Corp., Tokyo, Japan) at 80x magnification within clearly infarcted regions on the vWF stained cross-sections. The images were analysed with Visiopharm Integrated Systems (VIS) (Visiopharm A/S, Hørsholm, Denmark). Briefly, the software was trained to recognise vWF^{+}-structures after pre-processing steps that had enhanced the contrast of these structures relative to the surrounding

tissue. Vascularisation area was calculated as a percentage of the cardiac tissue present in the 4 images. Similarly vessel density was calculated as the number of vessels per mm^2 of infarcted cardiac tissue cross-section.

11. References

1. Rosamond, W.*, et al.* Heart disease and stroke statistics--2008 update: a report from the American Heart Association Statistics Committee and Stroke Statistics Subcommittee. *Circulation* **117**, e25-146 (2008).
2. Velagaleti, R.S.*, et al.* Long-term trends in the incidence of heart failure after myocardial infarction. *Circulation* **118**, 2057-2062 (2008).
3. Hirsch, A.T.*, et al.* Peripheral arterial disease detection, awareness, and treatment in primary care. *JAMA* **286**, 1317-1324 (2001).
4. Selvin, E. & Erlinger, T.P. Prevalence of and risk factors for peripheral arterial disease in the United States: results from the National Health and Nutrition Examination Survey, 1999-2000. *Circulation* **110**, 738-743 (2004).
5. Ostchega, Y., Paulose-Ram, R., Dillon, C.F., Gu, Q. & Hughes, J.P. Prevalence of peripheral arterial disease and risk factors in persons aged 60 and older: data from the National Health and Nutrition Examination Survey 1999-2004. *J Am Geriatr Soc* **55**, 583-589 (2007).
6. Carmeliet, P. Angiogenesis in life, disease and medicine. *Nature* **438**, 932-936 (2005).
7. Folkman, J. Tumor angiogenesis: therapeutic implications. *N Engl J Med* **285**, 1182-1186 (1971).
8. Gimbrone, M.A., Jr., Cotran, R.S. & Folkman, J. Human vascular endothelial cells in culture. Growth and DNA synthesis. *J Cell Biol* **60**, 673-684 (1974).
9. Gimbrone, M.A., Jr., Cotran, R.S., Leapman, S.B. & Folkman, J. Tumor growth and neovascularization: an experimental model using the rabbit cornea. *J Natl Cancer Inst* **52**, 413-427 (1974).
10. Gospodarowicz, D. Localisation of a fibroblast growth factor and its effect alone and with hydrocortisone on 3T3 cell growth. *Nature* **249**, 123-127 (1974).
11. White, C.W., Sondheimer, H.M., Crouch, E.C., Wilson, H. & Fan, L.L. Treatment of pulmonary hemangiomatosis with recombinant interferon alfa-2a. *N Engl J Med* **320**, 1197-1200 (1989).
12. Folkman, J. Successful treatment of an angiogenic disease. *N Engl J Med* **320**, 1211-1212 (1989).
13. Ferrara, N. & Henzel, W.J. Pituitary follicular cells secrete a novel heparin-binding growth factor specific for vascular endothelial cells. *Biochem Biophys Res Commun* **161**, 851-858 (1989).
14. Good, D.J.*, et al.* A tumor suppressor-dependent inhibitor of angiogenesis is immunologically and functionally indistinguishable from a fragment of thrombospondin. *Proc Natl Acad Sci U S A* **87**, 6624-6628 (1990).
15. Rastinejad, F., Polverini, P.J. & Bouck, N.P. Regulation of the activity of a new inhibitor of angiogenesis by a cancer suppressor gene. *Cell* **56**, 345-355 (1989).
16. Yanagisawa-Miwa, A.*, et al.* Salvage of infarcted myocardium by angiogenic action of basic fibroblast growth factor. *Science* **257**, 1401-1403 (1992).
17. Takeshita, S.*, et al.* Therapeutic angiogenesis. A single intraarterial bolus of vascular endothelial growth factor augments revascularization in a rabbit ischemic hind limb model. *J Clin Invest* **93**, 662-670 (1994).
18. Reynolds, L.P., Killilea, S.D. & Redmer, D.A. Angiogenesis in the female reproductive system. *FASEB J* **6**, 886-892 (1992).
19. Plendl, J. Angiogenesis and vascular regression in the ovary. *Anat Histol Embryol* **29**, 257-266 (2000).
20. Risau, W. Mechanisms of angiogenesis. *Nature* **386**, 671-674 (1997).
21. Ribatti, D., Vacca, A., Nico, B., Roncali, L. & Dammacco, F. Postnatal vasculogenesis. *Mech Dev* **100**, 157-163 (2001).
22. Asahara, T.*, et al.* Isolation of putative progenitor endothelial cells for angiogenesis. *Science* **275**, 964-967 (1997).

23. Young, P.P., Hofling, A.A. & Sands, M.S. VEGF increases engraftment of bone marrow-derived endothelial progenitor cells (EPCs) into vasculature of newborn murine recipients. *Proc Natl Acad Sci U S A* **99**, 11951-11956 (2002).
24. Hattori, K.*, et al.* Vascular endothelial growth factor and angiopoietin-1 stimulate postnatal hematopoiesis by recruitment of vasculogenic and hematopoietic stem cells. *J Exp Med* **193**, 1005-1014 (2001).
25. Heissig, B.*, et al.* Recruitment of stem and progenitor cells from the bone marrow niche requires MMP-9 mediated release of kit-ligand. *Cell* **109**, 625-637 (2002).
26. Asahara, T.*, et al.* VEGF contributes to postnatal neovascularization by mobilizing bone marrow-derived endothelial progenitor cells. *EMBO J* **18**, 3964-3972 (1999).
27. Li, H., Gerald, W.L. & Benezra, R. Utilization of bone marrow-derived endothelial cell precursors in spontaneous prostate tumors varies with tumor grade. *Cancer Res* **64**, 6137-6143 (2004).
28. Capillo, M.*, et al.* Continuous infusion of endostatin inhibits differentiation, mobilization, and clonogenic potential of endothelial cell progenitors. *Clin Cancer Res* **9**, 377-382 (2003).
29. Shaked, Y.*, et al.* Genetic heterogeneity of the vasculogenic phenotype parallels angiogenesis; Implications for cellular surrogate marker analysis of antiangiogenesis. *Cancer Cell* **7**, 101-111 (2005).
30. Sebzda, E.*, et al.* Syk and Slp-76 mutant mice reveal a cell-autonomous hematopoietic cell contribution to vascular development. *Dev Cell* **11**, 349-361 (2006).
31. Carmeliet, P. Mechanisms of angiogenesis and arteriogenesis. *Nat Med* **6**, 389-395 (2000).
32. Rossant, J. & Howard, L. Signaling pathways in vascular development. *Annu Rev Cell Dev Biol* **18**, 541-573 (2002).
33. Neufeld, G. & Kessler, O. Pro-angiogenic cytokines and their role in tumor angiogenesis. *Cancer Metastasis Rev* **25**, 373-385 (2006).
34. Maisonpierre, P.C.*, et al.* Angiopoietin-2, a natural antagonist for Tie2 that disrupts in vivo angiogenesis. *Science* **277**, 55-60 (1997).
35. Vestweber, D. Molecular mechanisms that control endothelial cell contacts. *J Pathol* **190**, 281-291 (2000).
36. Esser, S., Lampugnani, M.G., Corada, M., Dejana, E. & Risau, W. Vascular endothelial growth factor induces VE-cadherin tyrosine phosphorylation in endothelial cells. *J Cell Sci* **111 (Pt 13)**, 1853-1865 (1998).
37. Wright, T.J., Leach, L., Shaw, P.E. & Jones, P. Dynamics of vascular endothelial-cadherin and beta-catenin localization by vascular endothelial growth factor-induced angiogenesis in human umbilical vein cells. *Exp Cell Res* **280**, 159-168 (2002).
38. Rossant, J. & Hirashima, M. Vascular development and patterning: making the right choices. *Curr Opin Genet Dev* **13**, 408-412 (2003).
39. Suchting, S., Bicknell, R. & Eichmann, A. Neuronal clues to vascular guidance. *Exp Cell Res* **312**, 668-675 (2006).
40. Eichmann, A., Makinen, T. & Alitalo, K. Neural guidance molecules regulate vascular remodeling and vessel navigation. *Genes Dev* **19**, 1013-1021 (2005).
41. Klagsbrun, M. & Eichmann, A. A role for axon guidance receptors and ligands in blood vessel development and tumor angiogenesis. *Cytokine Growth Factor Rev* **16**, 535-548 (2005).
42. Weinstein, B.M. Vessels and nerves: marching to the same tune. *Cell* **120**, 299-302 (2005).
43. Noguera-Troise, I.*, et al.* Blockade of Dll4 inhibits tumour growth by promoting non-productive angiogenesis. *Nature* **444**, 1032-1037 (2006).
44. Davis, G.E. & Senger, D.R. Endothelial extracellular matrix: biosynthesis, remodeling, and functions during vascular morphogenesis and neovessel stabilization. *Circ Res* **97**, 1093-1107 (2005).
45. Zucker, S.*, et al.* Vascular endothelial growth factor induces tissue factor and matrix metalloproteinase production in endothelial cells: conversion of prothrombin to thrombin

results in progelatinase A activation and cell proliferation. *Int J Cancer* **75**, 780-786 (1998).
46. Chun, T.H.*, et al.* MT1-MMP-dependent neovessel formation within the confines of the three-dimensional extracellular matrix. *J Cell Biol* **167**, 757-767 (2004).
47. Itoh, Y. & Seiki, M. MT1-MMP: a potent modifier of pericellular microenvironment. *J Cell Physiol* **206**, 1-8 (2006).
48. Collen, A.*, et al.* Membrane-type matrix metalloproteinase-mediated angiogenesis in a fibrin-collagen matrix. *Blood* **101**, 1810-1817 (2003).
49. Roy, R., Zhang, B. & Moses, M.A. Making the cut: protease-mediated regulation of angiogenesis. *Exp Cell Res* **312**, 608-622 (2006).
50. van Hinsbergh, V.W., Engelse, M.A. & Quax, P.H. Pericellular proteases in angiogenesis and vasculogenesis. *Arterioscler Thromb Vasc Biol* **26**, 716-728 (2006).
51. Chang, C. & Werb, Z. The many faces of metalloproteases: cell growth, invasion, angiogenesis and metastasis. *Trends Cell Biol* **11**, S37-43 (2001).
52. Davis, G.E. & Senger, D.R. Extracellular matrix mediates a molecular balance between vascular morphogenesis and regression. *Curr Opin Hematol* **15**, 197-203 (2008).
53. Jain, R.K. Molecular regulation of vessel maturation. *Nat Med* **9**, 685-693 (2003).
54. Abramsson, A., Lindblom, P. & Betsholtz, C. Endothelial and nonendothelial sources of PDGF-B regulate pericyte recruitment and influence vascular pattern formation in tumors. *J Clin Invest* **112**, 1142-1151 (2003).
55. Uemura, A.*, et al.* Recombinant angiopoietin-1 restores higher-order architecture of growing blood vessels in mice in the absence of mural cells. *J Clin Invest* **110**, 1619-1628 (2002).
56. Carvalho, R.L.*, et al.* Defective paracrine signalling by TGFbeta in yolk sac vasculature of endoglin mutant mice: a paradigm for hereditary haemorrhagic telangiectasia. *Development* **131**, 6237-6247 (2004).
57. Sato, T.N.*, et al.* Distinct roles of the receptor tyrosine kinases Tie-1 and Tie-2 in blood vessel formation. *Nature* **376**, 70-74 (1995).
58. Carmeliet, P. Angiogenesis in health and disease. *Nat Med* **9**, 653-660 (2003).
59. Song, S., Ewald, A.J., Stallcup, W., Werb, Z. & Bergers, G. PDGFRbeta+ perivascular progenitor cells in tumours regulate pericyte differentiation and vascular survival. *Nat Cell Biol* **7**, 870-879 (2005).
60. Rajantie, I.*, et al.* Adult bone marrow-derived cells recruited during angiogenesis comprise precursors for periendothelial vascular mural cells. *Blood* **104**, 2084-2086 (2004).
61. Dor, Y.*, et al.* Conditional switching of VEGF provides new insights into adult neovascularization and pro-angiogenic therapy. *EMBO J* **21**, 1939-1947 (2002).
62. Baluk, P.*, et al.* Regulated angiogenesis and vascular regression in mice overexpressing vascular endothelial growth factor in airways. *Am J Pathol* **165**, 1071-1085 (2004).
63. Dimmeler, S., Haendeler, J., Rippmann, V., Nehls, M. & Zeiher, A.M. Shear stress inhibits apoptosis of human endothelial cells. *FEBS Lett* **399**, 71-74 (1996).
64. Kakisis, J.D., Liapis, C.D. & Sumpio, B.E. Effects of cyclic strain on vascular cells. *Endothelium* **11**, 17-28 (2004).
65. Chen, K.D.*, et al.* Mechanotransduction in response to shear stress. Roles of receptor tyrosine kinases, integrins, and Shc. *J Biol Chem* **274**, 18393-18400 (1999).
66. Fisher, A.B., Chien, S., Barakat, A.I. & Nerem, R.M. Endothelial cellular response to altered shear stress. *Am J Physiol Lung Cell Mol Physiol* **281**, L529-533 (2001).
67. Palumbo, R.*, et al.* Shear stress downregulation of platelet-derived growth factor receptor-beta and matrix metalloprotease-2 is associated with inhibition of smooth muscle cell invasion and migration. *Circulation* **102**, 225-230 (2000).
68. Magid, R., Murphy, T.J. & Galis, Z.S. Expression of matrix metalloproteinase-9 in endothelial cells is differentially regulated by shear stress. Role of c-Myc. *J Biol Chem* **278**, 32994-32999 (2003).
69. Yamaguchi, S.*, et al.* Cyclic strain stimulates early growth response gene product 1-mediated expression of membrane type 1 matrix metalloproteinase in endothelium. *Lab Invest* **82**, 949-956 (2002).

70. Davis, G.E., Bayless, K.J. & Mavila, A. Molecular basis of endothelial cell morphogenesis in three-dimensional extracellular matrices. *Anat Rec* **268**, 252-275 (2002).
71. Bayless, K.J. & Davis, G.E. Sphingosine-1-phosphate markedly induces matrix metalloproteinase and integrin-dependent human endothelial cell invasion and lumen formation in three-dimensional collagen and fibrin matrices. *Biochem Biophys Res Commun* **312**, 903-913 (2003).
72. Hiraoka, N., Allen, E., Apel, I.J., Gyetko, M.R. & Weiss, S.J. Matrix metalloproteinases regulate neovascularization by acting as pericellular fibrinolysins. *Cell* **95**, 365-377 (1998).
73. Hotary, K., Allen, E., Punturieri, A., Yana, I. & Weiss, S.J. Regulation of cell invasion and morphogenesis in a three-dimensional type I collagen matrix by membrane-type matrix metalloproteinases 1, 2, and 3. *J Cell Biol* **149**, 1309-1323 (2000).
74. Saunders, W.B., Bayless, K.J. & Davis, G.E. MMP-1 activation by serine proteases and MMP-10 induces human capillary tubular network collapse and regression in 3D collagen matrices. *J Cell Sci* **118**, 2325-2340 (2005).
75. Davis, G.E., Pintar Allen, K.A., Salazar, R. & Maxwell, S.A. Matrix metalloproteinase-1 and -9 activation by plasmin regulates a novel endothelial cell-mediated mechanism of collagen gel contraction and capillary tube regression in three-dimensional collagen matrices. *J Cell Sci* **114**, 917-930 (2001).
76. Simons, M. Angiogenesis: where do we stand now? *Circulation* **111**, 1556-1566 (2005).
77. Senger, D.R.*, et al.* Tumor cells secrete a vascular permeability factor that promotes accumulation of ascites fluid. *Science* **219**, 983-985 (1983).
78. Ferrara, N., Gerber, H.P. & LeCouter, J. The biology of VEGF and its receptors. *Nat Med* **9**, 669-676 (2003).
79. Heldin, C.H. & Westermark, B. Mechanism of action and in vivo role of platelet-derived growth factor. *Physiol Rev* **79**, 1283-1316 (1999).
80. Ferrara, N. & Davis-Smyth, T. The biology of vascular endothelial growth factor. *Endocr Rev* **18**, 4-25 (1997).
81. Ferrara, N. VEGF and the quest for tumour angiogenesis factors. *Nat Rev Cancer* **2**, 795-803 (2002).
82. Hanahan, D. & Folkman, J. Patterns and emerging mechanisms of the angiogenic switch during tumorigenesis. *Cell* **86**, 353-364 (1996).
83. Clauss, M.*, et al.* Vascular permeability factor: a tumor-derived polypeptide that induces endothelial cell and monocyte procoagulant activity, and promotes monocyte migration. *J Exp Med* **172**, 1535-1545 (1990).
84. Grunewald, M.*, et al.* VEGF-induced adult neovascularization: recruitment, retention, and role of accessory cells. *Cell* **124**, 175-189 (2006).
85. Heissig, B., Hattori, K., Friedrich, M., Rafii, S. & Werb, Z. Angiogenesis: vascular remodeling of the extracellular matrix involves metalloproteinases. *Curr Opin Hematol* **10**, 136-141 (2003).
86. Hiratsuka, S.*, et al.* MMP9 induction by vascular endothelial growth factor receptor-1 is involved in lung-specific metastasis. *Cancer Cell* **2**, 289-300 (2002).
87. Ferrara, N.*, et al.* Heterozygous embryonic lethality induced by targeted inactivation of the VEGF gene. *Nature* **380**, 439-442 (1996).
88. Fong, G.H., Rossant, J., Gertsenstein, M. & Breitman, M.L. Role of the Flt-1 receptor tyrosine kinase in regulating the assembly of vascular endothelium. *Nature* **376**, 66-70 (1995).
89. Fong, G.H., Zhang, L., Bryce, D.M. & Peng, J. Increased hemangioblast commitment, not vascular disorganization, is the primary defect in flt-1 knock-out mice. *Development* **126**, 3015-3025 (1999).
90. Shalaby, F.*, et al.* Failure of blood-island formation and vasculogenesis in Flk-1-deficient mice. *Nature* **376**, 62-66 (1995).
91. Zeng, H., Dvorak, H.F. & Mukhopadhyay, D. Vascular permeability factor (VPF)/vascular endothelial growth factor (VEGF) peceptor-1 down-modulates VPF/VEGF receptor-2-mediated endothelial cell proliferation, but not migration, through phosphatidylinositol 3-kinase-dependent pathways. *J Biol Chem* **276**, 26969-26979 (2001).

92. Rahimi, N., Dayanir, V. & Lashkari, K. Receptor chimeras indicate that the vascular endothelial growth factor receptor-1 (VEGFR-1) modulates mitogenic activity of VEGFR-2 in endothelial cells. *J Biol Chem* **275**, 16986-16992 (2000).
93. Ambati, B.K.*, et al.* Corneal avascularity is due to soluble VEGF receptor-1. *Nature* **443**, 993-997 (2006).
94. Tammela, T., Petrova, T.V. & Alitalo, K. Molecular lymphangiogenesis: new players. *Trends Cell Biol* **15**, 434-441 (2005).
95. Takahashi, T., Yamaguchi, S., Chida, K. & Shibuya, M. A single autophosphorylation site on KDR/Flk-1 is essential for VEGF-A-dependent activation of PLC-gamma and DNA synthesis in vascular endothelial cells. *EMBO J* **20**, 2768-2778 (2001).
96. Olsson, A.K., Dimberg, A., Kreuger, J. & Claesson-Welsh, L. VEGF receptor signalling - in control of vascular function. *Nat Rev Mol Cell Biol* **7**, 359-371 (2006).
97. Engelman, J.A., Luo, J. & Cantley, L.C. The evolution of phosphatidylinositol 3-kinases as regulators of growth and metabolism. *Nat Rev Genet* **7**, 606-619 (2006).
98. Ito, N., Wernstedt, C., Engstrom, U. & Claesson-Welsh, L. Identification of vascular endothelial growth factor receptor-1 tyrosine phosphorylation sites and binding of SH2 domain-containing molecules. *J Biol Chem* **273**, 23410-23418 (1998).
99. Autiero, M.*, et al.* Role of PlGF in the intra- and intermolecular cross talk between the VEGF receptors Flt1 and Flk1. *Nat Med* **9**, 936-943 (2003).
100. Kappert, K., Peters, K.G., Bohmer, F.D. & Ostman, A. Tyrosine phosphatases in vessel wall signaling. *Cardiovasc Res* **65**, 587-598 (2005).
101. Soker, S., Takashima, S., Miao, H.Q., Neufeld, G. & Klagsbrun, M. Neuropilin-1 is expressed by endothelial and tumor cells as an isoform-specific receptor for vascular endothelial growth factor. *Cell* **92**, 735-745 (1998).
102. Carmeliet, P.*, et al.* Role of HIF-1alpha in hypoxia-mediated apoptosis, cell proliferation and tumour angiogenesis. *Nature* **394**, 485-490 (1998).
103. Pugh, C.W. & Ratcliffe, P.J. Regulation of angiogenesis by hypoxia: role of the HIF system. *Nat Med* **9**, 677-684 (2003).
104. Frank, S.*, et al.* Regulation of vascular endothelial growth factor expression in cultured keratinocytes. Implications for normal and impaired wound healing. *J Biol Chem* **270**, 12607-12613 (1995).
105. Pertovaara, L.*, et al.* Vascular endothelial growth factor is induced in response to transforming growth factor-beta in fibroblastic and epithelial cells. *J Biol Chem* **269**, 6271-6274 (1994).
106. Warren, R.S., Yuan, H., Matli, M.R., Ferrara, N. & Donner, D.B. Induction of vascular endothelial growth factor by insulin-like growth factor 1 in colorectal carcinoma. *J Biol Chem* **271**, 29483-29488 (1996).
107. Ben-Av, P., Crofford, L.J., Wilder, R.L. & Hla, T. Induction of vascular endothelial growth factor expression in synovial fibroblasts by prostaglandin E and interleukin-1: a potential mechanism for inflammatory angiogenesis. *FEBS Lett* **372**, 83-87 (1995).
108. Cohen, T., Nahari, D., Cerem, L.W., Neufeld, G. & Levi, B.Z. Interleukin 6 induces the expression of vascular endothelial growth factor. *J Biol Chem* **271**, 736-741 (1996).
109. Grugel, S., Finkenzeller, G., Weindel, K., Barleon, B. & Marme, D. Both v-Ha-Ras and v-Raf stimulate expression of the vascular endothelial growth factor in NIH 3T3 cells. *J Biol Chem* **270**, 25915-25919 (1995).
110. Okada, F.*, et al.* Impact of oncogenes in tumor angiogenesis: mutant K-ras up-regulation of vascular endothelial growth factor/vascular permeability factor is necessary, but not sufficient for tumorigenicity of human colorectal carcinoma cells. *Proc Natl Acad Sci U S A* **95**, 3609-3614 (1998).
111. Zhang, X., Gaspard, J.P. & Chung, D.C. Regulation of vascular endothelial growth factor by the Wnt and K-ras pathways in colonic neoplasia. *Cancer Res* **61**, 6050-6054 (2001).
112. Tammela, T., Enholm, B., Alitalo, K. & Paavonen, K. The biology of vascular endothelial growth factors. *Cardiovasc Res* **65**, 550-563 (2005).
113. Karkkainen, M.J.*, et al.* Vascular endothelial growth factor C is required for sprouting of the first lymphatic vessels from embryonic veins. *Nat Immunol* **5**, 74-80 (2004).

114. Kukk, E.*, et al.* VEGF-C receptor binding and pattern of expression with VEGFR-3 suggests a role in lymphatic vascular development. *Development* **122**, 3829-3837 (1996).
115. Saharinen, P., Tammela, T., Karkkainen, M.J. & Alitalo, K. Lymphatic vasculature: development, molecular regulation and role in tumor metastasis and inflammation. *Trends Immunol* **25**, 387-395 (2004).
116. Skobe, M.*, et al.* Induction of tumor lymphangiogenesis by VEGF-C promotes breast cancer metastasis. *Nat Med* **7**, 192-198 (2001).
117. Karpanen, T. & Alitalo, K. Lymphatic vessels as targets of tumor therapy? *J Exp Med* **194**, F37-42 (2001).
118. Cao, Y.*, et al.* Vascular endothelial growth factor C induces angiogenesis in vivo. *Proc Natl Acad Sci U S A* **95**, 14389-14394 (1998).
119. Cao, R.*, et al.* Comparative evaluation of FGF-2-, VEGF-A-, and VEGF-C-induced angiogenesis, lymphangiogenesis, vascular fenestrations, and permeability. *Circ Res* **94**, 664-670 (2004).
120. Oh, S.J.*, et al.* VEGF and VEGF-C: specific induction of angiogenesis and lymphangiogenesis in the differentiated avian chorioallantoic membrane. *Dev Biol* **188**, 96-109 (1997).
121. Saaristo, A.*, et al.* Adenoviral VEGF-C overexpression induces blood vessel enlargement, tortuosity, and leakiness but no sprouting angiogenesis in the skin or mucous membranes. *FASEB J* **16**, 1041-1049 (2002).
122. Witzenbichler, B.*, et al.* Vascular endothelial growth factor-C (VEGF-C/VEGF-2) promotes angiogenesis in the setting of tissue ischemia. *Am J Pathol* **153**, 381-394 (1998).
123. Baluk, P.*, et al.* Pathogenesis of persistent lymphatic vessel hyperplasia in chronic airway inflammation. *J Clin Invest* **115**, 247-257 (2005).
124. Benest, A.V., Harper, S.J., Herttuala, S.Y., Alitalo, K. & Bates, D.O. VEGF-C induced angiogenesis preferentially occurs at a distance from lymphangiogenesis. *Cardiovasc Res* **78**, 315-323 (2008).
125. Maglione, D., Guerriero, V., Viglietto, G., Delli-Bovi, P. & Persico, M.G. Isolation of a human placenta cDNA coding for a protein related to the vascular permeability factor. *Proc Natl Acad Sci U S A* **88**, 9267-9271 (1991).
126. Shibuya, M. & Claesson-Welsh, L. Signal transduction by VEGF receptors in regulation of angiogenesis and lymphangiogenesis. *Exp Cell Res* **312**, 549-560 (2006).
127. Carmeliet, P.*, et al.* Synergism between vascular endothelial growth factor and placental growth factor contributes to angiogenesis and plasma extravasation in pathological conditions. *Nat Med* **7**, 575-583 (2001).
128. Lijnen, H.R.*, et al.* Impaired adipose tissue development in mice with inactivation of placental growth factor function. *Diabetes* **55**, 2698-2704 (2006).
129. van Royen, N.*, et al.* Stimulation of arteriogenesis; a new concept for the treatment of arterial occlusive disease. *Cardiovasc Res* **49**, 543-553 (2001).
130. Luttun, A.*, et al.* Revascularization of ischemic tissues by PlGF treatment, and inhibition of tumor angiogenesis, arthritis and atherosclerosis by anti-Flt1. *Nat Med* **8**, 831-840 (2002).
131. Ribatti, D. The discovery of the placental growth factor and its role in angiogenesis: a historical review. *Angiogenesis* **11**, 215-221 (2008).
132. Park, J.E., Chen, H.H., Winer, J., Houck, K.A. & Ferrara, N. Placenta growth factor. Potentiation of vascular endothelial growth factor bioactivity, in vitro and in vivo, and high affinity binding to Flt-1 but not to Flk-1/KDR. *J Biol Chem* **269**, 25646-25654 (1994).
133. Bottomley, M.J.*, et al.* Placenta growth factor (PlGF) induces vascular endothelial growth factor (VEGF) secretion from mononuclear cells and is co-expressed with VEGF in synovial fluid. *Clin Exp Immunol* **119**, 182-188 (2000).
134. Hattori, K.*, et al.* Placental growth factor reconstitutes hematopoiesis by recruiting VEGFR1(+) stem cells from bone-marrow microenvironment. *Nat Med* **8**, 841-849 (2002).
135. Kolakowski, S., Jr.*, et al.* Placental growth factor provides a novel local angiogenic therapy for ischemic cardiomyopathy. *J Card Surg* **21**, 559-564 (2006).
136. von Tell, D., Armulik, A. & Betsholtz, C. Pericytes and vascular stability. *Exp Cell Res* **312**, 623-629 (2006).

137. Winkler, F.*, et al.* Kinetics of vascular normalization by VEGFR2 blockade governs brain tumor response to radiation: role of oxygenation, angiopoietin-1, and matrix metalloproteinases. *Cancer Cell* **6**, 553-563 (2004).
138. Hawighorst, T.*, et al.* Activation of the tie2 receptor by angiopoietin-1 enhances tumor vessel maturation and impairs squamous cell carcinoma growth. *Am J Pathol* **160**, 1381-1392 (2002).
139. Brindle, N.P., Saharinen, P. & Alitalo, K. Signaling and functions of angiopoietin-1 in vascular protection. *Circ Res* **98**, 1014-1023 (2006).
140. Kim, I.*, et al.* Angiopoietin-1 regulates endothelial cell survival through the phosphatidylinositol 3'-Kinase/Akt signal transduction pathway. *Circ Res* **86**, 24-29 (2000).
141. Fujikawa, K.*, et al.* Role of PI 3-kinase in angiopoietin-1-mediated migration and attachment-dependent survival of endothelial cells. *Exp Cell Res* **253**, 663-672 (1999).
142. Papapetropoulos, A.*, et al.* Angiopoietin-1 inhibits endothelial cell apoptosis via the Akt/survivin pathway. *J Biol Chem* **275**, 9102-9105 (2000).
143. DeBusk, L.M., Hallahan, D.E. & Lin, P.C. Akt is a major angiogenic mediator downstream of the Ang1/Tie2 signaling pathway. *Exp Cell Res* **298**, 167-177 (2004).
144. Fiedler, U.*, et al.* The Tie-2 ligand angiopoietin-2 is stored in and rapidly released upon stimulation from endothelial cell Weibel-Palade bodies. *Blood* **103**, 4150-4156 (2004).
145. Holash, J.*, et al.* Vessel cooption, regression, and growth in tumors mediated by angiopoietins and VEGF. *Science* **284**, 1994-1998 (1999).
146. Gale, N.W.*, et al.* Angiopoietin-2 is required for postnatal angiogenesis and lymphatic patterning, and only the latter role is rescued by Angiopoietin-1. *Dev Cell* **3**, 411-423 (2002).
147. Hammes, H.P.*, et al.* Angiopoietin-2 causes pericyte dropout in the normal retina: evidence for involvement in diabetic retinopathy. *Diabetes* **53**, 1104-1110 (2004).
148. Zhang, L.*, et al.* Tumor-derived vascular endothelial growth factor up-regulates angiopoietin-2 in host endothelium and destabilizes host vasculature, supporting angiogenesis in ovarian cancer. *Cancer Res* **63**, 3403-3412 (2003).
149. Mandriota, S.J.*, et al.* Hypoxia-inducible angiopoietin-2 expression is mimicked by iodonium compounds and occurs in the rat brain and skin in response to systemic hypoxia and tissue ischemia. *Am J Pathol* **156**, 2077-2089 (2000).
150. Mandriota, S.J. & Pepper, M.S. Regulation of angiopoietin-2 mRNA levels in bovine microvascular endothelial cells by cytokines and hypoxia. *Circ Res* **83**, 852-859 (1998).
151. Fujiyama, S.*, et al.* Angiotensin AT(1) and AT(2) receptors differentially regulate angiopoietin-2 and vascular endothelial growth factor expression and angiogenesis by modulating heparin binding-epidermal growth factor (EGF)-mediated EGF receptor transactivation. *Circ Res* **88**, 22-29 (2001).
152. Cohen, B.*, et al.* Leptin induces angiopoietin-2 expression in adipose tissues. *J Biol Chem* **276**, 7697-7700 (2001).
153. Kim, I., Kim, J.H., Ryu, Y.S., Liu, M. & Koh, G.Y. Tumor necrosis factor-alpha upregulates angiopoietin-2 in human umbilical vein endothelial cells. *Biochem Biophys Res Commun* **269**, 361-365 (2000).
154. Dumont, D.J.*, et al.* Dominant-negative and targeted null mutations in the endothelial receptor tyrosine kinase, tek, reveal a critical role in vasculogenesis of the embryo. *Genes Dev* **8**, 1897-1909 (1994).
155. Suri, C.*, et al.* Requisite role of angiopoietin-1, a ligand for the TIE2 receptor, during embryonic angiogenesis. *Cell* **87**, 1171-1180 (1996).
156. Puri, M.C., Rossant, J., Alitalo, K., Bernstein, A. & Partanen, J. The receptor tyrosine kinase TIE is required for integrity and survival of vascular endothelial cells. *EMBO J* **14**, 5884-5891 (1995).
157. Thurston, G.*, et al.* Angiopoietin-1 protects the adult vasculature against plasma leakage. *Nat Med* **6**, 460-463 (2000).
158. Antoniades, H.N., Scher, C.D. & Stiles, C.D. Purification of human platelet-derived growth factor. *Proc Natl Acad Sci U S A* **76**, 1809-1813 (1979).

159. Heldin, C.H., Westermark, B. & Wasteson, A. Platelet-derived growth factor: purification and partial characterization. *Proc Natl Acad Sci U S A* **76**, 3722-3726 (1979).
160. Heldin, C.H., Wasteson, A. & Westermark, B. Platelet-derived growth factor. *Mol Cell Endocrinol* **39**, 169-187 (1985).
161. Li, X.*, et al.* PDGF-C is a new protease-activated ligand for the PDGF alpha-receptor. *Nat Cell Biol* **2**, 302-309 (2000).
162. Bergsten, E.*, et al.* PDGF-D is a specific, protease-activated ligand for the PDGF beta-receptor. *Nat Cell Biol* **3**, 512-516 (2001).
163. LaRochelle, W.J.*, et al.* PDGF-D, a new protease-activated growth factor. *Nat Cell Biol* **3**, 517-521 (2001).
164. Reigstad, L.J., Varhaug, J.E. & Lillehaug, J.R. Structural and functional specificities of PDGF-C and PDGF-D, the novel members of the platelet-derived growth factors family. *FEBS J* **272**, 5723-5741 (2005).
165. Kelly, J.D.*, et al.* Platelet-derived growth factor (PDGF) stimulates PDGF receptor subunit dimerization and intersubunit trans-phosphorylation. *J Biol Chem* **266**, 8987-8992 (1991).
166. Hubbard, S.R. Juxtamembrane autoinhibition in receptor tyrosine kinases. *Nat Rev Mol Cell Biol* **5**, 464-471 (2004).
167. Hellstrom, M., Kalen, M., Lindahl, P., Abramsson, A. & Betsholtz, C. Role of PDGF-B and PDGFR-beta in recruitment of vascular smooth muscle cells and pericytes during embryonic blood vessel formation in the mouse. *Development* **126**, 3047-3055 (1999).
168. Hirschi, K.K., Rohovsky, S.A. & D'Amore, P.A. PDGF, TGF-beta, and heterotypic cell-cell interactions mediate endothelial cell-induced recruitment of 10T1/2 cells and their differentiation to a smooth muscle fate. *J Cell Biol* **141**, 805-814 (1998).
169. Hellstrom, M.*, et al.* Lack of pericytes leads to endothelial hyperplasia and abnormal vascular morphogenesis. *J Cell Biol* **153**, 543-553 (2001).
170. Soriano, P. Abnormal kidney development and hematological disorders in PDGF beta-receptor mutant mice. *Genes Dev* **8**, 1888-1896 (1994).
171. Lindahl, P., Johansson, B.R., Leveen, P. & Betsholtz, C. Pericyte loss and microaneurysm formation in PDGF-B-deficient mice. *Science* **277**, 242-245 (1997).
172. Li, X.*, et al.* Revascularization of ischemic tissues by PDGF-CC via effects on endothelial cells and their progenitors. *J Clin Invest* **115**, 118-127 (2005).
173. Hsieh, P.C., Davis, M.E., Gannon, J., MacGillivray, C. & Lee, R.T. Controlled delivery of PDGF-BB for myocardial protection using injectable self-assembling peptide nanofibers. *J Clin Invest* **116**, 237-248 (2006).
174. Hsieh, P.C., MacGillivray, C., Gannon, J., Cruz, F.U. & Lee, R.T. Local controlled intramyocardial delivery of platelet-derived growth factor improves postinfarction ventricular function without pulmonary toxicity. *Circulation* **114**, 637-644 (2006).
175. Shing, Y.*, et al.* Heparin affinity: purification of a tumor-derived capillary endothelial cell growth factor. *Science* **223**, 1296-1299 (1984).
176. Shing, Y.*, et al.* Angiogenesis is stimulated by a tumor-derived endothelial cell growth factor. *J Cell Biochem* **29**, 275-287 (1985).
177. Folkman, J.*, et al.* A heparin-binding angiogenic protein--basic fibroblast growth factor--is stored within basement membrane. *Am J Pathol* **130**, 393-400 (1988).
178. Rusnati, M. & Presta, M. Interaction of angiogenic basic fibroblast growth factor with endothelial cell heparan sulfate proteoglycans. Biological implications in neovascularization. *Int J Clin Lab Res* **26**, 15-23 (1996).
179. Rusnati, M., Tanghetti, E., Dell'Era, P., Gualandris, A. & Presta, M. alphavbeta3 integrin mediates the cell-adhesive capacity and biological activity of basic fibroblast growth factor (FGF-2) in cultured endothelial cells. *Mol Biol Cell* **8**, 2449-2461 (1997).
180. Tanghetti, E.*, et al.* Biological activity of substrate-bound basic fibroblast growth factor (FGF2): recruitment of FGF receptor-1 in endothelial cell adhesion contacts. *Oncogene* **21**, 3889-3897 (2002).
181. Presta, M.*, et al.* Basic fibroblast growth factor bound to cell substrate promotes cell adhesion, proliferation, and protease production in cultured endothelial cells. *EXS* **61**, 205-209 (1992).

182. Presta, M.*, et al.* Fibroblast growth factor/fibroblast growth factor receptor system in angiogenesis. *Cytokine Growth Factor Rev* **16**, 159-178 (2005).
183. Presta, M., Moscatelli, D., Joseph-Silverstein, J. & Rifkin, D.B. Purification from a human hepatoma cell line of a basic fibroblast growth factor-like molecule that stimulates capillary endothelial cell plasminogen activator production, DNA synthesis, and migration. *Mol Cell Biol* **6**, 4060-4066 (1986).
184. Laham, R.J.*, et al.* Local perivascular delivery of basic fibroblast growth factor in patients undergoing coronary bypass surgery: results of a phase I randomized, double-blind, placebo-controlled trial. *Circulation* **100**, 1865-1871 (1999).
185. Simons, M.*, et al.* Pharmacological treatment of coronary artery disease with recombinant fibroblast growth factor-2: double-blind, randomized, controlled clinical trial. *Circulation* **105**, 788-793 (2002).
186. Ahn, A., Frishman, W.H., Gutwein, A., Passeri, J. & Nelson, M. Therapeutic angiogenesis: a new treatment approach for ischemic heart disease--part I. *Cardiol Rev* **16**, 163-171 (2008).
187. Beenken, A. & Mohammadi, M. The FGF family: biology, pathophysiology and therapy. *Nat Rev Drug Discov* **8**, 235-253 (2009).
188. Morrison, R.S.*, et al.* Fibroblast growth factor receptor gene expression and immunoreactivity are elevated in human glioblastoma multiforme. *Cancer Res* **54**, 2794-2799 (1994).
189. Rieck, P.W., Cholidis, S. & Hartmann, C. Intracellular signaling pathway of FGF-2-modulated corneal endothelial cell migration during wound healing in vitro. *Exp Eye Res* **73**, 639-650 (2001).
190. Giuliani, R., Bastaki, M., Coltrini, D. & Presta, M. Role of endothelial cell extracellular signal-regulated kinase1/2 in urokinase-type plasminogen activator upregulation and in vitro angiogenesis by fibroblast growth factor-2. *J Cell Sci* **112 (Pt 15)**, 2597-2606 (1999).
191. Eliceiri, B.P., Klemke, R., Stromblad, S. & Cheresh, D.A. Integrin alphavbeta3 requirement for sustained mitogen-activated protein kinase activity during angiogenesis. *J Cell Biol* **140**, 1255-1263 (1998).
192. Rusnati, M. & Presta, M. Extracellular angiogenic growth factor interactions: an angiogenesis interactome survey. *Endothelium* **13**, 93-111 (2006).
193. Wesley, U.V., McGroarty, M. & Homoyouni, A. Dipeptidyl peptidase inhibits malignant phenotype of prostate cancer cells by blocking basic fibroblast growth factor signaling pathway. *Cancer Res* **65**, 1325-1334 (2005).
194. Fontijn, D.*, et al.* CD13/Aminopeptidase N overexpression by basic fibroblast growth factor mediates enhanced invasiveness of 1F6 human melanoma cells. *Br J Cancer* **94**, 1627-1636 (2006).
195. Yang, C.*, et al.* Integrin alpha1beta1 and alpha2beta1 are the key regulators of hepatocarcinoma cell invasion across the fibrotic matrix microenvironment. *Cancer Res* **63**, 8312-8317 (2003).
196. Suyama, K., Shapiro, I., Guttman, M. & Hazan, R.B. A signaling pathway leading to metastasis is controlled by N-cadherin and the FGF receptor. *Cancer Cell* **2**, 301-314 (2002).
197. Giavazzi, R.*, et al.* Distinct role of fibroblast growth factor-2 and vascular endothelial growth factor on tumor growth and angiogenesis. *Am J Pathol* **162**, 1913-1926 (2003).
198. Fujii, T.*, et al.* Nonendothelial mesenchymal cell-derived MCP-1 is required for FGF-2-mediated therapeutic neovascularization: critical role of the inflammatory/arteriogenic pathway. *Arterioscler Thromb Vasc Biol* **26**, 2483-2489 (2006).
199. Naim, R., Chang, R.C., Sadick, H. & Hormann, K. Influence of hepatocyte growth factor/scatter factor (HGF/SF) on fibroblast growth factor-2 (FGF-2) levels in external auditory canal cholesteatoma (EACC) cell culture. *In Vivo* **19**, 599-603 (2005).
200. Castellon, R.*, et al.* Effects of angiogenic growth factor combinations on retinal endothelial cells. *Exp Eye Res* **74**, 523-535 (2002).
201. Jeon, O., Hwang, K.C., Yoo, K.J. & Kim, B.S. Combined sustained delivery of basic fibroblast growth factor and administration of granulocyte colony-stimulating factor:

synergistic effect on angiogenesis in mouse ischemic limbs. *J Endovasc Ther* **13**, 175-181 (2006).
202. Tille, J.C.*, et al.* Vascular endothelial growth factor (VEGF) receptor-2 antagonists inhibit VEGF- and basic fibroblast growth factor-induced angiogenesis in vivo and in vitro. *J Pharmacol Exp Ther* **299**, 1073-1085 (2001).
203. Auguste, P.*, et al.* Inhibition of fibroblast growth factor/fibroblast growth factor receptor activity in glioma cells impedes tumor growth by both angiogenesis-dependent and -independent mechanisms. *Cancer Res* **61**, 1717-1726 (2001).
204. Seghezzi, G.*, et al.* Fibroblast growth factor-2 (FGF-2) induces vascular endothelial growth factor (VEGF) expression in the endothelial cells of forming capillaries: an autocrine mechanism contributing to angiogenesis. *J Cell Biol* **141**, 1659-1673 (1998).
205. Kanda, S., Miyata, Y. & Kanetake, H. Fibroblast growth factor-2-mediated capillary morphogenesis of endothelial cells requires signals via Flt-1/vascular endothelial growth factor receptor-1: possible involvement of c-Akt. *J Biol Chem* **279**, 4007-4016 (2004).
206. Gabler, C., Plath-Gabler, A., Killian, G.J., Berisha, B. & Schams, D. Expression pattern of fibroblast growth factor (FGF) and vascular endothelial growth factor (VEGF) system members in bovine corpus luteum endothelial cells during treatment with FGF-2, VEGF or oestradiol. *Reprod Domest Anim* **39**, 321-327 (2004).
207. Cao, R.*, et al.* Angiogenic synergism, vascular stability and improvement of hind-limb ischemia by a combination of PDGF-BB and FGF-2. *Nat Med* **9**, 604-613 (2003).
208. Barde, Y.A. The nerve growth factor family. *Prog Growth Factor Res* **2**, 237-248 (1990).
209. Lindsay, R.M., Thoenen, H. & Barde, Y.A. Placode and neural crest-derived sensory neurons are responsive at early developmental stages to brain-derived neurotrophic factor. *Dev Biol* **112**, 319-328 (1985).
210. Sobue, G.*, et al.* Expression of mRNAs for neurotrophins (NGF, BDNF, and NT-3) and their receptors (p75NGFR, trk, trkB, and trkC) in human peripheral neuropathies. *Neurochem Res* **23**, 821-829 (1998).
211. Tucker, K.L., Meyer, M. & Barde, Y.A. Neurotrophins are required for nerve growth during development. *Nat Neurosci* **4**, 29-37 (2001).
212. Sofroniew, M.V., Howe, C.L. & Mobley, W.C. Nerve growth factor signaling, neuroprotection, and neural repair. *Annu Rev Neurosci* **24**, 1217-1281 (2001).
213. Huang, E.J. & Reichardt, L.F. Neurotrophins: roles in neuronal development and function. *Annu Rev Neurosci* **24**, 677-736 (2001).
214. Leibrock, J.*, et al.* Molecular cloning and expression of brain-derived neurotrophic factor. *Nature* **341**, 149-152 (1989).
215. Hofer, M., Pagliusi, S.R., Hohn, A., Leibrock, J. & Barde, Y.A. Regional distribution of brain-derived neurotrophic factor mRNA in the adult mouse brain. *EMBO J* **9**, 2459-2464 (1990).
216. Hohn, A., Leibrock, J., Bailey, K. & Barde, Y.A. Identification and characterization of a novel member of the nerve growth factor/brain-derived neurotrophic factor family. *Nature* **344**, 339-341 (1990).
217. Kolbeck, R., Jungbluth, S. & Barde, Y.A. Characterisation of neurotrophin dimers and monomers. *Eur J Biochem* **225**, 995-1003 (1994).
218. Lee, R., Kermani, P., Teng, K.K. & Hempstead, B.L. Regulation of cell survival by secreted proneurotrophins. *Science* **294**, 1945-1948 (2001).
219. Kim, H., Li, Q., Hempstead, B.L. & Madri, J.A. Paracrine and autocrine functions of brain-derived neurotrophic factor (BDNF) and nerve growth factor (NGF) in brain-derived endothelial cells. *J Biol Chem* **279**, 33538-33546 (2004).
220. Donovan, M.J.*, et al.* Brain derived neurotrophic factor is an endothelial cell survival factor required for intramyocardial vessel stabilization. *Development* **127**, 4531-4540 (2000).
221. Kermani, P.*, et al.* Neurotrophins promote revascularization by local recruitment of TrkB+ endothelial cells and systemic mobilization of hematopoietic progenitors. *J Clin Invest* **115**, 653-663 (2005).
222. Vacca, A.*, et al.* Bone marrow neovascularization, plasma cell angiogenic potential, and matrix metalloproteinase-2 secretion parallel progression of human multiple myeloma. *Blood* **93**, 3064-3073 (1999).

223. Vacca, A., Ribatti, D., Roccaro, A.M., Frigeri, A. & Dammacco, F. Bone marrow angiogenesis in patients with active multiple myeloma. *Semin Oncol* **28**, 543-550 (2001).
224. Hu, Y.*, et al.* Identification of brain-derived neurotrophic factor as a novel angiogenic protein in multiple myeloma. *Cancer Genet Cytogenet* **178**, 1-10 (2007).
225. Liu, Y., Sun, L., Huan, Y., Zhao, H. & Deng, J. Application of bFGF and BDNF to improve angiogenesis and cardiac function. *J Surg Res* **136**, 85-91 (2006).
226. Hiltunen, J.O., Laurikainen, A., Vakeva, A., Meri, S. & Saarma, M. Nerve growth factor and brain-derived neurotrophic factor mRNAs are regulated in distinct cell populations of rat heart after ischaemia and reperfusion. *J Pathol* **194**, 247-253 (2001).
227. Patist, C.M.*, et al.* Freeze-dried poly(D,L-lactic acid) macroporous guidance scaffolds impregnated with brain-derived neurotrophic factor in the transected adult rat thoracic spinal cord. *Biomaterials* **25**, 1569-1582 (2004).
228. Petit, I., Jin, D. & Rafii, S. The SDF-1-CXCR4 signaling pathway: a molecular hub modulating neo-angiogenesis. *Trends Immunol* **28**, 299-307 (2007).
229. Ara, T., Tokoyoda, K., Okamoto, R., Koni, P.A. & Nagasawa, T. The role of CXCL12 in the organ-specific process of artery formation. *Blood* **105**, 3155-3161 (2005).
230. Salvucci, O.*, et al.* Regulation of endothelial cell branching morphogenesis by endogenous chemokine stromal-derived factor-1. *Blood* **99**, 2703-2711 (2002).
231. Yamaguchi, J.*, et al.* Stromal cell-derived factor-1 effects on ex vivo expanded endothelial progenitor cell recruitment for ischemic neovascularization. *Circulation* **107**, 1322-1328 (2003).
232. Kryczek, I.*, et al.* CXCL12 and vascular endothelial growth factor synergistically induce neoangiogenesis in human ovarian cancers. *Cancer Res* **65**, 465-472 (2005).
233. Carr, A.N.*, et al.* Efficacy of systemic administration of SDF-1 in a model of vascular insufficiency: support for an endothelium-dependent mechanism. *Cardiovasc Res* **69**, 925-935 (2006).
234. Kollet, O.*, et al.* HGF, SDF-1, and MMP-9 are involved in stress-induced human CD34+ stem cell recruitment to the liver. *J Clin Invest* **112**, 160-169 (2003).
235. Shiba, Y.*, et al.* M-CSF accelerates neointimal formation in the early phase after vascular injury in mice: the critical role of the SDF-1-CXCR4 system. *Arterioscler Thromb Vasc Biol* **27**, 283-289 (2007).
236. Ponomaryov, T.*, et al.* Induction of the chemokine stromal-derived factor-1 following DNA damage improves human stem cell function. *J Clin Invest* **106**, 1331-1339 (2000).
237. Askari, A.T.*, et al.* Effect of stromal-cell-derived factor 1 on stem-cell homing and tissue regeneration in ischaemic cardiomyopathy. *Lancet* **362**, 697-703 (2003).
238. Wang, Y., Haider, H., Ahmad, N., Zhang, D. & Ashraf, M. Evidence for ischemia induced host-derived bone marrow cell mobilization into cardiac allografts. *J Mol Cell Cardiol* **41**, 478-487 (2006).
239. Pillarisetti, K. & Gupta, S.K. Cloning and relative expression analysis of rat stromal cell derived factor-1 (SDF-1)1: SDF-1 alpha mRNA is selectively induced in rat model of myocardial infarction. *Inflammation* **25**, 293-300 (2001).
240. Ma, J.*, et al.* Time course of myocardial stromal cell-derived factor 1 expression and beneficial effects of intravenously administered bone marrow stem cells in rats with experimental myocardial infarction. *Basic Res Cardiol* **100**, 217-223 (2005).
241. Lee, S.P.*, et al.* Integrin-linked kinase, a hypoxia-responsive molecule, controls postnatal vasculogenesis by recruitment of endothelial progenitor cells to ischemic tissue. *Circulation* **114**, 150-159 (2006).
242. De Falco, E.*, et al.* SDF-1 involvement in endothelial phenotype and ischemia-induced recruitment of bone marrow progenitor cells. *Blood* **104**, 3472-3482 (2004).
243. Yang, C.*, et al.* Enhancement of neovascularization with cord blood CD133+ cell-derived endothelial progenitor cell transplantation. *Thromb Haemost* **91**, 1202-1212 (2004).
244. Wang, J.*, et al.* Diverse signaling pathways through the SDF-1/CXCR4 chemokine axis in prostate cancer cell lines leads to altered patterns of cytokine secretion and angiogenesis. *Cell Signal* **17**, 1578-1592 (2005).
245. Petit, I.*, et al.* Atypical PKC-zeta regulates SDF-1-mediated migration and development of human CD34+ progenitor cells. *J Clin Invest* **115**, 168-176 (2005).

246. Zernecke, A.*, et al.* SDF-1alpha/CXCR4 axis is instrumental in neointimal hyperplasia and recruitment of smooth muscle progenitor cells. *Circ Res* **96**, 784-791 (2005).
247. Saxena, A.*, et al.* Stromal cell-derived factor-1alpha is cardioprotective after myocardial infarction. *Circulation* **117**, 2224-2231 (2008).
248. Hu, X.*, et al.* Stromal cell derived factor-1 alpha confers protection against myocardial ischemia/reperfusion injury: role of the cardiac stromal cell derived factor-1 alpha CXCR4 axis. *Circulation* **116**, 654-663 (2007).
249. Segers, V.F.*, et al.* Local delivery of protease-resistant stromal cell derived factor-1 for stem cell recruitment after myocardial infarction. *Circulation* **116**, 1683-1692 (2007).
250. Aoyama, H.*, et al.* Isolation and conformational analysis of fragment peptide corresponding to the heparin-binding site of hepatocyte growth factor. *Biochemistry* **36**, 10286-10291 (1997).
251. Jin, H., Wyss, J.M., Yang, R. & Schwall, R. The therapeutic potential of hepatocyte growth factor for myocardial infarction and heart failure. *Curr Pharm Des* **10**, 2525-2533 (2004).
252. Vale, P.R.*, et al.* Left ventricular electromechanical mapping to assess efficacy of phVEGF(165) gene transfer for therapeutic angiogenesis in chronic myocardial ischemia. *Circulation* **102**, 965-974 (2000).
253. Morishita, R.*, et al.* Therapeutic angiogenesis induced by human recombinant hepatocyte growth factor in rabbit hind limb ischemia model as cytokine supplement therapy. *Hypertension* **33**, 1379-1384 (1999).
254. Aoki, M.*, et al.* Angiogenesis induced by hepatocyte growth factor in non-infarcted myocardium and infarcted myocardium: up-regulation of essential transcription factor for angiogenesis, ets. *Gene Ther* **7**, 417-427 (2000).
255. Taniyama, Y.*, et al.* Therapeutic angiogenesis induced by human hepatocyte growth factor gene in rat and rabbit hindlimb ischemia models: preclinical study for treatment of peripheral arterial disease. *Gene Ther* **8**, 181-189 (2001).
256. Ueki, T.*, et al.* Hepatocyte growth factor gene therapy of liver cirrhosis in rats. *Nat Med* **5**, 226-230 (1999).
257. Mizuno, S., Matsumoto, K., Li, M.Y. & Nakamura, T. HGF reduces advancing lung fibrosis in mice: a potential role for MMP-dependent myofibroblast apoptosis. *FASEB J* **19**, 580-582 (2005).
258. Taniyama, Y.*, et al.* Potential contribution of a novel antifibrotic factor, hepatocyte growth factor, to prevention of myocardial fibrosis by angiotensin II blockade in cardiomyopathic hamsters. *Circulation* **102**, 246-252 (2000).
259. Soeki, T.*, et al.* Serum hepatocyte growth factor predicts ventricular remodeling following myocardial infarction. *Circ J* **66**, 1003-1007 (2002).
260. Yasuda, S.*, et al.* Enhanced secretion of cardiac hepatocyte growth factor from an infarct region is associated with less severe ventricular enlargement and improved cardiac function. *J Am Coll Cardiol* **36**, 115-121 (2000).
261. Miyagawa, S.*, et al.* Myocardial regeneration therapy for heart failure: hepatocyte growth factor enhances the effect of cellular cardiomyoplasty. *Circulation* **105**, 2556-2561 (2002).
262. Jayasankar, V.*, et al.* Gene transfer of hepatocyte growth factor attenuates postinfarction heart failure. *Circulation* **108 Suppl 1**, II230-236 (2003).
263. Azuma, J.*, et al.* Angiogenic and antifibrotic actions of hepatocyte growth factor improve cardiac dysfunction in porcine ischemic cardiomyopathy. *Gene Ther* **13**, 1206-1213 (2006).
264. Taniyama, Y.*, et al.* Therapeutic angiogenesis induced by human hepatocyte growth factor gene in rat diabetic hind limb ischemia model: molecular mechanisms of delayed angiogenesis in diabetes. *Circulation* **104**, 2344-2350 (2001).
265. Morishita, R.*, et al.* Safety evaluation of clinical gene therapy using hepatocyte growth factor to treat peripheral arterial disease. *Hypertension* **44**, 203-209 (2004).
266. Powell, R.J.*, et al.* Results of a double-blind, placebo-controlled study to assess the safety of intramuscular injection of hepatocyte growth factor plasmid to improve limb perfusion in patients with critical limb ischemia. *Circulation* **118**, 58-65 (2008).

267. Nachman, R.L. & Jaffe, E.A. Endothelial cell culture: beginnings of modern vascular biology. *J Clin Invest* **114**, 1037-1040 (2004).
268. Gimbrone, M.A., Jr., Cotran, R.S. & Folkman, J. Endothelial regeneration: studies with human endothelial cells in culture. *Ser Haematol* **6**, 453-455 (1973).
269. Jaffe, E.A., Nachman, R.L., Becker, C.G. & Minick, C.R. Culture of human endothelial cells derived from umbilical veins. Identification by morphologic and immunologic criteria. *J Clin Invest* **52**, 2745-2756 (1973).
270. Hamburger, V. A manual of experimental embryology. *Chicago: University of Chicago Press* **212**(1942).
271. Richardson, M. & Singh, G. Observations on the use of the avian chorioallantoic membrane (CAM) model in investigations into angiogenesis. *Curr Drug Targets Cardiovasc Haematol Disord* **3**, 155-185 (2003).
272. Fuchs, A. & Lindenbaum, E.S. The two- and three-dimensional structure of the microcirculation of the chick chorioallantoic membrane. *Acta Anat (Basel)* **131**, 271-275 (1988).
273. Taylor CM, W.J. The chick vitelline membrane as a test system for angiogenesis and antiangiogenesis. *Int. J. microsurc. clin. exp.* **3**, 337 (1984).
274. Norrby, K. In vivo models of angiogenesis. *J Cell Mol Med* **10**, 588-612 (2006).
275. Norrby, K., Jakobsson, A. & Sorbo, J. Quantitative angiogenesis in spreads of intact rat mesenteric windows. *Microvasc Res* **39**, 341-348 (1990).
276. Akhtar, N., Dickerson, E.B. & Auerbach, R. The sponge/Matrigel angiogenesis assay. *Angiogenesis* **5**, 75-80 (2002).
277. Auerbach, R. & Auerbach, W. Regional differences in the growth of normal and neoplastic cells. *Science* **215**, 127-134 (1982).
278. Auerbach, R., Morrissey, L.W., Kubai, L. & Sidky, Y.A. Regional differences in tumor growth: studies of the vascular system. *Int J Cancer* **22**, 40-46 (1978).
279. Kubai, L. & Auerbach, R. Regional differences in the growth of skin transplants. *Transplantation* **30**, 128-131 (1980).
280. Auerbach, R., Morrissey, L.W. & Sidky, Y.A. Regional differences in the incidence and growth of mouse tumors following intradermal or subcutaneous inoculation. *Cancer Res* **38**, 1739-1744 (1978).
281. Staton, C.A.*, et al.* Current methods for assaying angiogenesis in vitro and in vivo. *Int J Exp Pathol* **85**, 233-248 (2004).
282. Bezuidenhout, D. Porous polymeric superstructures as in-growth scaffolds for tissue-engineered vascular prostheses [PhD Thesis]. Cape Town:University of Stellenbosch. (2001).
283. Yancopoulos, G.D.*, et al.* Vascular-specific growth factors and blood vessel formation. *Nature* **407**, 242-248 (2000).
284. Lobov, I.B., Brooks, P.C. & Lang, R.A. Angiopoietin-2 displays VEGF-dependent modulation of capillary structure and endothelial cell survival in vivo. *Proc Natl Acad Sci U S A* **99**, 11205-11210 (2002).
285. Adams, R.H. & Alitalo, K. Molecular regulation of angiogenesis and lymphangiogenesis. *Nat Rev Mol Cell Biol* **8**, 464-478 (2007).
286. Elcin, A.E. & Elcin, Y.M. Localized angiogenesis induced by human vascular endothelial growth factor-activated PLGA sponge. *Tissue Eng* **12**, 959-968 (2006).
287. Smith, M.K., Peters, M.C., Richardson, T.P., Garbern, J.C. & Mooney, D.J. Locally enhanced angiogenesis promotes transplanted cell survival. *Tissue Eng* **10**, 63-71 (2004).
288. Richardson, T.P., Peters, M.C., Ennett, A.B. & Mooney, D.J. Polymeric system for dual growth factor delivery. *Nat Biotechnol* **19**, 1029-1034 (2001).
289. Zisch, A.H.*, et al.* Cell-demanded release of VEGF from synthetic, biointeractive cell ingrowth matrices for vascularized tissue growth. *FASEB J* **17**, 2260-2262 (2003).
290. Gosain, A.*, et al.* Exogenous pro-angiogenic stimuli cannot prevent physiologic vessel regression. *J Surg Res* **135**, 218-225 (2006).
291. Makanya, A.N.*, et al.* Microvascular endowment in the developing chicken embryo lung. *Am J Physiol Lung Cell Mol Physiol* **292**, L1136-1146 (2007).

292. Chan-Ling, T.*, et al.* Desmin ensheathment ratio as an indicator of vessel stability: evidence in normal development and in retinopathy of prematurity. *Am J Pathol* **165**, 1301-1313 (2004).
293. Benjamin, L.E., Hemo, I. & Keshet, E. A plasticity window for blood vessel remodelling is defined by pericyte coverage of the preformed endothelial network and is regulated by PDGF-B and VEGF. *Development* **125**, 1591-1598 (1998).
294. Baffert, F.*, et al.* Cellular changes in normal blood capillaries undergoing regression after inhibition of VEGF signaling. *Am J Physiol Heart Circ Physiol* **290**, H547-559 (2006).
295. Thurston, G., Baluk, P., Hirata, A. & McDonald, D.M. Permeability-related changes revealed at endothelial cell borders in inflamed venules by lectin binding. *Am J Physiol* **271**, H2547-2562 (1996).
296. Matsumoto, M.*, et al.* Hypoperfusion of peritubular capillaries induces chronic hypoxia before progression of tubulointerstitial injury in a progressive model of rat glomerulonephritis. *J Am Soc Nephrol* **15**, 1574-1581 (2004).
297. Murohara, T.*, et al.* Vascular endothelial growth factor/vascular permeability factor enhances vascular permeability via nitric oxide and prostacyclin. *Circulation* **97**, 99-107 (1998).
298. Schmetterer, L. & Polak, K. Role of nitric oxide in the control of ocular blood flow. *Prog Retin Eye Res* **20**, 823-847 (2001).
299. Peirce, S.M., Price, R.J. & Skalak, T.C. Spatial and temporal control of angiogenesis and arterialization using focal applications of VEGF164 and Ang-1. *Am J Physiol Heart Circ Physiol* **286**, H918-925 (2004).
300. Baffert, F.*, et al.* Age-related changes in vascular endothelial growth factor dependency and angiopoietin-1-induced plasticity of adult blood vessels. *Circ Res* **94**, 984-992 (2004).
301. Fischer, C.*, et al.* Anti-PlGF inhibits growth of VEGF(R)-inhibitor-resistant tumors without affecting healthy vessels. *Cell* **131**, 463-475 (2007).
302. Saunders, W.B.*, et al.* Coregulation of vascular tube stabilization by endothelial cell TIMP-2 and pericyte TIMP-3. *J Cell Biol* **175**, 179-191 (2006).
303. Spranger, J.*, et al.* Loss of the antiangiogenic pigment epithelium-derived factor in patients with angiogenic eye disease. *Diabetes* **50**, 2641-2645 (2001).
304. Duh, E.J.*, et al.* Pigment epithelium-derived factor suppresses ischemia-induced retinal neovascularization and VEGF-induced migration and growth. *Invest Ophthalmol Vis Sci* **43**, 821-829 (2002).
305. Doll, J.A.*, et al.* Pigment epithelium-derived factor regulates the vasculature and mass of the prostate and pancreas. *Nat Med* **9**, 774-780 (2003).
306. Chung, C.*, et al.* Pigment epithelium-derived factor is an angiogenesis and lipid regulator that activates peroxisome proliferator-activated receptor alpha. *Adv Exp Med Biol* **617**, 591-597 (2008).
307. Mori, K.*, et al.* Regression of ocular neovascularization in response to increased expression of pigment epithelium-derived factor. *Invest Ophthalmol Vis Sci* **43**, 2428-2434 (2002).
308. Wolpe, S.D.*, et al.* Identification and characterization of macrophage inflammatory protein 2. *Proc Natl Acad Sci U S A* **86**, 612-616 (1989).
309. Cao, Y., Chen, C., Weatherbee, J.A., Tsang, M. & Folkman, J. gro-beta, a -C-X-C- chemokine, is an angiogenesis inhibitor that suppresses the growth of Lewis lung carcinoma in mice. *J Exp Med* **182**, 2069-2077 (1995).
310. Lee, S., Jilani, S.M., Nikolova, G.V., Carpizo, D. & Iruela-Arispe, M.L. Processing of VEGF-A by matrix metalloproteinases regulates bioavailability and vascular patterning in tumors. *J Cell Biol* **169**, 681-691 (2005).
311. de Candia, P., Benera, R. & Solit, D.B. A role for Id proteins in mammary gland physiology and tumorigenesis. *Adv Cancer Res* **92**, 81-94 (2004).
312. Lyden, D.*, et al.* Id1 and Id3 are required for neurogenesis, angiogenesis and vascularization of tumour xenografts. *Nature* **401**, 670-677 (1999).
313. Mellick, A.S.*, et al.* Using the transcription factor inhibitor of DNA binding 1 to selectively target endothelial progenitor cells offers novel strategies to inhibit tumor angiogenesis and growth. *Cancer Res* **70**, 7273-7282 (2010).

314. Jessup, M. & Brozena, S. Heart failure. *N Engl J Med* **348**, 2007-2018 (2003).
315. McMurray, J.J. Clinical practice. Systolic heart failure. *N Engl J Med* **362**, 228-238.
316. Thygesen, K., Alpert, J.S. & White, H.D. Universal definition of myocardial infarction. *Eur Heart J* **28**, 2525-2538 (2007).
317. Grech, E.D. & Ramsdale, D.R. Acute coronary syndrome: unstable angina and non-ST segment elevation myocardial infarction. *BMJ* **326**, 1259-1261 (2003).
318. Thygesen, K.*, et al.* Universal definition of myocardial infarction. *Circulation* **116**, 2634-2653 (2007).
319. Libby, P. Inflammation in atherosclerosis. *Nature* **420**, 868-874 (2002).
320. Vayssier-Taussat, M.*, et al.* Effects of tobacco smoke and benzo[a]pyrene on human endothelial cell and monocyte stress responses. *Am J Physiol Heart Circ Physiol* **280**, H1293-1300 (2001).
321. Dimmeler, S., Haendeler, J., Galle, J. & Zeiher, A.M. Oxidized low-density lipoprotein induces apoptosis of human endothelial cells by activation of CPP32-like proteases. A mechanistic clue to the 'response to injury' hypothesis. *Circulation* **95**, 1760-1763 (1997).
322. Irani, K. Oxidant signaling in vascular cell growth, death, and survival : a review of the roles of reactive oxygen species in smooth muscle and endothelial cell mitogenic and apoptotic signaling. *Circ Res* **87**, 179-183 (2000).
323. Hsueh, W.A. & Anderson, P.W. Hypertension, the endothelial cell, and the vascular complications of diabetes mellitus. *Hypertension* **20**, 253-263 (1992).
324. Perez-Castellano, N.*, et al.* Influence of collateral circulation on in-hospital death from anterior acute myocardial infarction. *J Am Coll Cardiol* **31**, 512-518 (1998).
325. Koerselman, J., van der Graaf, Y., de Jaegere, P.P. & Grobbee, D.E. Coronary collaterals: an important and underexposed aspect of coronary artery disease. *Circulation* **107**, 2507-2511 (2003).
326. Libby, P., Ridker, P.M. & Maseri, A. Inflammation and atherosclerosis. *Circulation* **105**, 1135-1143 (2002).
327. Braunwald, E. & Kloner, R.A. The stunned myocardium: prolonged, postischemic ventricular dysfunction. *Circulation* **66**, 1146-1149 (1982).
328. Tennant T, W.C. Effect of coronary occlusion on myocardial contraction. *Am J Physiol 112: 351, 1935* **112**, 351 (1935).
329. Katz, A.M. Heart Failure: pathopysiology, molecular biology, and clinical management. (2009).
330. Opie, L. *Heart Physiology: from cell to circulation*, (2004).
331. Opie, L.H., Commerford, P.J., Gersh, B.J. & Pfeffer, M.A. Controversies in ventricular remodelling. *Lancet* **367**, 356-367 (2006).
332. Konstam, M.A. Reliability of ventricular remodeling as a surrogate for use in conjunction with clinical outcomes in heart failure. *Am J Cardiol* **96**, 867-871 (2005).
333. Cohn, J.N., Ferrari, R. & Sharpe, N. Cardiac remodeling--concepts and clinical implications: a consensus paper from an international forum on cardiac remodeling. Behalf of an International Forum on Cardiac Remodeling. *J Am Coll Cardiol* **35**, 569-582 (2000).
334. Hunter, J.J. & Chien, K.R. Signaling pathways for cardiac hypertrophy and failure. *N Engl J Med* **341**, 1276-1283 (1999).
335. Wang, N., Butler, J.P. & Ingber, D.E. Mechanotransduction across the cell surface and through the cytoskeleton. *Science* **260**, 1124-1127 (1993).
336. Heling, A.*, et al.* Increased expression of cytoskeletal, linkage, and extracellular proteins in failing human myocardium. *Circ Res* **86**, 846-853 (2000).
337. Shiojima, I.*, et al.* Disruption of coordinated cardiac hypertrophy and angiogenesis contributes to the transition to heart failure. *J Clin Invest* **115**, 2108-2118 (2005).
338. Braunwald, E. 50th anniversary historical article. Myocardial oxygen consumption: the quest for its determinants and some clinical fallout. *J Am Coll Cardiol* **34**, 1365-1368 (1999).
339. Lorell, B.H. & Carabello, B.A. Left ventricular hypertrophy: pathogenesis, detection, and prognosis. *Circulation* **102**, 470-479 (2000).

340. Creemers, E.E., Cleutjens, J.P., Smits, J.F. & Daemen, M.J. Matrix metalloproteinase inhibition after myocardial infarction: a new approach to prevent heart failure? *Circ Res* **89**, 201-210 (2001).
341. Spinale, F.G. Myocardial matrix remodeling and the matrix metalloproteinases: influence on cardiac form and function. *Physiol Rev* **87**, 1285-1342 (2007).
342. Jugdutt, B.I. Ventricular remodeling after infarction and the extracellular collagen matrix: when is enough enough? *Circulation* **108**, 1395-1403 (2003).
343. Holmes, J.W., Borg, T.K. & Covell, J.W. Structure and mechanics of healing myocardial infarcts. *Annu Rev Biomed Eng* **7**, 223-253 (2005).
344. Tyberg, J.V.*, et al.* An analysis of segmental ischemic dysfunction utilizing the pressure-length loop. *Circulation* **49**, 748-754 (1974).
345. Villarreal, F.J., Lew, W.Y., Waldman, L.K. & Covell, J.W. Transmural myocardial deformation in the ischemic canine left ventricle. *Circ Res* **68**, 368-381 (1991).
346. Diamond, G. & Forrester, J.S. Effect of coronary artery disease and acute myocardial infarction on left ventricular compliance in man. *Circulation* **45**, 11-19 (1972).
347. Bleifeld W, M.D., Hanrath P. Acute myocardial infarction. VI. Left ventricular wall stiffness in the acute phase and in the convalescent phase. . *Eur. J. Cardiol.* **2**, 191–198 (1974).
348. Fishbein, M.C., Maclean, D. & Maroko, P.R. The histopathologic evolution of myocardial infarction. *Chest* **73**, 843-849 (1978).
349. Hammerman, H., Kloner, R.A., Hale, S., Schoen, F.J. & Braunwald, E. Dose-dependent effects of short-term methylprednisolone on myocardial infarct extent, scar formation, and ventricular function. *Circulation* **68**, 446-452 (1983).
350. Mannisi, J.A., Weisman, H.F., Bush, D.E., Dudeck, P. & Healy, B. Steroid administration after myocardial infarction promotes early infarct expansion. A study in the rat. *J Clin Invest* **79**, 1431-1439 (1987).
351. Hammerman, H.*, et al.* Indomethacin-induced scar thinning after experimental myocardial infarction. *Circulation* **67**, 1290-1295 (1983).
352. Hammerman, H., Schoen, F.J., Braunwald, E. & Kloner, R.A. Drug-induced expansion of infarct: morphologic and functional correlations. *Circulation* **69**, 611-617 (1984).
353. Brown, E.J., Jr.*, et al.* Scar thinning due to ibuprofen administration after experimental myocardial infarction. *Am J Cardiol* **51**, 877-883 (1983).
354. Gupta, K.B., Ratcliffe, M.B., Fallert, M.A., Edmunds, L.H., Jr. & Bogen, D.K. Changes in passive mechanical stiffness of myocardial tissue with aneurysm formation. *Circulation* **89**, 2315-2326 (1994).
355. Lerman, R.H.*, et al.* Myocardial healing and repair after experimental infarction in the rabbit. *Circ Res* **53**, 378-388 (1983).
356. Jugdutt, B.I. & Amy, R.W. Healing after myocardial infarction in the dog: changes in infarct hydroxyproline and topography. *J Am Coll Cardiol* **7**, 91-102 (1986).
357. Connelly, C.M.*, et al.* Effects of reperfusion after coronary artery occlusion on post-infarction scar tissue. *Circ Res* **57**, 562-577 (1985).
358. Birnbaum, Y.*, et al.* Ventricular free wall rupture following acute myocardial infarction. *Coron Artery Dis* **14**, 463-470 (2003).
359. Wehrens, X.H. & Doevendans, P.A. Cardiac rupture complicating myocardial infarction. *Int J Cardiol* **95**, 285-292 (2004).
360. Bogen, D.K., Rabinowitz, S.A., Needleman, A., McMahon, T.A. & Abelmann, W.H. An analysis of the mechanical disadvantage of myocardial infarction in the canine left ventricle. *Circ Res* **47**, 728-741 (1980).
361. Swan, H.J., Forrester, J.S., Diamond, G., Chatterjee, K. & Parmley, W.W. Hemodynamic spectrum of myocardial infarction and cardiogenic shock. A conceptual model. *Circulation* **45**, 1097-1110 (1972).
362. Parmley, W.W., Chuck, L., Kivowitz, C., Matloff, J.M. & Swan, H.J. In vitro length-tension relations of human ventricular aneurysms. Relation of stiffness to mechanical disadvantage. *Am J Cardiol* **32**, 889-894 (1973).
363. Laird, J.D. & Vellekoop, H.P. The course of passive elasticity of myocardial tissue following experimental infarction in rabbits and its relation to mechanical dysfunction. *Circ Res* **41**, 715-721 (1977).

364. Janz, R.F. & Waldron, R.J. Predicted effect of chronic apical aneurysms on the passive stiffness of the human left ventricle. *Circ Res* **42**, 255-263 (1978).
365. Weisman, H.F. & Healy, B. Myocardial infarct expansion, infarct extension, and reinfarction: pathophysiologic concepts. *Prog Cardiovasc Dis* **30**, 73-110 (1987).
366. Olivetti, G., Capasso, J.M., Sonnenblick, E.H. & Anversa, P. Side-to-side slippage of myocytes participates in ventricular wall remodeling acutely after myocardial infarction in rats. *Circ Res* **67**, 23-34 (1990).
367. Gallagher, K.P.*, et al.* The distribution of functional impairment across the lateral border of acutely ischemic myocardium. *Circ Res* **58**, 570-583 (1986).
368. Feygin, J., Hu, Q., Swingen, C. & Zhang, J. Relationships between regional myocardial wall stress and bioenergetics in hearts with left ventricular hypertrophy. *Am J Physiol Heart Circ Physiol* **294**, H2313-2321 (2008).
369. Holmes, J.W. Candidate mechanical stimuli for hypertrophy during volume overload. *J Appl Physiol* **97**, 1453-1460 (2004).
370. Pfeffer, M.A.*, et al.* Effect of captopril on mortality and morbidity in patients with left ventricular dysfunction after myocardial infarction. Results of the survival and ventricular enlargement trial. The SAVE Investigators. *N Engl J Med* **327**, 669-677 (1992).
371. Effect of ramipril on mortality and morbidity of survivors of acute myocardial infarction with clinical evidence of heart failure. The Acute Infarction Ramipril Efficacy (AIRE) Study Investigators. *Lancet* **342**, 821-828 (1993).
372. Kober, L.*, et al.* A clinical trial of the angiotensin-converting-enzyme inhibitor trandolapril in patients with left ventricular dysfunction after myocardial infarction. Trandolapril Cardiac Evaluation (TRACE) Study Group. *N Engl J Med* **333**, 1670-1676 (1995).
373. Konstam, M.A.*, et al.* Effects of the angiotensin converting enzyme inhibitor enalapril on the long-term progression of left ventricular dilatation in patients with asymptomatic systolic dysfunction. SOLVD (Studies of Left Ventricular Dysfunction) Investigators. *Circulation* **88**, 2277-2283 (1993).
374. Greenberg, B.*, et al.* Effects of long-term enalapril therapy on cardiac structure and function in patients with left ventricular dysfunction. Results of the SOLVD echocardiography substudy. *Circulation* **91**, 2573-2581 (1995).
375. Randomised, placebo-controlled trial of carvedilol in patients with congestive heart failure due to ischaemic heart disease. Australia/New Zealand Heart Failure Research Collaborative Group. *Lancet* **349**, 375-380 (1997).
376. Hall, S.A.*, et al.* Time course of improvement in left ventricular function, mass and geometry in patients with congestive heart failure treated with beta-adrenergic blockade. *J Am Coll Cardiol* **25**, 1154-1161 (1995).
377. Cohn, J.N. & Tognoni, G. A randomized trial of the angiotensin-receptor blocker valsartan in chronic heart failure. *N Engl J Med* **345**, 1667-1675 (2001).
378. McMurray, J.J.*, et al.* Effects of candesartan in patients with chronic heart failure and reduced left-ventricular systolic function taking angiotensin-converting-enzyme inhibitors: the CHARM-Added trial. *Lancet* **362**, 767-771 (2003).
379. Jessup, M.*, et al.* 2009 focused update: ACCF/AHA Guidelines for the Diagnosis and Management of Heart Failure in Adults: a report of the American College of Cardiology Foundation/American Heart Association Task Force on Practice Guidelines: developed in collaboration with the International Society for Heart and Lung Transplantation. *Circulation* **119**, 1977-2016 (2009).
380. Packer, M. The neurohormonal hypothesis: a theory to explain the mechanism of disease progression in heart failure. *J Am Coll Cardiol* **20**, 248-254 (1992).
381. *Braunwald's Heart Disease: A Textbook of Cardiovascular Medicine*, (Saunders, 2007).
382. Mann, D.L. & Bristow, M.R. Mechanisms and models in heart failure: the biomechanical model and beyond. *Circulation* **111**, 2837-2849 (2005).
383. Fuchs, S.*, et al.* Transendocardial delivery of autologous bone marrow enhances collateral perfusion and regional function in pigs with chronic experimental myocardial ischemia. *J Am Coll Cardiol* **37**, 1726-1732 (2001).
384. Mangi, A.A.*, et al.* Mesenchymal stem cells modified with Akt prevent remodeling and restore performance of infarcted hearts. *Nat Med* **9**, 1195-1201 (2003).

385. Grossman, W., Jones, D. & McLaurin, L.P. Wall stress and patterns of hypertrophy in the human left ventricle. *J Clin Invest* **56**, 56-64 (1975).
386. Wall, S.T., Walker, J.C., Healy, K.E., Ratcliffe, M.B. & Guccione, J.M. Theoretical impact of the injection of material into the myocardium: a finite element model simulation. *Circulation* **114**, 2627-2635 (2006).
387. Segers, V.F. & Lee, R.T. Local delivery of proteins and the use of self-assembling peptides. *Drug Discov Today* **12**, 561-568 (2007).
388. Kofidis, T.*, et al.* Novel injectable bioartificial tissue facilitates targeted, less invasive, large-scale tissue restoration on the beating heart after myocardial injury. *Circulation* **112**, I173-177 (2005).
389. Dai, W., Wold, L.E., Dow, J.S. & Kloner, R.A. Thickening of the infarcted wall by collagen injection improves left ventricular function in rats: a novel approach to preserve cardiac function after myocardial infarction. *J Am Coll Cardiol* **46**, 714-719 (2005).
390. Christman, K.L.*, et al.* Injectable fibrin scaffold improves cell transplant survival, reduces infarct expansion, and induces neovasculature formation in ischemic myocardium. *J Am Coll Cardiol* **44**, 654-660 (2004).
391. Landa, N.*, et al.* Effect of injectable alginate implant on cardiac remodeling and function after recent and old infarcts in rat. *Circulation* **117**, 1388-1396 (2008).
392. Tsur-Gang, O.*, et al.* The effects of peptide-based modification of alginate on left ventricular remodeling and function after myocardial infarction. *Biomaterials* **30**, 189-195 (2009).
393. Yu, J.*, et al.* Restoration of left ventricular geometry and improvement of left ventricular function in a rodent model of chronic ischemic cardiomyopathy. *J Thorac Cardiovasc Surg* **137**, 180-187 (2009).
394. Jiang, X.J.*, et al.* Injection of a novel synthetic hydrogel preserves left ventricle function after myocardial infarction. *J Biomed Mater Res A* **90**, 472-477 (2009).
395. Wang, T.*, et al.* The inhibition of postinfarct ventricle remodeling without polycythaemia following local sustained intramyocardial delivery of erythropoietin within a supramolecular hydrogel. *Biomaterials* **30**, 4161-4167 (2009).
396. Fujimoto, K.L.*, et al.* Synthesis, characterization and therapeutic efficacy of a biodegradable, thermoresponsive hydrogel designed for application in chronic infarcted myocardium. *Biomaterials* **30**, 4357-4368 (2009).
397. Hubbell, J.A. Biomaterials in tissue engineering. *Biotechnology (N Y)* **13**, 565-576 (1995).
398. Park, Y. Bovine Primary Chondrocyte Culture in Synthetic Matrix Metalloproteinase-Sensitive Poly(ethylene glycol)-Based Hydrogels as a Scaffold for Cartilage Repair. *Tissue Engineering* **10**, 515-522 (2004).
399. Lin, C.C. & Anseth, K.S. PEG hydrogels for the controlled release of biomolecules in regenerative medicine. *Pharm Res* **26**, 631-643 (2009).
400. Lutolf, M.P., Raeber, G.P., Zisch, A.H., Tirelli, N. & Hubbell, J.A. Cell-Responsive Synthetic Hydrogels. *Advanced Materials* **15**, 888-892 (2003).
401. Lutolf, M.P. & Hubbell, J.A. Synthesis and Physicochemical Characterization of End-Linked Poly(ethylene glycol)-co-peptide Hydrogels Formed by Michael-Type Addition. *Biomacromolecules* **4**, 713-722 (2003).
402. van de Wetering, P., Metters, A.T., Schoenmakers, R.G. & Hubbell, J.A. Poly(ethylene glycol) hydrogels formed by conjugate addition with controllable swelling, degradation, and release of pharmaceutically active proteins. *J Control Release* **102**, 619-627 (2005).
403. Hennink, W.E. & van Nostrum, C.F. Novel crosslinking methods to design hydrogels. *Adv Drug Deliv Rev* **54**, 13-36 (2002).
404. Mather, B.D., Viswanathan, K., Miller, K.M. & Long, T.E. Michael addition reactions in macromolecular design for emerging technologies. *Progress in Polymer Science* **31**, 487-531 (2006).
405. Elbert, D.L., Pratt, A.B., Lutolf, M.P., Halstenberg, S. & Hubbell, J.A. Protein delivery from materials formed by self-selective conjugate addition reactions. *J Control Release* **76**, 11-25 (2001).

406. Friedman, M., Cavins, J.F. & Wall, J.S. Relative Nucleophilic Reactivities of Amino Groups and Mercaptide Ions in Addition Reactions with Œ±,Œ≤-Unsaturated Compounds1,2. *Journal of the American Chemical Society* **87**, 3672-3682 (1965).
407. Dobner, S., Bezuidenhout, D., Govender, P., Zilla, P. & Davies, N. A synthetic non-degradable polyethylene glycol hydrogel retards adverse post-infarct left ventricular remodeling. *J Card Fail* **15**, 629-636 (2009).
408. Lutolf, M.P.*, et al.* Synthetic matrix metalloproteinase-sensitive hydrogels for the conduction of tissue regeneration: engineering cell-invasion characteristics. *Proc Natl Acad Sci U S A* **100**, 5413-5418 (2003).
409. Lutolf, M.P. & Hubbell, J.A. Synthetic biomaterials as instructive extracellular microenvironments for morphogenesis in tissue engineering. *Nat Biotechnol* **23**, 47-55 (2005).
410. Lin, C.C. & Metters, A.T. Hydrogels in controlled release formulations: network design and mathematical modeling. *Adv Drug Deliv Rev* **58**, 1379-1408 (2006).
411. Peppas, N.A., Bures, P., Leobandung, W. & Ichikawa, H. Hydrogels in pharmaceutical formulations. *Eur J Pharm Biopharm* **50**, 27-46 (2000).
412. Weber, L.M. & Anseth, K.S. Hydrogel encapsulation environments functionalized with extracellular matrix interactions increase islet insulin secretion. *Matrix Biol* **27**, 667-673 (2008).
413. Mahoney, M.J. & Anseth, K.S. Three-dimensional growth and function of neural tissue in degradable polyethylene glycol hydrogels. *Biomaterials* **27**, 2265-2274 (2006).
414. Raeber, G.P., Lutolf, M.P. & Hubbell, J.A. Molecularly engineered PEG hydrogels: a novel model system for proteolytically mediated cell migration. *Biophys J* **89**, 1374-1388 (2005).
415. Fittkau, M.H.*, et al.* The selective modulation of endothelial cell mobility on RGD peptide containing surfaces by YIGSR peptides. *Biomaterials* **26**, 167-174 (2005).
416. Fairbanks, B.D.*, et al.* A Versatile Synthetic Extracellular Matrix Mimic via Thiol-Norbornene Photopolymerization. *Advanced Materials* **21**, 5005-5010 (2009).
417. Drury, J.L. & Mooney, D.J. Hydrogels for tissue engineering: scaffold design variables and applications. *Biomaterials* **24**, 4337-4351 (2003).
418. Mellott, M.B., Searcy, K. & Pishko, M.V. Release of protein from highly cross-linked hydrogels of poly(ethylene glycol) diacrylate fabricated by UV polymerization. *Biomaterials* **22**, 929-941 (2001).
419. Peppas, N.A., Keys, K.B., Torres-Lugo, M. & Lowman, A.M. Poly(ethylene glycol)-containing hydrogels in drug delivery. *J Control Release* **62**, 81-87 (1999).
420. Dinbergs, I.D., Brown, L. & Edelman, E.R. Cellular response to transforming growth factor-beta1 and basic fibroblast growth factor depends on release kinetics and extracellular matrix interactions. *J Biol Chem* **271**, 29822-29829 (1996).
421. Mann, B.K., Schmedlen, R.H. & West, J.L. Tethered-TGF-beta increases extracellular matrix production of vascular smooth muscle cells. *Biomaterials* **22**, 439-444 (2001).
422. Sakiyama-Elbert, S.E. & Hubbell, J.A. Controlled release of nerve growth factor from a heparin-containing fibrin-based cell ingrowth matrix. *J Control Release* **69**, 149-158 (2000).
423. Sakiyama-Elbert, S.E. & Hubbell, J.A. Development of fibrin derivatives for controlled release of heparin-binding growth factors. *J Control Release* **65**, 389-402 (2000).
424. Sakiyama-Elbert, S.E., Panitch, A. & Hubbell, J.A. Development of growth factor fusion proteins for cell-triggered drug delivery. *FASEB J* **15**, 1300-1302 (2001).
425. Zisch, A.H., Schenk, U., Schense, J.C., Sakiyama-Elbert, S.E. & Hubbell, J.A. Covalently conjugated VEGF--fibrin matrices for endothelialization. *J Control Release* **72**, 101-113 (2001).
426. Pike, D.B.*, et al.* Heparin-regulated release of growth factors in vitro and angiogenic response in vivo to implanted hyaluronan hydrogels containing VEGF and bFGF. *Biomaterials* **27**, 5242-5251 (2006).
427. DuBose, J.W., Cutshall, C. & Metters, A.T. Controlled release of tethered molecules via engineered hydrogel degradation: model development and validation. *J Biomed Mater Res A* **74**, 104-116 (2005).

428. Benoit, D.S.W., Collins, S.D. & Anseth, K.S. Multifunctional Hydrogels that Promote Osteogenic Human Mesenchymal Stem Cell Differentiation Through Stimulation and Sequestering of Bone Morphogenic Protein 2. *Advanced Functional Materials* **17**, 2085-2093 (2007).
429. Ehrbar, M.*, et al.* Cell-demanded liberation of VEGF121 from fibrin implants induces local and controlled blood vessel growth. *Circ Res* **94**, 1124-1132 (2004).
430. Schoenmakers, R.G., van de Wetering, P., Elbert, D.L. & Hubbell, J.A. The effect of the linker on the hydrolysis rate of drug-linked ester bonds. *J Control Release* **95**, 291-300 (2004).
431. Ferrara, N. & Kerbel, R.S. Angiogenesis as a therapeutic target. *Nature* **438**, 967-974 (2005).
432. Eichhorn, E.J. & Bristow, M.R. Medical therapy can improve the biological properties of the chronically failing heart. A new era in the treatment of heart failure. *Circulation* **94**, 2285-2296 (1996).
433. Greenhalgh, D.G., Sprugel, K.H., Murray, M.J. & Ross, R. PDGF and FGF stimulate wound healing in the genetically diabetic mouse. *Am J Pathol* **136**, 1235-1246 (1990).
434. Banai, S.*, et al.* Angiogenic-induced enhancement of collateral blood flow to ischemic myocardium by vascular endothelial growth factor in dogs. *Circulation* **89**, 2183-2189 (1994).
435. Tsurumi, Y.*, et al.* Direct intramuscular gene transfer of naked DNA encoding vascular endothelial growth factor augments collateral development and tissue perfusion. *Circulation* **94**, 3281-3290 (1996).
436. Giordano, F.J.*, et al.* Intracoronary gene transfer of fibroblast growth factor-5 increases blood flow and contractile function in an ischemic region of the heart. *Nat Med* **2**, 534-539 (1996).
437. Isner, J.M.*, et al.* Clinical evidence of angiogenesis after arterial gene transfer of phVEGF165 in patient with ischaemic limb. *Lancet* **348**, 370-374 (1996).
438. Schumacher, B., Pecher, P., von Specht, B.U. & Stegmann, T. Induction of neoangiogenesis in ischemic myocardium by human growth factors: first clinical results of a new treatment of coronary heart disease. *Circulation* **97**, 645-650 (1998).
439. Sellke, F.W., Laham, R.J., Edelman, E.R., Pearlman, J.D. & Simons, M. Therapeutic angiogenesis with basic fibroblast growth factor: technique and early results. *Ann Thorac Surg* **65**, 1540-1544 (1998).
440. Udelson, J.E.*, et al.* Therapeutic angiogenesis with recombinant fibroblast growth factor-2 improves stress and rest myocardial perfusion abnormalities in patients with severe symptomatic chronic coronary artery disease. *Circulation* **102**, 1605-1610 (2000).
441. Henry, T.D.*, et al.* Intracoronary administration of recombinant human vascular endothelial growth factor to patients with coronary artery disease. *Am Heart J* **142**, 872-880 (2001).
442. Hendel, R.C.*, et al.* Effect of intracoronary recombinant human vascular endothelial growth factor on myocardial perfusion: evidence for a dose-dependent effect. *Circulation* **101**, 118-121 (2000).
443. Vale, P.R.*, et al.* Randomized, single-blind, placebo-controlled pilot study of catheter-based myocardial gene transfer for therapeutic angiogenesis using left ventricular electromechanical mapping in patients with chronic myocardial ischemia. *Circulation* **103**, 2138-2143 (2001).
444. Rosengart, T.K.*, et al.* Angiogenesis gene therapy: phase I assessment of direct intramyocardial administration of an adenovirus vector expressing VEGF121 cDNA to individuals with clinically significant severe coronary artery disease. *Circulation* **100**, 468-474 (1999).
445. Grines, C.L.*, et al.* Angiogenic Gene Therapy (AGENT) trial in patients with stable angina pectoris. *Circulation* **105**, 1291-1297 (2002).
446. Henry, T.D.*, et al.* The VIVA trial: Vascular endothelial growth factor in Ischemia for Vascular Angiogenesis. *Circulation* **107**, 1359-1365 (2003).
447. Henry, T.D.*, et al.* Effects of Ad5FGF-4 in patients with angina: an analysis of pooled data from the AGENT-3 and AGENT-4 trials. *J Am Coll Cardiol* **50**, 1038-1046 (2007).

448. Marelli, D., Desrosiers, C., el-Alfy, M., Kao, R.L. & Chiu, R.C. Cell transplantation for myocardial repair: an experimental approach. *Cell Transplant* **1**, 383-390 (1992).
449. Chiu, R.C., Zibaitis, A. & Kao, R.L. Cellular cardiomyoplasty: myocardial regeneration with satellite cell implantation. *Ann Thorac Surg* **60**, 12-18 (1995).
450. Koh, G.Y., Klug, M.G., Soonpaa, M.H. & Field, L.J. Differentiation and long-term survival of C2C12 myoblast grafts in heart. *J Clin Invest* **92**, 1548-1554 (1993).
451. Taylor, D.A.*, et al.* Regenerating functional myocardium: improved performance after skeletal myoblast transplantation. *Nat Med* **4**, 929-933 (1998).
452. Tambara, K.*, et al.* Transplanted skeletal myoblasts can fully replace the infarcted myocardium when they survive in the host in large numbers. *Circulation* **108 Suppl 1**, II259-263 (2003).
453. Jain, M.*, et al.* Cell therapy attenuates deleterious ventricular remodeling and improves cardiac performance after myocardial infarction. *Circulation* **103**, 1920-1927 (2001).
454. Menasche, P.*, et al.* Myoblast transplantation for heart failure. *Lancet* **357**, 279-280 (2001).
455. Pagani, F.D.*, et al.* Autologous skeletal myoblasts transplanted to ischemia-damaged myocardium in humans. Histological analysis of cell survival and differentiation. *J Am Coll Cardiol* **41**, 879-888 (2003).
456. Hagege, A.A.*, et al.* Viability and differentiation of autologous skeletal myoblast grafts in ischaemic cardiomyopathy. *Lancet* **361**, 491-492 (2003).
457. Herreros, J.*, et al.* Autologous intramyocardial injection of cultured skeletal muscle-derived stem cells in patients with non-acute myocardial infarction. *Eur Heart J* **24**, 2012-2020 (2003).
458. Siminiak, T.*, et al.* Autologous skeletal myoblast transplantation for the treatment of postinfarction myocardial injury: phase I clinical study with 12 months of follow-up. *Am Heart J* **148**, 531-537 (2004).
459. Strauer, B.E.*, et al.* Repair of infarcted myocardium by autologous intracoronary mononuclear bone marrow cell transplantation in humans. *Circulation* **106**, 1913-1918 (2002).
460. Assmus, B.*, et al.* Transplantation of Progenitor Cells and Regeneration Enhancement in Acute Myocardial Infarction (TOPCARE-AMI). *Circulation* **106**, 3009-3017 (2002).
461. Perin, E.C.*, et al.* Transendocardial, autologous bone marrow cell transplantation for severe, chronic ischemic heart failure. *Circulation* **107**, 2294-2302 (2003).
462. Wollert, K.C.*, et al.* Intracoronary autologous bone-marrow cell transfer after myocardial infarction: the BOOST randomised controlled clinical trial. *Lancet* **364**, 141-148 (2004).
463. Asahara, T.*, et al.* Bone marrow origin of endothelial progenitor cells responsible for postnatal vasculogenesis in physiological and pathological neovascularization. *Circ Res* **85**, 221-228 (1999).
464. Goodell, M.A., Brose, K., Paradis, G., Conner, A.S. & Mulligan, R.C. Isolation and functional properties of murine hematopoietic stem cells that are replicating in vivo. *J Exp Med* **183**, 1797-1806 (1996).
465. Goodell, M.A.*, et al.* Dye efflux studies suggest that hematopoietic stem cells expressing low or undetectable levels of CD34 antigen exist in multiple species. *Nat Med* **3**, 1337-1345 (1997).
466. Pittenger, M.F. & Martin, B.J. Mesenchymal stem cells and their potential as cardiac therapeutics. *Circ Res* **95**, 9-20 (2004).
467. Jiang, Y.*, et al.* Pluripotency of mesenchymal stem cells derived from adult marrow. *Nature* **418**, 41-49 (2002).
468. Dimmeler, S., Zeiher, A.M. & Schneider, M.D. Unchain my heart: the scientific foundations of cardiac repair. *J Clin Invest* **115**, 572-583 (2005).
469. Murry, C.E., Field, L.J. & Menasche, P. Cell-based cardiac repair: reflections at the 10-year point. *Circulation* **112**, 3174-3183 (2005).
470. Murry, C.E.*, et al.* Haematopoietic stem cells do not transdifferentiate into cardiac myocytes in myocardial infarcts. *Nature* **428**, 664-668 (2004).
471. Alvarez-Dolado, M.*, et al.* Fusion of bone-marrow-derived cells with Purkinje neurons, cardiomyocytes and hepatocytes. *Nature* **425**, 968-973 (2003).

472. Balsam, L.B.*, et al.* Haematopoietic stem cells adopt mature haematopoietic fates in ischaemic myocardium. *Nature* **428**, 668-673 (2004).
473. Nygren, J.M.*, et al.* Bone marrow-derived hematopoietic cells generate cardiomyocytes at a low frequency through cell fusion, but not transdifferentiation. *Nat Med* **10**, 494-501 (2004).
474. Fernandez-Aviles, F.*, et al.* Experimental and clinical regenerative capability of human bone marrow cells after myocardial infarction. *Circ Res* **95**, 742-748 (2004).
475. Schachinger, V.*, et al.* Transplantation of progenitor cells and regeneration enhancement in acute myocardial infarction: final one-year results of the TOPCARE-AMI Trial. *J Am Coll Cardiol* **44**, 1690-1699 (2004).
476. Schachinger, V.*, et al.* Intracoronary bone marrow-derived progenitor cells in acute myocardial infarction. *N Engl J Med* **355**, 1210-1221 (2006).
477. Lunde, K.*, et al.* Intracoronary injection of mononuclear bone marrow cells in acute myocardial infarction. *N Engl J Med* **355**, 1199-1209 (2006).
478. Assmus, B.*, et al.* Transcoronary transplantation of progenitor cells after myocardial infarction. *N Engl J Med* **355**, 1222-1232 (2006).
479. Lazarous, D.F.*, et al.* Pharmacodynamics of basic fibroblast growth factor: route of administration determines myocardial and systemic distribution. *Cardiovasc Res* **36**, 78-85 (1997).
480. Kim, T.K. & Burgess, D.J. Pharmacokinetic characterization of 14C-vascular endothelial growth factor controlled release microspheres using a rat model. *J Pharm Pharmacol* **54**, 897-905 (2002).
481. Hariawala, M.D.*, et al.* VEGF improves myocardial blood flow but produces EDRF-mediated hypotension in porcine hearts. *J Surg Res* **63**, 77-82 (1996).
482. Lee, R.J.*, et al.* VEGF gene delivery to myocardium: deleterious effects of unregulated expression. *Circulation* **102**, 898-901 (2000).
483. Post, M.J., Laham, R., Sellke, F.W. & Simons, M. Therapeutic angiogenesis in cardiology using protein formulations. *Cardiovasc Res* **49**, 522-531 (2001).
484. Benjamin, L.E., Golijanin, D., Itin, A., Pode, D. & Keshet, E. Selective ablation of immature blood vessels in established human tumors follows vascular endothelial growth factor withdrawal. *J Clin Invest* **103**, 159-165 (1999).
485. Ziebart, T.*, et al.* Sustained persistence of transplanted proangiogenic cells contributes to neovascularization and cardiac function after ischemia. *Circ Res* **103**, 1327-1334 (2008).
486. Li, W. & Silverstein, R.L. Biological surgery: synergetic angiogenic therapy using coadministration of two progenitor cell populations. *Circ Res* **103**, 684-686 (2008).
487. Zisch, A.H., Lutolf, M.P. & Hubbell, J.A. Biopolymeric delivery matrices for angiogenic growth factors. *Cardiovasc Pathol* **12**, 295-310 (2003).
488. Tirelli, N., Lutolf, M.P., Napoli, A. & Hubbell, J.A. Poly(ethylene glycol) block copolymers. *J Biotechnol* **90**, 3-15 (2002).
489. Christman, K.L. & Lee, R.J. Biomaterials for the treatment of myocardial infarction. *J Am Coll Cardiol* **48**, 907-913 (2006).
490. Sanborn, T.J., Messersmith, P.B. & Barron, A.E. In situ crosslinking of a biomimetic peptide-PEG hydrogel via thermally triggered activation of factor XIII. *Biomaterials* **23**, 2703-2710 (2002).
491. Sabatine, M.S.*, et al.* Complementary roles for biomarkers of biomechanical strain ST2 and N-terminal prohormone B-type natriuretic peptide in patients with ST-elevation myocardial infarction. *Circulation* **117**, 1936-1944 (2008).
492. Christman, K.L., Fok, H.H., Sievers, R.E., Fang, Q. & Lee, R.J. Fibrin glue alone and skeletal myoblasts in a fibrin scaffold preserve cardiac function after myocardial infarction. *Tissue Eng* **10**, 403-409 (2004).
493. Twardowski, T., Fertala, A., Orgel, J.P. & San Antonio, J.D. Type I collagen and collagen mimetics as angiogenesis promoting superpolymers. *Curr Pharm Des* **13**, 3608-3621 (2007).
494. Nicolosi, G.L.*, et al.* The prognostic value of predischarge quantitative two-dimensional echocardiographic measurements and the effects of early lisinopril treatment on left ventricular structure and function after acute myocardial infarction in the GISSI-3 Trial.

Gruppo Italiano per lo Studio della Sopravvivenza nell'Infarto Miocardico. *Eur Heart J* **17**, 1646-1656 (1996).
495. Nelson, D.M., Ma, Z., Fujimoto, K.L., Hashizume, R. & Wagner, W.R. Intra-myocardial biomaterial injection therapy in the treatment of heart failure: Materials, outcomes and challenges. *Acta Biomaterialia* **7**, 1-15 (2011).
496. Lutolf, M.P.*, et al.* Repair of bone defects using synthetic mimetics of collagenous extracellular matrices. *Nat Biotechnol* **21**, 513-518 (2003).
497. Bezuidenhout, D., Davies, N. & Zilla, P. Effect of well defined dodecahedral porosity on inflammation and angiogenesis. *ASAIO J* **48**, 465-471 (2002).
498. Thurston, G., Baluk, P., Hirata, A. & McDonald, D. Permeability-related changes revealed at endothelial cell borders in inflamed venules by lectin binding. *Am J Physiol* **271**, H2547-2562 (1996).
499. Beckstead, J. A simple technique for preservation of fixation-sensitive antigens in paraffin-embedded tissues. *J Histochem Cytochem* **42**, 1127-1134 (1994).
500. Takagawa, J.*, et al.* Myocardial infarct size measurement in the mouse chronic infarction model: comparison of area- and length-based approaches. *J Appl Physiol* **102**, 2104-2111 (2007).